The development of novel automated technology to measure trace gas fluxes from agricultural systems

James Benjamin Keane

PhD

University of York

Biology

July 2015

Abstract

Anthropogenic climate change is driven by increasing emissions of greenhouse gases (GHGs), and the three biogenic GHGs with the greatest effect on radiative forcing are carbon dioxide (CO_2), methane (CH_4) and nitrous oxide (N_2O). One mitigation strategy is to substitute fossil fuels with biomass-derived energy, so a thorough understanding of the GHG budget of energy crop production is needed. Agriculture's biggest contribution to GHG emissions is N_2O as a consequence of nitrogenous (N) fertiliser applications.

Here two different novel automated systems, SkyBeam and SkyLine, are presented, capable of measuring net ecosystem exchange (NEE) of CO_2, CH_4 and N_2O on a near-continuous basis. Unlike micrometeorological methods, SkyBeam and SkyLine resolve to the plot scale, enabling manipulative experimentation to further understanding GHG fluxes. In fully replicated experiments, the effects on GHG of compost addition and different N fertiliser types were investigated in *Miscanthus x giganteus* and oilseed rape (OSR, *Brassica napus*). A further comparison of soil GHG flux under a *Miscanthus* field and a conventional arable field was made using flux chambers.

N_2O made a major contribution to the GHG balance in the arable field (14% total soil flux) and from the OSR, where it reduced the GHG sink by *ca.* 50%. N_2O flux was not a significant factor in *Miscanthus*, though compost addition increased N_2O emission. *Miscanthus* was a net GHG source, attributed to CO_2 emissions resulting from ploughing. Soil fluxes of N_2O and CH_4 were greater than those including vegetation.

Strong diurnal patterns were seen in all three GHGs measured, and these differed between crops. N_2O showed uptake during the day and emission at night from *Miscanthus*, whereas N_2O emissions were largest during the day from OSR. Diurnal peaks in soil respiration occurred at 15.00 under barley (*Hordeum vulgare*) at and under *Miscanthus* at 20.00. Continuous measurements are vital to characterise the diurnal pattern of GHG flux, or can be used to direct appropriately-timed daily measurements to calculate GHG budgets.

Table of Contents

List of Figures

List of Tables

Acknowledgements

The work presented here has been funded by the Energy Technology Institute (ETI) and the Natural Environment Research Council (NERC). I would like to thank both organisations for financing these projects, but in particular, Jonathan Oxley and Niall McNamara, for their patience in waiting for SkyBeam to be deployed (I trust you'll agree these results were worth the wait!) and Geri Newton-Cross and Geraint Evans for their guidance in presenting the work to the stakeholders. The role that NERC played in financing the design, development and deployment of SkyLine has also been invaluable. I'd like to thank all the people involved in the ELUM and GREENHOUSE projects, with whom I have worked. There are too many people, from various institutions, to name all of them individually, but thanks to Jon Finch and everyone from CEH Wallingford, for permission to use their data, likewise to Julia Drewer and everyone from CEH Edinburgh. Emanuel Blei and Rob Clement from University of Edinburgh have also provided great help and advice.

Huge thanks is due to Phil Ineson, my supervisor, who has not only provided me with excellent advice throughout my studentship, but also the motivation and the enthusiasm for research. It is safe to say that I would not be doing this for a living had it not been for his influence. I am also especially grateful to Sylvia Toet, who has offered support, advice, and most importantly, employment. My training panel, Simon McQueen-Mason and Kelly Redeker have helped me through the research process with their advice throughout. To James Stockdale and Kate Storer, both of whom have had to put up with sharing office space with me, patiently answering my many, many, questions, and ignoring the cursing at my computer screen, thank you.

The role played by the engineers from the workshops in the Department of Biology cannot be underestimated. Without the hard work of Mark Bentley, Steve Howarth, Trevor Illingworth and Richard, neither SkyBeam nor SkyLine would have progressed beyond sketches on paper. Steve and Mark particularly have made themselves available above and beyond the call of duty, taking many phone calls from me in remote locations at inconvenient times. They are a tremendous asset without which the University would be very much poorer.

I have been very lucky to have spent my time as a student as part of the D0 corridor in Biology. I could not have wished for a more friendly environment in which to work: the academic staff, Angela Hodge, Thorunn Helgason, Sue Hartley, Alastair Fitter

have always been approachable and friendly, and lab meetings have been a highlight of the week. Naomi Voke, Debbie Coldwell, David Sherlock, Tom Thirkell, Claudia Harflett, Sheila Davitt-Betts, Vicky Chadfield, Erin Haskell, Emma McLarnon, Tim Doheny-Adams and Lin Chen have all been good friends, as well as colleagues. Thanks to Mel Smee, for not just being a friend, but providing me with somewhere to live. I am especially grateful to Ruth, who has put up with my grumpiness and complaining, and without whom I might have gone mad this last year.

I cannot thank my family enough for the support throughout the last seven years. My parents have always been there for me, helping me financially, feeding me, putting a roof over my head, giving emotional support, helping look after George, and so many other ways. This would not have been possible without them, and I am eternally grateful. Thank you to my brother, Sam, who has to put up with me, and his wife, Kelly, who shouldn't but does; they have endured me live with them, and helped in many other ways. My Grandma, too, who was a constant source of support. Thank you to Jen, who has been so understanding and makes complicated things easy. Above all, thank you to George, who is my motivation, encouragement, and has been so patient with his Dad whilst I completed this work.

Author's declaration

I declare that this thesis is a presentation of original work and, with the exception of the work outlined below, I am the sole author. This work has not previously been presented for an award at this, or any other, University. All sources are acknowledged as References.

The eddy covariance data in Chapter 3 were collected using equipment maintained and deployed under the supervision of Jon Finch by Centre for Ecology and Hydrology (CEH), Wallingford, who also processed the raw data to provide flux half hourly fluxes. All analysis of those data presented here were conducted by me.

Hourly rainfall data, which were used in regression analyses in Chapters 2, 3 and 4 were provided courtesy of the Met Office and were accessed and used with permission from Centre for Environmental Data Archival (CEDA) via the MIDAS website.

The experimental design in Chapter 3 was conducted by myself, but I had substantial help deploying and maintaining the SkyBeam system in the field from Phil Ineson, Mark Bentley and James Stockdale. The experiments presented in Chapter 4 were designed by myself, Phil Ineson, Harry Vallack and Sylvia Toet, and the SkyLine system was installed and operated by all four. Additional technical help was provided in the field by Emanuel Blei. The manual chamber flux measurements and meteorological data were made by CEH Edinburgh, and the data are reproduced with their permission. Biomass measurements and soil pH measurements in Chapter 4 were made by Rebecca Rowe and Niall McNamara of CEH Lancaster, and used with permission. All the analyses here were performed by me.

1 General Introduction

1.1 Trace gases

Trace gases are those gases found in the atmosphere at very low concentrations, generally accepted to mean gases at less than 1% of total volume, i.e. they are present at concentrations lower than 10,000 parts per million (ppm), though Conrad (1996) suggests a lower concentration of 20 ppm. For the purpose of this thesis the less conservative definition will be considered, and thus encompasses a great many compounds including, *inter alia*, carbon dioxide (CO_2), methane (CH_4), nitrous oxide (N_2O), various chlorofluorocarbons (CFCs), nitric oxide (NO), ammonia (NH_3), carbon monoxide (CO) and other non-methane hydrocarbons (NMHCs). Short-lived species such as CO and NO vary greatly in concentrations across spatial scales (Matson & Harriss, 2009) whilst longer lived gases, such as CO_2 and N_2O, have more spatially consistent concentrations.

Of all the trace gases, it is those that play a role in the radiative balance of the planet that are of particular interest in the context of climate change. Gases that increase the radiative forcing of solar radiation are known collectively as greenhouse gases (GHG) and the GHGs that make the largest contribution to warming, after water vapour (H_2O), are CO_2, CH_4, CFCs and N_2O (IPCC, 2011). Whereas CFCs are artificially synthesised chemicals that have been widely phased out due to their ozone-destructive reactions in the stratosphere, CO_2, N_2O and CH_4 are all biogenic gases. A thorough understanding of the processes controlling the production and consumption of these latter three gases is key to our ability to manage land use to benefit the GHG balance.

Although it is now widely appreciated that the atmospheric concentration of CO_2 is rising rapidly, the importance of CH_4 and N_2O is frequently overlooked despite the fact that N_2O and CH_4 have, mole for mole over a 100 year timeframe, a global warming potential 298 and 34 times, respectively, that of CO_2 (see Forster *et al.*, 2007, Myhre, 2013). Indeed, some of the most sensible strategies for reducing national GHG burdens specifically tackle these more potent gases. Unfortunately, both N_2O and CH_4 can be emitted in rapid bursts directly from terrestrial systems (Ambus *et al.*, 2010) necessitating a more continuous approach for accurately quantifying their fluxes. Sources and sinks of trace gases

1.1.1.1 CO_2

Photosynthesis and respiration represent the major global biological sinks and sources of carbon (Reay & Grace, 2007); CO_2 is assimilated by plants through photosynthesis and converted to biomass, with the plants themselves, together with heterotrophic organisms, subsequently using this assimilated carbon for respiration, and produce CO_2 which is released back into the atmosphere. It is a combination of combustion of fossil fuels, specific industrial processes and land use change that are largely responsible for the elevation of atmospheric CO_2 (Stocker *et al.*, 2014) concentrations from levels of pre-industrial levels of 280 ppm to nearly 400 ppm in this decade.

For a summary of the fate of assimilated carbon, see Figure 1a in Singh *et al.*.(2010). It is thought that approximately 50% of anthropogenic CO_2 emissions are absorbed by terrestrial and oceanic carbon sinks annually (Sitch *et al.*, 2015). The major terrestrial CO_2 sinks are net primary production (NPP) and sequestration to the soil (Reay & Grace, 2007). Sequestration occurs where carbon accumulates in the soil, either because environmental conditions do not favour decomposition, which will lead to a buildup of organic material in the soil (e.g. peat lands), or where a proportion of decomposed biomass becomes 'inert' and is held back from the atmosphere for thousands of years (Reay & Grace, 2007). There is concern that with warming global temperatures, conditions will favour decomposition and increasing amounts of detritus will be respired back to the atmosphere rather than being sequestered in soils (Singh *et al.*, 2010).

Soil respiration is the largest biological source of CO_2 in terrestrial ecosystems (Bahn *et al.*, 2009). Factors controlling soil respiration include temperature (Singh *et al.*, 2010), soil moisture (Orchard & Cook, 1983), substrate availability and the nitrogen content of necromass (Raich & Tufekcioglu, 2000) and O_2 levels (Salome *et al.*, 2010). Practices to inhibit CO_2 losses from soil include reduced tillage in agricultural practice, and soil CO_2 losses can be managed through land use: deforestation and conversion of grassland to agricultural use can result in large soil C losses through respiration.

1.1.1.2 N_2O

N_2O is produced biologically by microbes through two processes, nitrification and denitrification (Firestone & Davidson, 1989). Nitrification is an aerobic process, through which ammonium (NH_4^+) is oxidised to nitrite (NO_2^-) and nitrate (NO_3^-);

denitrification is an anaerobic sequence of reactions through which NO_3^- is reduced to dinitrogen gas (N_2) via N_2O (Figure 1.1). A third pathway, nitrifier denitrication, is carried out by the same bacteria which oxidise NH_4 and are capable of reducing NO_2^- to N_2O (Wrage *et al.*, 2001). Whereas nitrification is an autotrophic process, denitrification is heterotrophic and requires a carbon (C) source (see Wrage *et al.*, 2001). The principal factors controlling nitrification are known to be NH_4 availability, soil temperature, moisture and pH (Parton *et al.*, 1996). The most important factor controlling denitrification is oxygen (O_2) concentration due to the sensitivity of nitrogen oxide reductase (NOR) enzymes which are inhibited in aerobic conditions (Knowles, 1982). Consequently, factors affecting O_2 availability will influence denitrification rates, and hence N_2O production. These factors include soil water content (Davidson *et al.*, 1993), and soil respiration, since at higher rates O_2 levels are depleted (Castaldi, 2000).

Apparent net N_2O uptake is seen when reduction of N_2O to N_2 exceeds the rate of N_2O production (Chapuis-Lardy *et al.*, 2007) and up to two thirds of N_2O produced at depth within a soil profile may be reduced to N_2 as it diffuses upwards to the atmosphere (Clough *et al.*, 1999). N_2O consumption in soils is generally held to occur at very high moisture levels which create anoxic conditions (Conen & Neftel, 2007) but N_2O uptake has been reported on several occasions from well aerated, dry soils (e.g. (Flechard *et al.*, 2005, Warneke *et al.*, 2015, Wu *et al.*, 2013), a process which has been attributed to aerobic denitrification (Bateman & Baggs, 2005), and which has been shown to be predominantly of biological origin (Warneke *et al.*, 2015).

The concentration of N_2O in the atmosphere has increased from 270 ppb prior to the industrial revolution to its current concentration of *ca.* 320 ppb (Forster *et al.*, 2007). The rise in atmospheric N_2O is largely a consequence of the increase in anthropogenic nitrogen (N) fixation via the Haber-Bosch process, principally for the production of nitrogenous fertilisers (Vitousek *et al.*, 1997). N_2O may be produced directly by microorganisms in soils or indirectly, when nitrogen (N) is leached from soils (e.g. as nitrate, NO_3) and a percentage subsequently converted into N_2O (Adler *et al.*, 2007). Hence, one principal driver of N_2O production from soils is the addition of N fertilisers to agricultural land (Forster *et al.*, 2007) and, very specifically, rapid bursts of N_2O production have frequently been seen in agricultural systems after wetting events (e.g. such as rainfall (Woli *et al.*, 2010)) and these emissions can constitute 20% of the annual flux, occurring over just a few days (Mummey *et al.*, 1997).

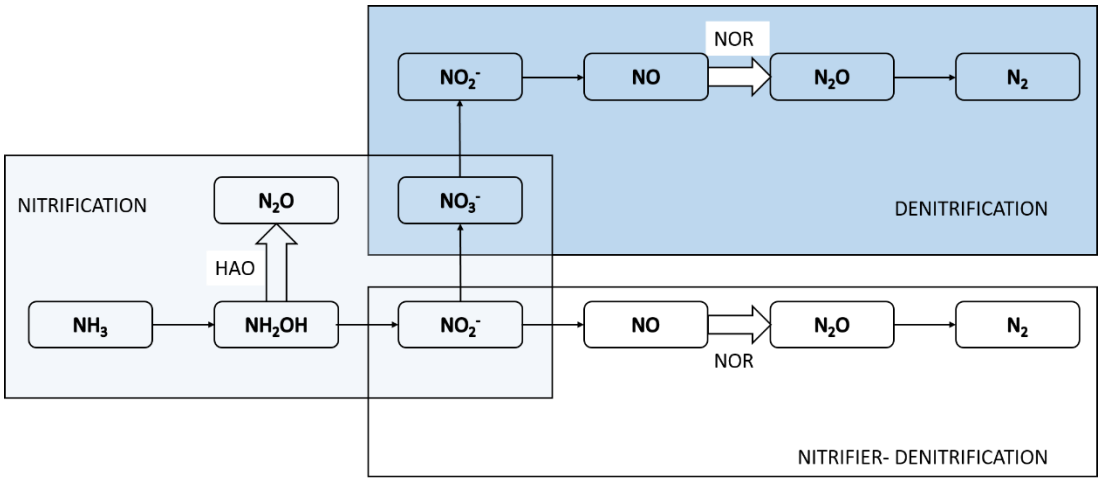

Figure 1.1 Elements of the nitrogen cycle showing nitrification and denitrification pathways. Enzymatic steps responsible for N_2O production are indicated by the large arrows; the enzymes hydroxylamine reductase (HAO) and nitric oxide reductase (NOR) are labelled adjacent to the arrows. Adapted from Wrage *et al.* (2001).

This high temporal variability represents a major challenge when attempting to quantify field fluxes for this gas.

1.1.1.3 CH_4

Atmospheric concentration of CH_4 has risen to around 1770 ppb, from a pre-industrial level of 770 ppb, constituting an increase of more than 250%, the largest percentage increase of any of CO_2, N_2O and CH_4 (Conrad, 2009). By far the largest global source of CH_4 is microbial in origin, which totals 69% of net CH_4 production (Conrad, 2009). The chemical reactions governing CH_4 production occur in anaerobic conditions, most commonly where acetate or CO_2 is reduced in the absence of alternative electron receptors (Figure 1.2; (Schutz *et al.*, 1988, Thauer, 1998)). CH_4 is produced by methanogenic archaea, predominantly from soils, ruminant guts, sediments and any system where a combination of available carbon and anaerobic conditions occur (Myhre, 2013), making the largest biological sources of CH_4 are wetlands, rice paddies, livestock and microbial processes in landfill sites (Myhre, 2013). The net system fluxes of CH_4 are greatly complicated by the fact that methanotrophic bacteria, in the presence of oxygen, can oxidise up to 90% of CH_4 produced (Le Mer & Roger, 2001), making net fluxes the result of these two processes. A third, and much less-well understood process, is anaerobic CH_4 oxidation, which is undertaken by a group of archaea in the presence of sulphate (Knittel & Boetius, 2009). Spatial heterogeneity in ecosystems, both vertically and horizontally, means that both CH_4 sources and sinks are often present, with the highest net fluxes to the atmosphere frequently associated with wetter regions (McNamara *et al.*, 2008), whilst drier soils within the same catchment may well be acting as effective CH_4 oxidation sites (Figure 1.2; (Bradford *et al.*, 2001). Factors governing whether a soil is a net producer or consumer of CH_4 include its physical properties (Smith *et al.*, 2003), available N content (Bender & Conrad, 1995, Reay & Nedwell, 2004), water content and pH (Bender & Conrad, 1995). Using a combination of land use, basic edaphic and climate information, combined with literature values, it is possible to estimate landscape CH_4 fluxes, but there still remain major data gaps; these are often associated with unusual land uses (e.g. willow energy crops on previous agricultural land) or critical interfaces between wet and dry or terrestrial and aquatic systems. Not unlike N_2O, CH_4 may be emitted from the soil in large bursts over short periods of time (Moore *et al.*, 1990) but there are a number of important and differing alternative pathways for CH_4 transport through plant-soil systems, in particular, diffusion through aerenchyma in wetland plant species allows CH_4 formed in sediments to reach the atmosphere (Kludze *et al.*, 1993)

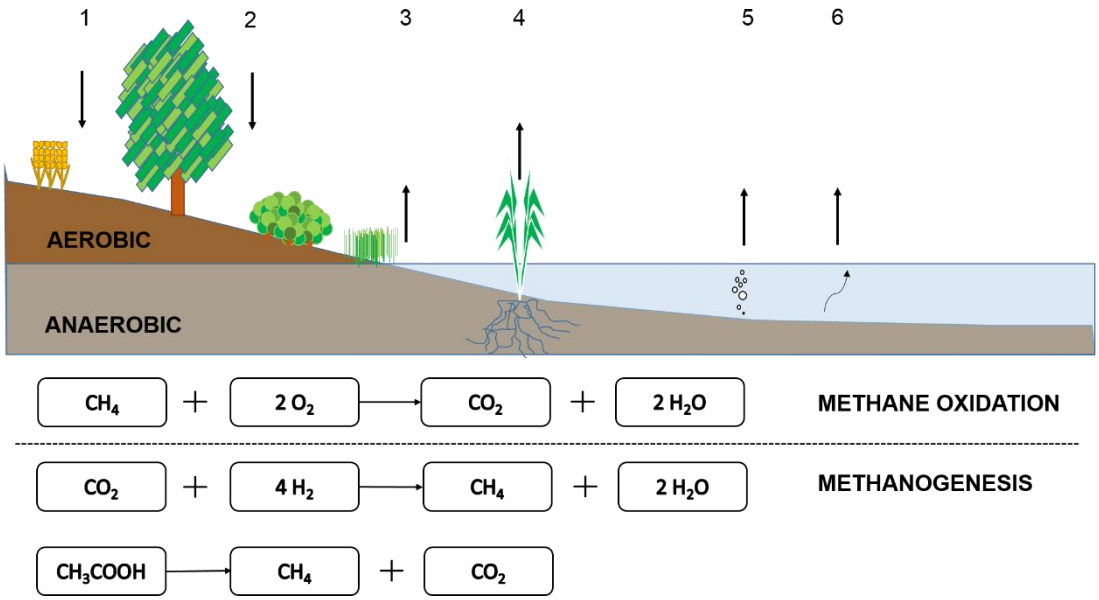

Figure 1.2 Methane fluxes across a landscape, the equations for production (methanogenesis) and consumption (oxidation) are shown. Methanogenesis occurs in anaerobic conditions and oxidation in aerobic. Upward arrows indicate where CH_4 is released to the atmosphere and downward arrows where uptake will occur. Uptake generally occurs in well aerated soils such as in agricultural and forest systems (1 & 2), whereas emission will occur where the water table is high (3), through direct transport via aerenchymous wetland plants (4), or from sediments via ebullition (5) or upward diffusion through a water body (6).

1.1.2 Trace gases and agricultural soils

In 2013, agriculture contributed approximately 8% of the UK's annual net GHG emissions, which made it a larger contributor than industrial processes and equated to more than half of the emissions from transport (DECC, 2015). The breakdown of UK agricultural emissions reveals that the three biggest sources are soil N_2O flux (*ca.* 50%), CH_4 from livestock (*ca.* 25%) and emissions from manure management (*ca.* 15%) (DEFRA, 2014a).

N_2O production by agricultural soil is derived principally from mineral N and manure applications to arable and grassland, and N excretion from livestock, with indirect emissions from NO_3 leaching and NH_3 volatilisation also important additional sources (Skiba *et al.*, 2012). The type of mineral N applied as fertiliser can affect N_2O fluxes (Dobbie & Smith, 2003a, Zhang *et al.*, 2014, Zhou *et al.*, 2014) and a range of mitigation techniques are available. However, due to the heterogeneity of N_2O fluxes, a fundamentally better understanding of the processes governing N_2O fluxes is needed in order to implement precision agriculture to effectively reduce future N_2O emissions (Rees *et al.*, 2013).

Whereas livestock agriculture is a large source of CH_4, soils under arable crop cultivation are often CH_4 sinks (Flessa *et al.*, 1998, Gregorich *et al.*, 2005, Meijide *et al.*, 2010, Sanz-Cobena *et al.*, 2014), and European crop lands are known to be a net sink for CH_4 (Ciais *et al.*, 2010). The sink effect is due to the aerobic nature of the majority of arable soils, and the sink effect diminishes depending on soil type, with the greatest oxidation seen in sandy-loams and the least in clay soils (Regina *et al.*, 2007). Grasslands are also often CH_4 sinks (Wei *et al.*, 2015), though this is by no means always the case (Hortnagl & Wohlfahrt, 2014), and the presence of grazing animals can shift a CH_4 sink to a net source (Schonbach *et al.*, 2012).

Tillage is known to increase soil respiration, particularly in the period immediately following disturbance (Alvaro-Fuentes *et al.*, 2007, Reicosky *et al.*, 1997, Roberts & Chan, 1990). Reducing, or halting tillage completely can reduce soil respiration and increase soil C sequestration (Jacobs *et al.*, 2009), and as such has been recommended as a GHG mitigation technique (Paustian *et al.*, 2000). However, soils under reduced tillage regimes have been shown to emit more N_2O than those under conventional tillage (Koga *et al.*, 2004), and modelled values have indicated that as

much as 300% of the gain in sequestered C from reduced tillage may be simply lost as N_2O flux to the atmosphere (Li *et al.*, 2005).

1.1.3 GHGs and bioenergy crops

With a growing world population, and a diminishing global reserve of fossil fuels, it is necessary for alternative sources of energy production to be investigated. Ethanol from biomass has long been used as a petroleum substitute (Nastari, 2012, Tyner, 2012), most commonly fermented from sugars obtained from corn (*Zea mays*) or sugar cane (*Saccharum* spp.). Diverting food crops into energy production would seem counter-productive, given that there is genuine concern regarding our ability to meet future global food demand (Godfray *et al.*, 2010). Crops such as corn, sugar cane, oilseed rape (OSR, *Brassica napus*) are considered first generation energy crops. Attention has recently turned to utilising lignocellulosic material: woody tissue and non-food crop by-products such, as corn stover. For this reason crops such as short rotation coppice (SRC) tree species such as willow (*Salix* spp.), poplar (*Populus* spp.), the perennial grasses *Miscanthus* (*Miscanthus x giganteus*) and switch grass (*Panicum virgatum*) and short rotation forestry (SRF) are being cultivated for energy production (Rowe *et al.*, 2009), and these are referred to as second generation energy crops. These are attractive since they do not deplete food supplies, have high yields (Oliver *et al.*, 2009), require less fertiliser input than annual arable crops (Don *et al.*, 2012), and can be grown on marginal agricultural land (Gopalakrishnan *et al.*, 2011). The challenge with utilising for lignocellulosic material for fuel production lies in degrading the hemicellulose to smaller carbon molecules which can be fermented to produce ethanol or transesterified for the production of biodiesel (Ragauskas *et al.*, 2006). Pretreatment must be undertaken to achieve this, which can be energy intensive, and is costly in terms of finance and GHG emissions. In order to make this process viable, maximum value in terms of by-products must be extracted from the 'biorefineries' where processing occurs (Ragauskas *et al.*, 2006), and much research into energy-efficient enzymatic digestion of hemicellulose is being carried out (Chandra *et al.*, 2015, Hong *et al.*, 2015, Yang *et al.*, 2015). In addition to liquid fuel production, energy may be derived from direct combustion of biomass in dedicated power stations, such as that found at the UK's largest power station, Drax, in North Yorkshire.

It is vital to consider the previous role of any land utilised for energy crop cultivation. The GHG fluxes associated with land use change to bioenergy production will largely

depend on the nature of the land use transition. The largest net gain in terms of GHG balance is predicted to come from converting conventional tilled arable land to either broad leaved forest or *Miscanthus,* mainly due to the reduction in N fertiliser usage (St Clair *et al.*, 2008), and any transition from grassland or forestry to energy cropping is likely to lead to a net emission of GHGs (Harris *et al.*, 2015). CH_4 may be similarly affected by land use change. Since CH_4 oxidation/production is heavily reliant on whether soils are anaerobic, an important factor in whether land is a source or sink of CH_4 is the impact on soil moisture status. If changes in the land use alter soil water relations, this may affect the rate at which CH_4 is produced or consumed. Converting forest to bioenergy crop production can stop CH_4 oxidation; in contrast the planting of oil palms may stimulate CH_4 oxidation (Cherubini *et al.*, 2009).

In order to obtain an accurate GHG budget for bioenergy, full life-cycle analyses (LCA) of bioenergy production must be undertaken (Kaltschmitt *et al.*, 1997). This accounts for the fluxes of all GHGs at each discrete stage of bioenergy production. If bioenergy production GHG balance is only considered in terms of CO_2, it may well encourage utilisation of crops with high nitrogen fertiliser requirements as feedstocks, which might lead to increased N_2O emissions which undermine any carbon gain (Reay *et al.*, 2012). An attributional LCA considers each phase of the process which may contribute a net production or consumption of GHGs (Figure 1.3); a consequential LCA considers the wider implications of energy production, including indirect land use change. However, the work in this thesis stops at the ‘farm gate’: only the GHG balance in terms of fluxes from soil and vegetation will be investigated.

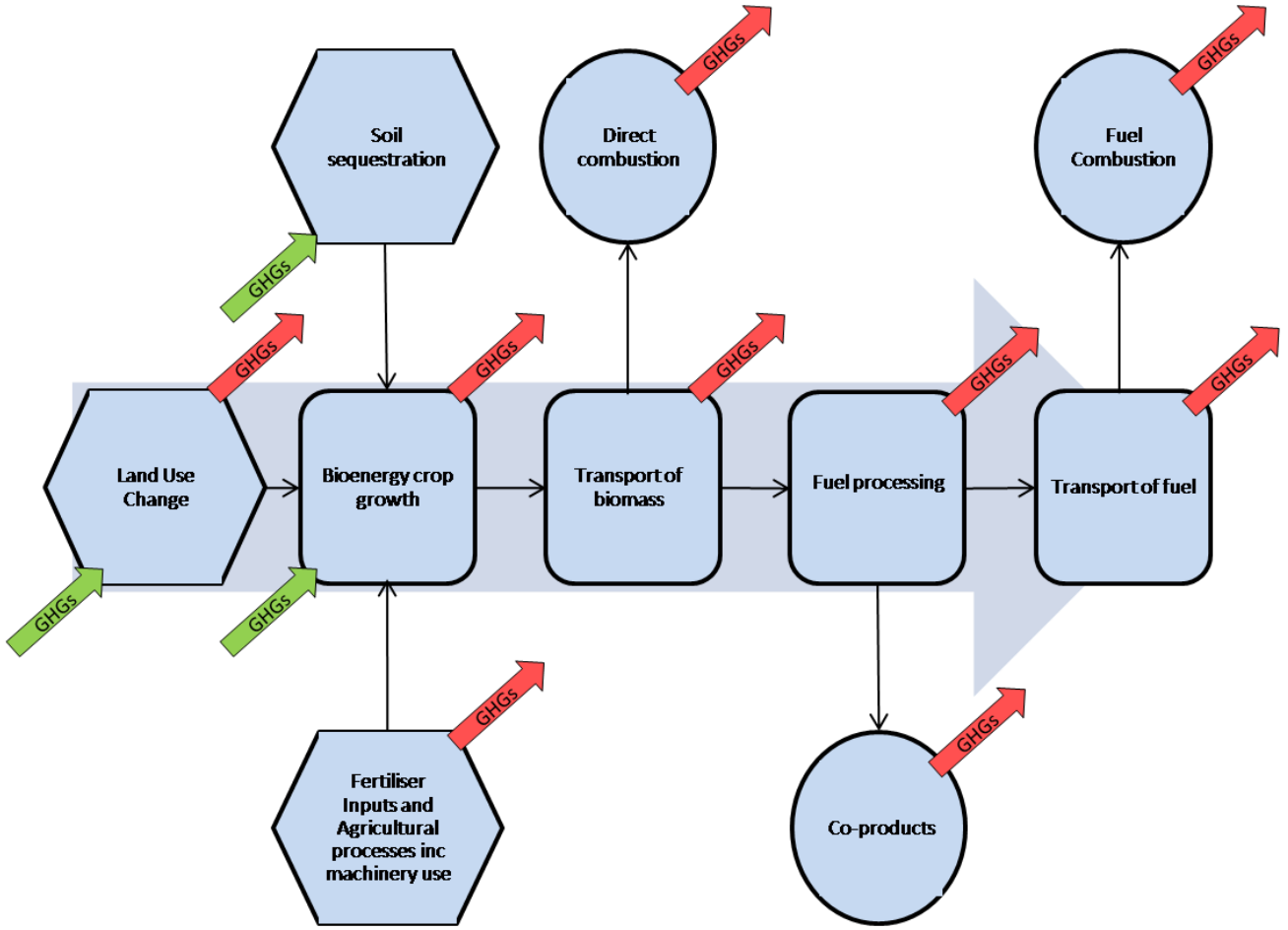

Figure 1.3 Conceptual biofuel life cycle analysis. Each stage must be considered in terms of greenhouse gas (GHG) production and consumption in order to quantify the GHG balance of bioenergy.

1.1.4 Soil fluxes vs net ecosystem fluxes

The net ecosystem GHG flux is the total flux of GHG gases, either positive or negative, once all the sources and sinks have been determined and accounted for. This is the most important figure when considering trace gas fluxes, especially with a view to extrapolating budgets at a landscape scale and larger (Mosier, 1998). It has been known for some time that CH_4 flux from soil to the atmosphere may be facilitated by aerenchymous tissue in rice plants (ButterbachBahl *et al.*, 1997), peatland plants such as *Eriophorum vaginatum* (Saarnio & Silvola, 1999) and other wetland species (Ding *et al.*, 2005). Trace gas emissions have been measured from the stems of non-aerenchymous plant species: Gauci *et al.* (2010) measured significant emissions of CH_4 from the stems of alders *(Alnus glutinosa*) and N_2O emissions have also been detected from stems of wetland trees (Rusch & Rennenberg, 1998) and non-wetland tree species (Pihlatie *et al.*, 2005). In order to be confident of the total net GHG exchange it is important to be able to measure both the fluxes of trace gases from the soils beneath vegetation, but also the fluxes from the vegetation itself.

1.2 Existing technologies for trace gas measurement

Several technologies exist for the quantification of trace gas fluxes and many studies have been conducted *ex situ* with soil incubated in laboratory studies. However, since it is field fluxes which are of most value to climate change research, so for the purposes of this thesis, the common techniques used for *in situ* field measurements of fluxes will be considered. Each method has various advantages and disadvantages, in terms of the quality of the data they can produce, and the cost at which those data are generated. Of particular interest are the spatial scale at which a method is able to measure and the frequency of the measurements (Figure 1.4), which can be key to detecting subtleties in the mechanisms controlling trace gas fluxes.

1.2.1 Chamber methods

Since the early twentieth century, chambers have been employed to measure trace gases (Matson & Harriss, 2009). Chambers may be classified as static/non-steady state or dynamic/steady state. Static chambers are also often referred to as cover-boxes and they usually consist of a sealed chamber placed over the soil with an air-tight sampling port through which volumes of air are removed, normally manually, at

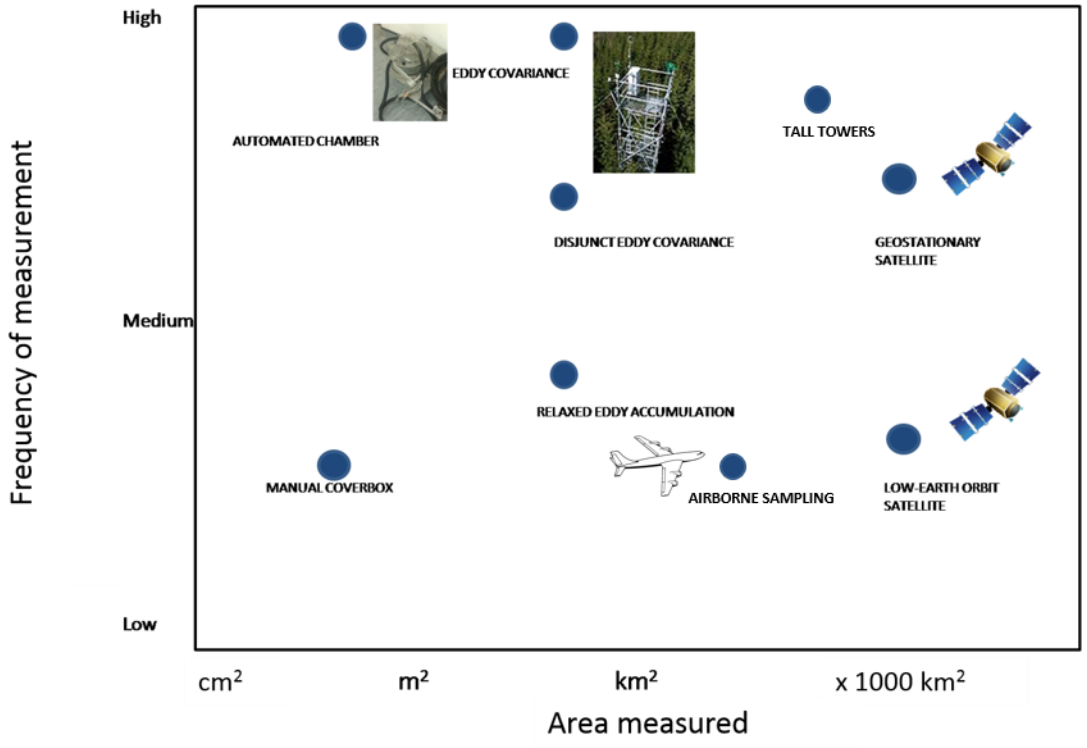

Figure 1.4 Common methods of trace gas measurements, considered in terms of the area at which they measure (horizontal axis) and the frequency of the measurements mad (vertical axis).

discrete intervals. Chambers may be a single unit placed on the soil, but more commonly they have a two-part construction, consisting of a base fitted into the soil and a separate cover box. The base, often referred to as a collar or core, is usually partially buried below the soil surface for the duration of the study, whilst the cover is deployed only during gas sampling periods. Gas samples are taken from the headspace at intervals and stored in gas tight containers which are usually pre-evacuated glass or metal containers or bags (e.g. Rochette & Erikson-Hamel, 2008). The gas samples are then normally returned to the laboratory where they are subsequently analysed to determine the time series of concentrations for the gases of interest. Flux rates are calculated using a regression of change in gas concentration over time (e.g. Venterea *et al.*, 2009), and much work has been done to suggest a standardised methodology (de Klein & Harvey 2012)

An alternative design for static chambers is to simply cycle the accumulating headspace gas from the chamber through an analyser such as an infrared gas analyser (IRGA), photoacoustic analyser or tunable diode laser. Such chambers are frequently designed for manual operation, which requires the investigator to place the chamber over the collar, and in the case of a field experimental comparison, to move the equipment sequentially between collars. In these systems, the chamber closes for a specified length of time and circulates headspace gas through the analyser which measures the concentration of the trace gas at a high frequency, typically 1Hz. Each chamber closure generates a series of concentrations over time which are used to plot a regression, from which the flux can be calculated. The data from such systems are normally stored as a file on the analyser or attached computer, and can be viewed in real time in the field. Commercial systems for CO_2 fluxes, with associated software, are available from PP Systems (UK) and Li-Cor (USA).

Automated chambers are also available, which are designed for longer term deployment over weeks, months or even years (Grace *et al.*, 2012). These automated chamber systems close for a programmable length of time in a preordained sequence and monitor fluxes at programmed intervals, and can be multiplexed into multiple chamber arrays across a landscape or experimental set up. It is recommended that chambers should incorporate a vent for equalising internal and external pressures (see below) since ‘pumping’ actions may affect flux measurements. Achieving this, whilst ensuring that no gas leakages occur, has resulted in the development of quite sophisticated vent designs, which are also discussed below.

One variant of the static chamber is the dynamic chamber which, instead of allowing an accumulation of air in the chamber, maintains a constant and measured air flow through the chamber, directly fed to a gas analyser. This approach has been used for several decades (Reiners, 1968) and relies on the difference in the concentrations of incoming and outgoing air to determine flux rates and an accurate measurement of flow rates. Again, these chambers usually consist of two components, *viz.* a collar inserted below the soil surface and the chamber itself, which sits on top of the collar, forming a seal in the same fashion as for a coverbox.

1.2.2 Gradient techniques

A major criticism of chamber approaches is that the chamber itself may affect the microclimate of the system under study, thus influencing the processes being measured. In practice, these criticisms do not apply to short flux measurement periods when chambers are removed between measurements, but the next stage in the development of *in situ* flux measurements is to try and avoid any chamber whatsoever. This led to the development of the so-called 'gradient methods' which relied on measuring the diffusive gradient of the gas over the system, taking simultaneous measurements of gas concentration at various different heights above the vegetation canopy. For example, using a tower with chemical traps (e.g. Duyzer *et al.*, 1992) or piped inlets at different heights serving a fast response analyser, it is possible to detect positive and negative gradients and to subsequently calculate ecosystem fluxes. Whilst avoiding any invasive chambers or manipulation of the system under study, the calculation of flux and requirement for a measurable gradient meant that the approach has been rapidly superseded by the development of the more sophisticated and analytically demanding eddy covariance (EC) approach. The technique was originally used for analysis of CO_2 fluxes but has also been used for other trace gases, including N_2O and CH_4, using fast response analysers (Hargreaves *et al.*, 1994).

A similar gradient approach has been applied to estimating fluxes of trace gases through the soil profile, using the quite marked gradients of gas concentrations frequently seen down soil profiles. Soil gas probes have been used to calculate fluxes of gases within a soil profile by measuring concentrations of gas at specific depths below the surface and applying diffusive models (e.g. Li & Kelliher, 2005). Additionally, approaches similar to those used for the above-ground chamber technique have been attempted. In these cases, the probes usually consist of hollow

tubes that are placed in the soil at a certain depth, achieved by driving the probe vertically into the soil or by excavating an opening for the probe directly in the soil. Some such soil probes have holes in the sub-surface end of the tube to allow diffusion of gas into the probes and the probe is sealed with a cap at the end exposed above the surface. It is from this end that samples may be taken for analysis, using the same techniques employed with chamber-based methods, such as a GC (Fierer *et al.*, 2005) and IRGA (Brummell & Siciliano, 2011). The probe itself is commonly made from corrosion proof metal such as stainless steel but other non-reactive materials such as bronze (Dowdell *et al.*, 1972) or plastics e.g. polyvinylchloride (Goodroad & Keeney, 1985) have been used. Other designs utilise gas permeable materials such as silicon (Kammann *et al.*, 2001a, Boon *et al.*, 2014), and therefore do not require holes for gas diffusion. Samples may be taken once the internal gas concentration has equilibrated with those of the soil, which may occur around seven hours after placement/flushing (Kammann *et al.*, 2001b). These probes are completely buried and have a gas sampling tube which extends from the probe to above the soil surface. Probes are designed to be left in the field for periods of weeks or months, with sampling being undertaken at intervals, as determined by the experimenter. As with chambers, probes may be sampled manually for discrete measurements, or they may be automated for near-continuous measurements (Albanito *et al.*, 2009). Probes are left uncapped outside of sampling periods and fluxes are calculated using the same regression approaches employed for chamber-based methods, with a number of assumptions being made (see below). Due to the reliance of soil probes on passive diffusion, the temporal resolution which they provide is generally very low, in the order of hours or days (Albanito *et al.*, 2009) since with any change in gradient a new equilibrium must be reached, and so they are wholly unsuitable for situations where fluxes rapidly change.

1.2.3 Box method

In a similar technique to the gradient air sampling described above, Denmead *et al.*. (1998) outlined a mass balance method for calculating trace gas fluxes within large square plots. In this case, gas concentrations were sampled at specific heights along the four boundaries of a 24 m x 24 m plot and the difference in concentrations (in addition to monitoring the wind direction) used for the calculation of fluxes within the plot using simple mass balance approaches. The equivalent calculations could be made from circular plots with concentrations measured in the centre, since the wind direction will always be towards the measuring equipment (Denmead, 1995). The

concentrations of the gases can be measured using rapid analysers, or an on-line GC (Denmead *et al.*, 1998). The principle has been used to extrapolate fluxes over much larger areas; see for example Kozlova *et al.* (2008), who used measurements from tall towers in Siberia and Shetland to infer large areal fluxes. The use of tall towers has enabled estimation of terrestrial fluxes at the national scale, such as the Mace Head tower in western Ireland (Biraud *et al.*, 2002), through back modelling the source of GHGs using naturally- occurring radioisotopes of radon and lead as tracers. A network of further towers around the UK is in development, with sites at Rigehill, Angus and Tacolneston. Similarly, measurements of GHG concentration made by aeroplane- mounted analysers have been used to infer regional fluxes through a mass balance approach (e.g. Pitt *et al.*, 2015).

1.2.4 Eddy covariance (EC) methods

Continuous measurements of flux may also be determined using the eddy covariance technique (EC). This is a micrometeorological method, as for the atmospheric gradient and box methods, but it relies on the fact that the lower atmosphere, or the atmospheric boundary layer (ABL), consists of turbulent rotational eddies of air moving laterally across the earth's surface (Caughey *et al.*, 1979). Consequently, each eddy has both a vertical and horizontal element and simultaneous measurement of these eddies at high frequency, coupled to monitoring of other atmospheric properties and high frequency gas analyses enables the calculation of various fluxes over a landscape; heat and moisture transfers have been measured for several decades using this process (McMillen, 1988). With the advent of high frequency gas analysers, the technique has been adapted to detect fluxes of infra-red absorbing trace gases such as CO_2 (Leuning & Moncrieff, 1990), CH_4 (Fowler *et al.*, 1995) and N_2O (Wienhold *et al.*, 1994).

EC systems have three general components: the first is a tower or structure to raise the equipment above the landscape of interest; the second element is a high frequency sonic anemometer to measure wind speed in three dimensions, and the third is a high frequency gas analyser. Eddy systems can only be reliably used to quantify trace gas fluxes over relatively homogeneous landscapes with a large "fetch", i.e. an unobstructed approach. As the technology and supporting software have improved, EC approaches are becoming more commonly used and have been used to measure CO_2 fluxes over forest canopies (Grace *et al.*, 1995, Miranda *et al.*, 1997),

grassland (Soussana *et al.*, 2007, Twine *et al.*, 2000), fens (Grondahl *et al.*, 2008) and agricultural land (Laville *et al.*, 1999, Zenone *et al.*, 2011).

Unfortunately, there are trace gases for which no appropriate fast response analysers (say, 10Hz) exist and alternatives to the conventional EC approach have been developed, involving collection of samples of gas over longer periods of time (e.g. on an hourly basis) for subsequent analysis and correlation to turbulence; examples of these techniques are relaxed eddy accumulation (REA) and disjunct eddy covariance (DEC; see (Rowe *et al.*, 2011)). REA consists of two reservoirs for collecting gas samples, one for holding samples from upward eddies and one for downward eddies. The amount sampled is proportional to the speed of the eddy and the flux of the gas of interest can be calculated from the volume collected in each reservoir and its concentration (Businger & Oncley, 1990). The gradient methods described above and REA are considered to be indirect methods of flux calculation, whereas DEC is a direct technique. Samples are taken for periods of less than 0.1 s, but they are separated by intervals of tens of seconds to allow the equipment to complete the analysis (Grabmer *et al.*, 2004). DEC has been used to sample volatile organic compounds (VOCs) as well as HNO_3, O_3, CO_2, CH_4, N_2O, and SO_2 (Turnipseed *et al.*, 2009). EC systems have been deployed on aircraft (Desjardins *et al.*, 1982) and used to measure trace gas fluxes over urban areas (Karl *et al.*, 2009, Mays *et al.*, 2009), Antarctica (King *et al.*, 2008) and various entire landscapes in Europe (Vellinga *et al.*, 2010).

The recent developments in laser technology, including high frequency cavity ring down (CRD), have opened the possibility of expanding EC approaches to any IR absorbing gas in a far more routine way, and of expansion to stable isotope monitoring; unfortunately these analytical devices are expensive (typically £35,000 to £75,000 per instrument).

1.2.5 Satellite-based measurements

Scanning imaging absorption spectrometer for atmospheric cartography (SCIAMACHY) is an example of a satellite-based sensing platform that records the intensity of solar radiation reflected from the earth's surface and from this calculates the concentration of trace gases, including CH_4, N_2O and CO_2 (Frankenberg *et al.*, 2005). This enables long-term measurements of fluxes on a global scale, taking measurements at a spatial resolution of 30 km x 60 km per pixel and it is able to cover

the whole globe in 6 days (Frankenberg *et al.*, 2005). Geo-synchronous satellites appear to be stationary over the equator and can monitor a much smaller area for extended periods: there are many satellites orbit capable of measuring trace gas emissions, and a comprehensive review can be found in Thies & Bendix (2011).

1.3 Evaluation of flux methods.

1.3.1 Chamber methods

There is often an inherent delay between sample collection and analysis when using manual chambers. Whilst an automated system using, for example, an IRGA may give results in real time, samples collected from cover boxes normally need to be analysed after return to the laboratory, though there are examples of field-deployed GCs designed for *in situ* analysis (Fest *et al.*, 2009). Delay between sample collection and analysis prevents any dynamic modification during field campaigns and, in extreme, can mean results are not seen until after the experiment is dismantled (Ma *et al.*, 2007, Brummell & Siciliano, 2011). This reduces an investigator's ability to react to a fault in the equipment, and any faults may go undetected until too late to rectify; it also means that sampling programmes cannot be readily modified in light of incoming information. Also, it is important to ensure that sample deterioration does not occur during storage and a number of studies have investigated a variety of storage and transport containers. Commercially available storage tubes (Exetainer 839W, Labco Ltd, High Wycombe, UK) are widely used and have been shown to maintain samples without deterioration for 8 weeks (Laughlin & Stevens, 2003) and this longevity of samples has several benefits for an experimenter. Additionally, the volume taken per sample may allow for analysis of several gases from the same sample, or for sequential analyses. It also gives the investigator the opportunity to dilute samples if the concentrations are outside the normal analytical range.

One key advantage of chambers is that they enable the investigator to collect flux data at a very high spatial resolution, with the basal area of chambers typically less than 1 m^2 (Matson & Harriss, 2009). This has helped to characterise the fluxes of trace gases in different vegetation and soil types and to identify and understand flux 'hot spots' within the landscape (Grondahl *et al.*, 2008). Use of collars with chambers also allows for the application of treatments in manipulation studies, such as nutrient additions (Zhang *et al.*, 2008, Yao *et al.*, 2009a, Jiang *et al.*, 2010), litter removal (Yan *et al.*, 2008) or biota exclusion (Heinemeyer *et al.*, 2011). In addition to treatments,

cover box studies provide the scope for replication, which adds considerable power within experimental and observational contrasts.

However, cover boxes are not without their problems and the use of sub-surface collars may create undesirable effects. Normally, cores are driven into the ground in order to avoid side “leakage” of the gases from the chamber which could lead to an underestimation of the flux (Rochette & Eriksen-Hamel, 2008). It has been shown that even when rings are minimally inserted into the soil “so as to avoid cutting fine roots” (e.g. 5 cm; (Zhang *et al.*, 2008)), CO_2 fluxes will be significantly reduced by collar insertion (Heinemeyer *et al.*, 2011). In fact, Heinemeyer *et al.* (2011) demonstrated that collar insertion can reduce CO_2 fluxes by up to 30% when compared to chambers placed over surface-resting collars. Whilst this may not be a major issue in comparative studies of treatment effects, it does raise significant questions as to the level to which soil flux data are underestimated, especially when the absolute flux forms part of a full life cycle GHG analysis.

The manual nature of sample collection normally employed in cover box work has both advantages and disadvantages. One clear advantage is that a manual approach does not require a field power source, enabling systems to be deployed virtually anywhere, no matter how remote. Brummell & Siciliano (2011) highlight the advantage of being able to gather samples from many separate experimental units (chambers) in a short space of time, thus being able to measure simultaneous fluxes across treatments, vegetation and soils comparisons, etc. This contrasts with flux measurements taken from automated chambers which require several minutes per measurement and, consequently, give staggered flux measurements across an experimental site. Questions have been raised, however, about the length of time that a chamber is left in place and the effect that this may have on the regression calculations arising from the measurements (Heinemeyer & McNamara, 2011).

Due to the nature of a static chamber, as the headspace gas concentration of a trace gas increases over time, it may tend to saturate, thus reducing the diffusion rate of gas from the soil (Davidson *et al.*, 2002). In this case if a flux is measured continuously the regression reveals an asymptote. Heinemeyer & McNamara (2011) show that by measuring headspace concentrations over longer periods, e.g. 75 minutes, as is typical of manual cover boxing, the regression can underestimate the level of the flux by up to 30% compared to a regression calculated with fewer measurements from the first 15 minutes after chamber closure. Moreover, the sampling method itself is

destructive and by actually removing the sample volume from the chamber headspace, the investigator is altering the gas composition within the chamber with implications for pressure within the chamber and the diffusion gradient.

Addition of a vent to chambers allows pressure equalisation with the atmosphere outside the chamber which reduces errors in the flux measurements from static chambers; the effectiveness of this varies depending on the porosity of the soil and speed of the wind passing over the chamber (Conen & Smith, 1998). Christiansen *et al.* (2011) confirm that a vent is required to avoid an overestimation in methane flux caused by disturbance when placing a chamber. However, poorly designed vents used to equalise internal and external pressure are known to cause overestimation of fluxes in windy conditions due to the Venturi effect (Davidson *et al.*, 2002), though such issues have now been largely addressed by improvements in vent design (Xu *et al.*, 2006).

One of the stated advantages of cover boxes is the reduced cost of the equipment, in comparison to that of automated chambers (Heinemeyer & McNamara, 2011), with typical unit costs of £10 and £5000 for manual and automatic units, respectively. However, such figures ignore the associated costs of manual sampling, which may be considerable. Automated dynamic chamber systems sample and store data continuously in large quantities, which only need to be downloaded relatively infrequently with consequent reductions in staff time costs; for equivalent manual measurements there are considerable staff time and travel & subsistence costs. Additional to the field costs associated with manual sampling are the staff and equipment costs associated with the subsequent laboratory analyses.

More importantly, frequently taken flux measurements will yield a more accurate flux estimate and automatic sampling always carries this advantage, whilst also avoiding time-based bias. When sampling manually, there is a tendency to sample during the daytime (Heinemeyer *et al.*, 2011) and this very strong bias towards day measurements is obvious from the refereed literature. For example, from the 40 refereed papers involving long-term manual cover box approaches resulting from a Web of Knowledge search, none reported any night time sampling of trace gases. Flux estimates based solely on measurements taken during daylight hours contain an inevitable bias and are open to criticism. Whilst work has been done to ascertain the most suitable time to sample to avoid bias (e.g. de Klein & Harvey, 2012), certain assumptions are made, chiefly that GHG fluxes are governed by soil temperature.

Dynamic chambers have many of the same benefits and problems associated with static chambers but sampling is non-destructive, and does not alter the physical composition of the headspace gas or cause step-wise alterations in the internal chamber pressure due to the removal of gas (Brummell & Siciliano, 2011). However, dynamic systems require a power source to maintain a flow of air through the chambers, and are more physically constrained because of the necessary sampling and inlet lines. They also require accurate flow control and monitoring, combined with continual analysis of the concentration of gas in the inlet stream. In comparisons of chamber-based techniques for CO_2 flux measurement, dynamic chambers have been shown to have a smaller variation in accuracy than static chambers (Pumpanen *et al.*, 2004) and the higher frequency of measurements per chamber closure provides a more reliable method of producing a regression (Heinemeyer & McNamara, 2011).

When chambers are automated they can provide near-continuous data for gas fluxes, and can be left in the field for weeks or months. This generates data appropriate for detecting and understanding temporal variation of fluxes which manual sampling may miss. However, depending on design, automated chambers may still not provide an entirely accurate estimate of flux (Yao *et al.*, 2009a, Yao *et al.*, 2009b) and a problem which Yao *et al.* (2009a) highlighted, and led to underestimated N_2O and CO_2 fluxes, was due to the chambers being extensively closed throughout their study, excluding precipitation from landing on the soil under the chamber. Additionally, their study also showed that the manual static chambers probably overestimated fluxes due to the lack of temporal resolution, in direct contrast with other studies (Norman *et al.*, 1997), some of whom attributed the underestimation to pressure artefacts (Davidson *et al.*, 2002, Pumpanen *et al.*, 2004) or development of modified diffusion gradients (Heinemeyer & McNamara, 2011). Automated chambers that only close for the period of measurement should be used where possible, avoiding problems that arise from isolating the soil from normal ambient conditions.

The relative merits of automated chambers versus manual coverboxes vary depending on the trace gas of interest. Whilst continuous measurements are the ideal for all three GHGs, it may not be achievable or cost effective and this is of particular importance if more than one site is to be studied. Automated portable CO_2 systems are so readily available that the savings on equipment made by using coverboxes are not justifiable in respect of the quality of the data they produce. For CH_4 and N_2O the situation is different. The analytical equipment needed to measure these in real-time with chambers is either ill-equipped for transportation, prohibitively expensive or both,

though in the last couple of years, steps have been made in the development of portable CH_4 analysers (e.g. the 15 kg UGGA, Los Gatos Research, CA USA). The flexibility required to sample multiple sites may not be provided by such equipment. Because they can be used to obtain gas samples for *post hoc* analysis, coverboxes can therefore provide an extremely effective way of obtaining flux data for N_2O and CH_4 to complement CO_2 data obtained from automated chamber systems (Norman *et al.*, 1997).

Perhaps the greatest shortcoming of chamber methods for measuring trace gas fluxes is their inability to capture vegetation fluxes. The size of commercial chambers (such as the Licor 8100-103) prevents measuring fluxes from all but very short vegetation: in fact the newest revision of Licor's long term chambers, which uses a lateral closing motion as opposed to an 'over the top' mechanism, further reduces the capacity to measure from anything but the very shortest vegetation. Whilst these systems are extremely effective for measuring fluxes between the soil-air interface, vegetation may be an extremely important component for CO_2, N_2O and CH_4 (ButterbachBahl *et al.*, 1997, Pihlatie *et al.*, 2005, Rusch & Rennenberg, 1998). Whilst larger bespoke chambers have been developed, the tendency is for them to be left *in situ* throughout a study, with resulting micro-environment changes (Mordacq *et al.*, 1991, Pape *et al.*, 2009).

Altering the micro-climate within a chamber is an issue inherent to all chamber based methodologies. Temperature increases within a closed chamber can be as large as 20^{o}C, and to avoid this, opaque insulated chambers are recommended for CH_4 (Butterbach-Bahl *et al.*, 2011) and N_2O measurements (Rochette & Eriksen-Hamel, 2008). These, however, are not suitable for long term deployment over vegetation, and will not accurately reflect day time CO_2 exchanges, as they prevent photosynthesis. Clear chambers allow photosynthesis to continue but are more prone to temperature increase. To reduce this, the period over which measurements are taken, and chambers are closed, should be kept as short as possible. Tall automated chambers such as those developed by Pape *et al.* (2009) have a lid that remains open except when measurements are taken, though the high-sided design of them still isolates the soil and vegetation within from ambient conditions. Whilst these concerns are of lesser importance in comparative studies, where all treatments are exposed to the same conditions, the same cannot be said when these data are needed for accurate flux budgets (Rochette & Eriksen-Hamel, 2008). When data are used for

this purpose, it is vital that they reflect as accurately as possible the fluxes under naturally occurring conditions.

1.3.2 Eddy covariance

A major advantage of EC systems over chamber measurements is the minimal alteration of the landscape that is being studied. This means that the data delivered are free from many of the biases inherent in chamber measurements and it is an increasingly popular method for obtaining non-invasive, high frequency flux data. Sampling is achieved by measuring the gas concentrations of the ambient atmosphere, quantifying the *in vivo* fluxes at the landscape scale. This puts such techniques at an advantage to chamber-based studies when calculating large-scale fluxes. Continuous data from high frequency analysers provide high temporal flux data, ensuring that short-term emissions after occurrences such as rainfall are not missed as might be the case using discrete sampling methods. Another major advantage of the EC system is that the gases that can be analysed are only limited by the availability of appropriate high frequency (*ca.* 10 Hz) analytical equipment and not by sample size. Due to the nature of that equipment, typically IRGAs and tunable diode lasers, the fluxes are calculated in near real-time in the field.

Eddy systems, however, are not suitable for use everywhere. Baldocchi (2003) outlines three major restrictions on their effectiveness: the terrain being measured must be flat; stable environmental conditions are necessary; the underlying vegetation needs to stretch “upwind for an extended distance”. The loss of accuracy when these conditions are breached seriously limits the locations where this technology to be deployed. The flux footprint (i.e. the area which an eddy system can measure) is normally at the scale of thousands of square metres, and this increases with tower height (Schmid, 1994). This lends the technology to measurement of fluxes of whole ecosystems and also means that the EC technique cannot provide high spatial resolution; clearly, EC is not really suited for trace gas flux quantification in experimental contrasts. Replication is hard to achieve with flux towers, due to the scale over which they are deployed, with the size of the equipment being prohibitive; towers in excess of 1.5 m cannot be erected indiscriminately. Recent developments in laser technologies now mean that EC for CO_2 and CH_4 are becoming routine but N_2O still remains a challenge for EC, but has been successfully deployed; the new generation of CRD lasers for the routine high frequency analyses of N_2O will revolutionise EC approaches for this gas.

The variations on EC, namely REA and DEC systems, are subject to the same limitations with regards to suitability of location and scale of spatial resolution. The temporal resolution of these is several orders of magnitude less than can be achieved with high frequency analysers. Despite this EC and REA have been shown to give similar flux estimates (Oncley *et al.*, 1993, Pryor *et al.*, 2008), and when discrepancies were found by Oncley *et al.* (1993), these were be attributed to the IRGA malfunctioning. DEC has also been shown to give similar flux estimates to EC, and has been successfully used with a range of trace gases (Turnipseed *et al.*, 2009).

The limitations of EC are not confined to the detection equipment and site topography. In their critique of EC, Loescher *et al.* (2006) list several additional sources of potential error which are inherent to the application of the theory behind the method. These include stratification of the boundary layer during the night time, periods of low turbulence that prevent flux measurement and vertical and horizontal advection which cause underestimation of fluxes. Each of these can cause gaps in the collected data and the methods for filling these gaps are also prone to error. Furthermore, where data are collected from night time measurements, they lose temporal resolution as the time period over which fluxes are estimated increases to as much as twelve hours (Loescher *et al.*, 2006).

1.3.3 Gradient methods

As a micrometeorological technique, like EC, above ground gradient sampling is limited in where it can be used. It has the same requirements for fetch and homogeneity as EC and, therefore, is not suitable for experimental plots or replication (Denmead, 2008). It has also been shown to give lower flux calculations than those obtained from chamber-based studies (Smith *et al.*, 1994). The temporal resolution of the flux data from this method is, as with other methods, controlled by the apparatus used for measuring the gas concentrations. This also governs the power requirement of the equipment which also restricts the technique's suitability to specific locations. This technique shares many of the advantages of EC, such as providing data over large areas, in long-term deployment, and it is non-invasive and the approach can also be used to sample for multiple gases. However, the requirement for measurements to be taken from multiple heights either prevents synchronous sampling or can introduce sources of error.

The above methods are used to measure fluxes from above the soil surface. This may include exchange from vegetation, or just from the soil air interface. Soil gas probes, however, allow measurements from an added dimension below the soil surface. This gives an additional layer of spatial resolution that is useful for investigating gas-evolving processes within the soil profile. As they are relatively small, it is possible to have replicates and to use them in manipulation experiments. They may be used to collect long-term fluxes, and the temporal resolution is dictated by the equipment used to measure gas concentrations, thus the relative merits in this respect are identical to those of automated and manual chambers. As a rather low-tech piece of equipment, individual probes are not expensive. Once again, though, the extra costs inherent in the sampling method used need to be accounted for, such as man-hours, travel and analysis apparatus.

Installation of probes is, however, an invasive process. Whether probes are driven in vertically through the soil column (Brummell & Siciliano, 2011) or horizontally into the face of an excavated pit face (Kammann *et al.*, 2001a), the disruption to the soil is unavoidable. Either method will cause root death, which affects fluxes as shown with collar insertion for chambers (Heinemeyer *et al.*, 2011, Mills *et al.*, 2011), and whilst in long-term studies root growth will recover, this factor should be considered if data are collected soon after the probes are inserted. Probes that are designed with holes in them face limitations as to where they can be used. In soils that are prone to water logging or have a high water table, the holes allow water to enter the internal space and prevent effectiveness. Furthermore, over a study period of months, soil particles may pass into the probe or block the holes, thereby preventing diffusion of gas into the probe (Fang & Moncrieff, 1998). The problems of blockage and water are negated by the use of sealed probes which separate the gas phase from the solid and liquid phases in the soil (Kammann *et al.*, 2001a). Silicone and other polymers used for these probes will support the growth of microbial biofilms (Dupin & McCarty, 1999), and these may have a direct effect on trace gas flux, especially CH_4 (Clapp *et al.*, 2004). Furthermore, growth of microbes on other polymers used for gas-permeable membranes such as polyethylene can cause them to degrade (Albertsson *et al.*, 1987).

1.3.4 Box method

This method is designed to bridge the gap in the spatial area that is able to be measured by chambers and micrometeorological methods. The ability to measure

fluxes from areas that are on the scale of tens of square metres is especially attractive as it allows for replication and treatments to be applied, but involves non-destructive sampling and is not dependent upon wind direction (Denmead *et al.*, 1998). However, Denmead *et al.* (1998) also highlight several flaws in the design of the technique, including the number of samples required to calculate the flux, which increases the source of error, and that it is inaccurate when measuring at low wind speeds. However, the results gained from mass balance studies are closer to those of models than the results from chamber measurements, which led Park *et al.* (2010) to conclude that it is the more accurate method.

1.3.5 Satellite-based measurements

These techniques are the best equipped to large-scale measurements and deliver column gas concentration and not flux, which has to be derived from some form of 'back-projection' modelling. Depending on whether the satellite platform is in a geostationary equatorial orbit or low earth orbit determines whether the equipment will be measuring a small area at high temporal resolution (i.e. every 10-15 minutes) (Thies & Bendix, 2011) or the whole globe over a period of days (Frankenberg *et al.*, 2005). Satellites are designed for long-term deployment and are capable of providing continuous data sets over many years. However, there have been problems with the longevity of the sensing equipment and in making appropriate post-capture corrections (Thies & Bendix, 2011). Maintenance of such equipment is hindered greatly by location and the equipment is very expensive to design, build and deploy into space, which severely restricts the availability of this technology. At present, the spatial resolution of such satellite imagery is poor - typically hundreds of km^2 - but will inevitably improve with time.

1.4 Summary

It is clear that no single existing technology for trace gas measurement satisfies all the desired qualities to a high degree (Table 1.1). Where some methods produce high frequency data, they are expensive and do not resolve spatially to the plot scale (e.g. EC). Lower cost methods such as manual chambers are an effective way of measuring multiple gases simultaneously to obtain comparisons between experimental contrasts, but they are labour intensive, yield low frequency data and there are issues in scaling up from the small scale to landscape values. Automation is the key to providing high frequency data, and in order to measure NEE, which is the key value to consider in terms of GHG balance, then a system which measures from both soil and vegetation is required to achieve this goal.

In this thesis, two novel automated chamber systems are presented, which are capable of measuring over vegetation (in one case from *Miscanthus*, which grows to heights in excess of 3 m), and can deliver the NEE of the three most important biogenic GHGs. The flexibility offered by a chamber based system has been utilised to investigate the effects of experimental manipulations, and the near-continuous data generated may shed light on previously unreported patterns in trace gas fluxes.

Table 1.1 Qualitative valuation of methods for trace gas flux measurements. Techniques are given a star rating from 1-5 depending on their performance in each category where 1 star = lowest and 5 stars = highest.

Method	Cost[1]	Area[2]	Spatial definition[3]	Sampling frequency[4]	Precision[5]	Accuracy[6]	Power requirement[7]
CHAMBERS							
Manual Static	★	★★	★★★★	★★	★★★★	★★	★
Automatic Static	★★★	★★	★★★★	★★★★	★★★★★	★★★	★★★
Automatic Dynamic	★★★	★★	★★★★	★★★★	★★★★★	★★★★	★★★
EDDY SYSTEMS							
Eddy covariance	★★★★	★★★★	★★	★★★★★	★★★★★	★★★★	★★★★★
Relaxed Eddy Acccumulation	★★★	★★★★	★★	★★★	★★★★	★★★	★★★
Disjunct Eddy Covariance	★★★★	★★★★	★★	★★★★	★★★★★	★★★★★	★★★★★
GRADIENT SYSTEMS							
Flux gradient method	★★★★	★★★★★	★★	★★★★★	★★★★★	★★	★★★★★
Soil gas probes	★★	★★	★★★	★★	★★★★	★★★★	★★★
Satellite SCIAMACHY	★★★★★	★★★★★	★	★★★★★	★★★★★	★★★★	★★★★★
Box Method	★★★★	★★★	★★★	★★★	★★★	★★★★	★★★

Table 1.1 breakdown of headings: 1. Cost. Covers the cost of equipment. **2.** Area: the scale over which a technique can quantify fluxes.**3.** Spatial definition. How sensitive a technique is, i.e. how good the spatial resolution is. **4.** Sampling frequency. How often measurements are taken, ranging from high (10 Hz) to low (days- weeks). **5.** Precision. The ability of a technique to produce repeatable results. **6.** Accuracy. How close to the actual flux that the estimate calculated is. **7.** Power requirement. This refers to the need for electrical power in the field.

1.5 Aims and hypotheses

Several broad aims were addressed during the course of this project:

- To develop a novel automated chamber system to deliver high frequency GHG flux data at a fine spatial scale from the large bioenergy crop *Miscanthus x giganteus*. It must be able to measure net ecosystem exchange of the three most important biogenic GHGs, CO_2, CH_4 and N_2O.
- To expand the development of a low cost automated chamber system for flexible deployment in more conventional crops, providing high frequency and fine spatial resolution with the capacity for more than 20 replicates.
- To compare in-field GHG fluxes from a bioenergy crop, *Miscanthus x giganteus*, to conventional arable crops.
- To investigate the drivers of GHG fluxes across a variety of agricultural systems.

The primary specific hypotheses investigated experimentally whilst completing the above objectives were:

1. GHG fluxes would be significantly higher from the soil under conventional cropping than under *Miscanthus x giganteus*.
2. There would be a significant difference between cumulative soil CO_2 flux from an arable crop measured on a monthly and a sub-daily frequency.
3. GHG flux, in particular N_2O emissions, would be greater from *Miscanthus x giganteus* treated with green waste compost than from untreated controls.
4. N_2O emissions from oilseed rape would significantly differ between mineral nitrogen forms applied to the crop (NH_4 and NO_3), and that applying double the nitrogen as NH_4NO_3 would significantly increase N_2O emissions.

Further emergent hypotheses were investigated based upon observations made during the course of experimentation, and on opportunities available through collaboration. These included **i** NEE of CO_2 from *Miscanthus* measured using EC and large a large clear automated chamber would not significantly differ **ii** there would be no significant difference between fluxes of N_2O measured using manual static chambers and a novel automated chamber system **iii** sunlight is a key driver of N_2O emission from soil under oilseed rape. The outlined aims and hypotheses were

undertaken across three experimental field campaigns, and are described in the following chapters.

2 A comparison of trace gas fluxes from soil under a bioenergy crop and a conventional arable crop system

2.1 Introduction

Global atmospheric carbon dioxide (CO_2) levels have exceeded 400 parts per million (ppm), constituting a rise of 120 ppm from pre-industrial levels (see Tjiputra *et al.*, 2014). This increase is largely attributed to emissions from the combustion of fossil fuels for the generation of energy. Carbon dioxide, amongst other greenhouse gases (GHGs), has properties which cause the atmosphere to warm, with warming resulting from human activity referred to as anthropogenic climate change. It is a widely-held opinion that a rise of more than 2 ^{o}C will have hugely detrimental effects on the global biosphere, and in order to remain within this 2 ^{o}C target, atmospheric CO_2 should not exceed 500 ppm (IPCC, 2014). The optimal way of achieving this, in the absence of efficient technology for the removal of CO_2 from the atmosphere (Boot-Handford *et al.*, 2014), is to drastically reduce emissions (Smith *et al.*, 2014). The United Kingdom has pledged to reduce CO_2 emissions to below 1990 levels by 2030, in part by ensuring 15 % of the nation's energy requirements are met by so-called renewable sources by 2020 (DECC, 2011). Bioenergy, or energy derived directly from biomass, has been identified as one route through which these reductions can be realised (DECC, 2011).

Bioenergy crops are those grown specifically to provide a feedstock for energy production, whether from processing for production of liquid transportation fuels or for direct combustion in power plants. The fundamental attraction of bioenergy crops with regard to GHG balance is that they are considered a "carbon-neutral" alternative to fossil fuel-derived energy (Clifton-Brown *et al.*, 2004). This neutrality is predicated upon the direct carbon emissions from the combustion of biomass being in equilibrium with the carbon sequestered during photosynthesis. The growing phase of bioenergy crops can result in a net uptake of CO_2 from photosynthesis (Cadoux *et al.*, 2014), and for this reason, fast growing woody species such as poplar (*Populus* spp.) and willow (*Salix* spp.) are increasingly being used as bioenergy crops, as well as perennial grasses such as switchgrass (*Panicum virgatum*) and *Miscanthus* (*Miscanthus x giganteus*) (Lewandowski *et al.*, 2000, van der Weijde *et al.*, 2013). Such non-food crops are referred to as second generation energy crops. Additional

carbon may be sequestered in the soil through the growth of plant root tissues and litter fall from senescing plants (Clifton-Brown *et al.*, 2007, Don *et al.*, 2012).

Further gains in terms of GHG balance have been modelled as a result of converting conventional tilled arable land to *Miscanthus*, with half of this gain being made from reduced N_2O emissions due to lower nitrogenous fertiliser application (St Clair *et al.*, 2008). *Miscanthus* has a low nitrogen requirement (van der Weijde *et al.*, 2013), possibly because it increases nitrogen mineralisation rates in the soil (Davis *et al.*, 2013) and recycles nitrogen very efficiently when left to senesce over winter (Strullu *et al.*, 2011). It has been suggested that *Miscanthus* may play a role in nitrogen fixation (Davis *et al.*, 2010, Keymer & Kent, 2014). However, previous land use must be considered; for example, converting pasture to short rotation forestry (SRF) can increase N_2O emissions (Palmer *et al.*, 2014). Additionally it has been estimated that the carbon benefits of energy derived from first generation energy crops such as corn (*Zea mays*) would be undermined in totality by the fertiliser-driven N_2O during growth (Crutzen *et al.*, 2008).

In addition to the emission of CO_2 from respiration, soil can be both a source and sink of the biogenic GHGs methane (CH_4) and nitrous oxide (N_2O). These two important gases are, mole for mole, 34 and 298 times more potent in terms of global warming potential (GWP) than CO_2 (Myhre, 2013). CH_4 production occurs in wetter soils in anaerobic conditions and is consumed through oxidation by methanotrophic microbes in aerated soil (Bradford *et al.*, 2001). The largest natural sources of CH_4 are wetlands and peat uplands (Ciais, 2013, McNamara *et al.*, 2008), whereas forest and agricultural soils are commonly strongly oxidising (Bradford *et al.*, 2001, Flessa *et al.*, 1998). By far the biggest contribution to soil N_2O results comes from the application of nitrogenous fertiliser to agricultural soil (Myhre, 2013). Processes governing N_2O are complex and our knowledge of them is continually growing (Butterbach-Bahl *et al.*, 2013), but broadly speaking two processes are responsible for its generation. N_2O is produced as a by-product of ammonium (NH_4) oxidisation through nitrification and as a product of nitrate (NO_3) reduction during denitrification (Firestone & Davidson, 1989). Negative fluxes have been shown to occur and are commonly attributed to further reduction of N_2O to dinitrogen gas (N_2) which requires anoxic conditions (Chapuis-Lardy *et al.*, 2007). N_2O consumption is rather enigmatic, and has also been reported in dry, well aerated soils (Chapuis-Lardy *et al.*, 2007). In order to accurately assess the GHG balance of bioenergy production full life cycle analyses (LCA) must be undertaken, quantifying the emissions or uptake of trace gases at every stage of

their production, including the intrinsic emissions associated with fertiliser production, harvest and transportation of biomass and subsequent downstream processing (Cherubini *et al.*, 2009). A full LCA is beyond the scope of this study, which ends at 'the farm gate', but equally essential is the quantification of the trace gas fluxes from the soils during the cultivation of these crops.

Chamber-based methods are commonly used for measuring trace gas fluxes from soils, and, placed on the soil surface, they measure the change in concentration of the gases of interest in a known enclosed volume over time, typically 1-2 hours for N_2O and CH_4, less for CO_2. Situating chambers throughout a landscape enables a representative estimate of flux to be gathered at a high spatial resolution. Manual chambers are a low-cost method which allow an experimenter to measure many replicates concurrently with no requirement for power (Heinemeyer & McNamara, 2011), which makes them appropriate for field work in remote locations (Brummell & Siciliano, 2011). However, due to the high demand for manpower, they tend to be measured on a weekly or monthly basis (Drewer *et al.*, 2012, Guckland *et al.*, 2010, Toma *et al.*, 2011, von Arnold *et al.*, 2005). Automated chambers increase the temporal resolution of measurements, but their power requirement and higher cost means they are less commonly used. Commercial automated systems are available to buy for CO_2 flux measurement, but equivalent systems for CH_4 and N_2O fluxes are not commonly available, but may be constructed by adapting CO_2 systems with the addition of supplementary analysers. For a detailed description and evaluation of various chamber techniques see Chapter 1.

Methodological comparisons of trace gas fluxes measured using manual chambers and near-continuous systems (e.g. eddy covariance and automated chambers) can be split into two categories: those which focus on absolute values of point measurements (Ambus & Robertson, 1998, Heinemeyer & McNamara, 2011, Matsuura *et al.*, 2011) and those investigating the effect on cumulative estimated fluxes over time as a consequence of measurement frequency (Burrows *et al.*, 2005, Laville *et al.*, 1997, van der Weerden *et al.*, 2013, Yao *et al.*, 2009a, Yu *et al.*, 2013b). All of the latter, however, compare the methodologies within a single land use or vegetation type, and it is generally accepted that by making daily, weekly or monthly manual measurements simultaneously from multiple experimental treatments or land uses, a valid comparison of GHG fluxes can be made. It is more questionable whether the long-term estimate of flux from such discrete measurements is reliable. A comparison of the frequency at which measurements are made, from two land uses

under the same physical conditions, and the effect of estimated cumulative flux over long periods of time will therefore be of value in terms of knowing how reliable GHG budgets based upon manual sampling regimes actually are. Such a comparison would also provide to a comparison of automated and manual systems, due to the difference in measurement frequency employed by the different methods.

In the current study, soil GHG measurements were made with manual static chambers on a monthly basis from two adjacent fields, one of which was used to cultivate the bioenergy crop *Miscanthus*, the other being used for conventional arable crop production, over the course of 18 months. The total flux of CO_2, N_2O and CH_4 was calculated from these data to test the hypothesis that the total soil GHG flux would be significantly lower from the field in which *Miscanthus* was grown.

Automated soil CO_2 chambers were deployed for the entirety of the study in the *Miscanthus* field, and for a period of four months in the arable field, during which time spring barley (*Hordeum vulgare*) was grown. These measurements allowed a comparison of the total soil CO_2 flux calculated using both monthly and continuous data to be made. Both the manual and automated CO_2 measurements were made using the same infrared gas analyser (IRGA) and measured the exact same positions in the crops.

2.2 Methods and materials

2.2.1 Site

The study site was a working farm, on which both perennial crops used for bioenergy production (willow (*Salix* spp.) and *Miscanthus*) and combinations of conventional arable crops, namely wheat (*Triticum aestivum*), barley (*Hordeum vulgare*) and oilseed rape (OSR; *Brassica napus*) in a rotation, were grown. Short rotation coppice (SRC) willow is harvested every three years, but *Miscanthus* is harvested annually, in the spring.

Two adjacent (on a north-south orientation) fields under different cropping strategies were chosen to compare the different trace gas fluxes associated with arable crop and *Miscanthus* production. The *Miscanthus* field used in this study had been established seven years prior to the start of measurements; the two most recent rotations in the arable field had been winter wheat and OSR, respectively. At the start of this study in September 2012, the field had been too wet to plough and so was left fallow until it was drilled with spring barley in April 2013. The barley was harvested in September 2013 and the subsequent crop of OSR was sown almost immediately. The two previous arable rotations had received approximately 200 kg-N fertiliser ha^{-1} per annum, and 179 kg-N ha^{-1} was applied to the barley as ammonium nitrate in three doses between the end of April and the beginning of June 2013. Chamber bases were left *in situ* during the applications, in the understanding that even application would be achieved by the agricultural machinery.

Unusually for *Miscanthus*, the field was tilled in April 2013, following a disappointing harvest of ca 7.5 tonnes ha^{-1} in the previous year. The tillage was undertaken in an attempt to spread the rhizomes more evenly and thus increase yield.

Due to the nature of the crop production in the arable field, this study was divided into three Campaigns: Campaign 1 covers the period the arable field was left fallow, Campaign 2 the period during which barley was grown and Campaign 3 covered the first months of OSR production until the harvest of *Miscanthus* in spring 2014.

2.2.2 Trace gas flux measurements

2.2.2.1 Monthly measurements

Measurements of CO_2, CH_4 and N_2O flux were made on approximately a monthly basis starting in October 2012. CH_4 and N_2O fluxes were measured using the manual static chamber technique and a Licor survey chamber (LI- 8100-103, Licor. Lincoln NE) attached to an infrared gas analyser (LI-8100 IRGA, Licor, Lincoln NE) was used to measure soil CO_2 flux. Both types of chamber used the same collars (opaque polyvinyl chloride (PVC), diameter 20 cm, height 10 cm) which were inserted into the soil to a depth of approximately 2 cm at the start of each Campaign and left in place so that the same positions were measured throughout the Campaign. The collars in the *Miscanthus* were, throughout the entire study period, shared with automated chambers which measured soil CO_2 flux on a near-hourly basis in between the monthly schedule. In Campaign 2 automated chambers were also deployed in the arable crop, and these also shared the collars with the manual chambers. Where necessary a good seal with the surrounding soil was achieved by putting fine building sand around the base of the collars. Collars were distributed at random within the area within which the automated chamber system could function (limited to ca 160 m^2 due to the length of the gas lines), and during Campaigns 2 and 3 the *Miscanthus* collars were arranged within the plots of a controlled compost addition experiment (see Chapter 3). Collars were kept free of aboveground biomass, but did not exclude roots.

Soil CO_2 fluxes measured with the survey chamber and IRGA were calculated using the internal Licor software; the chamber closure was set to two minutes with a 30 second 'dead band' at the beginning of the measurement to allow for mixing of the headspace gas. The linear regression of the short-term changes in CO_2 concentration over time was used to provide the flux, and the software made the required adjustments for chamber volume, area and temperature.

Manual chambers were deployed immediately after the Licor survey chamber measurements. Manual chambers were made of the same cylindrical opaque PVC pipe as the surface collars, with a flat circular lid (height 24 cm, diameter 20 cm). To minimise internal heating the chambers were covered with an insulating layer of aluminium thermal foil and chambers were sealed onto the collars using a 5 cm wide rubber band. A septum through which gas samples were removed was formed using a Subaseal (SubaSeal No. 25, Sigma-Aldrich, St Louis, MO, USA) pushed into a 1

cm circular hole in the centre of the chamber lid. In order to minimise disturbance to the soil surrounding the collar, samples were taken through a 1.5 m length of vacuum tubing (Tygon Formulation R-3603 Tubing, Part number AAC00002, Saint-Gobain Performance Plastics, Akron, OH, USA) which passed through the septum. Samples were taken using 20 cm^3 plastic syringes and transferred to pre-evacuated 12 cm^3 vials (Exetainer 839W, Labco Ltd, High Wycombe, UK). Syringes were pumped three times prior to sampling in order to mix the chamber headspace and gas within the tubing. Chambers were closed for two hours and were sampled five times at 30 minute intervals (at 0, 30, 60, 90 and 120 minutes).

Concentrations of N_2O, CH_4 and CO_2 were determined by gas chromatograph (GC; PerkinElmer Instruments, Shelton, CT, USA) fitted with an electron capture detector (ECD) and a flame ionisation detector (FID) at the University of York, usually within a week of sampling. The overpressure of the sample vials enabled the flow of the gas through the equipment's autosampler, and the GC was calibrated using a reference gas (BOC Gases, Guildford, Surrey, UK) on average every 8 samples.

Fluxes were calculated as the change in concentration over time as determined by linear regression, and were adjusted for area, volume and temperature, which was measured at the time of sampling. Outliers were identified by calculating the studentised residual of each individual point of a regression, which is the ratio of the residual to the estimated error variance with that point removed from the regression, and a studentised residual greater than 2 indicates a point with undue influence on the regression (SAS 9.3, SAS Institute Inc., NC), thus any such point was excluded from the analysis.

2.2.2.2 Sub-daily measurements

Throughout the entire study period, soil CO_2 fluxes were measured from under the *Miscanthus* using an automated chamber system. Licor automated chambers (LI-8100-101, Licor, Lincoln NE) were attached to an IRGA via a multiplexer (Electronic workshops, Department of Biology, University of York, York UK); chambers were programmed to close according to the same protocol used for the monthly survey chamber measurements and fluxes were similarly calculated using the Licor software. Measurements cycled continuously between chambers, and chambers were placed over the exact same collars used for the monthly measurements.

During Campaign 1 eight chambers were deployed in the *Miscanthus* whilst six chambers were used during Campaigns 2 and 3, but were arranged with two chambers within each of three experimental plots. Therefore the fluxes from the two chambers within each plot were averaged prior to any statistical analyses for the latter two Campaigns. During Campaign 2, four chambers were deployed within the arable field, again deployed on the same collars used for monthly measurements.

2.2.3 Environmental variables

At the end of the two hour chamber closure for the monthly measurements, soil moisture within each collar was measured using a soil moisture sensor (SM200, Delta-T, Cambridge UK) attached to a multi-meter. The millivolts reading was converted to a volumetric soil moisture value *post hoc* using the formula for mineral soil provided in the Delta-T manual .

Air temperature was measured during chamber closures using a digital thermometer and soil temperature at 10 cm depth was also determined in each field. Throughout Campaign 2 soil moisture and temperature in both fields (and the *Miscanthus* for most of Campaign 3) were logged as hourly averages (SM200 moisture probes, ST1 soil temperature sensors; DL2 and GP1 loggers, Delta-T, Cambridge UK).

Meteorological data (air temperature, solar radiation, humidity) were measured and recorded on site using a weather station (WP1, Delta-T, Cambridge UK) and rainfall data for 2013 were provided by a research group from Centre for Ecology and Hydrology who were working at the same site. Hourly data were also retrieved from the Met Office station at Scampton, *ca.* two miles from the study site.

2.2.4 Data analysis

Automated chamber fluxes were calculated using the internal Licor software. Analysis of manual chamber measurements were performed using linear regression, and cumulative fluxes were calculated using trapezoidal integration in SAS (SAS 9.3, SAS Institute USA). Statistical analyses (e.g. analysis of variance, mixed effects models, t-tests) were all performed in SAS and graphs were produced using Sigmaplot (Sigmaplot 12.3, Systat software, IL USA) and SAS. Data were tested for normality and where necessary transformations (log and reciprocal) were performed.

2.3 Results

2.3.1 Monthly gas flux measurements

2.3.1.1 CO_2 fluxes

Soil CO_2 flux was characterised by lower values during the winter months, increasing through spring to peak in the summer (Figure 2.1). Fluxes from the arable field peaked in June 2013 at 892 ± 160 mg m^{-2} h^{-1} and slightly later, in July 2013, from the *Miscanthus* field at 817 ± 50 mg m^{-2} h^{-1}. There was a significant difference in CO_2 flux between the fields over the whole study period, $F_{[1,147]}$= 11.78, p< 0.0001; sampling date was also significant, $F_{[15,147]}$= 43.39, p<0.0001 and there was a significant interaction between sampling date and crop regime, $F_{[14,147]}$= 7.74, p< 0.0001.

The fluxes from the two fields differed during Campaign 1 $F_{[1,78]}$=43.21, p< 0.0001, approached significance in Campaign 2, $F_{[1,28]}$=3.00, p= 0.09 and were not different during Campaign 3, $F_{[1,28]}$= 1.02, p= 0.32 (see Figure 2.1). The fluxes were significantly higher in the arable field on every measurement day during the first Campaign. During this period the arable field was left fallow, and the fluxes were probably driven by the input of carbon from the decomposing roots and residue from the preceding wheat crop. There were higher CO_2 fluxes from the arable soil during Campaign 2 on the two measurement days following fertiliser application to the barley crop, and these days are mostly responsible for the larger cumulative fluxes from the arable field. Fluxes were similar from both crops in late July 2013, yet higher from the *Miscanthus* in August; at this point the *Miscanthus* was still growing whereas the barley was mature and almost ready for harvest. Fluxes were remarkably similar from both fields throughout Campaign 3, with the exception of higher fluxes from *Miscanthus* in December 2013, as the fluxes declined through winter.

The total CO_2 flux was higher from the arable field in Campaign 1: 390 ± 55 g m^{-2} compared to 110 ± 17 g m^{-2}, $t_{[22]}$= 4.87, p<0.001. In Campaign 2 the total flux from the arable field (930 ± 130 g m^{-2}) was nearly twice as large as that from the *Miscanthus* (460 ± 28 g m^{-2}), $t_{[7]}$= 2.48, p<0.05, but there was no difference in the total CO_2 flux between the fields during Campaign 3, when the OSR was developing (arable 750 ± 120 g m^{-2}, *Miscanthus* 930 ± 140 g m^{-2}), $t_{[7]}$= -0.92, p> 0.3.

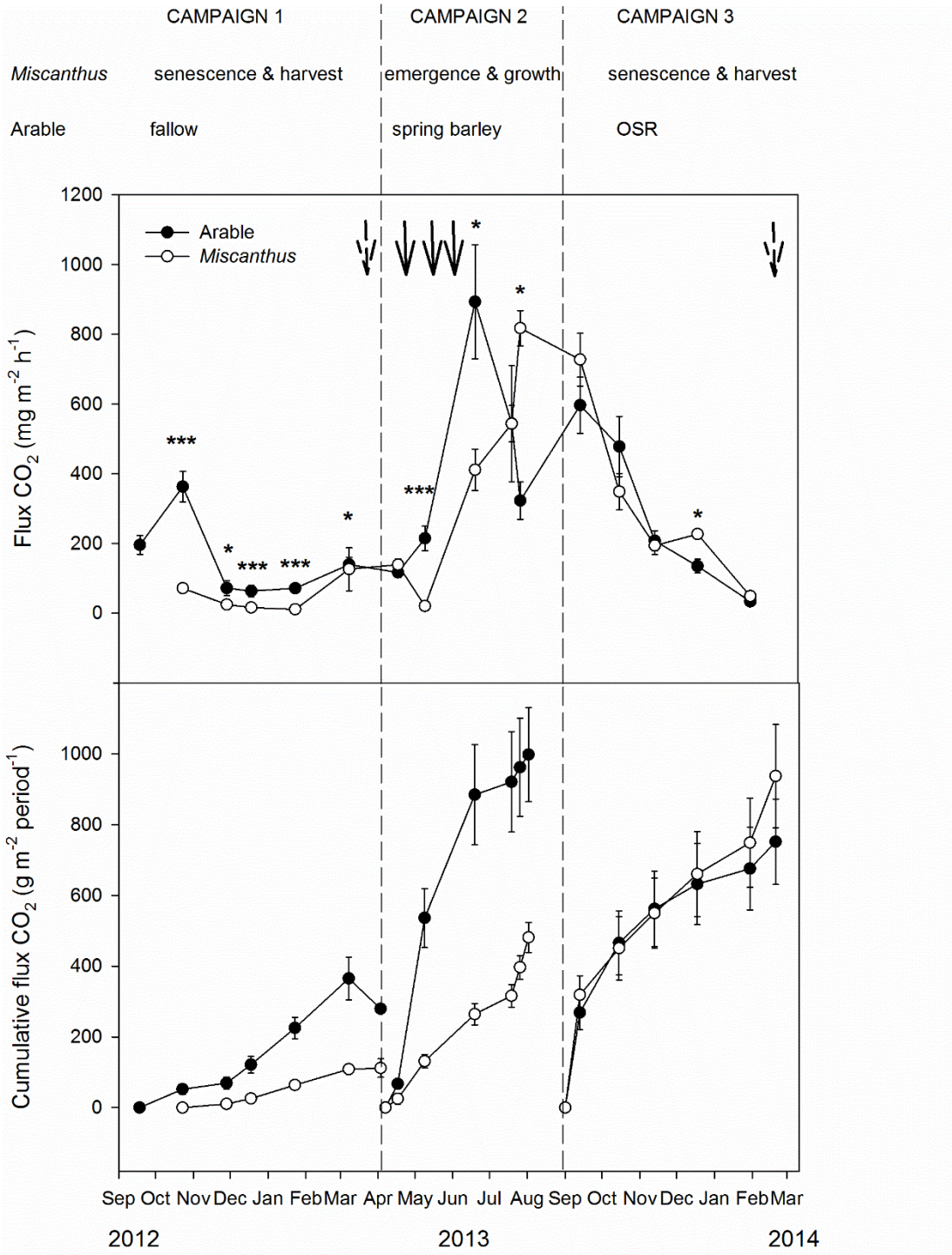

Figure 2.1 Mean flux (top panel) and cumulative flux (bottom panel) ± 1SE of soil CO_2 flux measured using a Licor survey chamber and IRGA, from fields under an energy crop and adjacent arable crop. Dashed vertical lines separate 'Campaigns' where the practices in the arable were fallow, spring barley and OSR respectively. Solid arrows indicate N fertiliser application to the arable crop and dashed arrows indicate the timing of *Miscanthus* harvest. Significant differences in flux are indicated: * p<0.05, ** p<0.01, *** p<0.001.

2.3.1.2 N_2O fluxes

Soil N_2O fluxes from the arable field exhibited three distinct peaks in March (127 ± 35 µg m^{-2} h^{-1}), June (307 ± 42 µg m^{-2} h^{-1}) and July (258± 67 µg m^{-2} h^{-1}) 2013 (Figure 2.2). In contrast N_2O fluxes were close to zero in the *Miscanthus*, with the highest value of 24 ± 1 µg m^{-2} h^{-1} seen in July 2013. N_2O flux was significantly higher from the arable field for the entire study period $F_{[1,76]}$= 11.6, p<0.02, and there was a significant effect of sampling date $F_{[17,76]}$= 4.95, p<0.001 and significant interaction between date and crop regime $F_{[25,76]}$= 2.36, p<0.009.

Fluxes were higher on two occasions during the fallow period in the arable field (Campaign 1), and on every day measurements were taken during Campaign 2 (Figure 2.2). Emissions of N_2O increased dramatically following fertiliser applications at the end of April 2013, but whilst there was a trend for higher fluxes from the arable during Campaign 3, there was no single day on which they were significantly different.

The total flux of N_2O was higher from the arable field in all three Campaigns. In Campaign 1 the total emissions from arable, 154 ± 45 mg m^{-2} were thirty times higher than those from the *Miscanthus*, 5 ± 2 mg m^{-2}, $t_{[22]}$= 4.3, p< 0.0001. In the second Campaign, emissions were much greater than the first Campaign, and the total flux from arable (413 ± 52 mg m^{-2}) was closer to forty times that from the *Miscanthus* (11 ± 2 mg m^{-2}), $t_{[7]}$= 5.04, p< 0.002. The third Campaign was typified by decreased emissions from the arable field, and the total flux of 102 ± 23 mg m^{-2} $period^{-1}$ was the lowest seen from this field. In contrast, Campaign 3 saw the highest total flux from the *Miscanthus*, although at 34 ± 2 mg m^{-2} it was still three times lower than the arable flux, $t_{[7]}$= 3.6, p< 0.009.

2.3.1.3 CH_4 fluxes

CH_4 fluxes were very low for most of the study period, and when they differed from zero they tended to be negative, indicating net uptake by the soil (Figure 2.3). The total flux from Campaigns 1 and 2 suggest that both systems were weak net sinks for CH_4. However, in Campaign 3 a peak in emission (217 ± 137 µg m^{-2} h^{-1}) during December 2013 from the *Miscanthus* shifted this field into a net source over the Campaign. On the same day the arable showed the largest negative flux for the entire study period (-176 ± 176 µg m^{-2} h^{-1}). Due to the large variation between chambers in both crops, there were no significant differences between fluxes on any measurement day, nor were there any significant differences in the total fluxes.

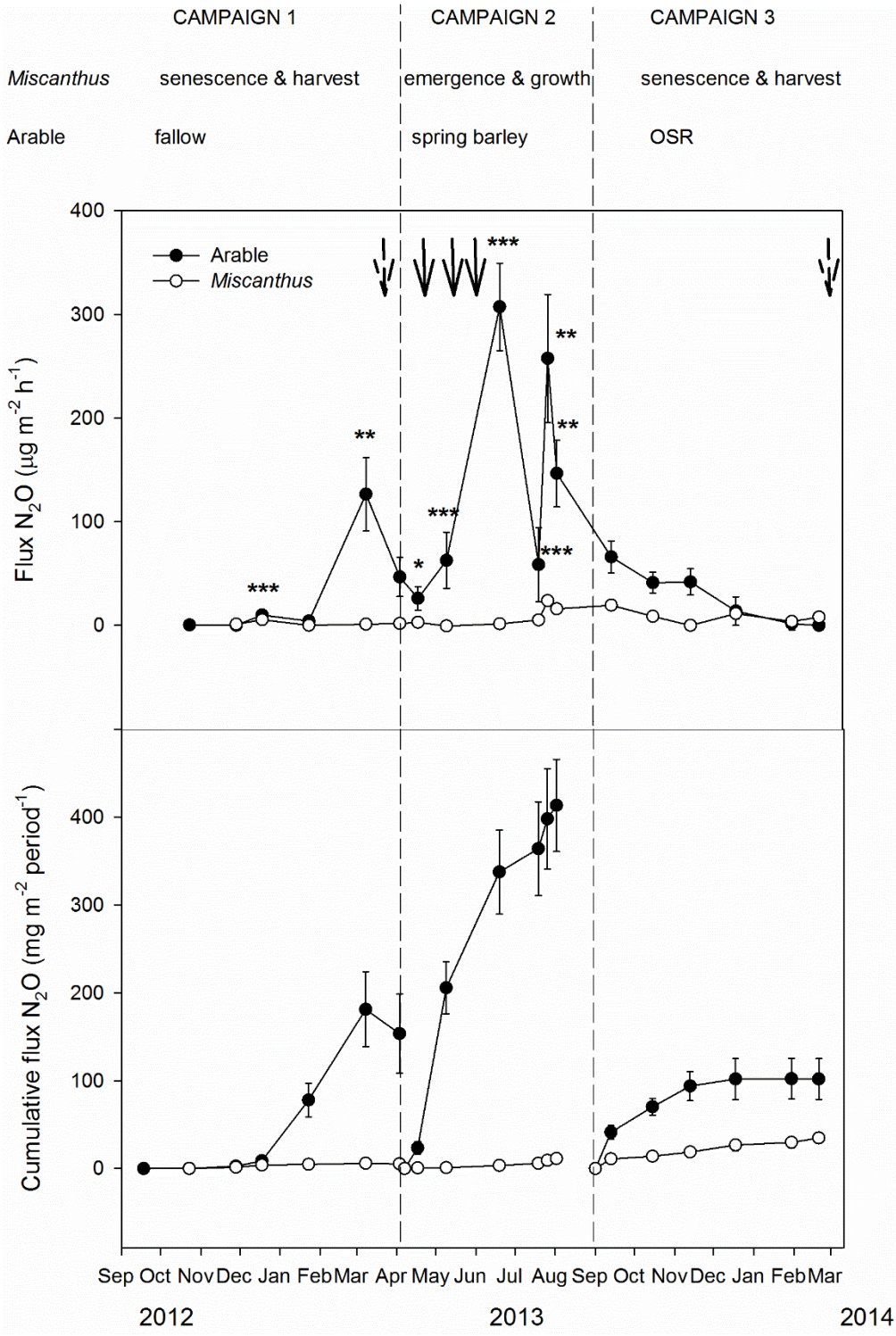

Figure 2.2 Mean flux N_2O and cumulative flux ± 1SE from an arable field and adjacent *Miscanthus* crop. Vertical dashed lines separate different Campaigns with different crops in the arable field. Significant differences between fluxes are shown: * $p<0.05$, ** $p<0.01$, *** $p<0.001$. Solid arrows show nitrogen fertiliser application to the arable and dashed arrows *Miscanthus* harvest.

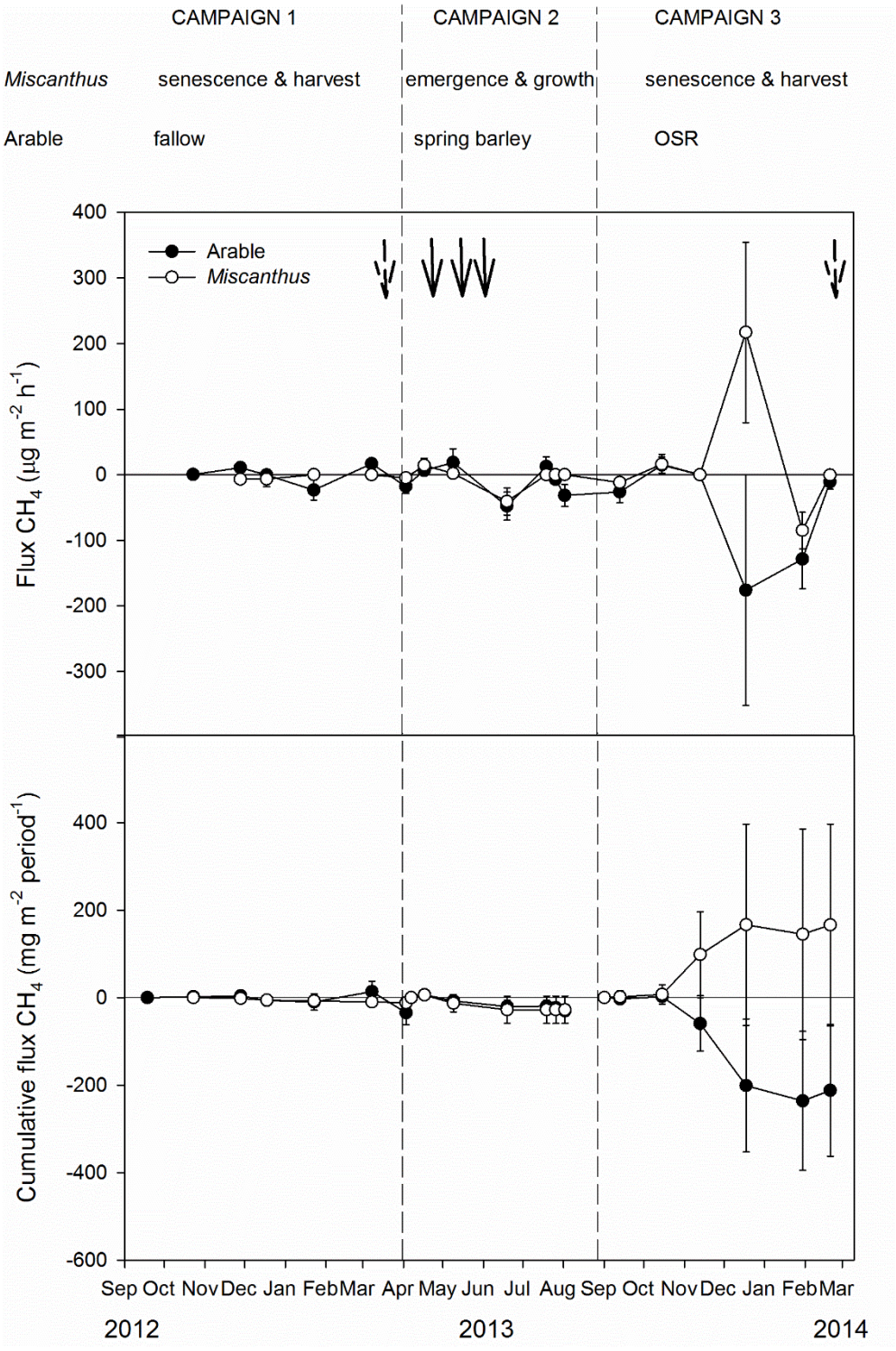

Figure 2.3 Mean flux CH_4 and cumulative flux ± 1SE from soil under arable and *Miscanthus* crops, measured using manual static chambers. Dashed vertical lines denote different crops in the arable field. Solid arrows represent timing of nitrogen fertiliser application to the arable crop and dashed arrows time of *Miscanthus* harvests.

2.3.2 GHG Balance

CO_2 was the largest contributor to the total GHG balance for both crops (Figure 2.4). In absolute terms Campaign 2 saw the greatest flux of GHGs of the whole study, produced from the arable field. The total N_2O flux of 123 g CO_2-eq m^{-2} for Campaign 1 was more than 10 % of the total soil respiration from that field during the same period (997 g CO_2-eq m^{-2}). Total N_2O flux from the arable field during Campaign 1 also represented a substantial proportion of the total soil GHG flux, which at 53 g CO_2-eq m^{-2} equated to 14 % of the CO_2 flux. In Campaign 3, the total N_2O flux of 30 g CO_2-eq m^{-2} was lower, amounting to just 4 % of the total CO_2 flux. As a proportion of total soil GHG flux, N_2O was lower from the *Miscanthus* field, however, and was the equivalent to just 1.4 %, 1.1 % and 0.9 % of the total CO_2 flux for Campaigns 1, 2 and 3. The contribution of CH_4 to the total flux of GHGs from both fields was negligible (Figure 2.4). It is important to emphasise that the fluxes measured in this study were from soil only and the total GHG flux presented is not the net ecosystem exchange, which, by accounting for CO_2 uptake by vegetation would greatly reduce, if not reverse, the total GHG emissions.

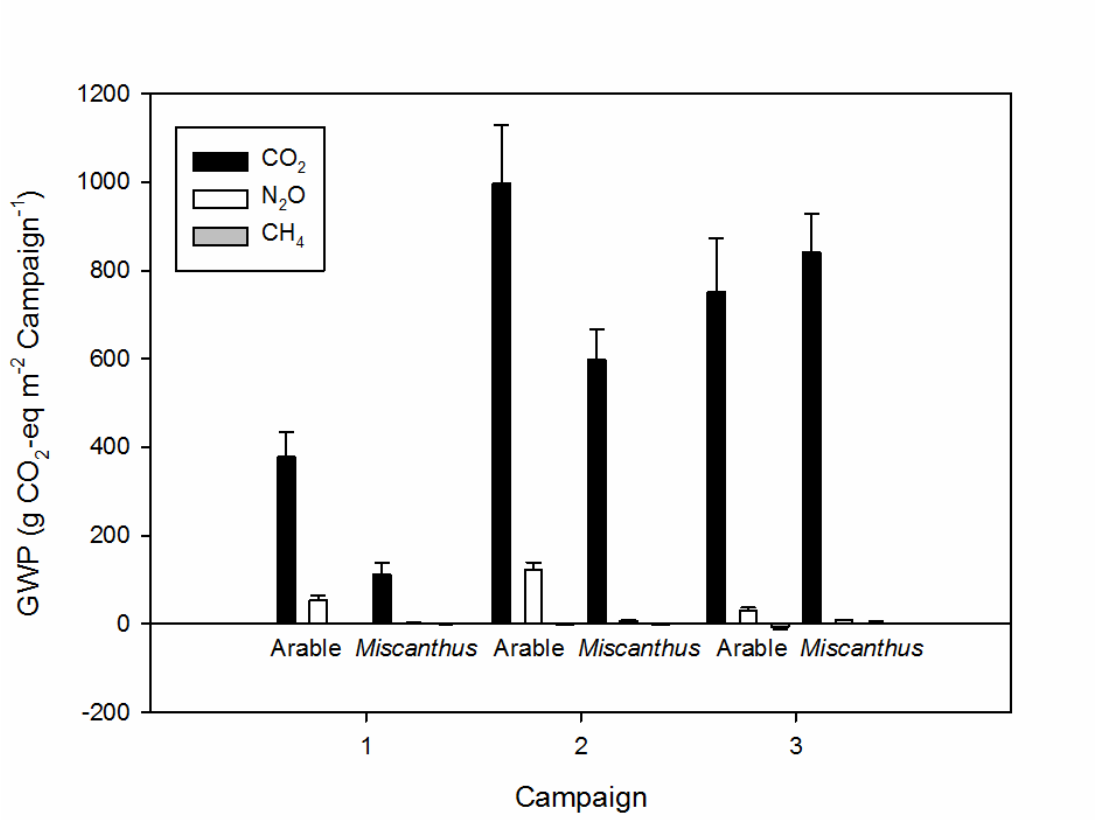

Figure 2.4 Total soil flux of three GHGs expressed in CO_2 equivalents (Myhre *et al.*, 2013) from an arable field and a *Miscanthus* field. Campaigns represent periods of varying length during which the arable field was used for different crop production and cover the period from September 2012 to March 2014. Values are means ± 1 SE.

2.3.3 Sub-daily measurements

Automated chamber measurements of soil CO_2 flux from beneath *Miscanthus* showed a similar pattern to the data from the manual chamber, with low fluxes through the winter of 2012-13, higher fluxes through summer 2013 followed by a decline into autumn and winter 2013 (Figure 2.5). A point of interest is the variation between the fluxes during autumn between 2012 and 2013: peak fluxes in October 2012 were well below 200 mg m^{-2} h^{-1}, declining to below 100 mg m^{-2} h^{-1} by the end of the month. In contrast, at the start of October 2013 maximum fluxes were still above 600 mg m^{-2} h^{-1} and were still greater than 300 mg m^{-2} h^{-1} by the end of this month. This variation was also detected in the survey chamber measurements, which were below 100 mg m^{-2} h^{-1} in October 2012 and below 400 mg m^{-2} h^{-1} in October 2013. During Campaign 2 in summer 2013 there was an initial peak in soil CO_2 flux in late May, followed by a decline in early June before fluxes increased to their annual peak of *ca.* 700 mg m^{-2} h^{-1} through late July and August. Unfortunately, instrumental malfunction meant that no data were collected for the majority of August, though the shape of the trend, allied to the data from the survey chamber, suggests that soil fluxes probably continued to rise slightly to a maximum during the intervening period. The reduction in flux throughout the end of summer was punctuated by a brief and rapid increase to around 1100 mg m^{-2} h^{-1} in early September 2013, a peak not detected under the monthly measurement regimen.

The scatter in the automated data demonstrates the diel variation in fluxes, which is reflected in the daily mean values (Figure 2.5, bottom panel). The daily means more clearly show fluctuations in the fluxes between days, with peaks and troughs shown over periods of a few days.

Measurements from the arable field during Campaign 2 in summer 2013 show that soil CO_2 fluxes were slower to increase under the barley then they were in the *Miscanthus* (Figure 2.6). Fluxes from the *Miscanthus* increased during late May to over 600 mg m^{-2} h^{-1}, whilst arable fluxes were still below 400 mg m^{-2} h^{-1}. However, when fluxes increased under the barley they did so rapidly, reaching a maximum of *ca.* 1500 mg m^{-2} h^{-1} during early July. Fluxes under arable were declining through late July, whilst *Miscanthus* fluxes were still increasing. By the end of the measurement period in late July, just prior to harvest, fluxes under the barley crop had reduced to less than 400 mg m^{-2} h^{-1}.

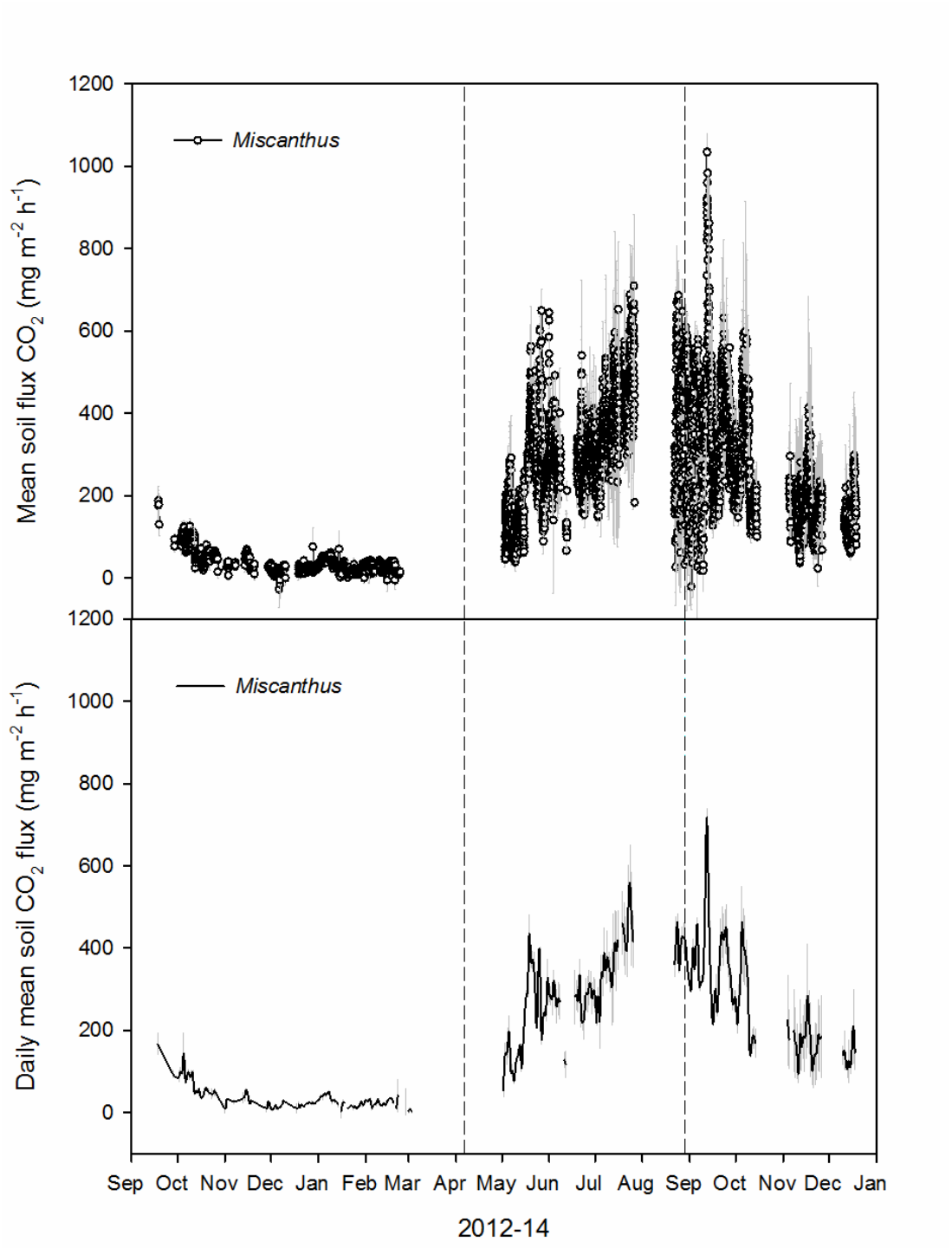

Figure 2.5 Mean ± 1 SE soil CO_2 flux from automated Licor chambers under *Miscanthus*. Top panel shows means of each cycle of chamber closure (ca 1 hour in frequency) and the bottom panel shows the daily mean. Dashed lines represent the timings of harvests in the adjacent arable field.

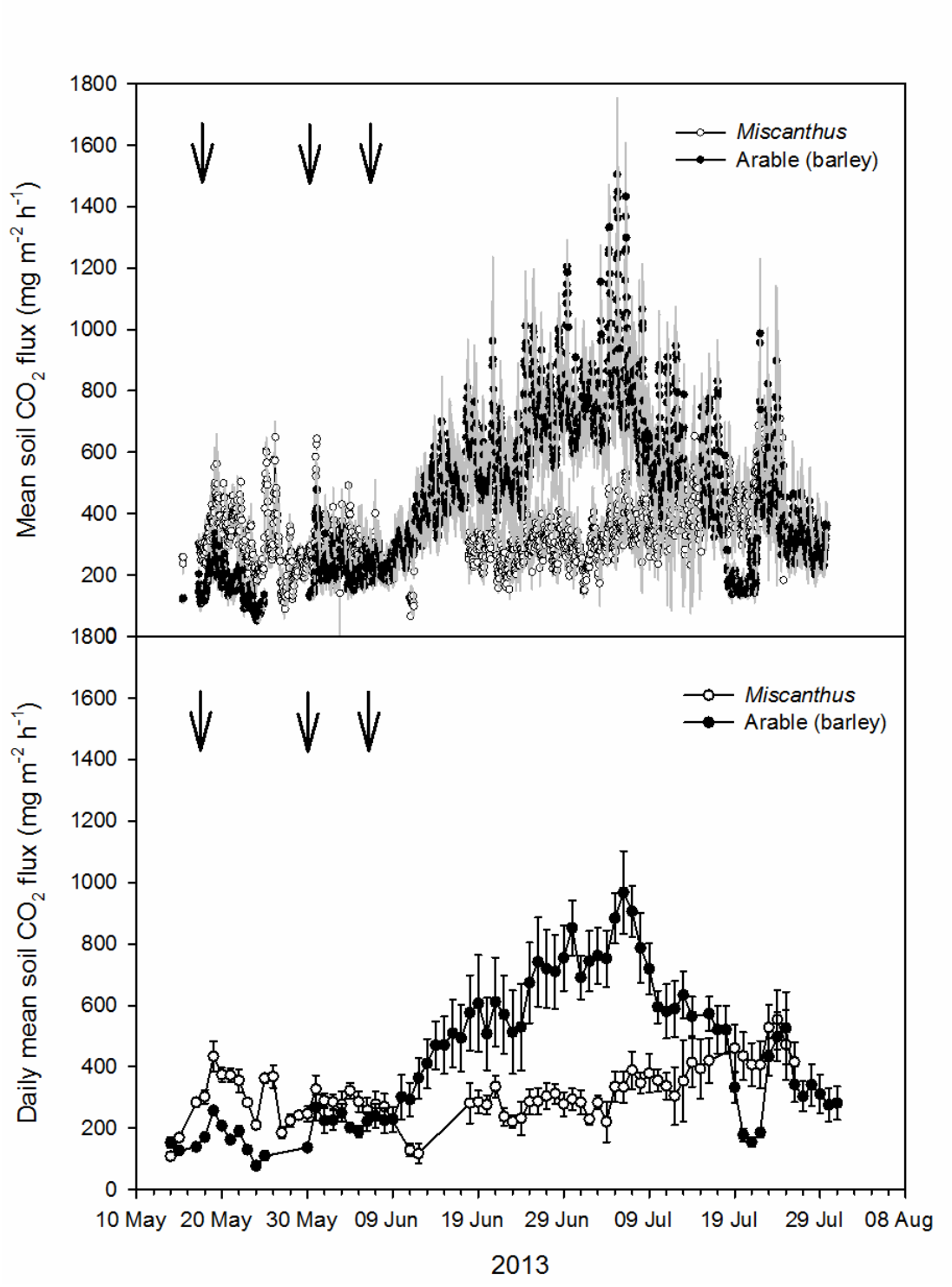

Figure 2.6 Mean soil CO_2 ± 1 SE flux measured using automated Licor chambers from under *Miscanthus* (open circles) and an arable crop (closed circles, spring barley) during Campaign 2. Means are based on a cycle of chamber closures at *ca.* 1 hour frequency (top panel) and daily means are also shown (bottom panel). Arrows indicate timing of nitrogen fertiliser applications to the arable crop.

Scatter within the sub-daily measurements in the arable again reflects the diel variation in soil CO_2 flux, which was at its greatest during peak emissions at the beginning of July 2013, where the daily mean (ca 900 mg m^{-2} h^{-1}) was approximately 60% of the daily maximum flux (ca 1500 mg m^{-2} h^{-1}) (Figure 2.6).

Analysis of the data from the automated chambers matches the data from the manual chamber measurements, showing significant differences between soil CO_2 flux from the arable field and the *Miscanthus* field $F_{[1,453]}$= 4.72, p<0.04, a significant effect of date $F_{[128,453]}$= 14.12, p<0001 and an interaction between date and crop $F_{[63,453]}$= 11.6, p<0.0001.

The calculated total CO_2 flux from the soil under *Miscanthus* was lower using automated data than when calculated using monthly manual measurements (Figure 2.7) in Campaign 2 ($T_{[5]}$= -3.17, p<0.03) and Campaign 3 ($T_{[5]}$= -5.06 p<0.004), and approached significance in Campaign 1 ($T_{[7]}$= -1.92 p< 0.1). Using automated data from the arable field did not significantly affect the calculated total soil CO_2 flux in Campaign 2 ($T_{[3]}$= -1.29, p= 0.29), the only period during which these chambers were available for use in this field.

2.3.4 Diurnal trends in soil CO_2 flux

Data from the automated chambers show that soil CO_2 flux varied throughout the day both in the *Miscanthus* field and under the arable crop (Figure 2.8) during Campaign 2. The trends are strikingly different for the two fields, with the lowest daily flux under *Miscanthus* occurring between 9.00 and 10.00 and peak emissions throughout the late evening. Fluxes from the arable field, on the other hand, peaked during the afternoon around 15.00 and the lowest fluxes were seen during the early morning. Depending on the time of day, the mean *Miscanthus* flux ranged from 83% (at 21.00) to 46% (at 14.00) of the arable flux, which introduces the potential for a massive bias in measurements.

The diurnal trend under the *Miscanthus* was similar in both Campaigns 2 and 3, though there was a difference in the absolute values of these fluxes, with higher values during Campaign 2 of summer 2013 than the subsequent Campaign during winter of that year (Figure 2.8). Campaign 1 did not show such a strong diel trend, although the fluxes during that period were much smaller than the other two Campaigns.

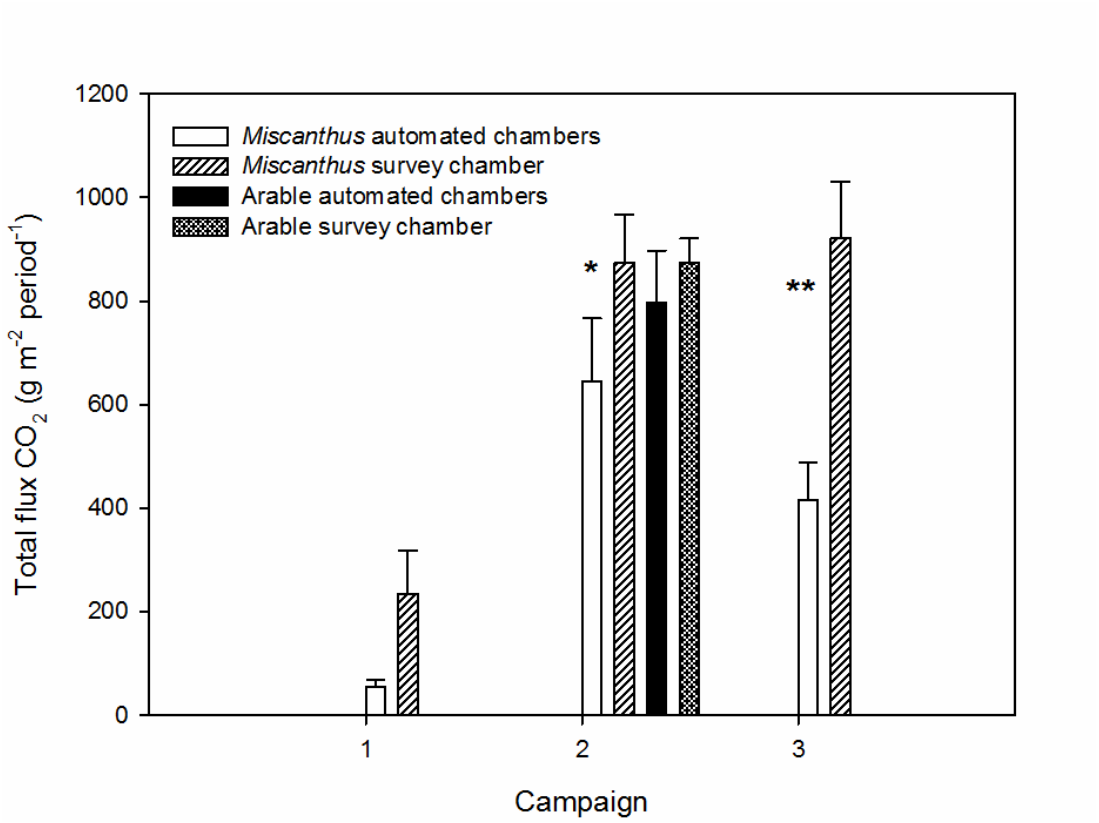

Figure 2.7 Total CO_2 flux from soil under *Miscanthus* and arable cropping, measured using and IRGA and automated chambers (*ca.* hourly measurements) or a manual survey chamber (*ca.* monthly measurements). Campaigns represent periods of different crop production in the arable field (1- fallow, 2- spring barley, 3- oilseed rape). Automated and manual measurements were made from the same positions: results of paired t-tests show significant differences between the total flux calculated from automated and manual measurements, * $p< 0.05$, ** $p< 0.01$.

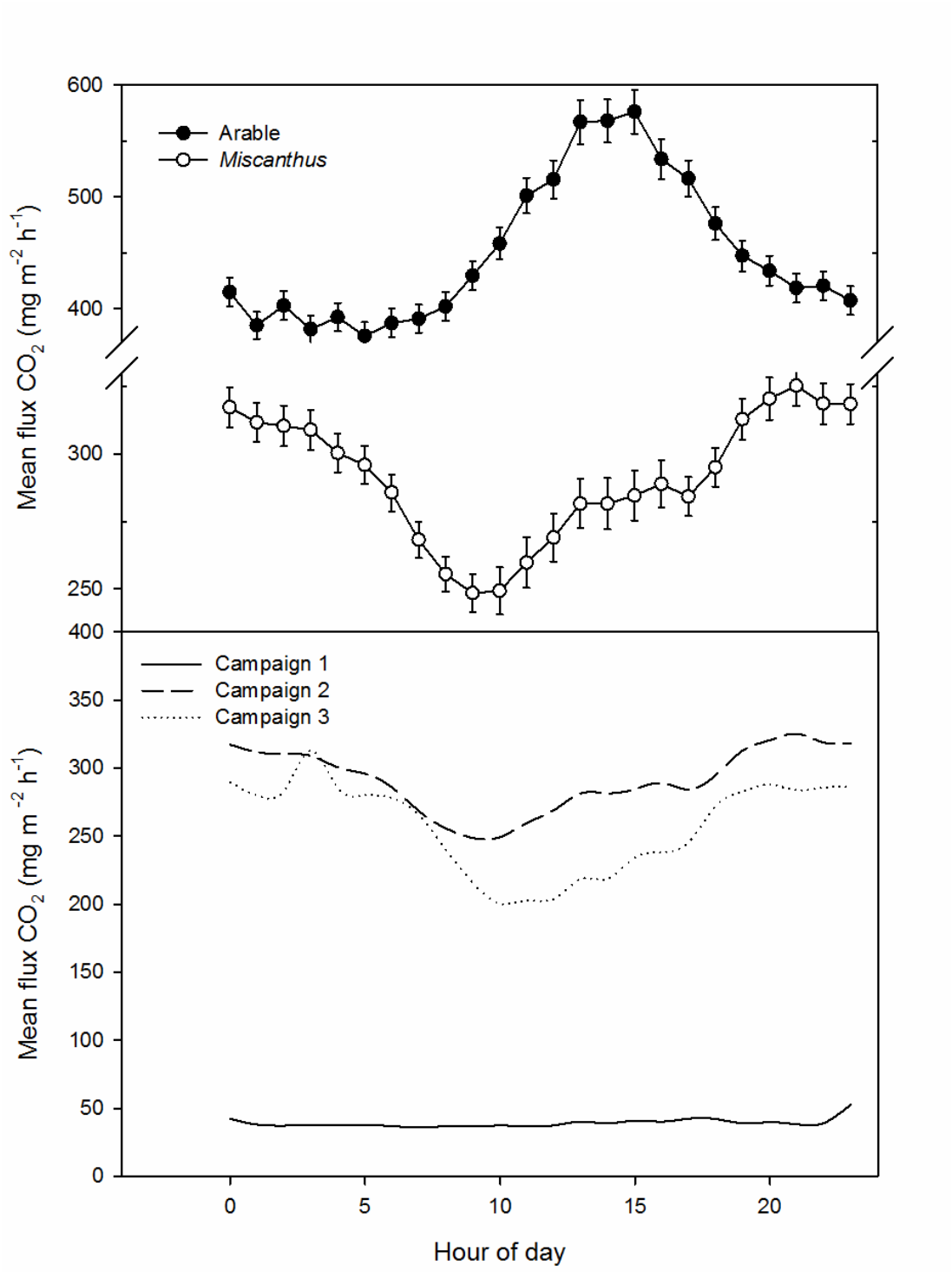

Figure 2.8 The diurnal variation in soil CO_2 flux from an arable field and a *Miscanthus* field. Top panel: *Miscanthus* and arable (spring barley) fields from the same Campaign show contrasting daily cycles (*Miscanthus* n= 480, arable n= 320). Values are means ± 1SE, note the axis break. Bottom panel: soil CO_2 flux under *Miscanthus* over three Campaigns (1- winter 2012-13, 2- summer 2013, 3- winter 2013-4).

2.3.5 Environmental variables

The pattern of solar radiation was somewhat predictable, peaking in 2013 during the middle of June (Figure 2.9). Perhaps surprisingly, there was a brief increase in solar radiation towards the end of February 2013, but otherwise it was characterised by lower values during the winters of 2012-3 and 2013-4. The contrast between the values for September 2012 and 2013 is worth noting: daily maxima of solar radiation during the former, approaching 800 W m^{-2}, were higher than those during the latter, which were closer to 500 W m^{-2}. The values during the rest of autumn for both years were more similar.

Air temperature also peaked during summer, but it lagged behind values of solar radiation, peaking during late July and the beginning of August 2013 (Figure 2.9). Temperatures reached the lowest of the study period during January 2013. Soil temperatures exhibited a similar pattern to air temperature, though was generally higher. Soil temperature in both the *Miscanthus* and arable fields were similar.

Soil moisture (at 5 cm depth) was measured throughout the summer and autumn 2013. Peaks in soil moisture could be seen following periods of rainfall (Figure 2.9), and was followed by rapid drops in the intervening periods. During June and July the arable field appeared to be wetter than the adjacent *Miscanthus* field. Soil moisture was lowest at the start of September 2013, but following sustained period of precipitation during September and October, moisture peaked in the *Miscanthus* field during late October 2013. The arable field was wettest during May 2013, but dried out to similar levels to the *Miscanthus* field by the end of July.

The periods that received the most rainfall were the winters (Figure 2.9). A lack of rain through April and into the first half of May 2013 left the site close to drought conditions. This was followed by sustained rainfall for the remainder of May, but the first half of June and most of July 2013 were also very dry.

2.3.6 Relationship between environmental variables and fluxes

The measured environmental variables were used to explain the patterns in the observed fluxes in both the monthly and sub-daily data. In addition to concurrent measurements, daily maxima and minima were used to explain monthly fluxes.

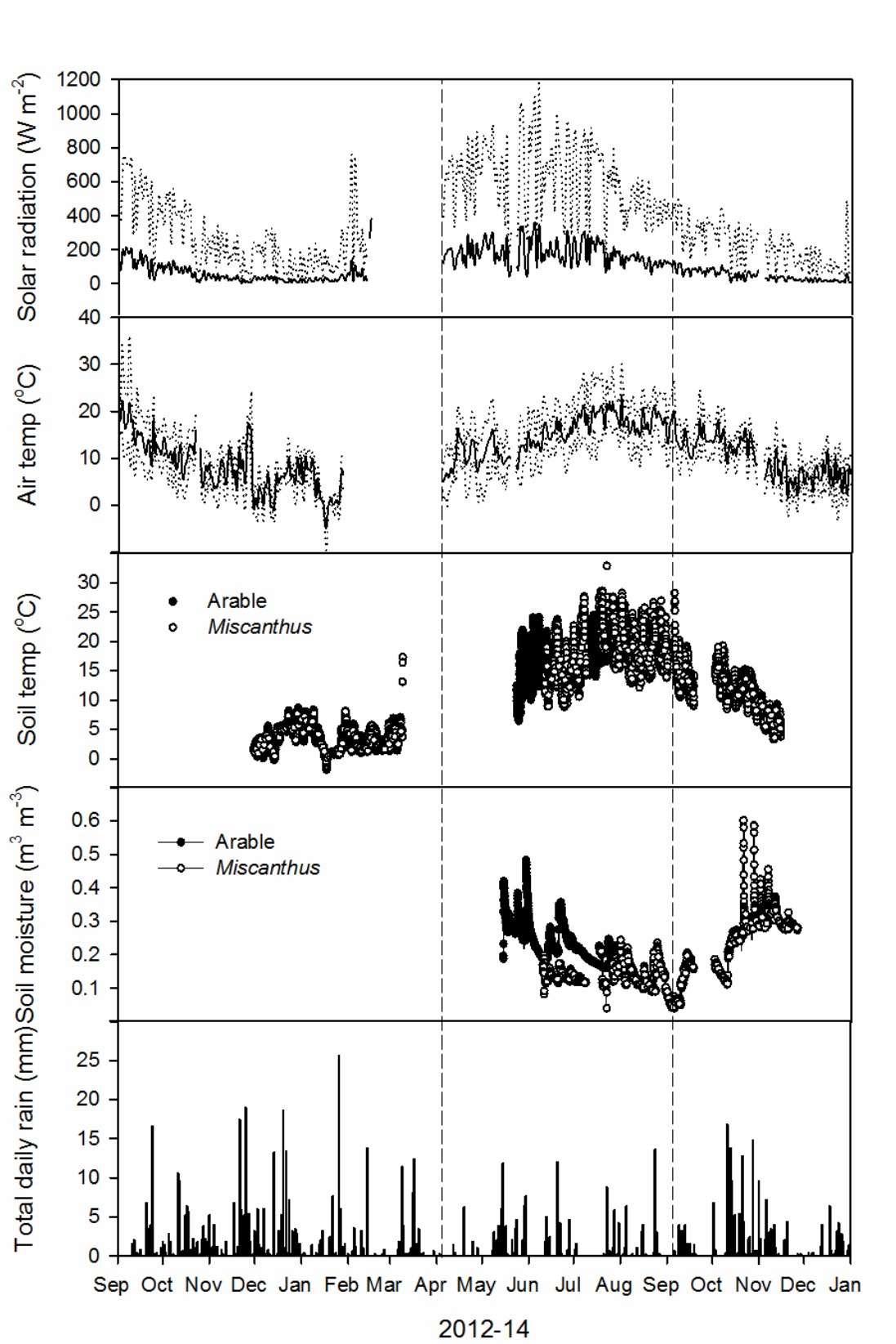

Figure 2.9 Environmental and meteorological variables measured at the study site across three Campaigns (separated by vertical dashed lines). Solar radiation and air temperature are daily means (of hourly measurements; solid line). Daily maximum values are shown for both

air temperature and radiation, and daily minimum values for temperature (dotted lines), since minimum solar radiation values were all zero they are not shown. Soil temperature and soil moisture show hourly mean values from the *Miscanthus* field (open circles) and the arable field (closed circles), and rainfall data are daily total values. Rainfall data were collected from the met station on site; however, during periods of instrumental error the rainfall data from a Met Office station approximately two miles from the site were used.

2.3.6.1 Monthly gas fluxes

Soil CO_2 flux displayed strong linear relationships with several environmental variables (Figure 2.10). These relationships were consistent across both the arable and *Miscanthus* fields, and for the most part were similar in terms of the strength and direction of the relationship. The variable explaining most of the variance in the arable field was soil temperature (R^2= 0.46, p< 0.0001), which had a strong positive correlation with CO_2 flux. Concurrent air temperature, daily minimum temperature and maximum solar radiation all demonstrated strong positive relationships with soil respiration from the arable field, explaining 44%, 37% and 32% of the variation, respectively. Maximum daily solar radiation did not exhibit a significant relationship with fluxes from under the *Miscanthus*, although concurrent solar radiation does seem to have been important for CO_2 flux from the *Miscanthus* field: this variable explained the variation soil respiration most closely (R^2= 0.83, p< 0.0001), which was in contrast to the much weaker, though significant, relationship of this variable with the arable fluxes (R^2= 0.16, p< 0.01). Fluxes from the *Miscanthus* field also showed strong positive linear relationships with soil temperature (R^2= 0.67, p<0.0001), air temperature (R^2= 0.53, p< 0.0001) and minimum daily temperature (R^2= 0.49, p< 0.0001), though this last variable did not have as strong an effect on fluxes from the *Miscanthus* field as for the arable, as shown from the gradient of the regression lines (Figure 2.10). The relationship between soil CO_2 flux and soil temperature was improved slightly with a quadratic model for *Miscanthus* (R^2= 0.69 versus R^2= 0.67 for a linear fit), but did not alter the R^2 value for the arable field. No other relationship between CO_2 flux and environmental variable was improved with a non-linear model.

Two variables showed significant negative relationships with soil respiration in both fields. Somewhat surprisingly, soil respiration declined with increasing soil moisture in a similar fashion under both crops, explaining 25% of the variation in the arable field and 35% in the *Miscanthus* field. Relative humidity showed a closer relationship in both the arable (R^2= 0.30, p< 0.0001) and the *Miscanthus* fields (R^2= 0.65, p< 0.0001).

N_2O fluxes were less well described by environmental variables, and in all cases the relationships were stronger from the arable field than from the *Miscanthus* field (Figure 2.11). Perhaps surprisingly, the variable which explained the most variation in N_2O flux was maximum daily solar radiation for the arable field (R^2= 0.53, p< 0.0001), as fluxes increased with radiation, but this did not show a significant

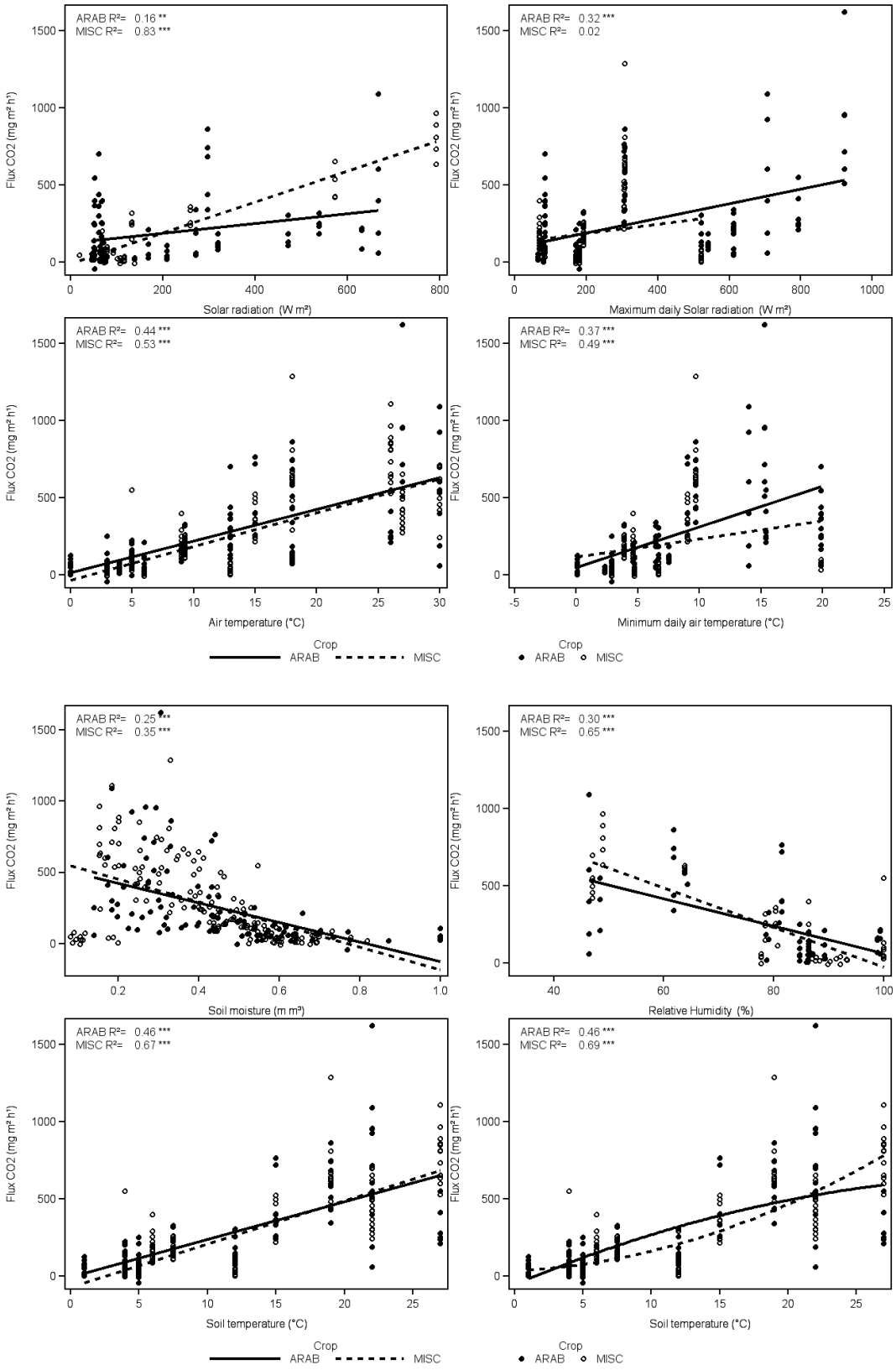

Figure 2.10 Monthly soil CO_2 flux measurements using a Licor survey chamber from an arable (ARAB) and a *Miscanthus* field (MISC) plotted against environmental variables. All panels (except the bottom right) display linear regression lines, with the R^2 statistic (*** denotes

p<0.001). The bottom right panel compares a quadratic fit with the linear fit for the same data (soil temperature) in the adjacent panel. All other variables were best described with a linear relationship.

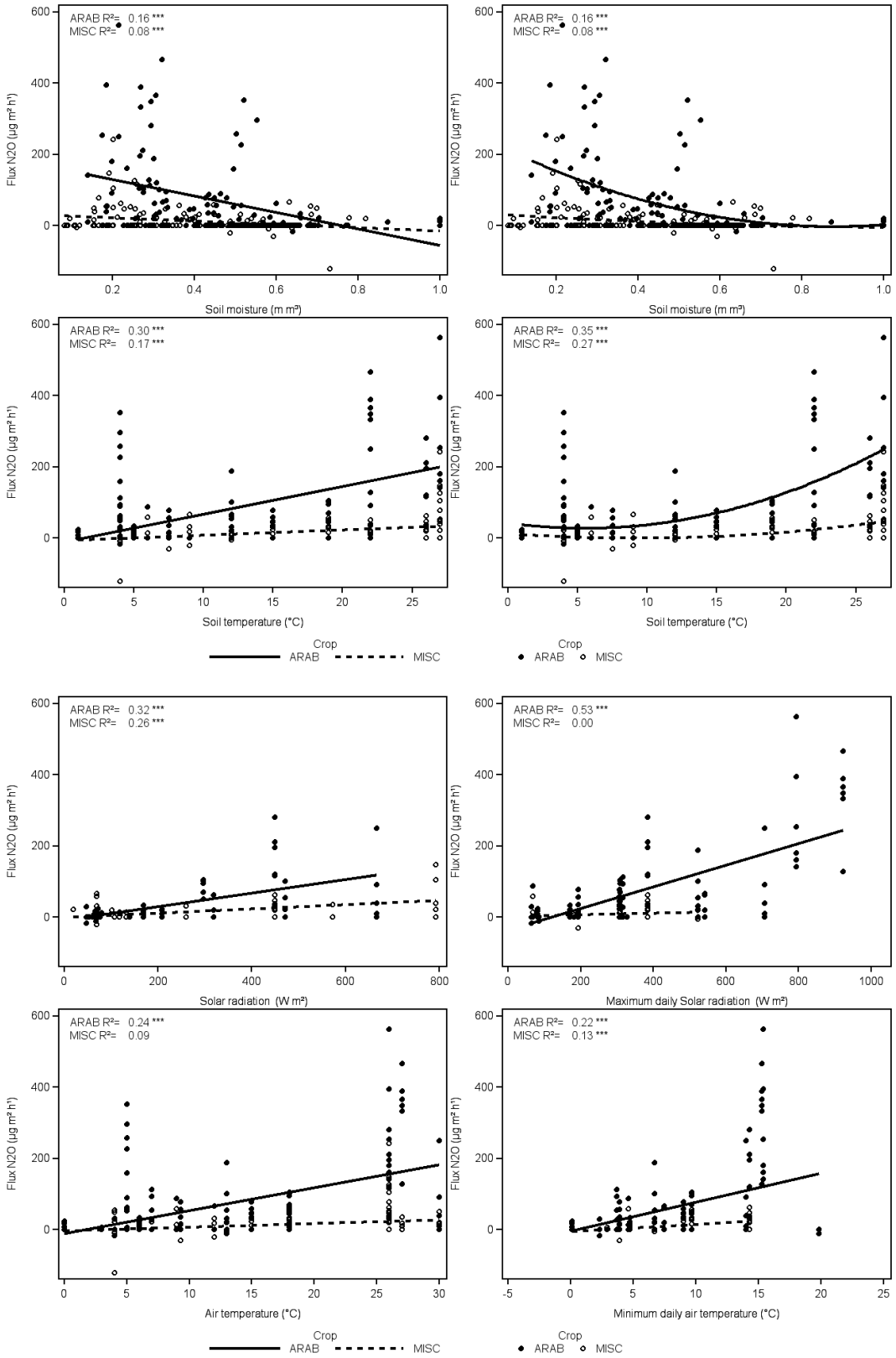

Figure 2.11 Monthly N_2O flux measurements from an arable and a *Miscanthus* field, made using static chambers, and their relationship with various environmental variables. The R^2 statistic is displayed in each panel, where *** denotes p< 0.001. The top two rows compare

the same variable with a linear fit (left panel) and a curve fit (right panel). No other variables were improved by the use of non-linear regression.

relationship with fluxes of N_2O from *Miscanthus* soil. Instantaneous solar radiation was less important in explaining the N_2O fluxes in the arable field (R^2= 0.32, p< 0.0001), but there was a significant relationship with fluxes from the *Miscanthus* (R^2= 0.26, p< 0.0001), which was second only to soil temperature in this crop. Soil temperature displayed a strong positive relationship with arable fluxes (R^2= 0.35, p< 0.0001) and also appeared important in controlling fluxes from the *Miscanthus* (R^2= 0.27, p< 0.0001). This relationship was better described with a quadratic model than a linear fit for both crops (Figure 2.11). Minimum daily temperature and concurrent air temperature both positively affected N_2O fluxes from the arable field, explaining 22% and 24% of the variation respectively, and whilst the minimum daily temperature was also important for fluxes from *Miscanthus* (R^2= 0.13, p< 0.001), concurrent air temperature was not significant.

Perhaps a little counterintuitively, soil moisture displayed a significant negative relationship with N_2O flux in both fields, though with R^2 values of 0.16 and 0.08 in from the arable and *Miscanthus* respectively, the relationships were not particularly strong. Despite this, the regressions suggest that N_2O emission will cease at a soil moisture level of *ca.* 0.7 m^3 m^{-3}. The relationship between fluxes and soil moisture was equally well described by linear and non-linear models.

No environmental variable was shown to be significantly associated with CH_4 fluxes, from either field (Table 2.1). Stepwise multiple regression showed no improvement in describing CH_4 flux from the *Miscanthus* field, but it was significant for fluxes from the arable field (Equation 2.2). This analysis indicated that soil moisture was the most important control over CH_4 flux, with fluxes becoming more positive with increasing soil moisture, and that solar radiation also played a role. Multiple regression models also indicate that soil temperature was the most important factor controlling soil CO_2 flux in the arable field (Equation 2.3), and that soil moisture and maximum daily air temperature were significantly related variables. This model was a better predictor (R^2= 0.60, p< 0.0001) than any individual variable, and fluxes from the *Miscanthus* were also very well described (R^2= 0.91, p< 0.0001) by a model including air temperature, solar radiation and relative humidity (Equation 2.4).

Table 2.1 Correlation matrix for monthly fluxes of CO_2, N_2O and CH_4 with measured environmental variables. Values shown are Pearson correlation statistics. * p < 0.05, ** p< 0.01, *** p<0.001, ns= not significant.

CROP	Variable	Soil Temp	Air temp	Soil Moisture	Solar Radiation	Relative Humidity	Daily mean air temp	Daily maximum air temp	Daily Maximum radiation	N_2O flux	CH_4 flux	CO_2 flux	Log CO_2 flux
Arable	Soil temp	1	0.96***	-0.68***	0.84***	-0.81***	0.97***	0.97***	0.95***	0.55***	0.04 ns	0.69***	0.71***
	Air temp	0.96***	1	-0.71***	0.83***	-0.83***	0.97***	0.98***	0.96***	0.5***	0.03 ns	0.67***	0.69***
	Soil moisture	-0.68***	-0.71***	1	-0.72***	0.7***	-0.7***	-0.72***	-0.72***	-0.41***	0.01 ns	-0.52***	-0.68***
	Solar radiation	0.84***	0.83***	-0.72***	1	-0.69***	0.1	0.16***	0.22***	0.61***	0.08 ns	0.31**	0.35***
	Relative humidity	-0.81***	-0.83***	0.7***	-0.69***	1	-0.2***	-0.3***	-0.36***	-0.25*	-0.01 ns	-0.58***	-0.51***
	Dailymean temp	0.97***	0.97***	-0.7***	0.1***	-0.2***	1	0.9***	0.6***	0.46***	0.01 ns	0.63***	0.6***
	Daily max air temp	0.97***	0.98***	-0.72***	0.16***	-0.3***	0.9***	1	0.8***	0.46***	0 ns	0.63***	0.62***
	Daily max radiation	0.95***	0.96***	-0.72***	0.22***	-0.36***	0.6***	0.8***	1	0.4***	0.04 ns	0.68***	0.63***
	N_2O flux	0.55***	0.5***	-0.41***	0.61***	-0.25*	0.46***	0.46***	0.4***	1	0.04 ns	0.42***	0.41***
	CH_4 flux	0.04 ns	0.03 ns	0.01 ns	0.08 ns	-0.01 ns	0.01 ns	0 ns	0.04 ns	0.04 ns	1	0.02 ns	0.09 ns
	CO_2 flux	0.69***	0.67***	-0.52***	0.31*	-0.58***	0.63***	0.63***	0.68***	0.42***	0.02 ns	1	0.85***
	Log CO_2 flux	0.71***	0.69***	-0.68***	0.35***	-0.51***	0.6***	0.62***	0.63***	0.41***	0.09 ns	0.85***	1

CROP	Variable	Soil Temp	Air temp	Soil Moisture	Solar Radiation	Relative Humidity	Daily mean air temp	Daily maximum air temp	Daily Maximum radiation	N_2O flux	CH_4 flux	CO_2 flux	Log CO_2 flux
Misc'	Soil temp	1	0.96***	-0.77***	0.91***	-0.79***	0.97***	0.97***	0.95***	0.4***	-0.01 ns	0.82***	0.76***
	Air temp	0.96***	1	-0.76***	0.87***	-0.82***	0.96***	0.98***	0.91***	0.32***	0 ns	0.74***	0.75***
	Soil moisture	-0.77***	-0.76***	1	-0.83***	0.74***	-0.8***	-0.83***	-0.77***	-0.27***	-0.07 ns	-0.55***	-0.51***
	Solar radiation	0.91***	0.87***	-0.83***	1	-0.63***	0.22***	0.24***	0.33***	0.46***	-0.12 ns	0.92***	0.67***
	Relative humidity	-0.79***	-0.82***	0.74***	-0.63***	1	-0.29***	-0.31***	-0.43***	-0.33***	0.07 ns	-0.81***	-0.68***
	Dailymean temp	0.97***	0.96***	-0.8***	0.22***	-0.29***	1	0.98***	0.7***	0.45***	-0.02 ns	0.79***	0.79***
	Daily max air temp	0.97***	0.98***	-0.83***	0.24***	-0.31***	0.98***	1	0.77***	0.43***	-0.02 ns	0.78***	0.85***
	Daily max radiation	0.95***	0.91***	-0.77***	0.33***	-0.43***	0.7***	0.77***	1	0.43***	-0.1 ns	0.82***	0.68***
	N_2O flux	0.4***	0.32***	-0.27***	0.46***	-0.33***	0.45***	0.43***	0.43***	1	0.2*	0.45***	0.31***
	CH_4 flux	-0.01 ns	0 ns	-0.07 ns	-0.12 ns	0.07 ns	-0.02 ns	-0.02 ns	-0.1 ns	0.2*	1	0.07 ns	0.07 ns
	CO_2 flux	0.82***	0.74***	-0.55***	0.92***	-0.81***	0.79***	0.78***	0.82***	0.45***	0.07 ns	1	0.84***
	Log CO_2 flux	0.76***	0.75***	-0.51***	0.67***	-0.68***	0.79***	0.85***	0.68***	0.31***	0.07 ns	0.84***	1

Arable:

N_2O µg m^{-2} h^{-1} = 3.90 soil temp (°C) - 7.49

R^2= 0.41, p< 0.0001 **(Eq 2.1)**

CH_4 µg m^{-2} h^{-1}= 35.81 soil moist (m^3 m^{-3}) - 0.04 radiation (W m^{-2}) - 14.45

R^2= 0.14, p= 0.05 **(Eq 2.2)**

Log_{10} CO_2 mg m^{-2} h^{-1}= 0.23 soil temp (°C) - 1.80 soil moist (m^3 m^{-3}) - max temp (°C) +3.90

R^2= 0.60, p< 0.0001 **(Eq 2.3)**

***Miscanthus*:**

Log_{10} CO_2 mg m^{-2} h^{-1}= 0.30 Air temp (°C) - 0.01 radiation (W m^{-2}) - 0.09 RH (%) + 10.62

R^2= 0.91, p< 0.0001 **(Eq 2.4)**

2.3.6.2 Sub-daily soil CO_2 fluxes

Soil respiration was positively related to soil temperature (Figure 2.12) in the *Miscanthus* (R^2= 0.60, p< 0.0001), where it was the variable showing the strongest correlation with respiration, and in the arable field, though here the relationship was much weaker (R^2= 0.09, p< 0.0001). There was also a weak, but significant, positive relationship between CO_2 fluxes and solar radiation in both fields, explaining 3% and 7% of the variation from the arable and *Miscanthus* fields, respectively (Figure 2.12). The relationship between soil respiration and air temperature was less straight forward. For both fields, the data were better described by a non-linear model (Figure 2.12), which indicates a positive effect on CO_2 flux below a threshold temperature, and a subsequent decline as temperatures increased further. These relationships suggest an optimum air temperature for soil respiration of around 25 °C

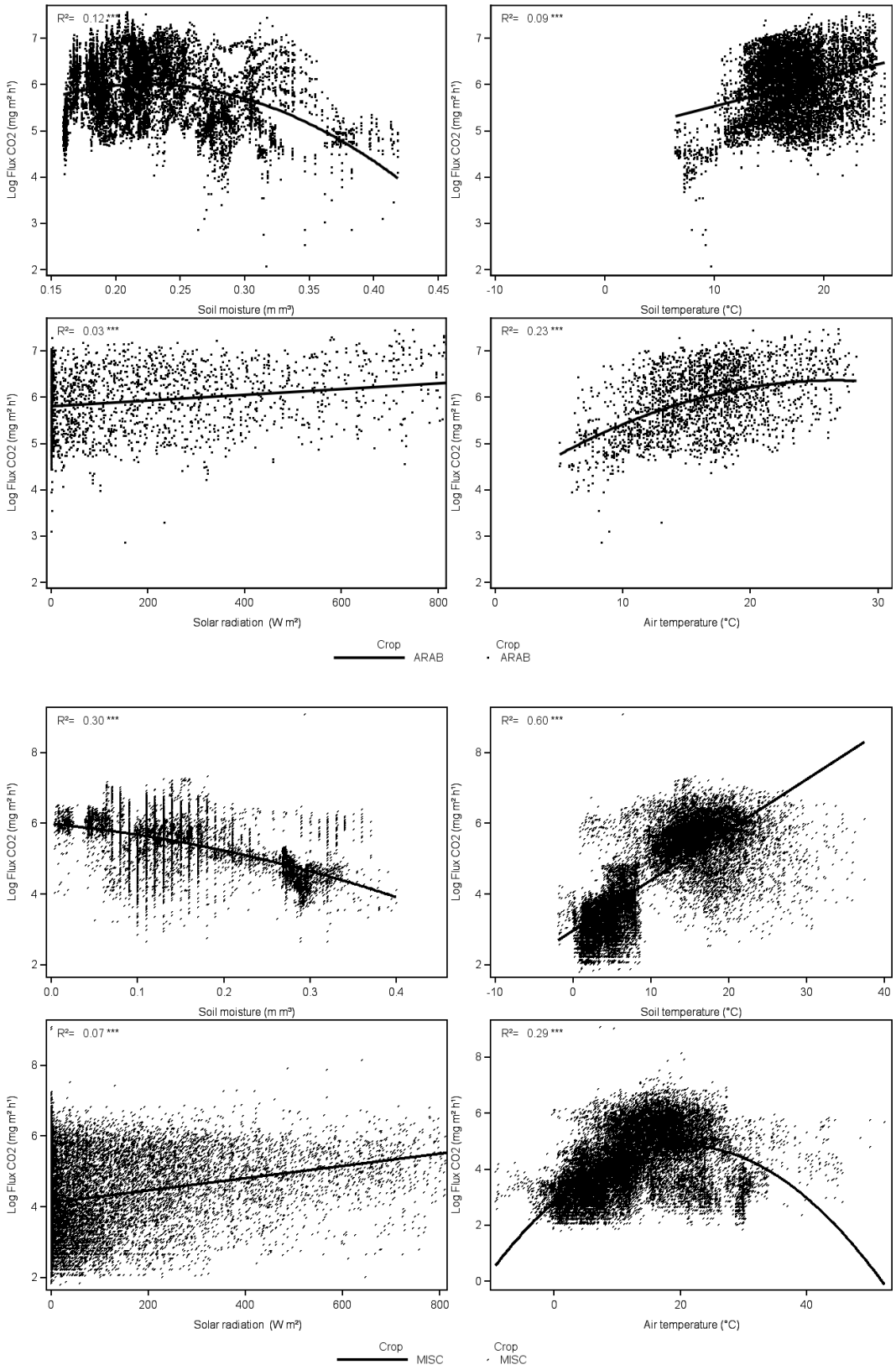

Figure 2.12 Relationship of environmental variables to log_{10} transformed soil CO_2 fluxes measured using automated chambers, from and arable field (top four panels) and a *Miscanthus* field (bottom four panels).

in the arable field, but lower, ca 20 ^{o}C in the *Miscanthus*.

The relationship of CO_2 flux with soil moisture was also best described by a non-linear fit, with respiration in both fields declining more quickly above a threshold: this was more severe in the arable field, where it seems that fluxes tended to zero at moisture levels *ca.* 0.5 m^3 m^{-3}, as opposed to 0.6 m^3 m^{-3} in the *Miscanthus* field. Even when moisture levels in the upper 5 cm of the soil were very low (< 0.05 m^3 m^{-3}) in the *Miscanthus* field, soil respiration continued.

The diurnal pattern in soil CO_2 flux from the arable field can be seen to follow closely air temperature, the variable with which it was most closely associated (Figure 2.13). This was not so clear for the *Miscanthus* field, where CO_2 fluxes did not appear to be as synchronous with soil temperature, with which they were most closely related. This discrepancy suggests that another factor is an important control of soil CO_2 flux. However, multiple regression models including additional measured environmental variables were not a significant improvement on regressions with any single variable.

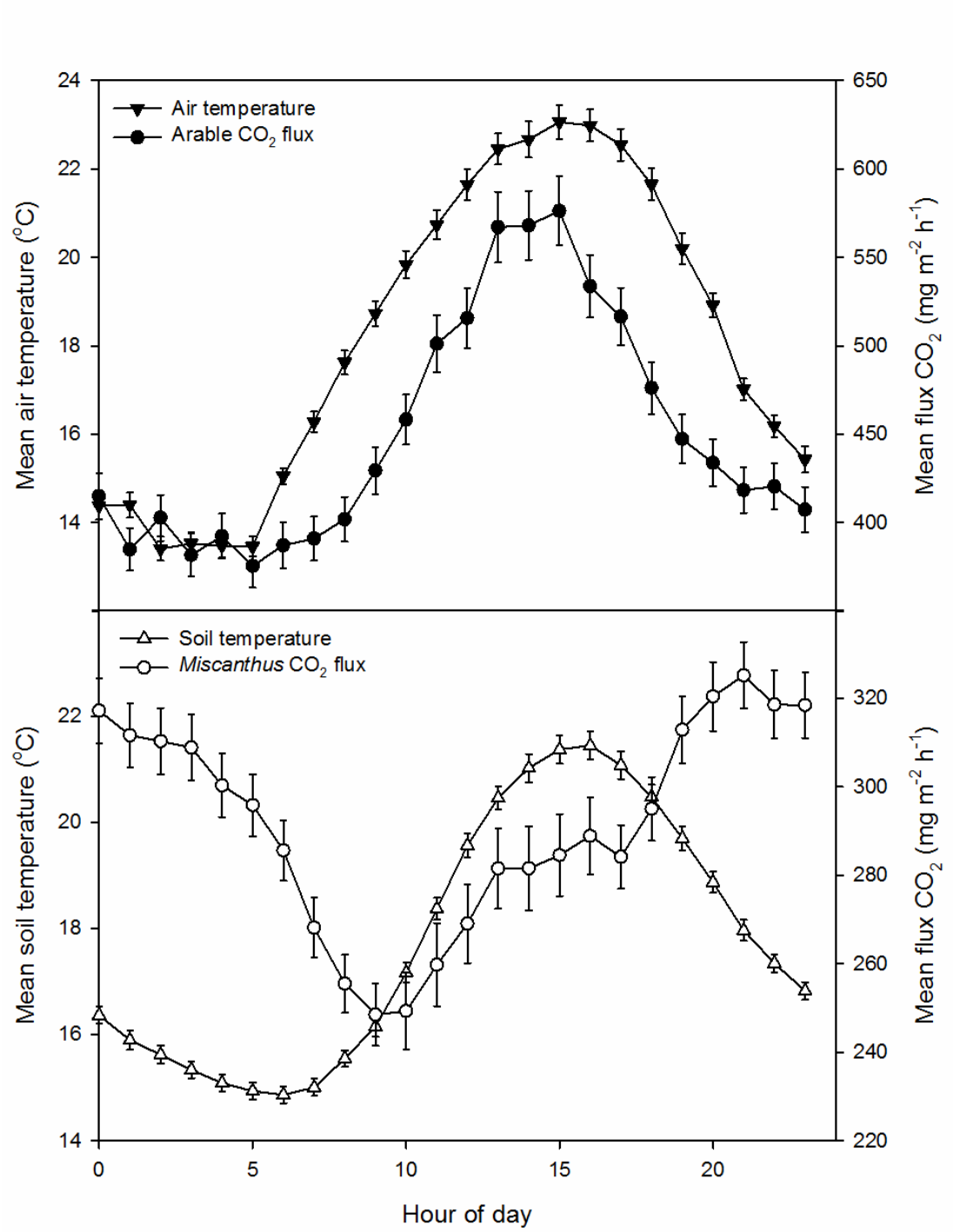

Figure 2.13 Diurnal pattern of CO_2 fluxes measured over 80 days from an arable field (top panel, n=320) and a *Miscanthus* field (bottom panel n=480) with the environmental variable with which the fluxes were most closely related. Values are means ± 1SE, measured during May- July 2013.

2.4 Discussion

2.4.1 Monthly soil GHG fluxes

The arable field consistently produced higher fluxes of GHGs from the soil than the *Miscanthus* field across the whole study period. This was expected, especially for N_2O, principally due to the history of fertiliser amendment; fertiliser application to the crops during this study totalled 179 kg-N ha^{-1} to the arable field, compared to zero to the *Miscanthus*. The N_2O fluxes reported from the *Miscanthus* here were of a similar order of magnitude to those reported elsewhere. In a similar study at the same site, Drewer *et al.* (2012) saw peak N_2O emissions of *ca.* 110 µg m^{-2} h^{-1} from *Miscanthus*, and a cumulative flux of 152 kg CO_2-eq ha^{-1} y^{-1}. The peak emissions presented here of 24 µg m^{-2} h^{-1} were lower, but the cumulative flux over the entire 485 day period equated to *ca.* 100 kg CO_2-eq ha^{-1} y^{-1}. Other studies have seen a similar range of N_2O fluxes from unfertilised *Miscanthus* in Denmark (Jorgensen *et al.*, 1997), North America (Behnke *et al.*, 2012) and Japan (Mori *et al.*, 2005, Toma *et al.*, 2011).

N_2O emissions from arable crops are typically in the range of 0.3- 3 % of the applied total N fertiliser (De Klein *et al.*, 2006), which here would amount to 0.57- 5.73 kg-N ha^{-1} y^{-1}, or 0.84- 8.43 kg N_2O ha^{-1} y^{-1}. The cumulative N_2O flux from the arable field of 669 mg N_2O m^{-2} for the entire study equates to 3.1 kg N_2O-N ha^{-1} y^{-1}, an intermediate level of emissions, though it is towards the upper bound of those reported from cereal crops by Stehfest & Bouwman (2006), and greater than the total flux associated with spring barley in a Scottish study, in which the total emission of 0.8 kg N_2O-N ha^{-1} y^{-1} equated to an emission factor of 0.67 % of the applied N fertiliser (Smith *et al.*, 1998a). If the total flux from the unfertilised *Miscanthus* soil is taken as a baseline, then an emission factor (EF) of 1.54 % of the 179 kg applied over the period can be estimated. The peak emission measured from the arable field in this study was slightly more than 300 µg m^{-2} h^{-1}, occurring in the weeks following fertiliser addition to the barley crop, in June 2013. This figure is comparable to other studies from fertilised barley, where peaks ranging from *ca.* 60 µg m^{-2} h^{-1} (Petersen, 1999), *ca.* 300 µg m^{-2} h^{-1} (Chatskikh & Olesen, 2007), and *ca.* 440 µg m^{-2} h^{-1} (Kaiser *et al.*, 1998) have been published. However, in some circumstances fluxes in excess of 4000 µg m^{-2} h^{-1} have been seen from organic arable soils (Petersen *et al.*, 2012).

The soil CO_2 fluxes (0- 1000 mg m^{-2} h^{-1}) from both fields were in the typical range reported for soil respiration from arable soils (Chirinda *et al.*, 2010, Drewer *et al.*,

2012, Poll *et al.*, 2013). Highest fluxes were seen here during the summer months, when the air and soil temperatures were highest and maximum carbon input to the soil via the crop root system would have been occurring. During Campaign 2 it is clear from the monthly data that respiration was higher from the barley crop than the *Miscanthus* during the first weeks. Later in this Campaign, soil respiration was higher under the *Miscanthus* and this is most probably a consequence of the different growth trajectories of the two crops. Through May and June the barley was in its rapid growth phase, with a high rate of photosynthesis ensuring high root exudates and fuelling soil respiration. At this point the *Miscanthus* had only recently emerged and lagged behind in terms of green shoot growth. During July the barley had matured and photosynthesis slowed as grain filled and soil respiration also slowed under this crop (Sreenivasulu & Schnurbusch, 2012). Conversely the *Miscanthus* continued to grow well into September, probably maintaining a strong carbon supply to the soil and thus driving the higher soil respiration seen in this crop during July into August. The presence of more above-ground biomass in the *Miscanthus* field compared to the arable field during December 2013 was probably linked to the occurrence of higher respiration seen during Campaign 3.

Higher rates of soil respiration were consistently seen from the arable field during Campaign 1, during its fallow period. In contrast, the CO_2 fluxes from both fields were similar for the most part of winter 2013-14 (Campaign 3). The fallow period of Campaign 1 was the result of the land being inaccessible to farm machinery, and so the roots and other residues of the previous rotation crop (wheat) had been left in the soil. It is suggested here that decomposition of this residual material was the driver for the higher respiration seen from this field during this time.

CH_4 fluxes did not statistically differ between the two fields. The fluxes were small, and for the majority of the study they were negative, indicating oxidation was occurring in the soil. Whilst agricultural soils are known to be a net sink for CH_4 (Flessa *et al.*, 1998), nitrogen addition to soils, particularly as fertiliser, is known to inhibit the enzymes required for CH_4 oxidation (Arif *et al.*, 1996, Hutsch, 2001). In light of this it might have been expected that greater uptake would have been seen under the *Miscanthus* crop. The absence of a difference between the two fields might perhaps be down to the additional inhibitory effect of any herbicides applied to both crops, since these are also known to reduce CH_4 oxidation (Arif *et al.*, 1996). Ultimately, the role CH_4 played in the overall GHG balance for this site was very minor.

2.4.2 GHG balance

Without net ecosystem exchange (NEE) of CO_2 from both crops it is not possible to provide the final GHG balance for the two fields in this study but it is possible to make inferences using the data collected. During Campaign 1, when the arable field was fallow, it is possible to conclude that the arable field was a net source for GHGs, since there was no photosynthesis to offset soil respiration. It may be that during the winter months, when the *Miscanthus* senesced that this crop was also a net source for GHGs. It is possible to make an estimate of CO_2 uptake from gross primary productivity (GPP), or, more accurately, from the yield of the crops. In 2013 the mean yield from barley in the UK was 5.8 t ha^{-1} (DEFRA, 2013), which equates to 580 g m^{-2} of grain, and if a harvest index of 50% is assumed (Bertholdsson & Brantestam, 2009) this would equate to 1160 g m^{-2} total biomass. A 44% carbon content of this biomass (Elsgaard *et al.*, 2012) would give an estimate of 510 g-C m^{-2} in the biomass alone, and does not account for additional carbon sequestered to the soil or soil biota. The total soil respiration during the cultivation of the barley crop in Campaign 2 was 997 g CO_2 m^{-2} (271 g CO_2-C m^{-2}) which would mean in terms of carbon dynamics the arable field was a net sink of around 239 g C m^{-2}. The role N_2O plays in the GHG balance becomes critical, since, with an emission of 123 g CO_2-eq m^{-2} for the Campaign, N_2O emissions move the balance further towards being a net GHG source. It is essential, therefore, to have highly robust estimates of both N_2O flux and NEE from arable land in order to accurately assess the full impact of agriculture on climate change. It is also important to note that this study makes no consideration for the intrinsic GHG emissions associated with harvest, production or fertiliser manufacture which will undoubtedly tip the balance well into a net source of GHGs for the production of this crop.

Due to the lower CO_2 fluxes from the *Miscanthus* (Campaigns 1 and 2) and the negligible N_2O fluxes throughout the study, it is likely that the *Miscanthus* field was a net sink for GHGs, confirming previous reports (Drewer *et al.*, 2012) which makes *Miscanthus* attractive as a bioenergy crop. These estimates, based upon monthly measurements, assume that the time of day at which samples are taken is representative of the daily mean, in order to generate reliable data.

2.4.3 Measurement frequency and diurnal variation of CO_2 fluxes

High frequency measurements of CO_2 with automated chambers gave a lower estimate of total CO_2 flux from the *Miscanthus* field during Campaigns 2 and 3 than that calculated using monthly measurements. This can be attributed to the inherent bias involved in measuring at discrete intervals. The bias is two-fold: first, in respect to the day on which sampling takes place, and second, regarding the time of day at which measurements are taken. As shown by the hourly data, there was substantial daily variation between fluxes, and also a strong diurnal variation. If the monthly sampling day happens to have particularly high or low fluxes, this would skew the estimate of the flux for the entire month. Perhaps more importantly, by sampling during the afternoon, as was dictated by the logistics of the field work in the current study, the monthly data do not include measurements from the part of the day when fluxes were at their lowest. This led to an overestimation of the total flux from this crop for the two Campaigns during which the diurnal cycle of soil respiration was strongest. During Campaign 1, when the diurnal variation was much less pronounced, there was no difference between the hourly and monthly derived estimates.

A striking characteristic of the hourly CO_2 data is the marked difference in the diurnal cycles between the arable field and the *Miscanthus* field, shown by the mean hourly flux from both fields during Campaign 2. At 05.00 soil respiration in the arable field began to increase, until it peaked at around 15.00. In the *Miscanthus* field, fluxes began to decrease at 05.00 towards a daily minimum at around 09.00. After this time respiration began to increase until it reached the daily maximum in the late afternoon and early evening. Unlike respiration in the arable field, the rate of flux did not decline sharply after peaking, but stayed relatively stable throughout the night. The time of day at which fluxes are measured is crucial, especially if the purpose is to compare fluxes from the two different crops. Measuring between 09.00 and 15.00 will exaggerate the differences between the fields, whereas fluxes between 18.00 and 05.00 are much more similar in both fields. This has implications not only for this study, but any investigation which uses a single daily flux measurement with which to measure an experimental contrast.

There are a huge number of papers relying on a single time point sampling schedules (Barrena *et al.*, 2013, Finocchiaro *et al.*, 2014, Gauder *et al.*, 2012, Jeuffroy *et al.*, 2013, Johnson *et al.*, 2010, Perdomo *et al.*, 2009, Shvaleva *et al.*, 2014, von Arnold *et al.*, 2005, Zhang *et al.*, 2013), which compare fluxes of all or some of CO_2, N_2O and

CH_4 from different land uses or crop types. Some authors acknowledge the importance of selecting the appropriate time for sampling, though most do not. Zhang *et al.* (2013) state that they performed their sampling between 09.00 and 11.00, since that was representative of the daily mean flux; however, they did not measure this themselves, and the reference cited providing this information (Lin *et al.*, 2009), also stated this as a fact without either offering any data to support this claim or a reference as evidence. Likewise, Perdomo *et al.* (2009) state they chose sampling times to be representative of the daily mean, which is also based upon another study which asserts that 10.00- 12.00 is typical of the daily mean flux (Kessavalou *et al.*, 1998), but without any supporting evidence.

The cause of this diurnal pattern in soil respiration was probably the availability of carbon to microbes in the form of root exudates and root respiration itself. Since barley has been specifically bred to be short, the time taken for photosynthate to move through the plant will be shorter than in the much taller *Miscanthus*. It would be expected, therefore, that the amount of labile carbon in each field peaked at a different time, hence the asynchrony in soil respiration patterns. With this in mind, this particularly calls into question studies which compare fluxes under forests with arable or grassland fluxes by using a daily measurement regime. For example, it has been shown that respiration under forests can be uncoupled from soil temperature (Liu *et al.*, 2006).

It is possible that the difference in the diurnal pattern of soil respiration is attributable to the different photosynthetic pathways used by the barley (C3) and the *Miscanthus* (C4). The diurnal pattern of soil respiration of the C4 species maize has also been shown to be dependent on soil temperature (Han *et al.*, 2008), which resembled more closely the pattern seen here under the barley than under the *Miscanthus*. Barley bundle sheath cells move assimilated carbon rapidly to the phloem (Leegood, 2008), which suggests that the translocation of photosynthate to the soil occurs relatively more quickly than may occur in *Miscanthus*.

2.4.4 Environmental controls of GHG flux

2.4.4.1 CO_2

The controls on soil respiration differed between the two fields and, indeed, varied depending on whether monthly or hourly measurements are considered. The clear message is that temperature played a key role in both fields: the close relationship

between soil CO_2 flux and both air temperature (Bouma *et al.*, 1997, Raich & Schlesinger, 1992) and soil temperature (Kane *et al.*, 2003, Kutsch & Kappen, 1997) is commonly reported. Whilst the monthly data indicated that the response of CO_2 flux to temperature was similar in both fields, the automated data revealed differences; soil temperature was the best predictor of flux from in the *Miscanthus* field, air temperature was better for the arable field.

It is notable that monthly CO_2 flux in the *Miscanthus* field was very significantly correlated with solar radiation, but much less so for the arable soil CO_2 fluxes. This relationship was still present in the hourly data, but much less strong. A link with solar radiation is to be expected, since photosynthesis will increase with solar radiation and this, in turn, will increase the availability of carbon substrate for soil. It is clear that there is a fraction of soil respiration that is decoupled from temperature control at this site, which has been shown before in forests (Liu *et al.*, 2006, Makita *et al.*, 2014, Savage *et al.*, 2013), in agricultural systems (Oikawa *et al.*, 2014) and grasslands (Bahn *et al.*, 2009). Carbon supply certainly controls respiration in plant roots (Lotscher & Gayler, 2005, Savage *et al.*, 2013) and since root respiration may account for as much as 50 % of total soil respiration (Bond-Lamberty *et al.*, 2004) it is highly probable that this contributes to the difference in diurnal pattern of soil respiration between the two fields. The time taken for assimilated carbon to be respired from the soil varies between plant species, with transfer through taller vegetation taking longer (Kuzyakov & Gavrichkova, 2010), so it follows that *Miscanthus* photosynthate reaching the soil will peak later in the day than that of barley. Furthermore, the *Miscanthus*, as a perennial crop, has a bigger more established root system, which will provide a greater proportion of total soil respiration than rotation arable crops.

The negative relationship of soil respiration and soil moisture was consistently seen in both the monthly and hourly data, and can be explained by increasing moisture limiting O_2 availability for respiration.

2.4.4.2 N_2O

N_2O fluxes were positively correlated to soil temperature in both fields, as might be expected, and whilst concurrent air temperature was also positively related to flux in the arable field, there was no relationship with concurrent air temperature and N_2O fluxes from the *Miscanthus* field. The minimum daily air temperature was significantly related to fluxes from both fields, and the conclusion to be drawn is that on warmer

days the soil environment is more favourable to microbes producing N_2O, be that through nitrification or denitrification. The strong positive relationship between N_2O flux and solar radiation in the arable field was somewhat unexpected. It may be explained as the product of heterotrophic denitrification, which requires a carbon source (Firestone & Davidson, 1989). It follows that increased solar radiation will stimulate more photosynthesis and therefore an increase in carbon substrate for denitrifiers. The lack of such a relationship in the *Miscanthus* field can be attributed to the low fluxes in this field, with the drier soil conditions not favouring denitrification coupled to lower N availability.

There was a negative relationship between N_2O flux and soil moisture in both fields. This is somewhat surprising if the predominant process through which N_2O is produced is denitrification as suggested from the apparent relationship with root carbon supply; N_2O would be expected to increase with soil moisture through the creation of more anaerobic conditions and therefore favour N_2O emission. An alternative conclusion might be that the N_2O emissions at this site are driven by nitrification and so increasing soil moisture reduces oxygen availability and thus inhibits N_2O production. In actuality the soil in this study was often over or near field capacity. The soil at this site has previously been assessed as having a bulk density of 1.5 g cm^{-3} (Case *et al.*, 2014) which, if a particle density of 2.65 g cm^{-3} is assumed, gives a porosity of 57%. A volumetric soil moisture content of 0.57 m^3 m^{-3} therefore approximates to 100 % water-filled pore space (WFPS); maximum N_2O production through denitrification is known to occur at around 70% WFPS (Bateman & Baggs, 2005, Rabot *et al.*, 2015), which in this soil equates to *ca.* 0.4 m^3 m^{-3} soil moisture. Above this water level N_2O production generally declines, and fluxes can become negative due to complete reduction of N_2O to dinitrogen gas (Chapuis-Lardy *et al.*, 2007), which may explain the lowest N_2O fluxes seen at this site in the wettest soil conditions.

2.5 Conclusions

Trace gas fluxes were greater from the soil in the arable field than from the *Miscanthus* field. The greatest contribution was from CO_2 in both fields, yet this is likely to have been at least offset by photosynthesis. To confirm this, it is essential that NEE of CO_2 be quantified for both crops, which is beyond the capability of traditional chamber techniques. N_2O made a substantial contribution to the total GHG flux from the soil in the arable field but not in the *Miscanthus*, which did not receive any nitrogen fertiliser. N_2O emissions have the potential to transform a net GHG sink into a net source, and this will have fundamental implications should it become general practice for fertiliser to be applied to bioenergy crops.

Automated measurements show that soil respiration exhibits a distinct diurnal pattern which differs between fields, and it is inferred that this is due to the covering vegetation type. This calls into question any comparison between fluxes from different land uses or crop types which is based upon single daily measurements. In order to have confidence in such comparisons it is absolutely essential that the underlying diurnal pattern of flux is established in order to ensure that measurements are made during the period that is best representative of the daily mean.

Whilst this study has shown the diurnal pattern in soil CO_2 flux, no such data were collected to establish whether a similar cycle took place for either N_2O or CH_4 at this site. It remains a crucial question which needs to be addressed: do all trace gas fluxes exhibit a diurnal pattern? Without this knowledge any such research from which GHG inventories are derived, or upon which policy is made, must be questioned. It is possible that estimates of flux which are extrapolated to the regional, national or global scale may also, consequently, be inaccurate. The need for continuous, or near continuous measurement systems for trace gas monitoring is clear and immediate.

3 Skybeam: a novel automated chamber system for high frequency measurement of the net ecosystem exchange of three trace gases

3.1 Introduction

One strategy for reducing GHG emissions to the atmosphere is to replace fossil fuel combustion with that of biomass (DECC, 2011, Rowe *et al.*, 2009). This relies on the principle that the CO_2 emitted to the atmosphere from biomass combustion is in equilibrium with the CO_2 drawn down by the plant as it was growing, thus having no net loading effect on the atmosphere. In order to fully account for the GHG budget of energy produced in this manner, a full life cycle assessment (LCA) must be conducted (Kaltschmitt *et al.*, 1997), which will quantify the net effect on GHGs for each stage of energy production. In addition to the growing stage, this will include other steps e.g. direct emissions from agricultural vehicles used for sowing and tending the crops in the field, harvesting the crop, transportation to its place of combustion, and any intrinsic emissions from downstream processing and fertiliser manufacture. Whilst EU assessment of global warming potential (GWP) of bioenergy production accounts for the consequences of many of these stages, it is only through quantification of further indirect processes, such as indirect land use change (iLUC) that the total net balance can be assessed, which is referred to as consequential LCA (CLCA) (e.g. Styles *et al.*, 2015).

One of the attractions of *Miscanthus* as such an energy crop is its low demand for N fertiliser (St Clair *et al.*, 2008), due to its efficiency at recycling nutrients from above ground biomass and storing them below-ground in its rhizome when it senesces over winter (Strullu *et al.*, 2011). Various studies have investigated the effect of fertiliser on *Miscanthus* yields, with mixed results, with some authors reporting increased yields (e.g. Larsen *et al.*, 2014, Smith & Slater, 2010) and others no effect (see Maughan *et al.*, 2012, Teat *et al.*, 2015). In Chapter 2 of this thesis it was shown that unfertilised *Miscanthus* had a smaller soil-GHG footprint than an arable crop grown at the same site, largely due to the high N_2O fluxes seen from the fertilised arable crop. However, if agricultural practices alter, and it becomes common practice to apply fertiliser to energy crops, it may fundamentally change the GHG balance of producing that crop, and therefore negate any gains in GHG emission from bioenergy production.

Diurnal patterns in soil respiration were demonstrated in the previous Chapter. Furthermore, this diurnal variation was different between fields under different crops at the same site and it is possible that similar diurnal patterns exist in N_2O and CH_4 fluxes. If there is no such variation, then measuring fluxes once a day, at any time, will give data sufficiently accurate to produce an estimate representative of cumulative flux from a system. If, however, there are diurnal variations in these fluxes, it is vital that flux measurements are taken regularly enough to account for this diurnal pattern, to eliminate bias, or to ensure measurements are taken at a time when fluxes are typical of the daily mean. Ideally flux data would be collected continuously over the long term to produce reliable GHG budgets for bioenergy production.

The need for continuous ecosystem gas flux data has led to the development of the eddy covariance (EC) technique, which quantifies net ecosystem-atmosphere gas transfers (commonly CO_2) over a comparatively large area, typically hundreds of square metres; (see Baldocchi & Wilson, 2001, Reichstein *et al.*, 2003). Whilst the development of this technique has advanced *in situ* estimation of ecosystem-atmosphere CO_2 exchanges, the technique cannot be used for quantification of exchanges at normal field trial or plot scales because of stringent 'fetch' requirements. The importance of being able to measure at the plot or management unit scale becomes clear when consideration is given to how trace gas fluxes can be managed though land use. It is at the management unit scale (e.g. methane production from cattle pastures) rather than at the landscape scale (e.g. agricultural land as a whole) that land management with beneficial GHG balances will be achieved. It is only when one attempts to find an appropriate location for an EC system that these stringent site requirements reveal how few sites across a typical landscape are actually appropriate for EC measurements; fences & hedges, streams, small hills, buildings, trees and human activity are all to be avoided, biasing location and, hence, attempts to up-scale.

Additionally, there is still active debate about some of the assumptions upon which the EC technique relies (see, for example, Mahrt, 2010) and the technique is still far from routine for monitoring the major GHG gases besides CO_2. Increasingly, we need measurements at smaller 'field' scales, enabling flux comparisons across heterogeneous landscapes or gradients (e.g. pastures, wetlands, water bodies) and across field manipulations (e.g. N additions, warming, elevated CO_2).

Mass balance approaches can rarely be used to quantify C or N flux differences, particularly under field conditions, because they invariably require the detection of a small change against a background of a large ecosystem stock (see, for example, Heath *et al.*, 2005). In a number of limited circumstances, stable isotopes can be used to detect these changes (e.g. ^{15}N dilution; C_3 plants in C_4 soils, after Ineson *et al.*, 1996) but not without disturbance of the systems under study. In contrast, chamber methods can detect quite subtle changes in net C and N balance and can also be used to identify underlying controlling factors, such as rainfall events and weather fronts. Initial comparisons of flux estimates made using EC and chamber methods have yielded similar results (e.g. Laine *et al.*, 2006), but the confounding influence of spatial and temporal heterogeneity actually make such direct comparisons very difficult. Burrows *et al.* (2005) have shown the clear value of automated chambers for determining CO_2 flux estimates at high frequency, but automated chambers frequently present problems of power supply, centralised gas analysis, expensive multiplexing, and, critically, they cannot be easily applied to tall vegetation. Whilst existing automated chamber systems such as that made by Licor can measure fluxes from over short (10 cm) vegetation, no such system yet exists that can provide the same data from perennial grasses used as bioenergy crops, e.g. *Miscanthus x giganteus,* which grow to heights in excess of 3 m. Establishing automated chambers in large numbers across spatially separated plots is prohibitively expensive and there is an urgent need for techniques to enable alternative automatic effective NEE and GHG measurements at the plot scale.

Here, a novel automated system is presented. The system is called SkyBeam and has been designed as a single chamber, which can automatically move repeatedly to the same points within a crop, then closing to make a flux measurement. The chamber is large enough to measure from over vegetation as tall as 3 m, ensuring that the flux measurements delivered are NEE and not just soil derived fluxes. By using a clear chamber photosynthesis may continue, and using a short chamber closure ensures that the crop is exposed to ambient conditions for as much of the study period as possible. Circulating the headspace gas through multiple analysers allows the quantification of NEE of the three most important biogenic GHGs from a single chamber closure. The system was deployed to measure GHG fluxes from *Miscanthus x giganteus* in late spring 2013 and was in operation until December of that year. That particular year the farmer elected to apply a green waste compost to the crop, and SkyBeam allowed the effects of compost addition on the GHG balance to be investigated in a fully replicated experimental contrast.

3.2 Methods and materials

3.2.1 Site description

The following work was undertaken at a working farm in the East Midlands of the United Kingdom (UK), within a field producing *Miscanthus x giganteus* (henceforth *Miscanthus*) at the same site as described in Chapter 2 of this thesis. The *Miscanthus* field was used for production of a crop which ultimately would be used to produce electricity by direct combustion of the biomass at Drax power station in North Yorkshire, UK. The crop was harvested each spring, during March or April, and the crop regrew during May-June growing rapidly until October. The crop was allowed to senesce over winter before being harvested the following spring, thus completing the annual cycle. The *Miscanthus* crop had been planted seven years previously and had not received any fertiliser for at least the two years prior to this experimental work and the soil type has been defined as of Beccles 1 association (Drewer *et al.*, 2012), fine silt over clay. In spring 2013 the field was harrowed in an attempt to redistribute the rhizomes more evenly, with a view to improving yield. In July 2013 the field received an application of a green compost, consisting largely of wood waste, at a rate of 4 T ha^{-1}. The part of the field in which this work was conducted was deliberately excluded from receiving compost, but this was added shortly after in a controlled experiment.

3.2.2 Trace gas flux measurements

3.2.2.1 SkyBeam design

SkyBeam, an automated chamber system, was developed at the University of York by the Electronic and Mechanical Engineers at the Department of Biology. Testing of the system was initially undertaken on the University of York campus and, subsequently, at the field site in Lincolnshire, prior to commencing experimental work (see Appendix A).

The design of the SkyBeam consisted of a single chamber suspended from a trolley, mounted on a gantry comprising a rigid aluminium beam and two pairs of scaffolding towers for support (Figure 3.1). The gantry was built to a height of 6 m to allow for clearance above a fully grown *Miscanthus* crop of 3 m. Suspending the chamber from a beam allowed repeated measurements to be taken from preselected points along a transect directly underneath the beam. A 10 m beam allowed for six separate measurement positions to be sited under the system.

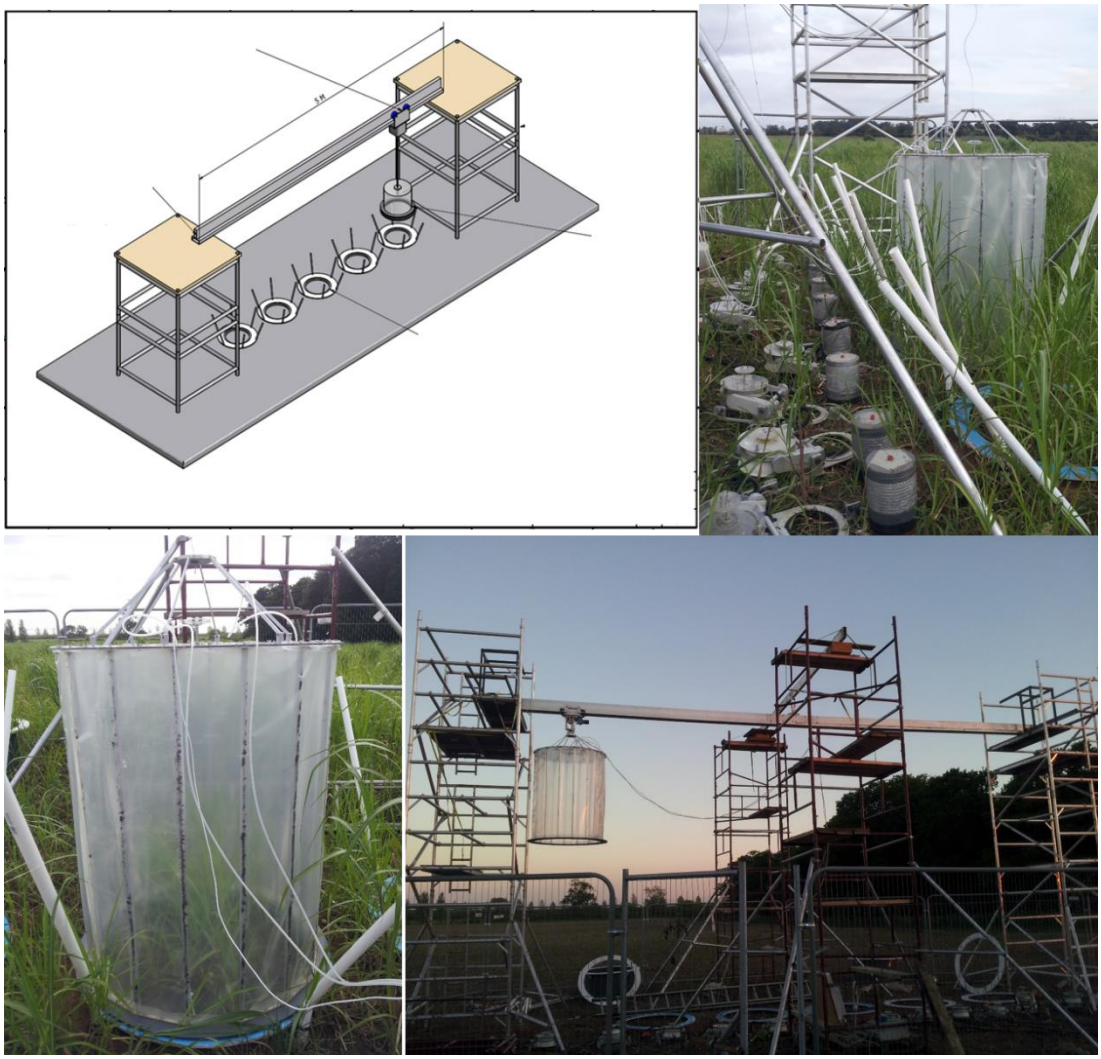

Figure 3.1 The design, construction and deployment of SkyBeam. The initial design (top left) illustrates the concept of a single chamber suspended over the area to be measured. The chamber was mounted on a trolley which traversed the beam in order to repeatedly measure the same positions. A hoist lowered the chamber and raised it on completion of a measurement. The final design (bottom right) included an additional pair of scaffold towers with a secondary beam perpendicular to the main beam, for supplementary support. The height of the main beam was 6 m and it spanned 10 m, allowing for 6 measurement positions. Accurate landing was achieved with guide rods (bottom left) which were customised white PVC pipes. Within the plot surrounding each landing base, collars were installed for measurement of soil respiration using Licor automated chambers, and manual static chambers for CH_4 and N_2O fluxes (top right). Here manual chambers can be seen *in situ*, whilst the automated chambers have been removed from the collars for the manual measurements to be made.

A single measurement consisted of the chamber being lowered over the designated position for a specified length of time, before being raised at the end of the measurement, at which point the trolley moved to the next position and the process repeated. The automation of the system was achieved by developing an interface with a Licor system (LI-8100, Licor, Lincoln NE USA), which used an infrared gas analyser (IRGA) and automated chambers to measure soil CO_2 fluxes. Here the IRGA controlled the opening and closing of the large SkyBeam chamber (through raising and dropping), which replaced the very much smaller normal Licor-built automated soil flux chambers. The system was a dynamic closed-chamber system, where the headspace gas continually circulated via a 10 m length of polyethylene tubing (Bev-A-Line IV, Cole-Parmer, London UK) through the analyser throughout the chamber closure period. The Licor software was used to program the length of chamber closure and the number of observations to be made during an experimental run. The Licor software also calculated the CO_2 flux, and full details of the equations used are published the instrument's manual, following Healy *et al.* (1996). SkyBeam's firmware was developed to be fully programmable in terms of the number of landing positions (replicates) and the sequence in which they were sampled, permitting the adoption of flexible, randomised experimental designs.

The trolley used for the lateral movement of SkyBeam and the winch for vertical movement were powered using a 12 V DC supply, for ease of use in field environments. Additional analysers, such as the LGR CH_4 and N_2O analysers (Los Gatos Research, CA USA) used during the field campaigns in Lincolnshire required mains electricity (230 V AC), supplied from marine batteries and inverter charged from a diesel generator. The generator was situated so that the prevailing wind removed emissions from the study area, so as not to interfere with any of the eddy covariance (EC) measurements being taken at the site. In addition a conditional 'start' module was programmed to prevent generator operation if the wind direction was unsuitable.

The position of the SkyBeam trolley was determined and controlled through the use of 'location' magnets positioned on the underside of the beam. Sensors on the trolley were triggered when they passed a magnet, which was placed above each of the specific location points to be measured. The 'drop' distance required for each sampling position was programmed during the initial setting of the system, and relied on the time taken for the chamber to descend to the correct height.

3.2.2.2 SkyBeam chamber design

The chamber design was a cage-like structure, with a circular clear Perspex roof for the chamber sitting on top of a framework of vertical aluminium rods (Figure 3.2). The dimensions of the chamber were 1 m internal diameter and 1.5 m in height; extensions were built to accommodate the growing crop, but were unnecessary due to poor crop growth that year. The base of the chamber was a flat circular acrylic flange and the walls of the chamber were formed by stretching clear 720 gauge (180 µm) polythene (Cat No. PM0026, First Tunnels, Barrowford, UK), around the framework, sealed using fibreglass tape.

Pressure inside the chamber was equalised with ambient pressure through the inclusion of a vent, after Xu *et al.* (2006). Pressure was monitored by the Licor system for accurate flux calculation and gas concentrations were also adjusted for temperature, which was measured using a thermistor within the chamber headspace. The landing bases consisted of flat circular flanges on which the bases of the chamber sat (Figure 3.2) and three concentric rings of rubber seal were fixed to the base of the chamber to ensure an airtight seal when the chamber was closed. Bases were positioned on the soil surface and packed with fine building sand to form a seal with the soil.

3.2.2.3 Gas measurements and flux calculations

The SkyBeam chamber was deployed from June to December 2013, and was programed to close for 10 minutes per measurement, with a delay separating each measurement as the chamber moved between positions, to allow the gas lines to purge with ambient air. CO_2 fluxes from the SkyBeam system were calculated using the internal Licor software, with a 'dead band' of 30 seconds to allow for mixing. The flux was calculated as a linear regression over two minutes, which was found to best describe the instantaneous flux at the time of closure. Regressions over a longer period saw CO_2 concentrations approach an asymptote, especially during daylight measurements and, therefore, an underestimate of the flux.

CH_4 and N_2O fluxes were measured over two campaigns of approximately two weeks each (between July and October 2013) during the study. During these periods, two cavity ring down laser (CRD) analysers- a fast GHG analyser for CH_4 and an N_2O analyser (Los Gatos Research, CA USA)- were incorporated into the SkyBeam assembly, drawing the headspace gas from the exhaust of the IRGA before returning it to the chamber (see Appendix B). Both CRD analysers measured at 1 Hz, and

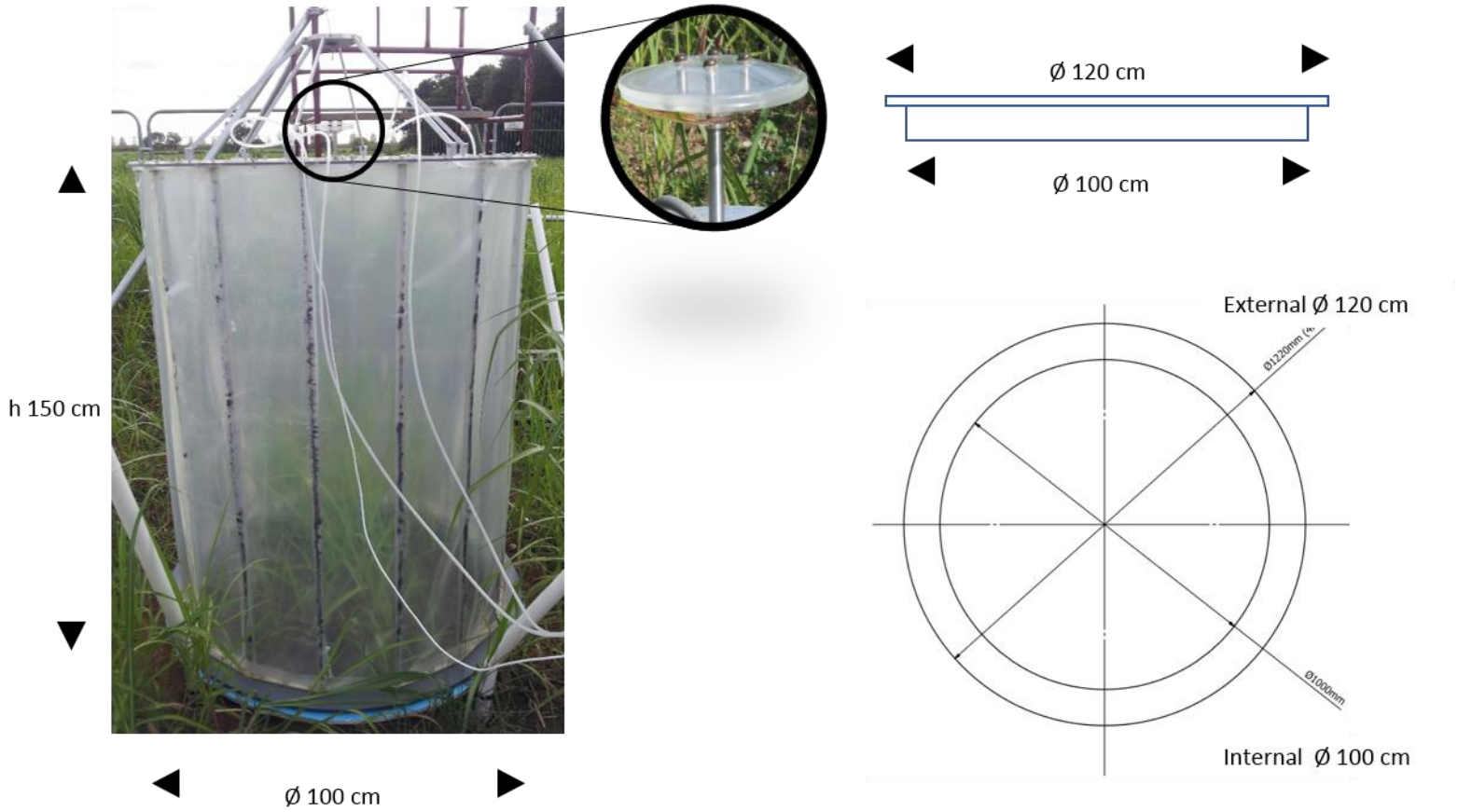

Figure 3.2 Design of the SkyBeam chamber and landing bases. The chamber stood 1.5 m tall with an internal diameter of 1 m (left). Internal pressure was equalised with ambient using a vent (inset, centre), and the landing base comprised a flat circular flange and a perpendicular collar, whose sides were vertical *viz* the soil surface (top right: side profile, bottom right: top profile).

fluxes were calculated as the linear regression of the change in concentration over time during the period 200 to 440 seconds following chamber closure. Fluxes were adjusted for chamber temperature volume and area. Further adjustment was made to the CO_2 fluxes during daylight hours based upon the light attenuation of the chamber material, after Heinemeyer *et al.* (2013) (Appendix C).

3.2.2.4 Soil trace gas fluxes

Soil respiration was measured using an automated chamber system with an IRGA (LI-8100-101 chambers, Licor, Lincoln NE) from the same plots as used by the SkyBeam system. Two collars were placed within each of six plots, and were inserted to a depth of 2 cm. For a full description of the measurement protocol see Chapter 2 of this thesis. CO_2 fluxes were calculated using the linear regression function within the Licor internal software. Soil N_2O and CH_4 fluxes were measured using manual static chambers placed over the same collars used by the automated respiration chambers, approximately once a month. The protocol used is outlined in Chapter 2 of this thesis.

3.2.2.5 Eddy covariance measurements

An eddy covariance (EC) tower was sited within the same *Miscanthus* field as the SkyBeam system, under the stewardship of Centre for Ecology and Hydrology (CEH). The system measured CO_2 concentration at a rate of 10 Hz and CO_2 fluxes were integrated as 30 minute averages (EddyPro, Licor, Lincoln NE), producing data for the net ecosystem exchange (NEE) of CO_2.

3.2.3 Experimental design

3.2.3.1 Compost addition

The experimental area was selected following harvest of the *Miscanthus* crop and subsequent harrowing of the field in spring 2013. Six plots were demarcated, each containing one landing base for the SkyBeam system (Figure 3.4). The emerging shoots across the field were surveyed and plots were sited in an area representative of the field. Two 20 cm diameter collars were installed within each of the six plots, to be used by automated chambers and for manual flux measurements (Figure 3.4). Automated chambers were deployed during May 2013, and the first manual measurements were made the same month.

Figure 3.3 Aerial view of experimental site. Arrow marked “N” indicates the direction of North. The prevailing wind direction is denoted by the elongated arrow. The circle in the north-eastern region of the field shows the location of the EC system, and the rectangle in the northwest corner is the SkyBeam system. The square containing “G” symbolises the diesel generator for powering the equipment. The northern half of the western boundary of the *Miscanthus* field was bordered by a mature deciduous wood, exceeding 10 m in height. The southern half of the western boundary was adjacent to another *Miscanthus* field, as was the western half of the south boundary. The neighbouring field at the eastern half of the south boundary was dedicated to conventional arable crop rotation (barley and oilseed rape during the experimental period), as were the two fields to the north of the *Miscanthus*. The entire eastern side of the *Miscanthus* was bordered by a short rotation coppice stand which was approximately 3 m tall during the study.

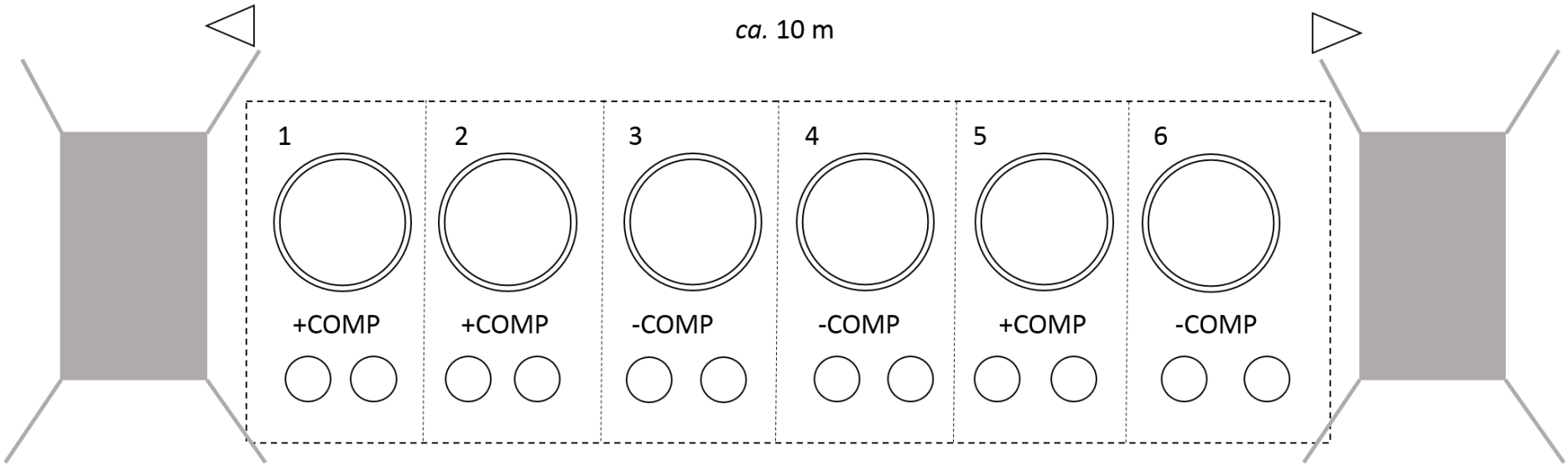

Figure 3.4 Overhead schematic of the plots beneath the SkyBeam system. Dashed lines show the margins of each plot. Plot numbers are indicated, and the treatment they received: +COMP= with compost, -COMP= control. The large circles represent the SkyBeam landing bases, and the small circles represent the collars used for manual and automated chambers. Grey shaded areas represent support towers. Not to scale.

In July 2013 a green compost was applied (5 T ha^{-1}) to the soil surface *Miscanthus* field at large; a subsample of this compost was taken and well mixed and applied to the experimental plots by hand, at an equivalent rate, a few days later. The compost consisted of decomposed woody material composed of pieces smaller than 5 cm to fine sawdust-like particles and included timber and included timber and composite materials. It was hypothesised that the addition of compost would increase the soil moisture and availability of nitrogen (N), and so would stimulate production of N_2O. Plots were therefore paired according to the flux of N_2O prior to compost application, and one plot within each pair was designated at random to receive compost (+COMP), the other kept as a control (-COMP). Biomass was harvested by hand at the end of the measurement period in spring 2014. Vegetation from within each plot was cut at height analogous to mechanical harvesting, and dried at 70^{o}C until at constant weight.

3.2.3.2 Methodological comparison

The presence of a CO_2 EC system within the *Miscanthus* provided the opportunity to directly compare the measured NEE of CO_2 using both the SkyBeam and EC techniques. Automated chambers delivered high frequency measurements of soil respiration, which enabled the assumptions regarding night time fluxes made during EC data processing to be investigated.

It was further hypothesised that there would be a significant difference between the total estimated flux of N_2O and CH_4 made using manual chamber data and high frequency NEE measurements from SkyBeam.

3.2.3.3 Partitioning of carbon fluxes

Both the EC system and SkyBeam delivered NEE of CO_2, and for the purposes of this analysis, NEE is defined as

$$NEE = R_{eco} - \text{photosynthesis}$$

where R_{eco} is ecosystem respiration. R_{eco} can be defined as

$$R_{eco} = R_a + R_h$$

where R_a is autotrophic respiration and R_h is heterotrophic respiration. However, in this study, in the absence of root exclusion collars, R_{eco} can only be partitioned into

soil respiration (R_{soil}) and above ground autotrophic respiration (R_{plant}). So we can define R_{eco} as

$$R_{eco} = R_{soil} + R_{plant}.$$

However, during the night, no photosynthesis occurs, thus

$$NEE = R_{eco}.$$

For the purposes of analysis, night is defined here as any period with PAR levels of zero. The night time data from the automated soil chambers under SkyBeam were used to establish the relationship between R_{eco} and R_{soil}, which was then extrapolated to day time data and the derived values for day time R_{eco} were used to estimate photosynthesis. The relationship between day time and night time R_{eco} was used to estimate day time values for R_{eco} from the EC data, which allowed a further calculation of photosynthesis to be made.

3.2.4 Environmental variables

Soil moisture and temperature were measured within each of the six experimental plots using SM200 moisture probes and ST1 temperature sensors, and logged as hourly averages on GP1 and DL2 dataloggers (Delta-T, Cambridge, UK). Meteorological data (air temperature, solar radiation and humidity) were recorded as hourly averages using an onsite weather station (WP1, Delta-T, Cambridge, UK). Rainfall data were retrieved from the Met Office weather station *ca.* two miles from the site, and additional measurements of air temperature, and solar radiation were measured and provided by CEH concurrently with the EC measurements.

3.2.5 Data processing

All statistical analyses were performed using SAS (SAS 9.3, SAS Institute, NC USA). Gas fluxes were calculated by linear regression, and cumulative fluxes were estimated from trapezoidal integration. Repeated measures analysis of variance in fluxes between compost treatments were conducted using mixed effects models. Graphs were produced using Sigmaplot (Sigmaplot 12.3, Systat software, IL USA).

3.3 Results

3.3.1 NEE data from SkyBeam

3.3.1.1 CO_2

At the beginning of the study during June 2013 fluxes of CO_2 from the *Miscanthus* remained positive throughout the whole day (Figure 3.5). From July onwards fluxes increased, both negative and positive: negative fluxes are defined as a flux from the atmosphere to the ecosystem and were seen during the daylight hours as the crop photosynthesised, and positive fluxes were seen during the night when photosynthesis halted (Figure 3.6). Negative fluxes steadily increased through the summer to a maximum of *ca.* 2500 mg m^{-2} h^{-1} from the amended plots (+COMP) and more than 3000 mg m^{-2} h^{-1} from the control (-COMP) plots, which occurred during late September 2013. Highest emissions of CO_2 were seen during August for both treatments and were *ca.* 3000 mg m^{-2} h^{-1} and 3500 mg m^{-2} h^{-1} for +COMP and -COMP respectively, though generally during this time the daily maximum fluxes were between 1000 and 2000 mg m^{-2} h^{-1}. Fluxes decreased in magnitude through autumn into the winter, tending towards zero by December, though there were still isolated occurrences of negative NEE which indicates that there was still some photosynthetic activity at this time. There was no significant effect of compost addition on the daily mean CO_2 flux ($F_{[1, 455]}$= 1.27, p= 0.26).

The cumulative NEE of CO_2 shows that for both treatments the *Miscanthus* was a net source of carbon emissions (Figure 3.7). Daily total fluxes of NEE were exclusively positive for July and the first week of August for both treatments. During the second week in August there were isolated days where the net CO_2 flux was negative, initially in the -COMP plots, but by the middle of the month both treatments were increasingly taking up more CO_2 than they were emitting over the course of a day (Figure 3.7, top panel). Through September there were more days of net uptake, particularly in the second half of the month. These days slowed the cumulative emission of CO_2, particularly in the -COMP plots, and over the last few days of September into the beginning of October the system was accumulating carbon in both treatments, demonstrated by the decrease in the cumulative NEE of CO_2. There were no data collected between 2nd October and 9th November, and so the periods either side have been treated as separate. It is entirely possible that had data been collected during this interval the system would have been shown to be a net sink for CO_2. At the end

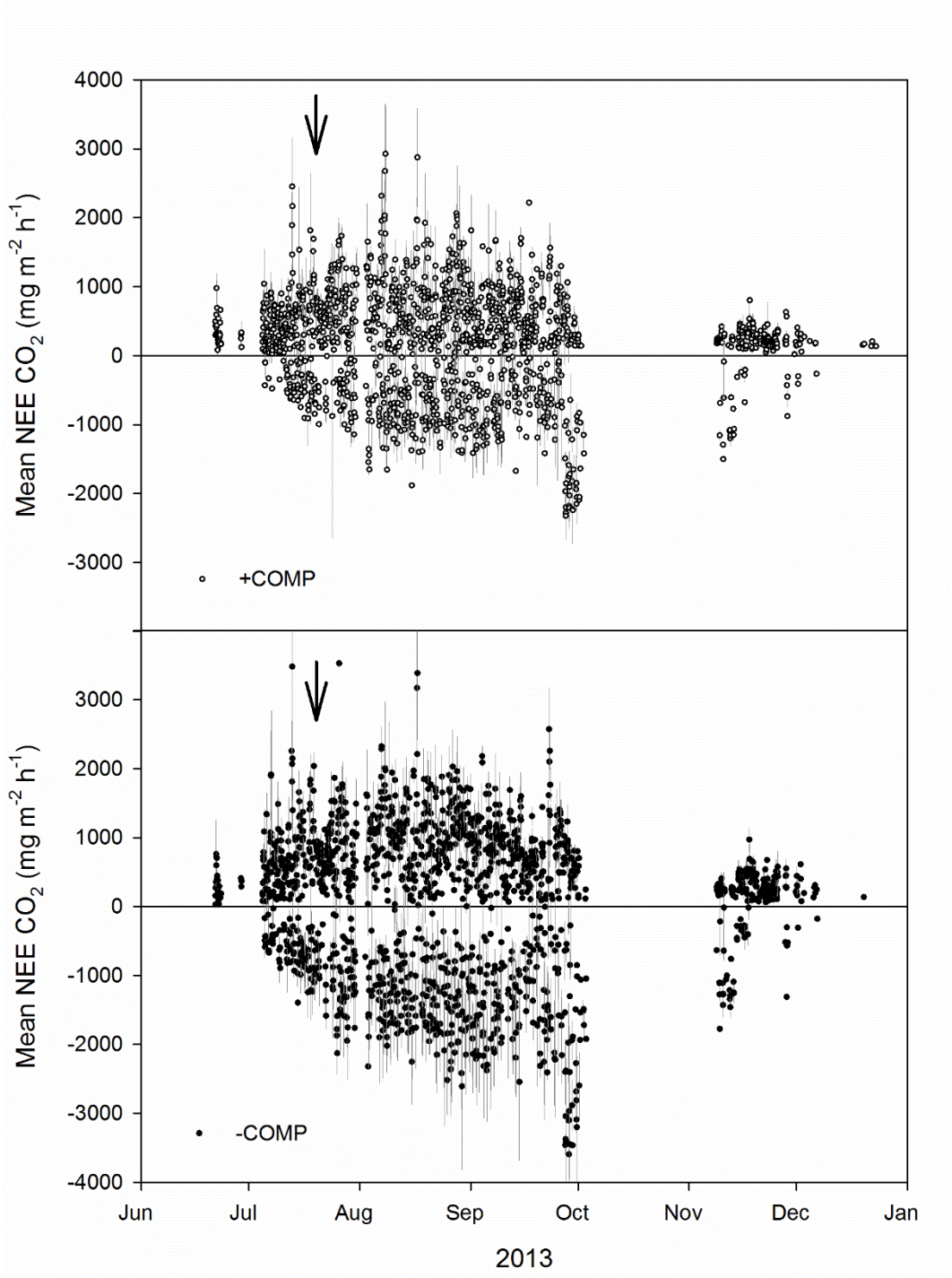

Figure 3.5 Mean ± 1SE (n=3) net ecosystem exchange (NEE) of CO_2 from over *Miscanthus* measured using the SkyBeam system approximately hourly. Top panel shows fluxes from plots amended with green compost (open symbols) bottom panel shows unamended plots (closed symbols), vertical arrows indicate timing of addition. Negative fluxes indicate uptake and positive fluxes emissions.

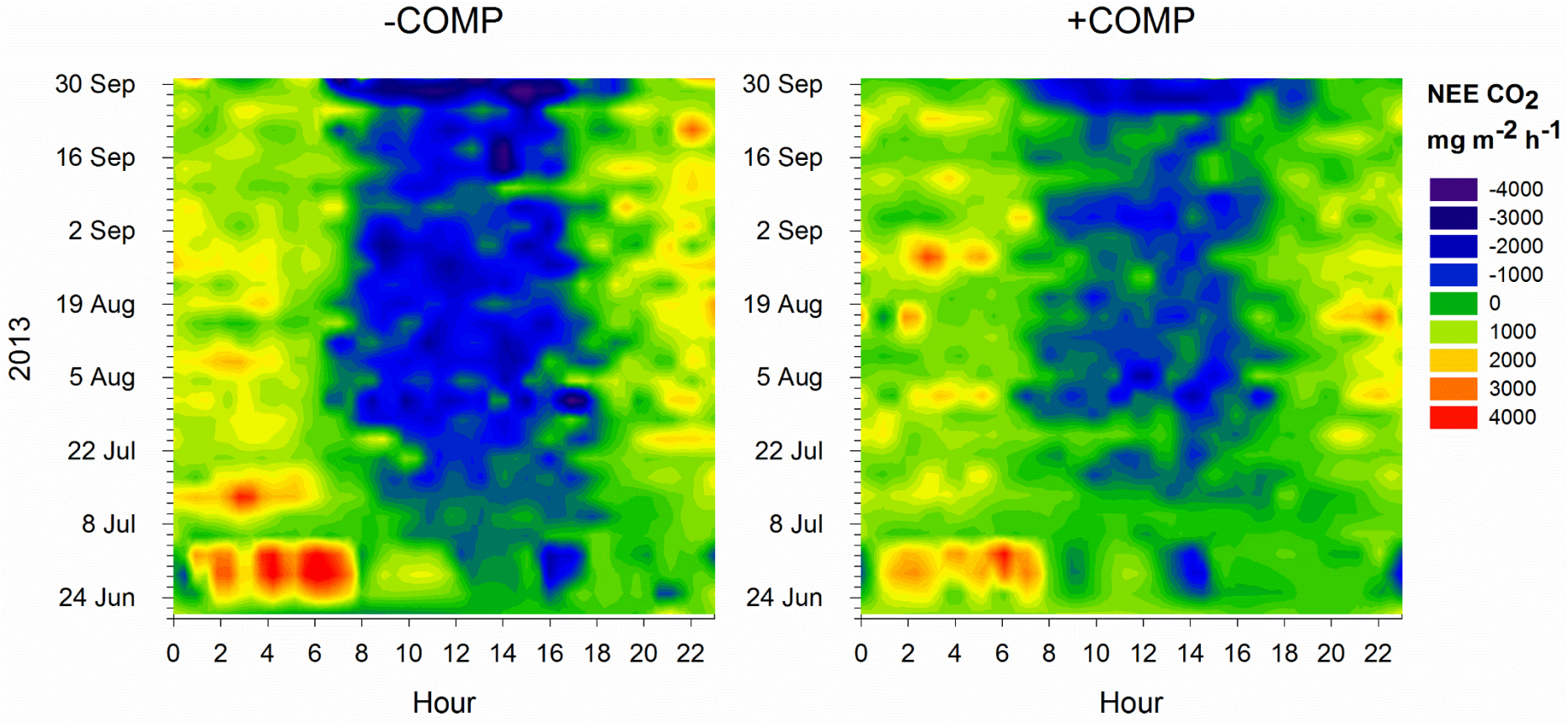

Figure 3.6 Fingerprint map of NEE CO_2 measured using SkyBeam over *Miscanthus* during summer 2013. Measurements were taken from a compost addition experiment, with plots amended with compost (+COMP, right hand panel) or un-amended controls (-COMP, left hand panel). Fluxes varied with time of day (horizontal axis) and time of year (vertical axis). Negative values indicate net uptake of CO_2 and positive values net release.

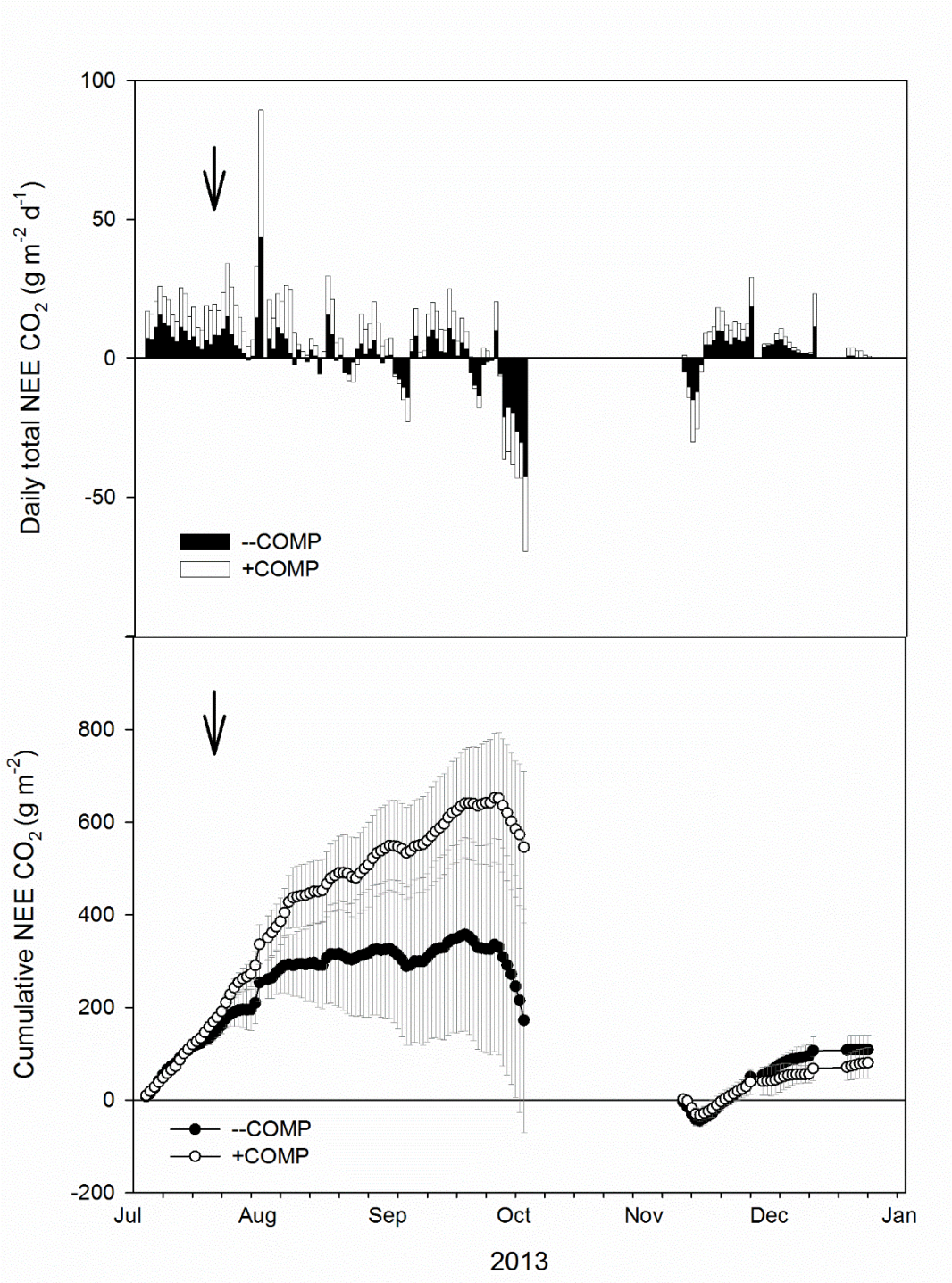

Figure 3.7 Mean ± 1SE (n=3) cumulative NEE (bottom panel) and daily total flux (top panel) of CO_2 from *Miscanthus* measured using SkyBeam. Plots were either amended with green compost (+COMP) or un-amended (-COMP), vertical arrows indicate timing of application. Due to the absence of data for October, the cumulative fluxes are calculated as two separate periods.

of the first period the total NEE of CO_2 was 172 ± 241 g m^{-2} for the -COMP plots and 546 ± 164 g m^{-2} from the +COMP, indicating that at this point in the growth cycle the *Miscanthus* was a net source of carbon emissions. When data collection recommenced in the second week of November the crop was still photosynthesising, to such an extent that the daily net fluxes were negative, for both the -COMP and +COMP. Within a week, however, net daily fluxes were positive, and by the end of the study the system was a net source for both treatments, with total emissions of 108 ± 31 g CO_2 m^{-2} $period^{-1}$ and 80 ± 33 g CO_2 m^{-2} $period^{-1}$ from the –-COMP and +COMP plots respectively. The total NEE of CO_2 was not significantly different between compost treatments for either the period July to October ($t_{[2]}$= -0.92, p= 0.45), or the period November to December ($t_{[2]}$= 0.48, p=0.68).

3.3.1.2 N_2O

N_2O fluxes were initially small (< 100 µg m^{-2} h^{-1}, Figure 3.8). In fact, the majority of fluxes from both treatments were negative, indicating net uptake of N_2O by the system. Six days after measurements began, there was a short-lived period of large N_2O emissions from both treatments, peaking at *ca.* 1500 µg m^{-2} h^{-1} in the –-COMP plots and more than 2000 µg m^{-2} h^{-1} in the +COMP. This period of emission coincided with a day of heavy rain (more than 7 mm) on the 21st July 2013, which was the first precipitation in more than two weeks at the site (Figure 3.8, top panel). Within 48 hours the previous pattern of small and negative fluxes resumed. A similar, though much smaller, burst of positive N_2O fluxes occurred around September 11th 2013, following several days of rain preceded by a prolonged dry period. Fluxes during the second period of measurements were smaller (-100 to 100 µg m^{-2} h^{-1}), and predominantly negative for both treatments (Figure 3.8).

The two measurement periods were analysed separately. There was a significant effect of compost addition on individual rates of N_2O flux during the first period ($F_{[1,4]}$= 8.64, p< 0.043), with fluxes being higher from the +COMP plots. Fluxes significantly differed ($F_{[352,1380]}$= 10.32, p<0.0001), but there was no interaction between treatment and time. There was no effect of compost on NEE of N_2O during the second period of measurements.

During the first measurement period the *Miscanthus* was a net source for N_2O, but a net sink in the second period from both treatments (Figure 3.9). Whilst the total NEE from the +COMP plots tended to be higher, the total flux was not significantly different

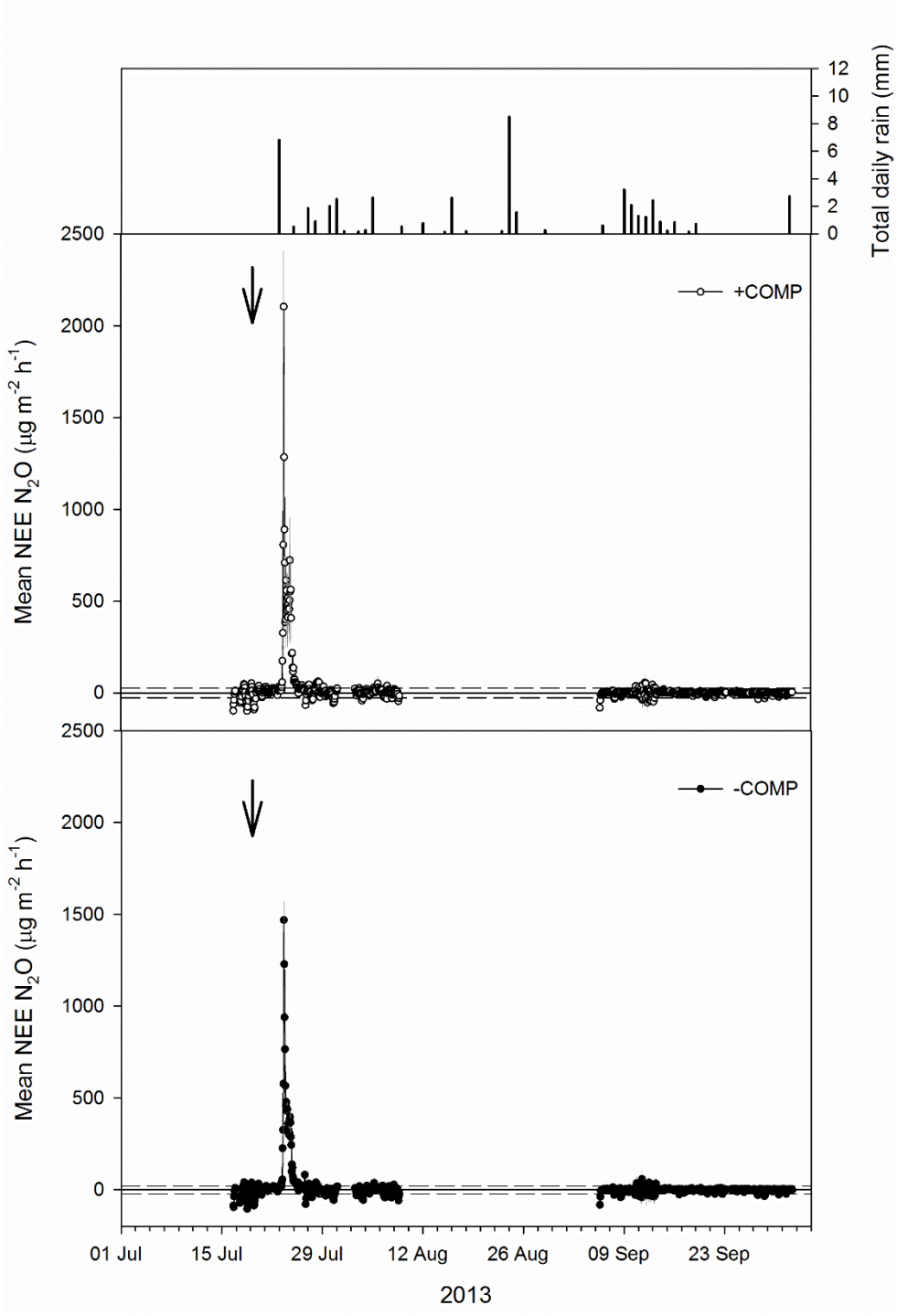

Figure 3.8 Mean ± 1SE (n=3) NEE of N_2O from *Miscanthus* following a compost addition measured using the SkyBeam system. Unamended plots (-COMP, closed circles) are shown in the bottom panel, amended plots (+COMP, open circles) in the top panel. Measurements were made approximately hourly. Negative fluxes indicate uptake of N_2O and positive fluxes release and the dashed horizontal lines represent an estimated detection limit for N_2O flux, based on Cowan *et al.*, (2014). The total daily rainfall for the study period is shown in the top panel. Vertical arrows indicate timing of compost addition.

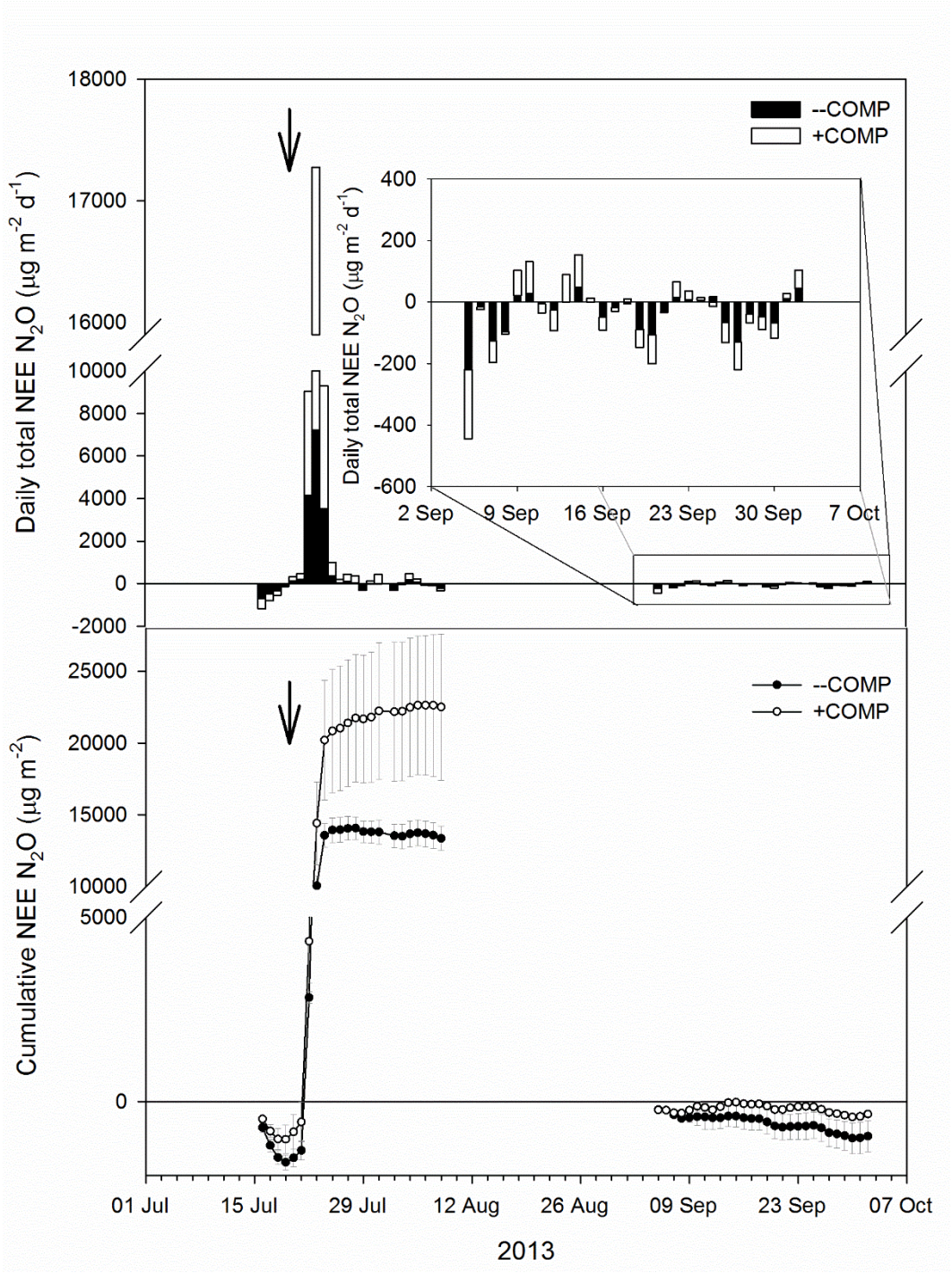

Figure 3.9 Mean (± 1SE, n=3) cumulative (bottom panel) and total (top panel) NEE of N_2O from *Miscanthus* measured using SkyBeam, following a green compost addition. Open symbols represent amended plots (+COMP) and closed symbols untreated controls (-COMP), vertical arrows denote timing of compost addition. Note the break in the axes on both panels. For clarity the daily totals from the second period of measurements has been expanded (top panel, inset). Negative fluxes indicate uptake, positive fluxes emission.

at the end of either period. Negative and positive daily totals of NEE were seen during both periods, but the cause of the *Miscanthus* being an overall net source for N_2O over the first period was attributable the aforementioned three day period of high fluxes from 21-23rd July 2013 (Figure 3.9).

3.3.1.3 CH_4

CH_4 fluxes were for the most part negative, indicating that there was net uptake by the system (Figure 3.10). This was consistent across both treatments and measurement periods. Fluxes varied between *ca.* -130 to 50 µg m^{-2} h^{-1}, though were typically in the -100 to 0 µg m^{-2} h^{-1} range, for both +COMP and –-COMP plots, and there was no significant difference between the treatments. The greatest uptake was seen during the beginning of the study throughout July, and reduced over the course of the summer, so that by the end of September uptake was rarely stronger than -50 µg m^{-2} h^{-1}.

The *Miscanthus* system was a net sink for CH_4 over both periods for both treatments (Figure 3.11). Despite there being occasional positive CH_4 fluxes, there were only two days over which the *Miscanthus* was a net source; on both days the total emissions were close to zero, and they both occurred during the first measurement period (Figure 3.11).

3.3.2 Soil trace gas fluxes

3.3.2.1 CO_2

Soil CO_2 fluxes at the start of May were generally below 300 mg m^{-2} h^{-1}, and the overall pattern from both treatments saw CO_2 fluxes increase over the summer into August, after which they began to decline through autumn into the winter months November and December, when fluxes rarely exceeded 200 µg m^{-2} h^{-1} (Figure 3.12). During August, an equipment failure prevented data collection, but either side of this gap the fluxes reached a peak for both treatments of *ca.* 600 and 800 µg m^{-2} h^{-1} for the –-COMP and +COMP treatments respectively. The general trend in soil CO_2 flux was punctuated by two distinct periods of high fluxes (Figure 3.12). During mid-May there was a sustained period of approximately two weeks during which fluxes reached 600 µg m^{-2} h^{-1} for plots which were to receive both treatments. Following this period fluxes declined to 300- 400 µg m^{-2} h^{-1} and continued the gradual increase that typified the pattern previously. The second distinct period of especially high fluxes occurred

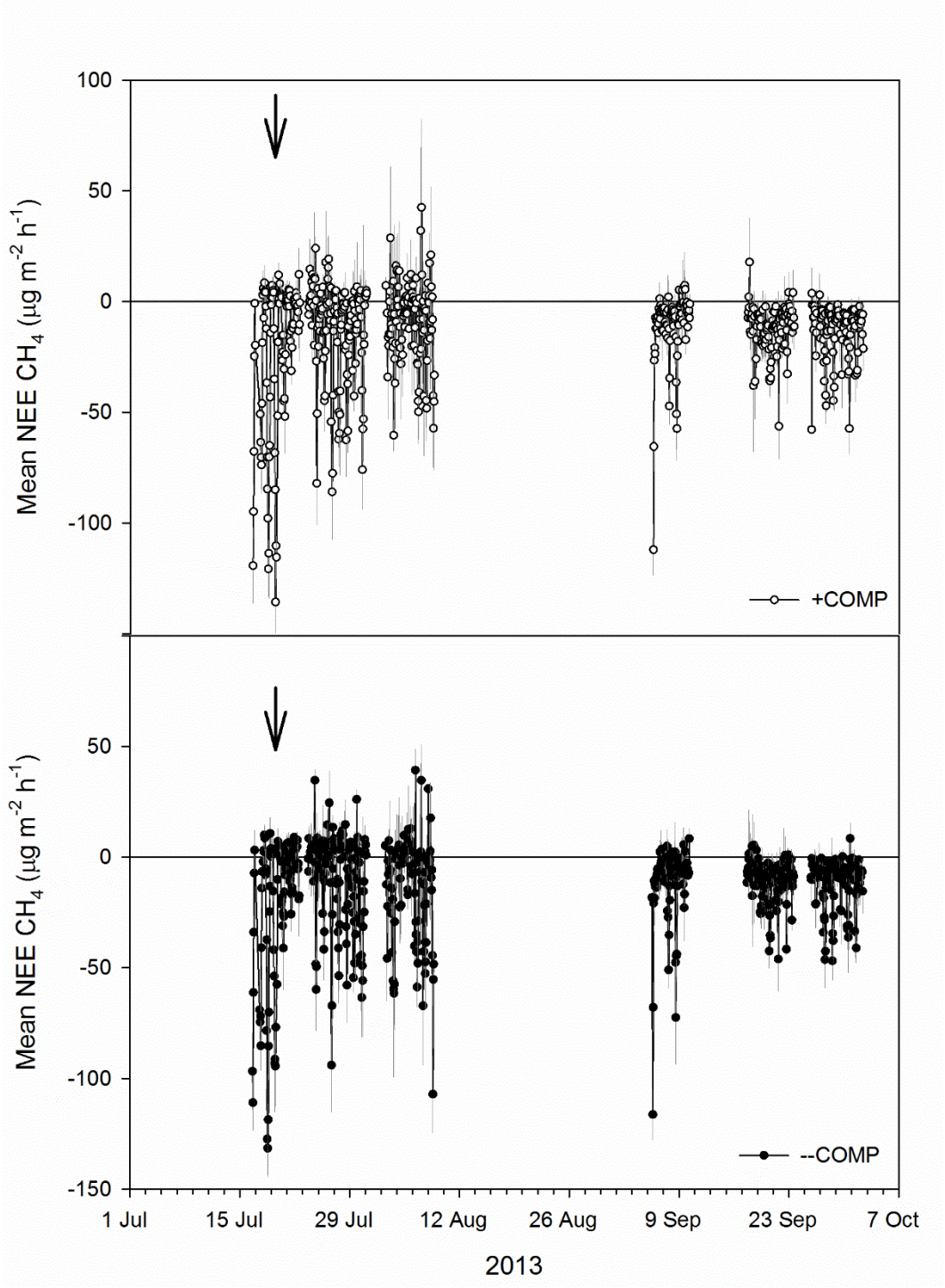

Figure 3.10 Mean ± 1SE (n=3) NEE of CH_4 from *Miscanthus* following a compost addition (open circles, top panel) and from untreated controls (bottom panel, closed circles). Vertical arrows indicate timing of compost addition.

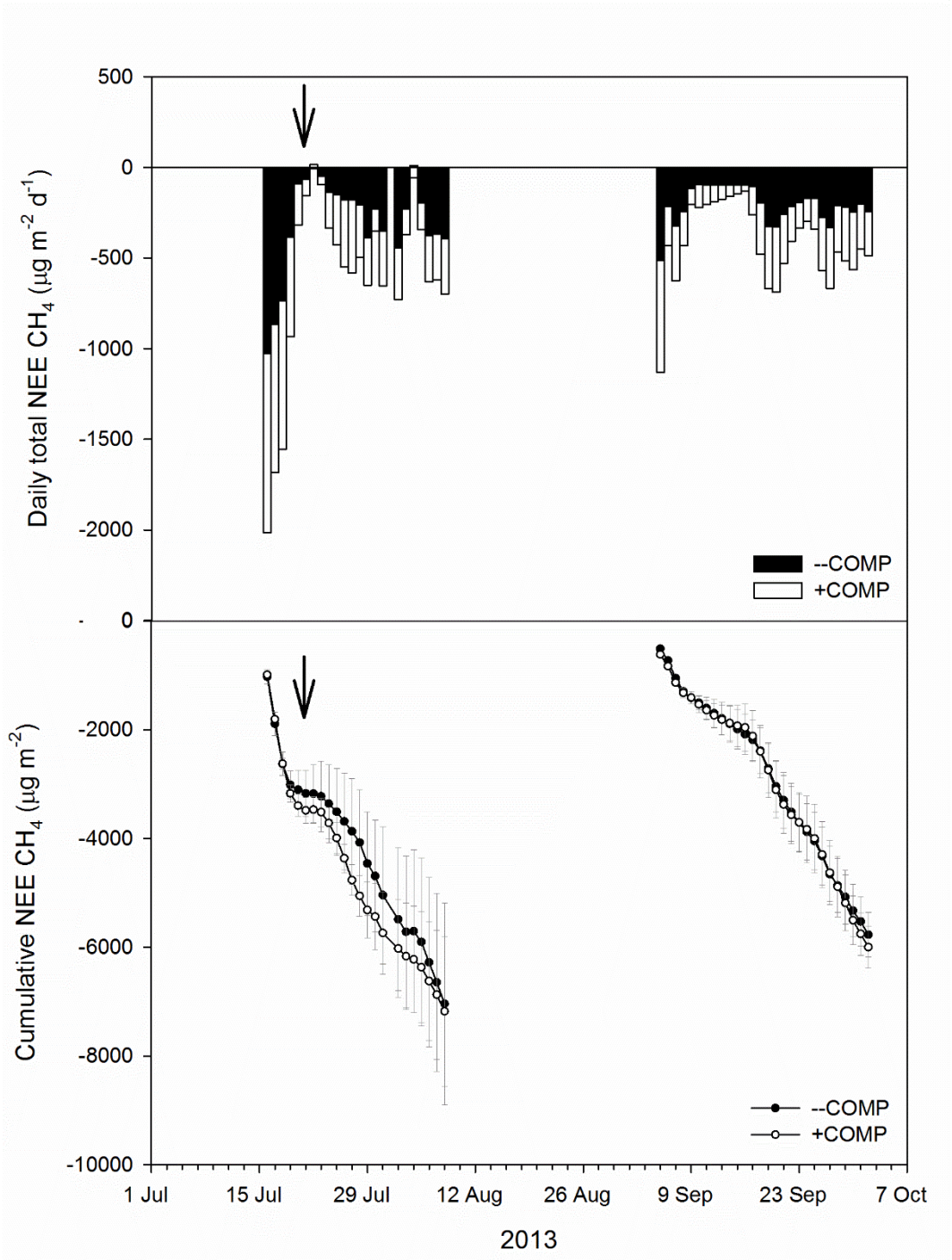

Figure 3.11 Mean (± 1SE, n=3) cumulative (bottom panel) and total (top panel) NEE of CH_4 from *Miscanthus* measured using SkyBeam, following a green compost addition. Open symbols represent amended plots (+COMP) and closed symbols untreated controls (-COMP), vertical arrows indicate timing of addition. Note the break in the axes on both panels. Negative fluxes indicate uptake, positive fluxes emission.

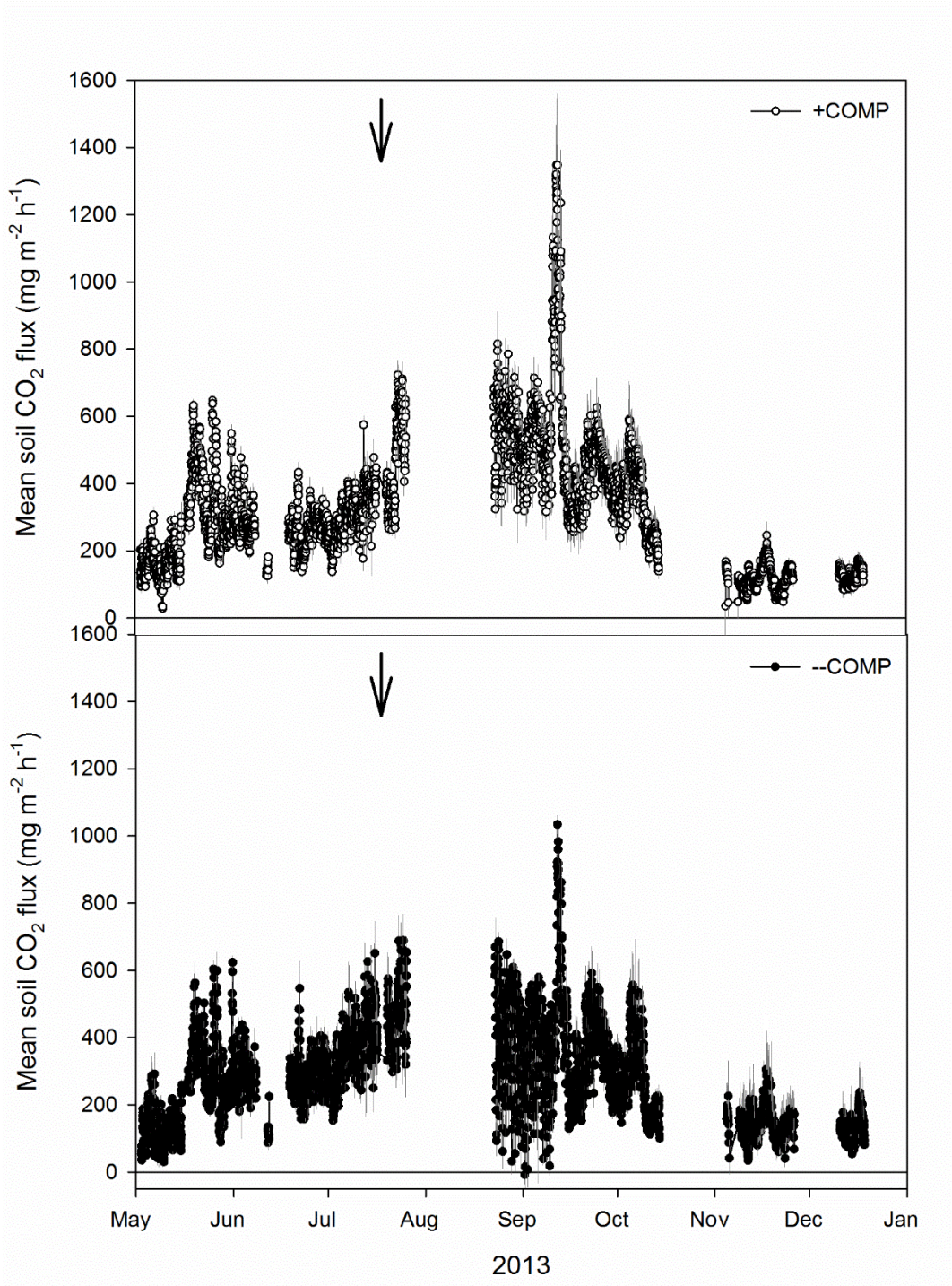

Figure 3.12 Mean ± 1SE (n=3) soil CO_2 flux from under *Miscanthus* following a compost addition measured using automated chambers. Closed circles represent control plots (-COMP) and open circles plots treated with compost (+COMP), vertical arrows indicate timing of addition.

over two days during the second week of September, and it was at this time that the maximum annual soil fluxes in excess of 1000 µg m^{-2} h^{-1} from the –-COMP and 1300 µg m^{-2} h^{-1} +COMP plots were seen. These high fluxes occurred following sustained rain which ended an approximately two week period with no precipitation. Prior to the application of compost, there was no significant difference in the daily mean soil CO_2 flux between the +COMP and –-COMP plots $F_{[1,284]}$< 0.00, p> 0.98, nor was there a difference over the entire study after treatment application, $F_{[1,628]}$= 0.39, p<0.54. However, there was a trend for higher CO_2 fluxes from the +COMP plots in the six weeks immediately after treatment, and if the fluxes from these weeks are analysed separately then this trend approached significance, $F_{[1,96]}$= 3.05, p= 0.084. The total soil CO_2 flux following compost addition did not differ between treatments, $t_{[2]}$= 0.02, p > 0.98 (Figure 3.13).

3.3.2.2 N_2O

Like N_2O NEE measured using SkyBeam, soil N_2O fluxes were generally very small (< 20 µg m^{-2} h^{-1}) throughout the study period, from both treatments (Figure 3.14). However, with the exception of one occasion in November 2013, fluxes were always positive. At this time, as with several other sampling days, zero was within the standard error of the mean flux.

N_2O emissions peaked on the 26th July 2013, four days after compost addition. Fluxes of *ca.* 115 µg m^{-2} h^{-1} and 25 µg m^{-2} h^{-1} were seen from the +COMP and –-COMP plots respectively. The peak in N_2O fluxes coincided with the largest values recorded with SkyBeam, though the manual measurements were undertaken several days after the maximum seen from the automated system.

There was no significant difference in soil N_2O flux between the compost treatments during the whole study period ($F_{[1,35]}$= 1.55, p< 0.23), though fluxes significantly differed between sampling days ($F_{[8,32]}$= 5.68, p< 0.0003), and there was a significant interaction between treatment and time ($F_{[8,32]}$= 2.43, p< 0.04). The fluxes seen closest to the compost addition appeared to differ between the treatments, and indeed if this day is analysed separately, emissions were significantly higher from the +COMP plots than from the controls, ($t_{[4]}$= 4.71, p< 0.01). The total cumulative flux for the period July 2013 to March 2014 did not differ between the –-COMP (59 mg m^{-2} $period^{-1}$) and the +COMP plots (63 mg m^{-2} $period^{-1}$) ($t_{[4]}$= 0.30, p< 0.78).

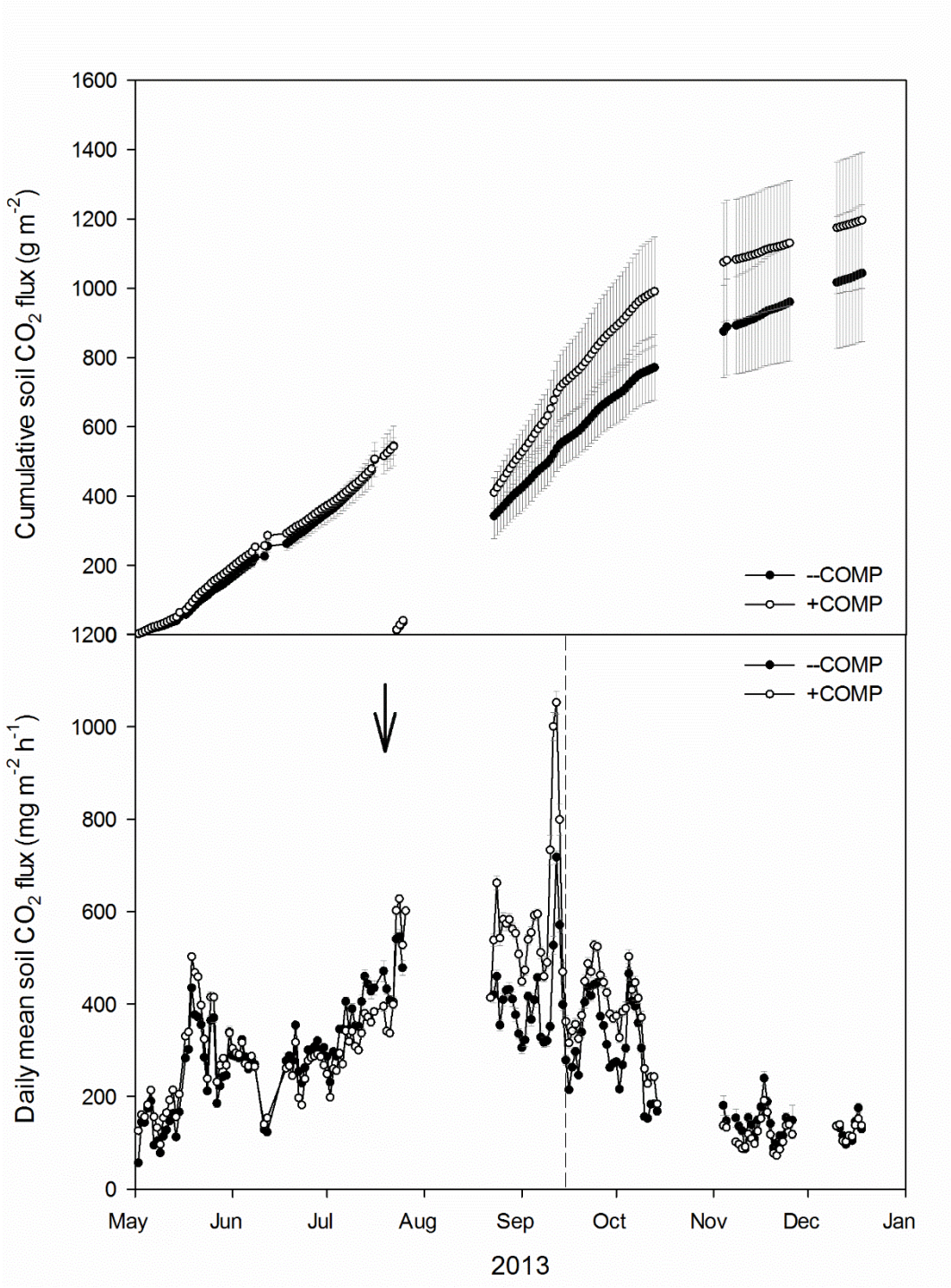

Figure 3.13 Daily mean and cumulative ± 1SE (n=3) soil CO_2 flux under *Miscanthus* up to and following compost addition. The arrow indicates the timing of application and the dashed vertical line bounds the six week period following compost addition during which fluxes tended to be higher from the amended plots (see text for details). Cumulative curves are shown for before and after compost addition.

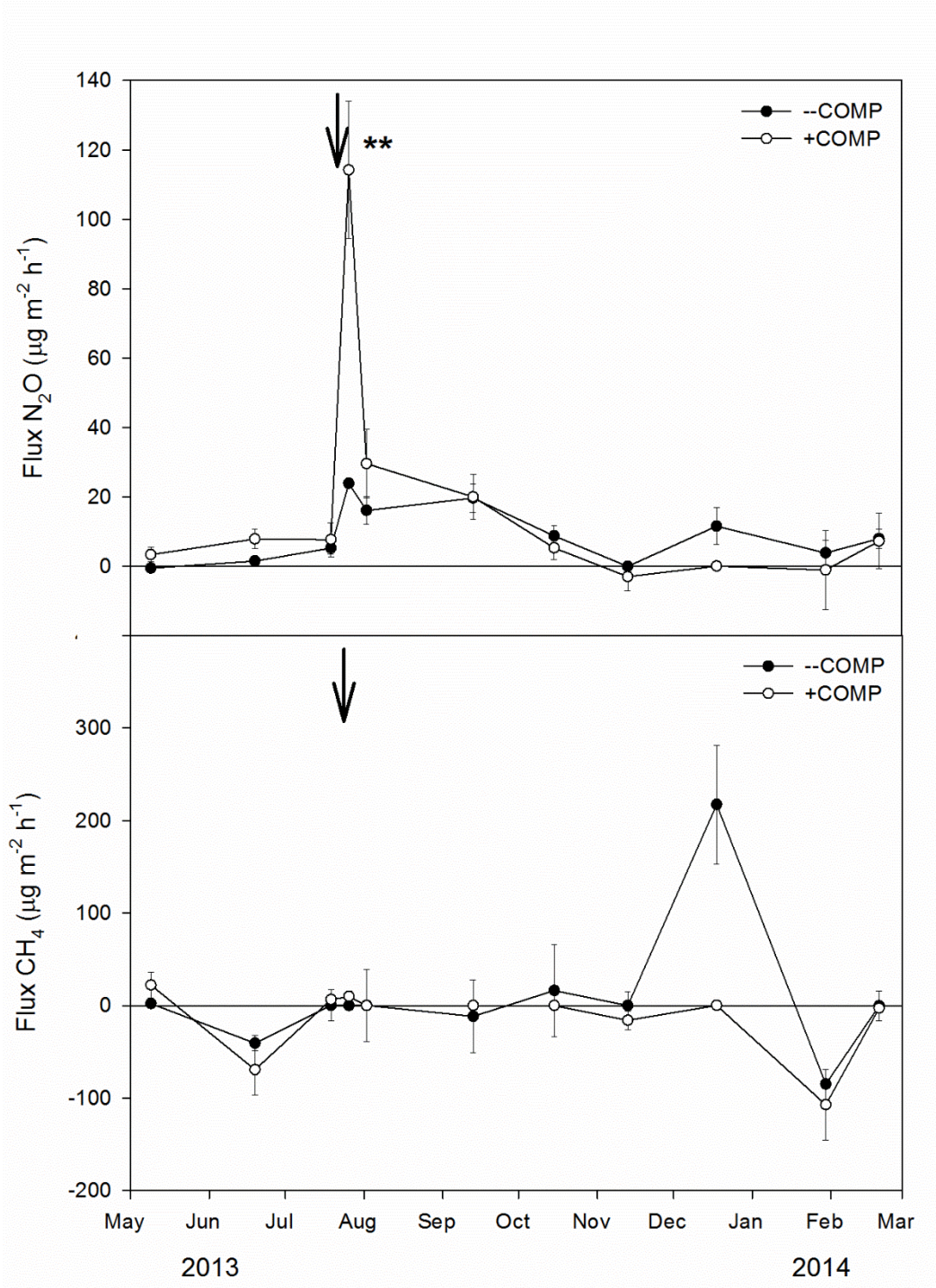

Figure 3.14 Mean flux N_2O and CH_4 ± 1SE from the soil under *Miscanthus* in plots treated with green compost (+COMP) and no compost (-COMP). Measurements were made using manual static chambers. Negative fluxes indicate net uptake and positive fluxes emission. Arrows denote timing of compost application, ** represents $p < 0.01$, t-test.

3.3.2.3 CH_4

CH_4 fluxes were close to zero for both treatments throughout the study (Figure 3.14). When the fluxes differed from zero they tended to be negative (-100 to 0 µg m^{-2} h^{-1}), which indicated that, as shown by the parallel measurements from SkyBeam, the soil was taking up CH_4. There was one sampling day, in December 2013, where an emission of > 200 µg m^{-2} h^{-1} was seen from the –-COMP plots, which was in contrast to the flux of *ca.* 0 µg m^{-2} h^{-1} from the +COMP plots. There was no significant difference in fluxes between treatments over the entire study ($F_{[1,32]}$= 0.79, p< 0.39), neither did they differ with sampling date ($F_{[8,32]}$= 1.89, p< 0.10) and there was no interaction between date and treatment ($F_{[8,32]}$= 0.92, p< 0.52). By the end of the study period, the –-COMP plots were a net source of CH_4 (160 mg m^{-2} $period^{-1}$), but the +COMP plots appeared to be a net sink (-68 mg m^{-2} $period^{-1}$); the variation within each treatment, however, was large and the two treatments did not significantly differ ($t_{[4]}$= -0.97, p< 0.39).

3.3.3 Comparison of trace gas fluxes from SkyBeam and manual chambers

The period from 19th July 2013 to 2nd August 2013 was used to compare the fluxes of CH_4 and N_2O measured from the soil, using manual chambers, and of NEE of CH_4 and N_2O measured using SkyBeam. Soil fluxes were measured three times during this period, and SkyBeam operated continuously throughout.

NEE for both gases, as measured by SkyBeam was consistently lower than the soil measurements: the closest (temporally) automated measurement from SkyBeam was significantly lower than from the manual chamber within the same plot for N_2O, ($t_{[19]}$= 7.99, p< 0.0001), and CH_4, ($t_{[14]}$= 2.32, p< 0.036). The same was also true for the daily mean fluxes based upon the continuous SkyBeam measurements, for N_2O, ($t_{[23]}$= 5.74, p< 0.0001), and CH_4, ($t_{[17]}$= 4.30, p, 0.0005).

The manual chamber measurements yielded a higher estimate of cumulative N_2O flux compared to that derived from the hourly SkyBeam measurements. Cumulative soil N_2O flux from coverboxes was 68 ± 17 mg m^{-2} for the period and significantly greater than 19 ± 3 mg m^{-2} for the same period based upon SkyBeam data ($t_{[5]}$= 3.12, p< 0.027). There was no significant difference between the estimate of cumulative CH_4 flux between static chambers and SkyBeam ($t_{[5]}$= -1.3, p> 0.2).

3.3.4 Biomass harvested from compost treatments

Above-ground biomass from the control plots tended to be greater than that from the +COMP plots (Figure 3.15). The total biomass from the –-COMP plots was 203 ± 20 g m^{-2} compared to 129 ± 18 g $m^{-2}$from the +COMP plots, though they did not significantly differ ($t_{[4]}$= -2.61, p=0.06), and scaled up, this would represent a yield of 2.03 and 1.29 odt ha^{-1}.

3.3.5 Greenhouse gas budget of NEE of three trace gases.

The GHG balance of trace gases, over both periods in which NEE of all three gases was measured using SkyBeam, did not differ between compost treatments. The contribution of CO_2 to the overall budget was between 3 and 4 orders of magnitude greater than that of either N_2O or CH_4 (Figure 3.16). Despite CH_4 acting as a net carbon sink, it was dwarfed by the emissions of CO_2 from both treatments, and whilst N_2O acted as a sink in the first period and a source in the second, it had very little bearing on the overall GHG balance.

3.3.6 EC derived NEE of CO_2

3.3.6.1 Comparison of EC and SkyBeam

At the start of the study period (early July 2013) the CO_2 NEE measured using EC were in the range of *ca.* -1200 to 1500 mg CO_2 m^{-2} h^{-1} (Figure 3.17). Through the summer the negative range of values decreased quickly, so that by the end of August 2013 minima NEE of < -3000 mg m^{-2} h^{-1} were seen (Figure 3.18). Throughout this time the maximum values of NEE remained fairly constant around 1500 mg m^{-2} h^{-1}. Uptake reduced through September, though even at the end of the month there were isolated fluxes of *ca.* -3000 mg m^{-2} h^{-1}. During September maximum fluxes also diminished to approximately 1000 mg m^{-2} h^{-1}. From November onwards fluxes were predominantly positive, and were of the range 0- 500 mg m^{-2} h^{-1}.

The number of EC flux values that made were retained after quality control totalled much fewer than those from the SkyBeam system (Figure 3.17), and these tended to be at the extremes of the daily range: there were fewer fluxes close to zero in the EC data than were seen by the SkyBeam system. In order to calculate daily mean fluxes from the EC data, any days with fewer than 6 measurements (half hourly averages) were removed, as this was deemed not to be representative of a 24 hour period,

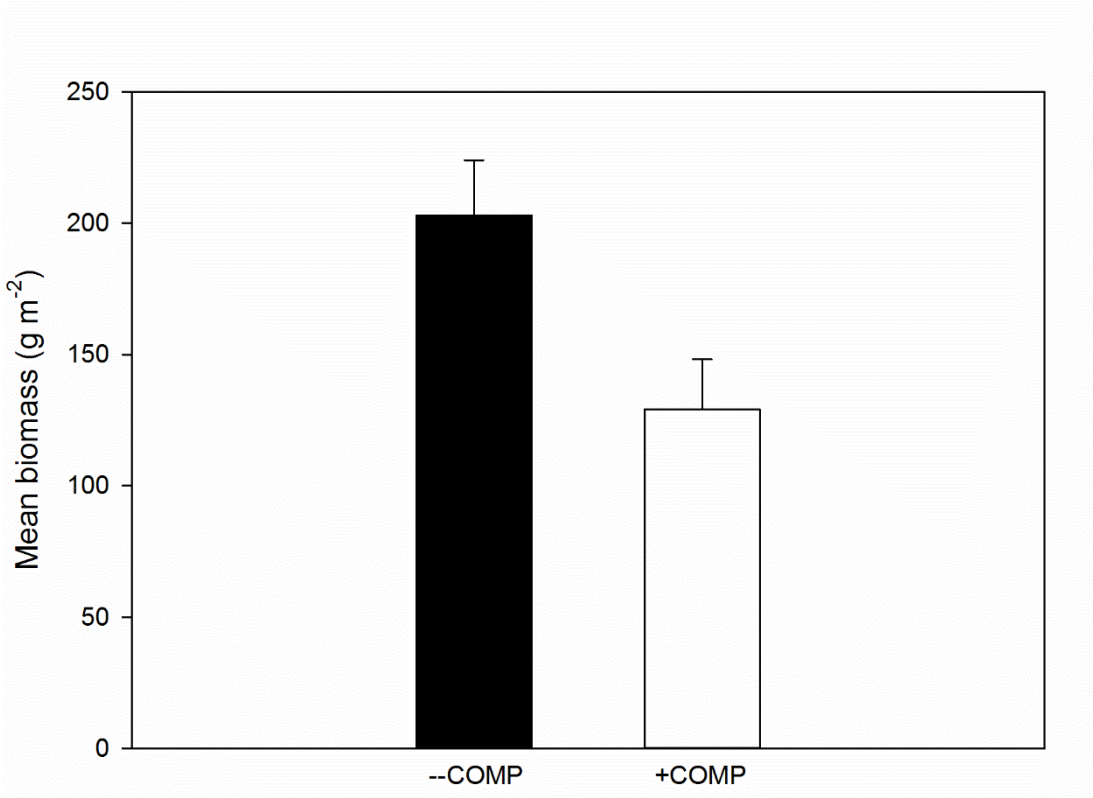

Figure 3.15 Oven-dried biomass of *Miscanthus* from growing season 2013-2014 from plots amended with compost (+COMP) and controls (-COMP). Values are means ± 1SE, n=3.

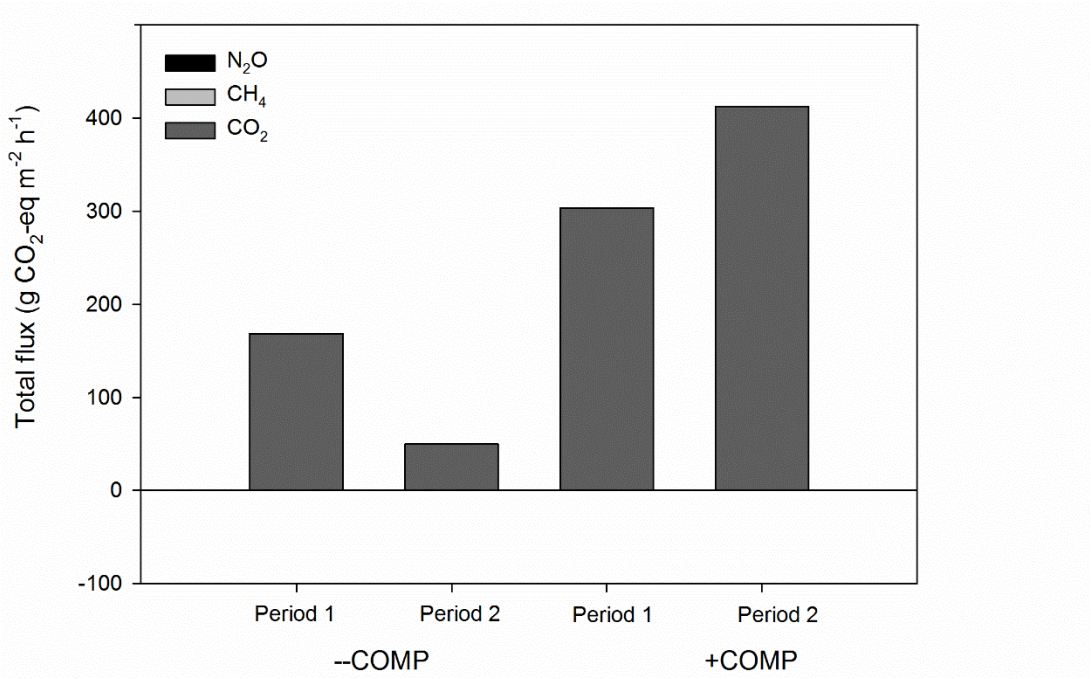

Figure 3.16 GHG balance expressed as CO_2 equivalents (CO_2-eq, (Myhre *et al.*, 2013)) derived from the cumulative NEE of three trace gases, CO_2, N_2O and CH_4. The contribution of N_2O and CH_4 is so small to see on this scale.

especially since SkyBeam data were *ca.* hourly in frequency. The daily mean NEE of CO_2, as measured by the EC system was negative throughout July and August (Figure 3.19, middle panel): net flux of CO_2 was in the region of 0 to -500 mg m^{-2} d^{-1}, and this decreased to a minimum of *ca.* -1000 mg m^{-2} d^{-1} during the first half of August. By the start of September the net daily flux was becoming more positive, tending towards zero, and there were days of positive net emission, which increased in frequency towards the end of the month. This pattern is reflected in the cumulative NEE of CO_2 from the EC data, where there was a steady accumulation of carbon by the system until the end of August, after which an equilibrium was reached, until at the end of September it appears that the *Miscanthus* system began to lose carbon (Figure 3.19, bottom panel).

In contrast, the data from SkyBeam indicate that for the early part of the summer, the *Miscanthus* was a net source of CO_2, with daily means in the range of 0 to 1000 mg m^{-2} d^{-1} (Figure 3.19, top panel). From mid-August there were days on which the daily mean NEE of CO_2 was negative, indicating net uptake of CO_2 on these occasions. These occurrences increased in frequency, so that by the start of October, the running average was negative, which would suggest that at this point the *Miscanthus* was starting to accumulate carbon, at the point where the EC data indicate the opposite was happening. The cumulative flux calculated from SkyBeam reflects that of the EC data from around August 28th, where emission and uptake are in equilibrium and the cumulative flux remains static for approximately the next four weeks (Figure 3.19, bottom panel). From September 25th, however, the SkyBeam data reflect a net accumulation of carbon by the *Miscanthus*, at the very time that the EC data show a release of carbon.

For the entire study period, the daily mean NEE of CO_2 measured by the EC system was lower than that from SkyBeam ($t_{[57]}$= -6.85, $p< 0.0001$). However, the cumulative flux CO_2 calculated with the data from both systems remained largely static during the period 26th August to 23rd September 2013 (Figure 3.19), and indeed during this period the daily mean NEE CO_2 did not differ between the two systems ($t_{[28]}$= -1.95, $p> 0.06$).

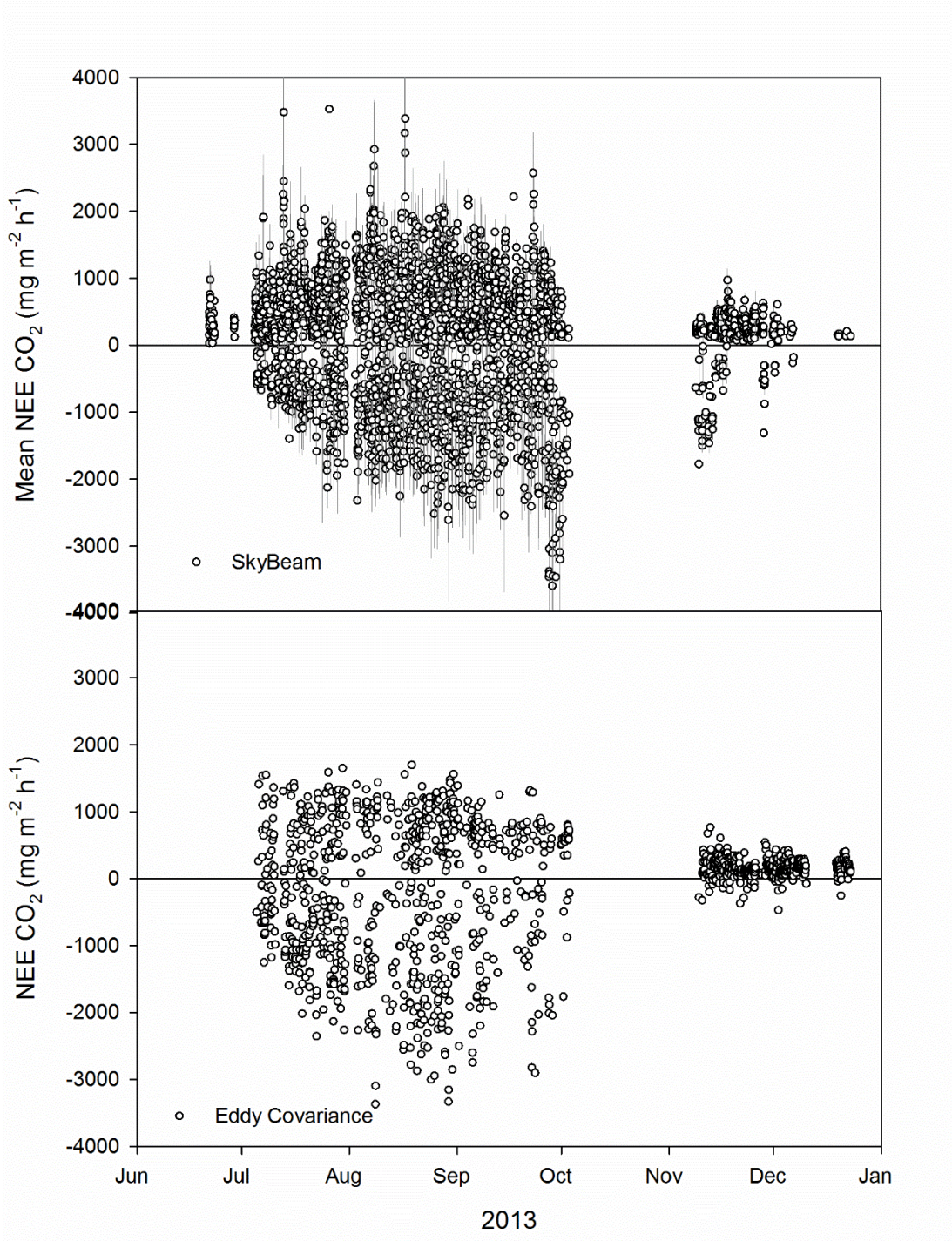

Figure 3.17 NEE of CO_2 from *Miscanthus* measured using EC system (bottom panel) and the SkyBeam system (top panel, mean ± 1SE, n=3). Negative fluxes indicate net uptake of CO_2 and positive fluxes emission. EC data are the means of 30 minute period

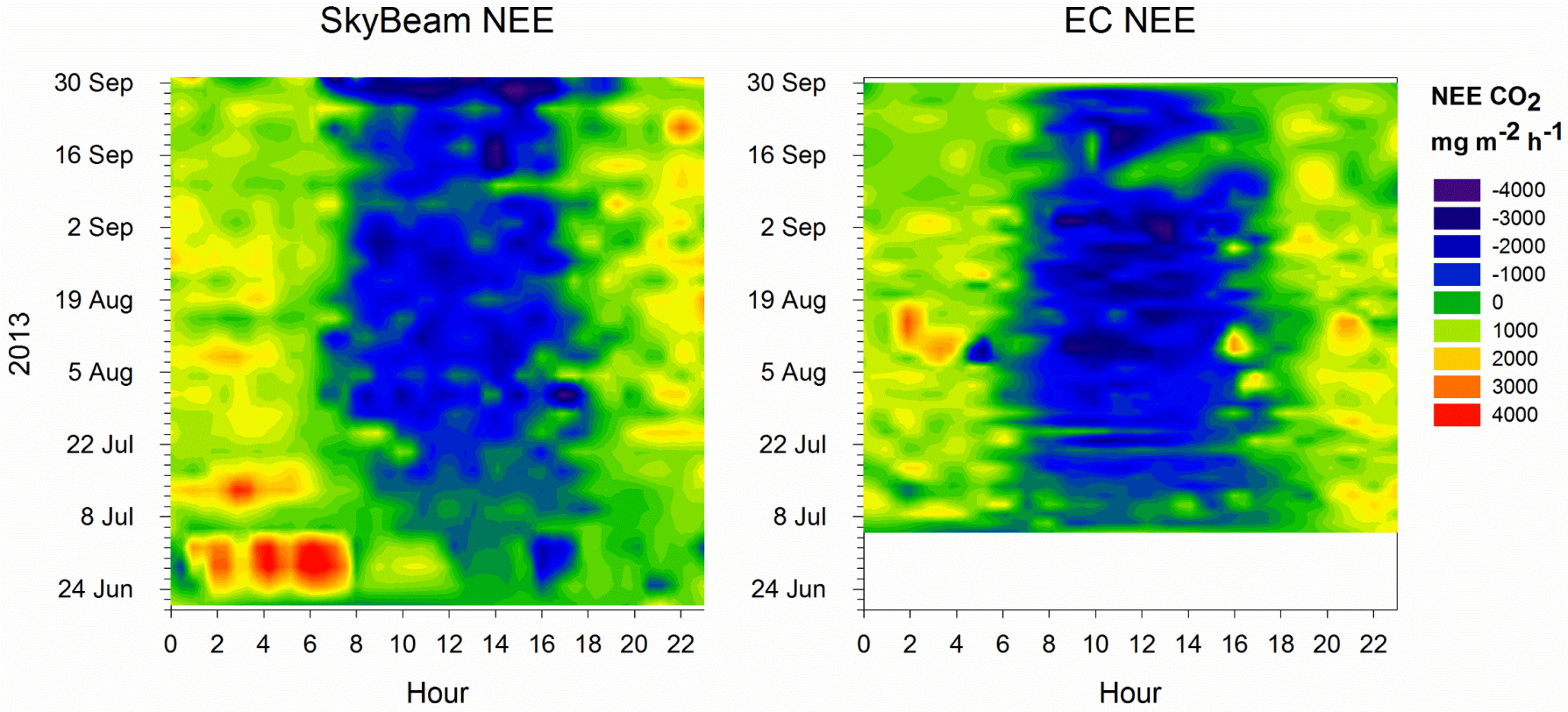

Figure 3.18 Fingerprint maps of NEE of CO_2 measured using SkyBeam (left) and EC (right). Positive fluxes represent net release of CO_2 and negative fluxes net uptake.

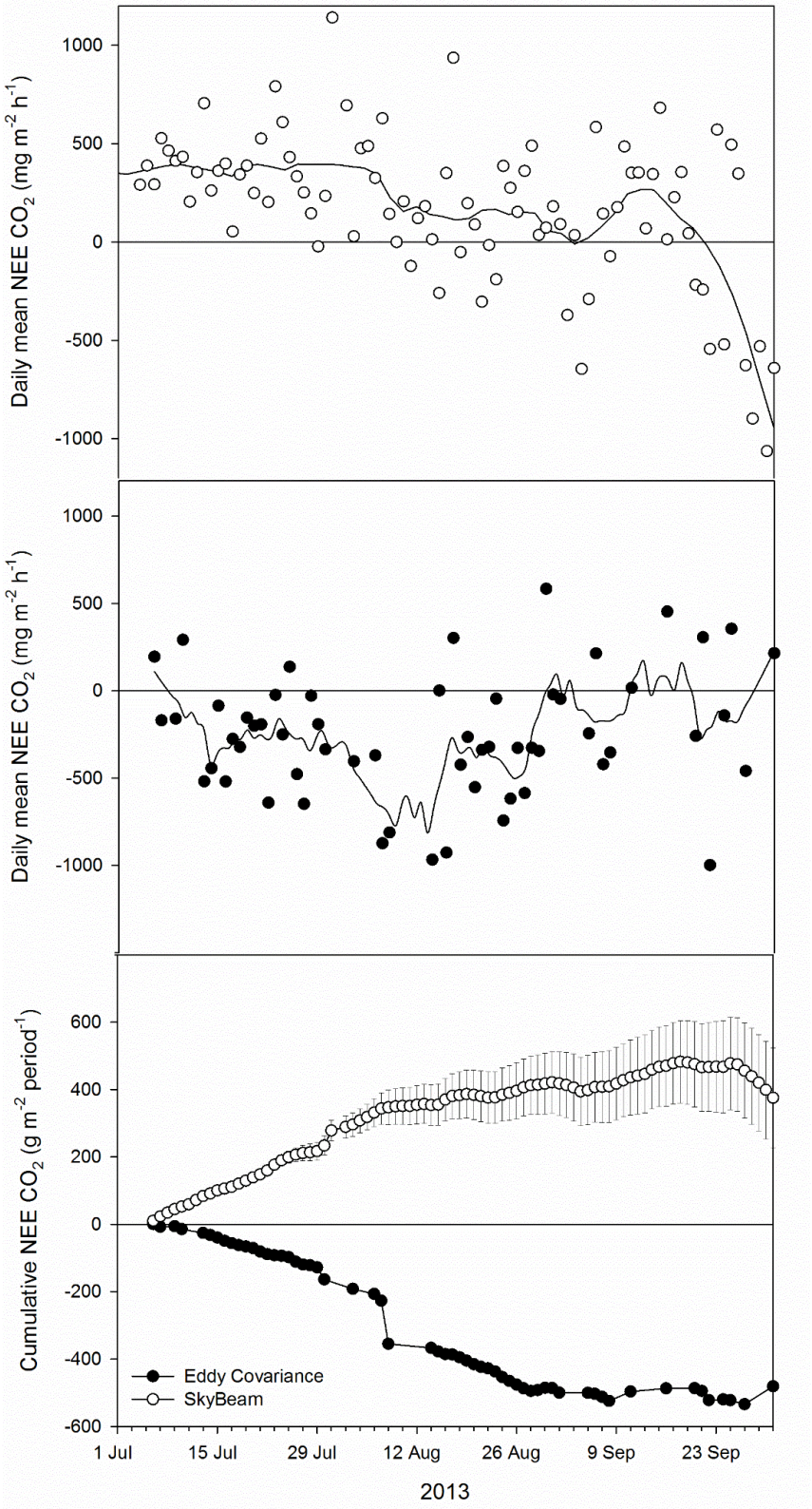

Figure 3.19 Daily mean (top and middle panels) and cumulative (bottom panel) NEE of CO_2 from *Miscanthus* measured using EC (closed circles) and SkyBeam (open circles). Daily means are accompanied by a 1 week running average (solid lines). Cumulative values from

SkyBeam data are means ± 1SE (n=6), EC data are not replicated. Negative values of NEE indicate net uptake pf CO_2 and positive values net release.

Due to the conservative quality control for the EC data, for the period 4th July to 1st October 2013, 2486 half-hourly flux measurements were rejected, as opposed to just 1785 which were retained. As such, a more relevant comparison between SkyBeam data and EC values is derived from the hourly averages of the data. Comparing the hourly means from both systems shows that SkyBeam tended to yield higher (more positive) flux values than those from the EC system ($t_{[2147]}$= 16.74, p< 0.001). This was particularly evident at high rates of uptake, during highest rates of photosynthesis (Figure 3.20).

3.3.6.2 Partitioning of carbon fluxes from EC and SkyBeam

Night time hourly ecosystem respiration (R_{eco}) from SkyBeam was higher than soil respiration (R_{soil}) measured data from the automated chambers, and this displayed a good linear relationship (Figure 3.21). This relationship was used to extrapolate values for R_{eco} during the day time from concurrent R_{soil} measurements. The mean daily night time R_{eco} was estimated to be *ca.* 12% lower than day time R_{eco} (Figure 3.22), and allowed for an estimate of photosynthetic activity to be made.

Photosynthesis, as calculated from EC data, increased from the end of July to daily means in excess of 2500 mg m^{-2} h^{-1} during August. During the beginning of September photosynthetic rates dropped, but increased again for the second half of that month (Figure 3.23). Data from SkyBeam suggests that photosynthesis was much lower in that particular part of the field during July, where rates increased steadily from *ca.* 100 mg m^{-2} h^{-1} to more than 500 mg m^{-2} h^{-1}. These values were approximately 1000 mg m^{-2} h^{-1} lower than for the field as a whole, as shown in the EC data (Figure 3.23). However, during August the estimated rates of photosynthesis became much more similar for both systems' data, and by the beginning of September there were days on which the area of the field measured by SkyBeam was photosynthesising more than the mean of the EC's fetch.

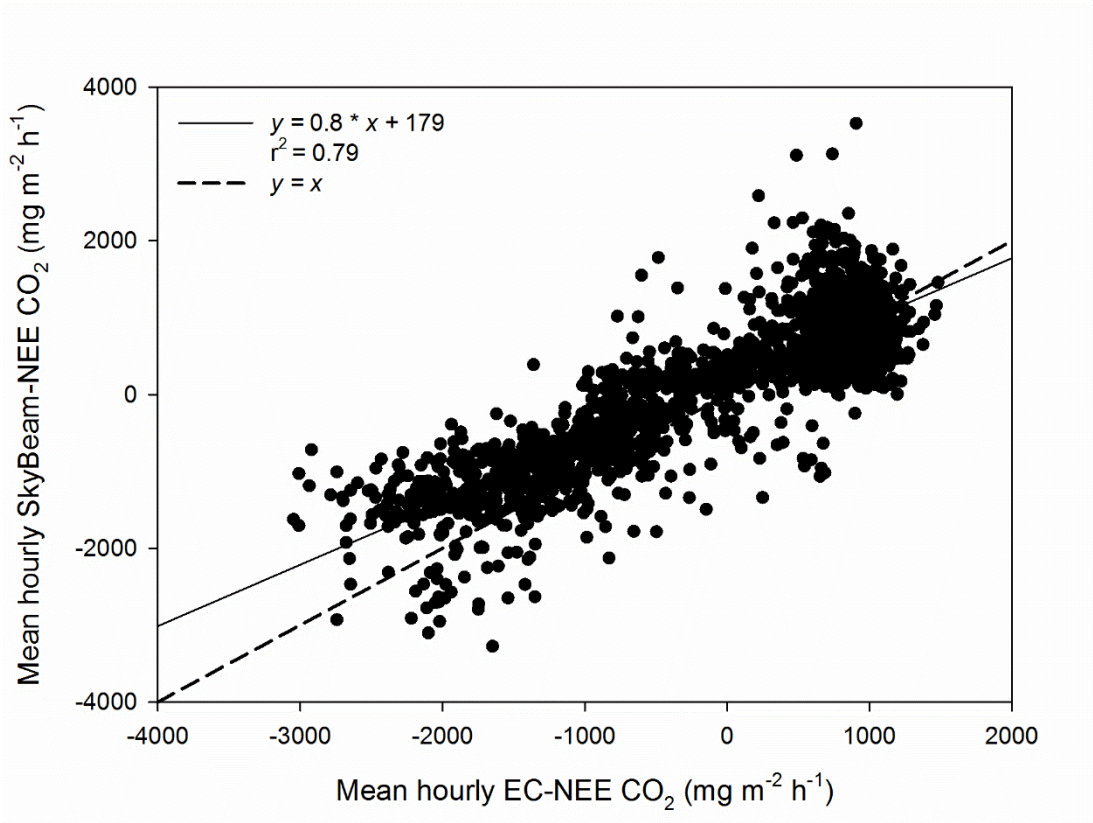

Figure 3.20 Comparison of hourly mean values of NEE from both the EC system and SkyBeam from a *Miscanthus x giganteus* field. The solid line shows the linear regression of the two variables, the dashed line represents the one to one relationship.

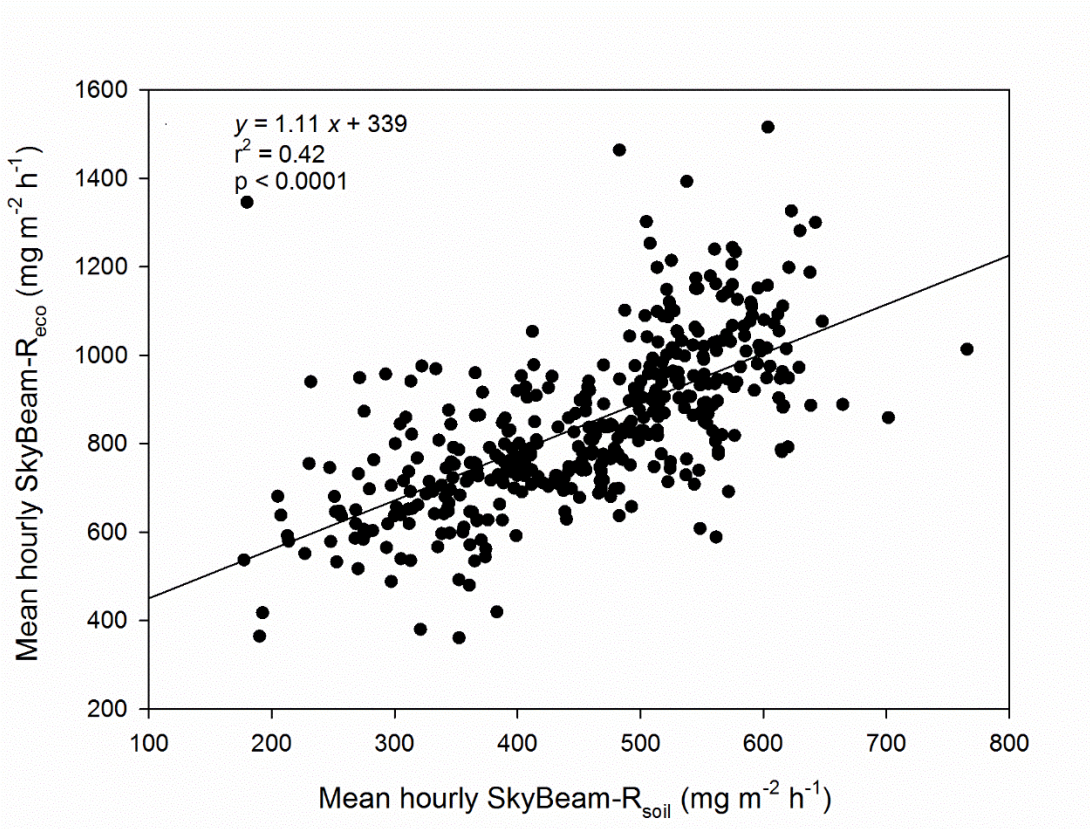

Figure 3.21 Relationship between soil respiration (R_{soil}), measured using automated chambers and ecosystem respiration (R_{eco}), measured using SkyBeam during the night. This relationship was used to extrapolate day time values of R_{eco} from R_{soil} measurements.

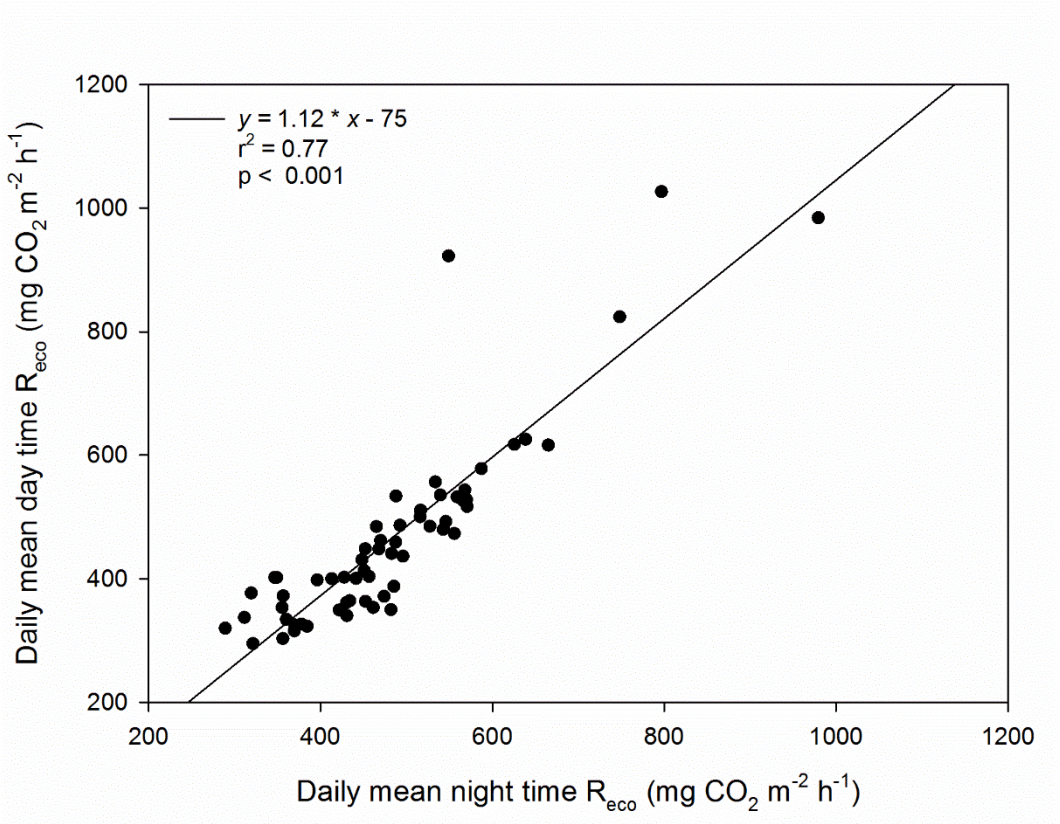

Figure 3.22 Relationship between the mean night time ecosystem respiration (R_{eco}), measured using SkyBeam, and mean day time R_{eco}, calculated from R_{soil} measured using automated chambers.

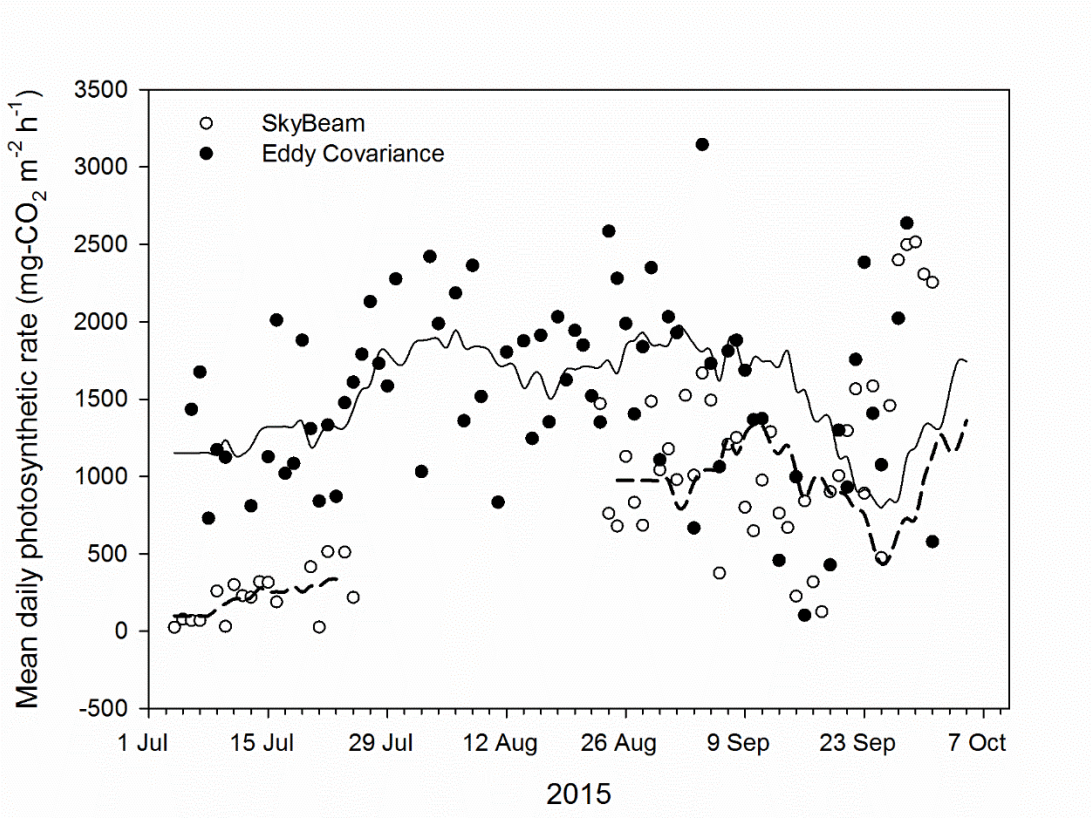

Figure 3.23 Daily mean values of photosynthesis, expressed in terms of mg CO_2 m^{-2} h^{-1}, calculated from NEE data measured using SkyBeam and EC from a *Miscanthus* field. A running 7-day average is shown for both EC data (solid line) and SkyBeam (dashed line).

3.3.7 Environmental variables and their relationship to trace gas fluxes

3.3.7.1 Patterns in environmental variables

During May the daily average air temperature of approximately 10^{o}C included daily ranges extending from near-zero to more than 20^{o}C. Daily means rose to a peak of more than 20^{o}C in early August and the highest temperature recorded was also during this month, when a maximum greater than 30^{o}C was reached (Figure 3.24). Soil temperature followed a similar pattern to air temperature, with maximum values occurring at the same time, though the soil was consistently warmer than the air (Figure 3.24). Soil temperature did not differ between the +COMP and –-COMP treated plots ($F_{[1,291]}$= 0.11, p> 0.72). The annual peak in solar radiation occurred earlier than that of temperature, with a maximum daily mean of over 200 W m^{-2} achieved in June (Figure 3.24). The highest recorded level of radiation was more than 1000 W m^{-2} and this was also seen in June. Interdiel fluctuations could be quite pronounced, and consecutive daily means sometimes differed by a factor of three.

Prolonged rainfall during May was followed by a dry first half of June; there was also a period of more than two weeks during July in which no rain fell at all (Figure 3.24). There was no significant difference in soil moisture prior to compost addition. The compost treatment was applied during this dry spell and following the application the +COMP plots were significantly wetter ($F_{[1,91]}$= 7.40, p< 0.008). A significant interaction between treatment and date ($F_{[82,91]}$= 15.25, p< 0.0001), indicated that the treatment effect changed, and *post hoc* tests showed that it was following rainfall that the treatments differed (Figure 3.24). After a summer characterised by periods of consecutive dry days, punctuated by sporadic precipitation, rain fell on the vast majority of days from the beginning of October into the middle of November. This was reflected in the soil moisture readings, which rarely exceeded 0.25 m^{3} m^{-3} until November, when moisture levels were maintained above 0.3 m^{3} m^{-3}. By this time moisture levels were consistent between the two compost treatments.

3.3.7.2 Correlation matrix

All four gas fluxes (NEE CO_2, N_2O and CH_4 and soil respiration) were significantly positively correlated with each other (Table 3.1), reflecting the likelihood they were affected by common factors. Other variables showing positive correlations were solar radiation and air temperature and soil temperature, and relative humidity was significantly negatively correlated with air temperature and solar radiation (Table 3.1).

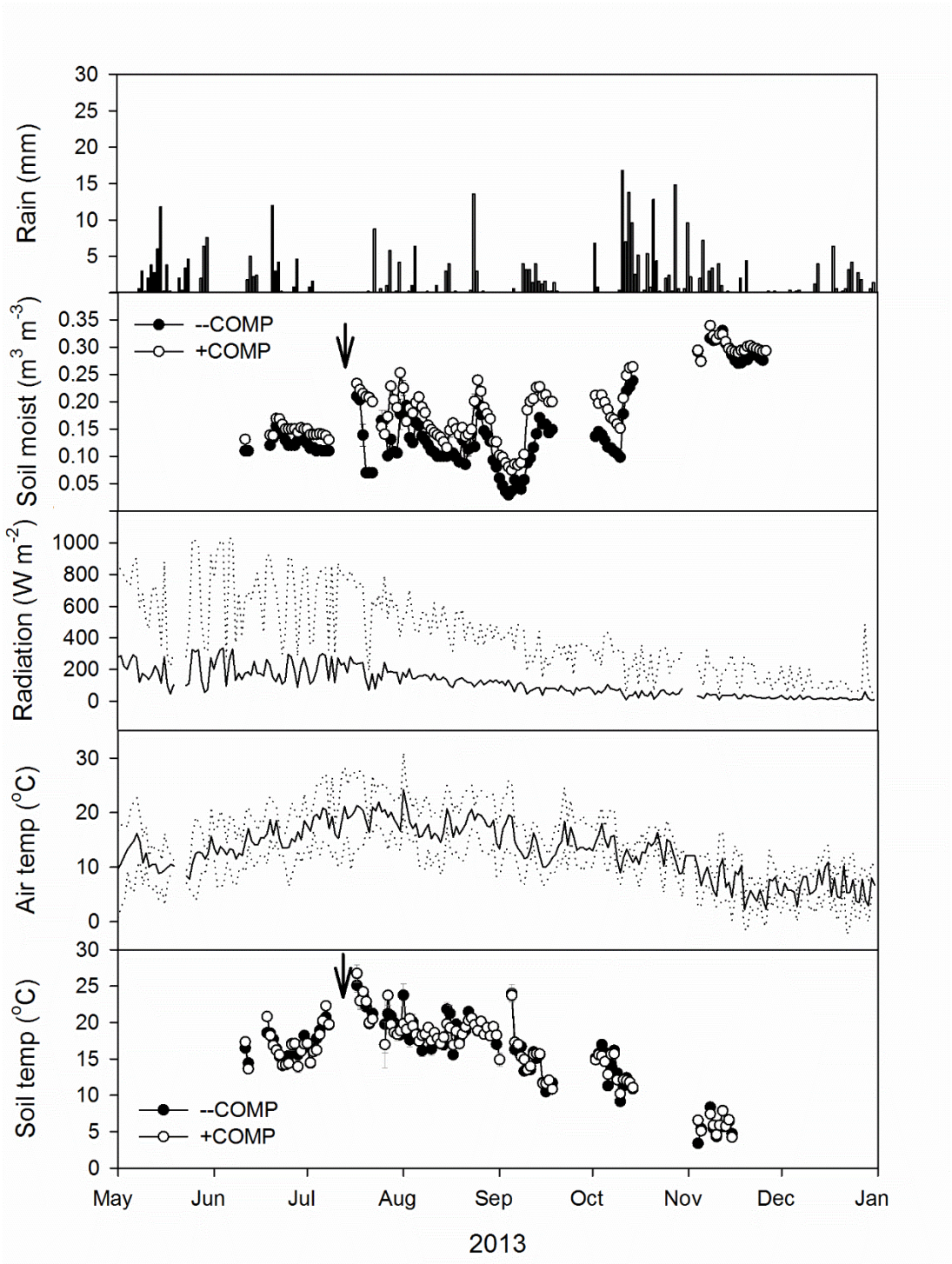

Figure 3.24 Environmental and meteorological variables recorded throughout the study period. With the exception of rainfall (daily totals), values shown are daily means of hourly measurements; for soil moisture and soil temperature the data are daily means ± 1SE, n=3. The dashed lines for air temperature represent the daily maximum and minimum, and for solar radiation (radiation) the maximum, since the daily minimum was always zero. Vertical arrows indicate timing of compost addition.

Table 3.1 Correlation matrix of trace gas fluxes measured using SkyBeam and automated chambers (soil respiration only) and environmental variables. Values shown are Pearson correlation coefficients, significance levels are denoted (* p< 0.05, ** p< 0.01, *** p< 0.001).

TREAT	Variable	Flux N_2O	Flux CH_4	NEE CO_2	Soil respiration	Solar radiation	Air temp	Relative humidity	Soil moisture	Soil temp	Hourly rain	Daily rain
	Flux N_2O	1	0.23 ***	0.11 ***	0.18 ***	-0.02ns	0.15 ***	0.12 ***	0.07ns	-0.32 ***	0.08*	0.32 ***
	Flux CH_4	0.23 ***	1	0.33 ***	0.21 ***	-0.54 ***	-0.36 ***	0.59 ***	-0.04ns	-0.46 ***	0.11*	0.11 ***
	NEE CO_2	0.11 ***	0.33 ***	1	0.37 ***	-0.65 ***	-0.29 ***	0.69 ***	0.01ns	-0.21 ***	0.03ns	0.05***
	Soil respiration	0.18 ***	0.21 ***	0.37 ***	1	-0.01ns	0.44 ***	0.1**	-0.55 ***	0.35 ***	-0.06*	-0.1 ***
-COMP	Solar radiation	-0.02ns	-0.54 ***	-0.65 ***	-0.01ns	1	0.56 ***	-0.76 ***	-0.31 ***	0.32 ***	-0.02ns	-0.05ns
	Air temperature	0.15 ***	-0.36 ***	-0.29 ***	0.44 ***	0.56 ***	1	-0.59 ***	-0.6 ***	0.87 ***	0.05ns	0.05***
	Relative humidity	0.12 ***	0.59 ***	0.69 ***	0.1**	-0.76 ***	-0.59 ***	1	0.39 ***	-0.38 ***	0.04ns	0.15 ***
	Soil moisture	0.07ns	-0.04ns	0.01ns	-0.55 ***	-0.31 ***	-0.6 ***	0.39 ***	1	-0.6 ***	0	0.12 ***
	Soil temperature	-0.32 ***	-0.46 ***	-0.21 ***	0.35 ***	0.32 ***	0.87 ***	-0.38 ***	-0.6 ***	1	0	-0.15 ***
	Hourly rain	0.08*	0.11*	0.03ns	-0.06*	-0.02ns	0.05ns	0.04ns	0	0	1	0.27 ***
	Daily rain	0.32 ***	0.11 ***	0.05***	-0.1 ***	-0.05ns	0.05***	0.15 ***	0.12 ***	-0.15 ***	0.27 ***	1

TREATMENT	Variable	Flux N_2O	Flux CH_4	NEE CO_2	Soil respiration	Solar radiation	Air temp	Relative humidity	Soil moisture	Soil temp	Hourly rain	Daily rain
+COMP	Flux N_2O	1	0.14 ***	0.16 ***	0.1 **	0.06 ***	0.19 ***	0.05 ns	0.07 ns	-0.24 ***	0 ns	0.22 ***
	Flux CH_4	0.14 ***	1	0.34 ***	0.13 ***	-0.45 ***	-0.38 ***	0.51 ***	-0.07 ns	-0.34 ***	0.04 ns	0.11 ***
	NEE CO_2	0.16 ***	0.34 ***	1	0.26 ***	-0.61 ***	-0.25 ***	0.66 ***	0.03 ns	-0.16 ***	0.04 ns	0.07 ***
	Soil respiration	0.1 **	0.13 ***	0.26 ***	1	0 ***	0.43 ***	-0.01 ns	-0.51 ***	0.37 ***	-0.01 ns	-0.02 **
	Solar radiation	0.06 ns	-0.45 ***	-0.61 ***	-0.04 ns	1	0.55 ***	-0.76 ***	-0.29 ***	0.4 ***	-0.04 ns	-0.1 ***
	Air temperature	0.19 ***	-0.38 ***	-0.25 ***	0.43 ***	0.55	1	-0.58 ***	-0.53 ***	0.87 ***	0.03 ns	0.05 ***
	Relative humidity	0.05 ns	0.51 ***	0.66 ***	-0.01 ns	-0.76 ***	-0.58 ***	1	0.38 ***	-0.43 ***	0.08 **	0.15 ***
	Soil moisture	0.07 ns	-0.07 ns	0.03 ns	-0.51 ***	-0.29 ***	-0.53 ***	0.38 ***	1	-0.61 ***	0.09 *	0.16 ***
	Soil temperature	-0.24 ***	-0.34 ***	-0.16 ***	0.37 ***	0.4 ***	0.87 ***	-0.43 ***	-0.61 ***	1	0 ns	-0.13 ***
	Hourly rain	0 ns	0.04 ns	0.04 ns	-0.01 ns	-0.04 ns	0.03 ns	0.08 **	0.09 *	0 ns	1	0.35 ***
	Daily rain	0.22 ***	0.11 ***	0.07 ***	-0.02 **	-0.1 ***	0.05 ***	0.15 ***	0.16 ***	-0.13 ***	0.35 ***	1

The relationship between soil moisture and temperature was also significantly negative

3.3.7.3 NEE CO_2 and environmental variables

The variable which showed the strongest relationship with NEE of CO_2, for both treatments, was solar radiation (Figure 3.25), which consistently accounted for at least 60% of the variation in NEE. For both the –-COMP and +COMP plots, NEE was strongly negatively related to the instantaneous rate of solar radiation. The relationship in the control plots (-COMP) was best described as a non-linear function (R^2= 0.60), where maximum uptake occurred at radiation levels between 400 and 600 W m^{-2} (Figure 3.25). A non-linear model also fitted well to the +COMP treatment (R^2= 0.49), but was best described by a linear model (R^2= 0.66), perhaps due to the reduced biomass present in these plots (Figure 3.1), meaning that maximum uptake was not achieved in this treatment. At 0 W m^{-2} NEE was positive, since with no light no photosynthesis occurred, and NEE consisted of ecosystem respiration at this point.

Relative humidity was positively related to NEE for both treatments, and explained 51% and 53% of the variance in the –-COMP and +COMP plots respectively (Figure 3.25). NEE became positive as relative humidity approached 80%, indicating that above this emission exceeded uptake. The only other variable to show a significant relationship with NEE of CO_2 was air temperature, which was very weakly significant (R^2= 0.04, both treatments) and with uptake increasing slightly with higher temperatures. Neither soil temperature nor soil moisture displayed significant relationships with NEE.

3.3.7.4 Soil respiration

Relative humidity and air temperature were the two variables significantly associated with soil respiration across both compost treatments (Figure 3.26). Air temperature had the biggest effect on soil respiration, best described as a non-linear relationship which explained 15% and 19% of the variation in the –-COMP and +COMP treatments respectively. It is suggested that soil respiration peaked at around 20 ^oC (Figure 3.26). Soil respiration increased very slightly with relative humidity in both treatments, though where this relationship was decidedly weak in the +COMP plots (R^2= 0.03), it was stronger in the –-COMP plots (R^2= 0.14).

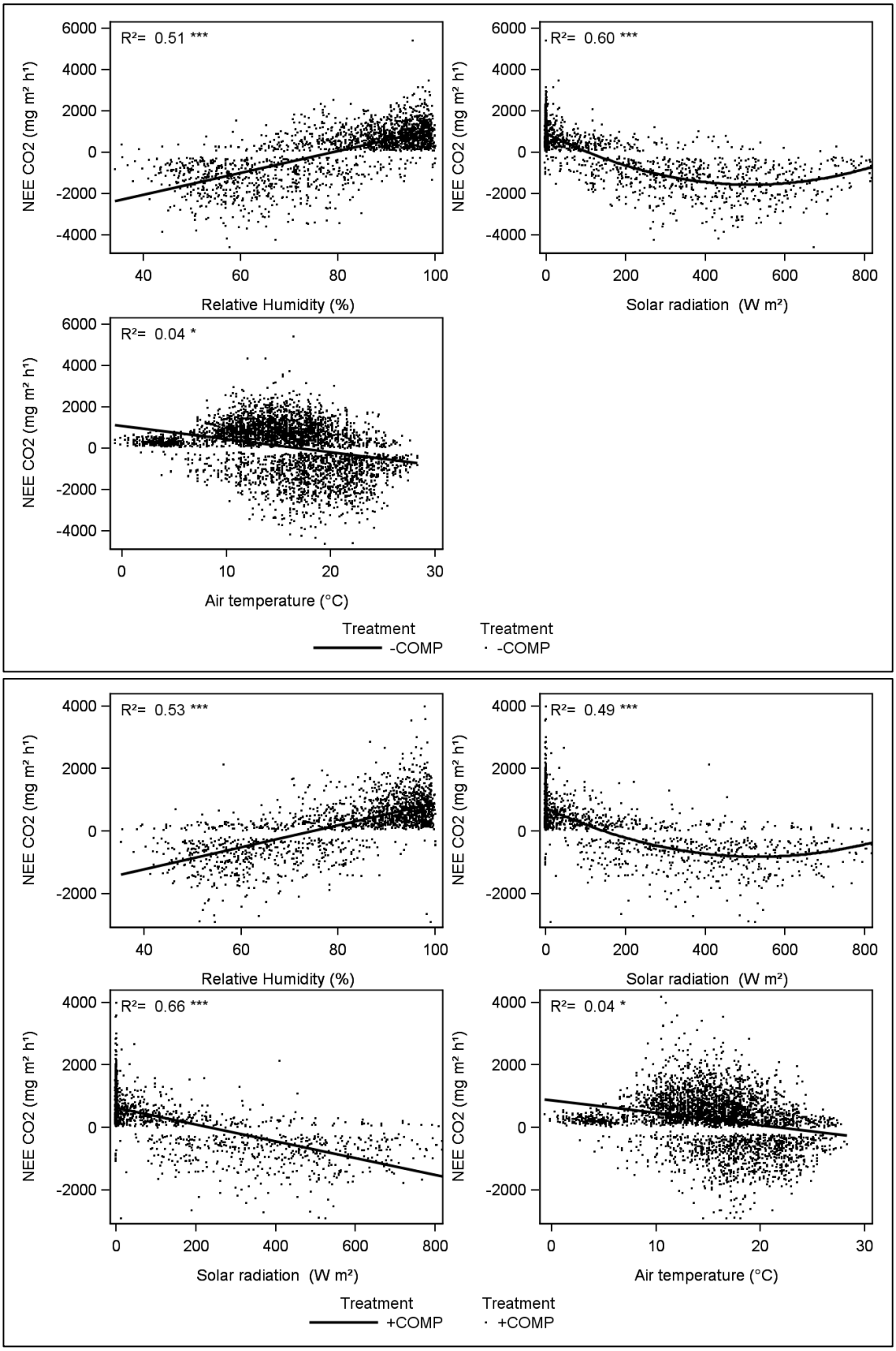

Figure 3.25 Environmental variables which demonstrated a significant relationship with NEE of CO_2 measured using SkyBeam, for -COMP (top three panels) and +COMP plots (bottom four panels). R^2 values and significance level are shown, (* p< 0.05, ** p< 0.01, *** p< 0.001).

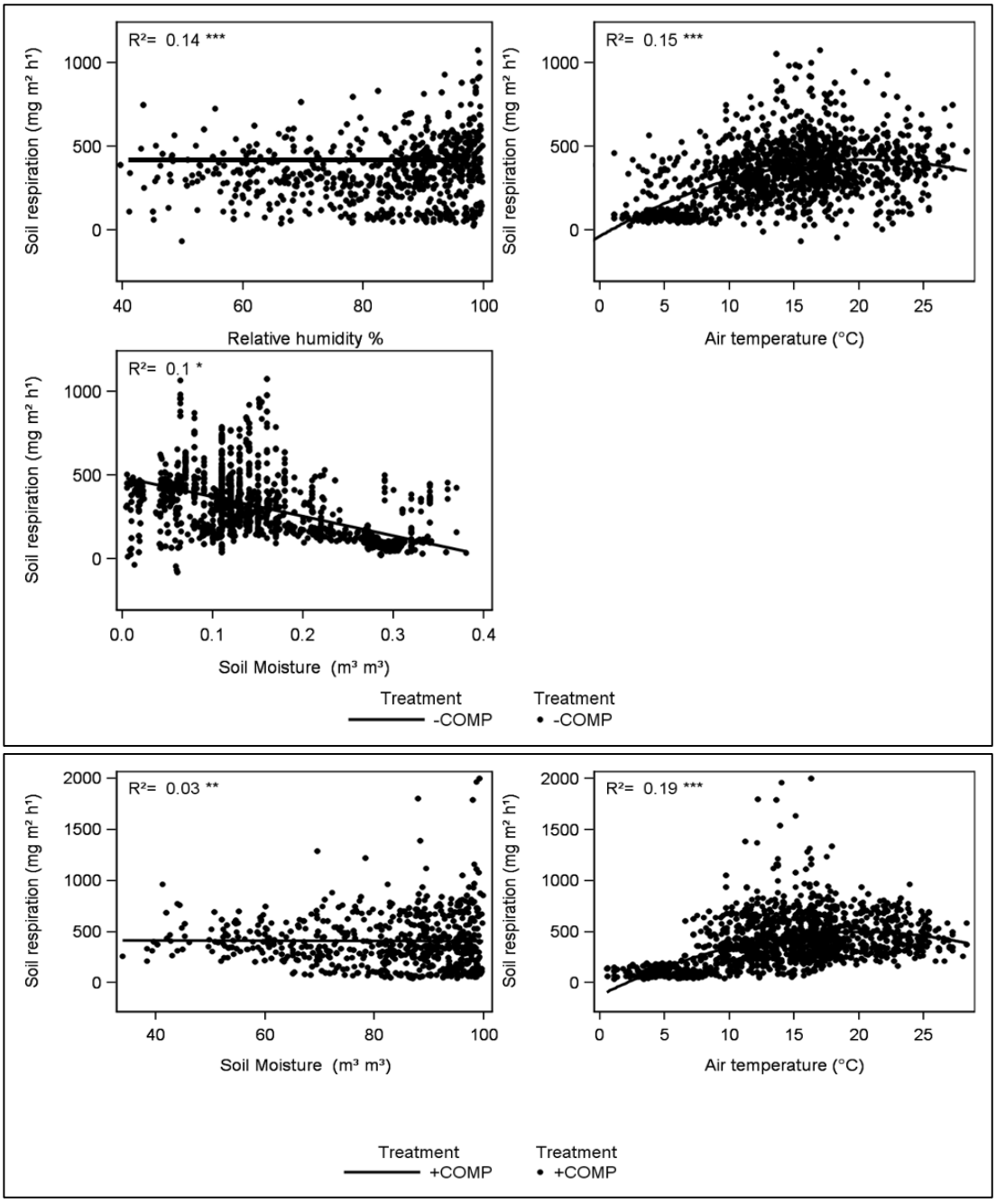

Figure 3.26 Relationship of soil respiration to environmental variables from plots treated with compost (+COMP, bottom panel) and controls (-COMP top panel). R^2 values and significance level are shown, (* p< 0.05, ** p< 0.01, *** p< 0.001). The model, linear or non-linear, with the best fit is displayed.

The effect of soil moisture on respiration was different between the two treatments. Whereas it was not significantly related in the +COMP plots, it there was a negative relationship in the control plots, where it explained 10 % of the variation (Figure 3.26). This relationship would suggest that as volumetric soil moisture approached 40%, soil respiration approached zero in this treatment.

3.3.7.5 N_2O and environmental variables

As seen for soil respiration, air temperature and relative humidity were the two variables consistently significantly related to the NEE of N_2O from both compost treatments (Figure 3.27). Relative humidity showed a weak positive relationship with both the –-COMP plots (R^2= 0.02) and the +COMP plots (R^2- 0.04). The variable which explained most of the variation in flux of N_2O was air temperature, for the -COMP treatment (R^2= 0.11), and whilst this variable had a slightly better relationship with the +COMP plots (R^2= 0.13), it was soil moisture that explained most of the variation in N_2O flux from these plots (R^2= 0.14), with which N_2O flux had a positive relationship (Figure 3.27).

The relationship of N_2O and environmental variables differed somewhat for the monthly coverbox data (Figure 3.28). The variable which explained the greatest variation (R^2= 0.30) in the –-COMP treatment was the daily minimum value of relative humidity, with soil N_2O fluxes declining with increased humidity. Daily minimum temperature also had a big influence, (R^2= 0.26) with fluxes increasing with temperature, and concurrent soil temperature (R^2= 0.20) and air temperature (R^2= 0.16) were also significantly related to soil N_2O flux (Figure 3.28). The relationship with soil temperature indicated that fluxes increased exponentially above 10^{o}C, and that air temperature > 20^{o}C were required for the highest fluxes (Figure 3.28).

Similarly, in the +COMP plots N_2O fluxes increased above a soil temperature threshold of 10 ^{o}C, and this was the best predictor of fluxes (R^2= 0.44, Figure 3.28). The relationship with concurrent air temperature was not so strong in the +COMP treatment (R^2= 0.16), though fluxes did increase with temperature, and this was clearer in the relationship with minimum daily air temperature, which explained 32%

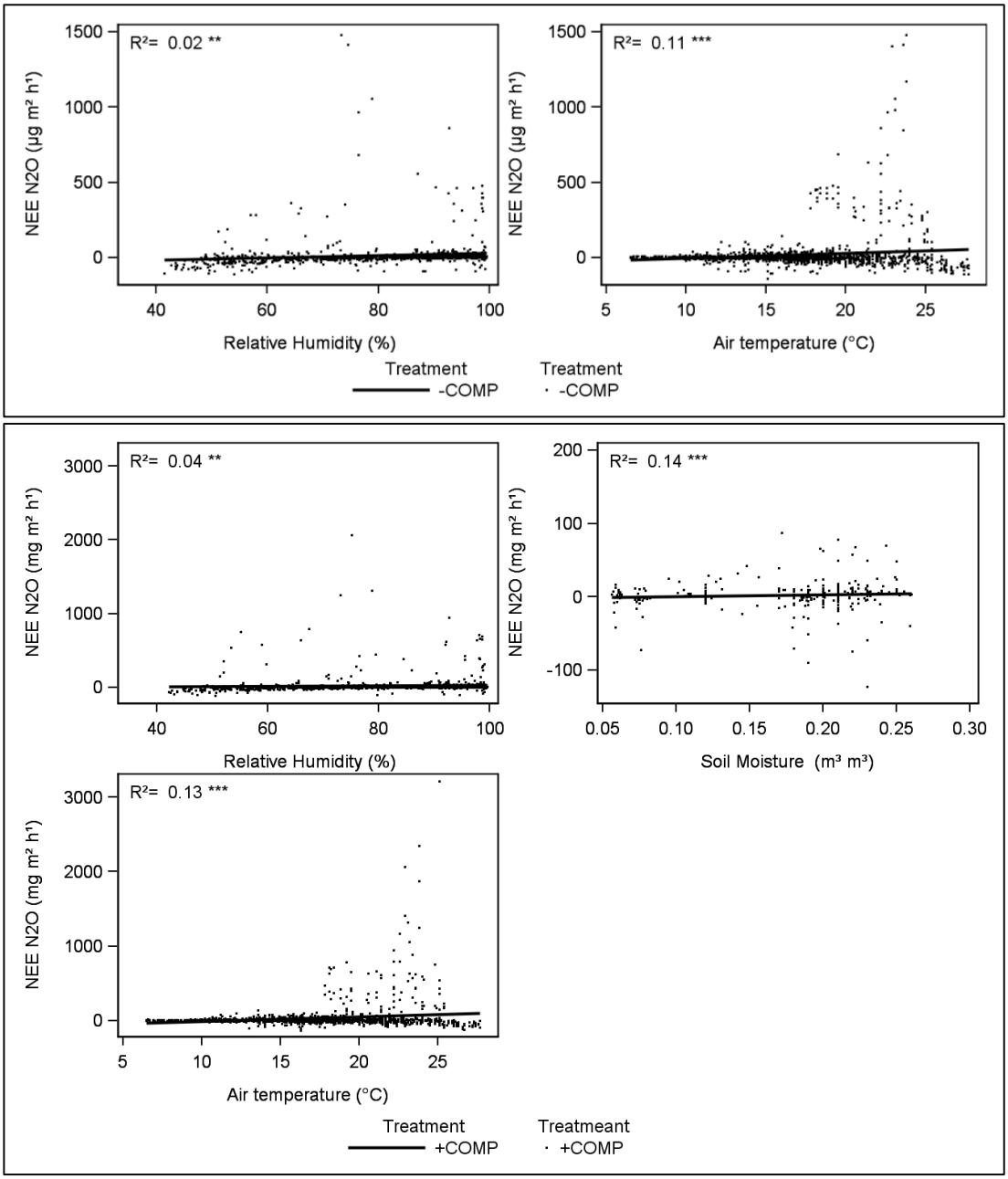

Figure 3.27 Relationship of NEE of N_2O measured using SkyBeam to environmental variables from plots treated with compost (+COMP bottom panel) and controls (-COMP top panel). R^2 values and significance level are shown, (* p< 0.05, ** p< 0.01, *** p< 0.001). The model, linear or non-linear, with the best fit is displayed.

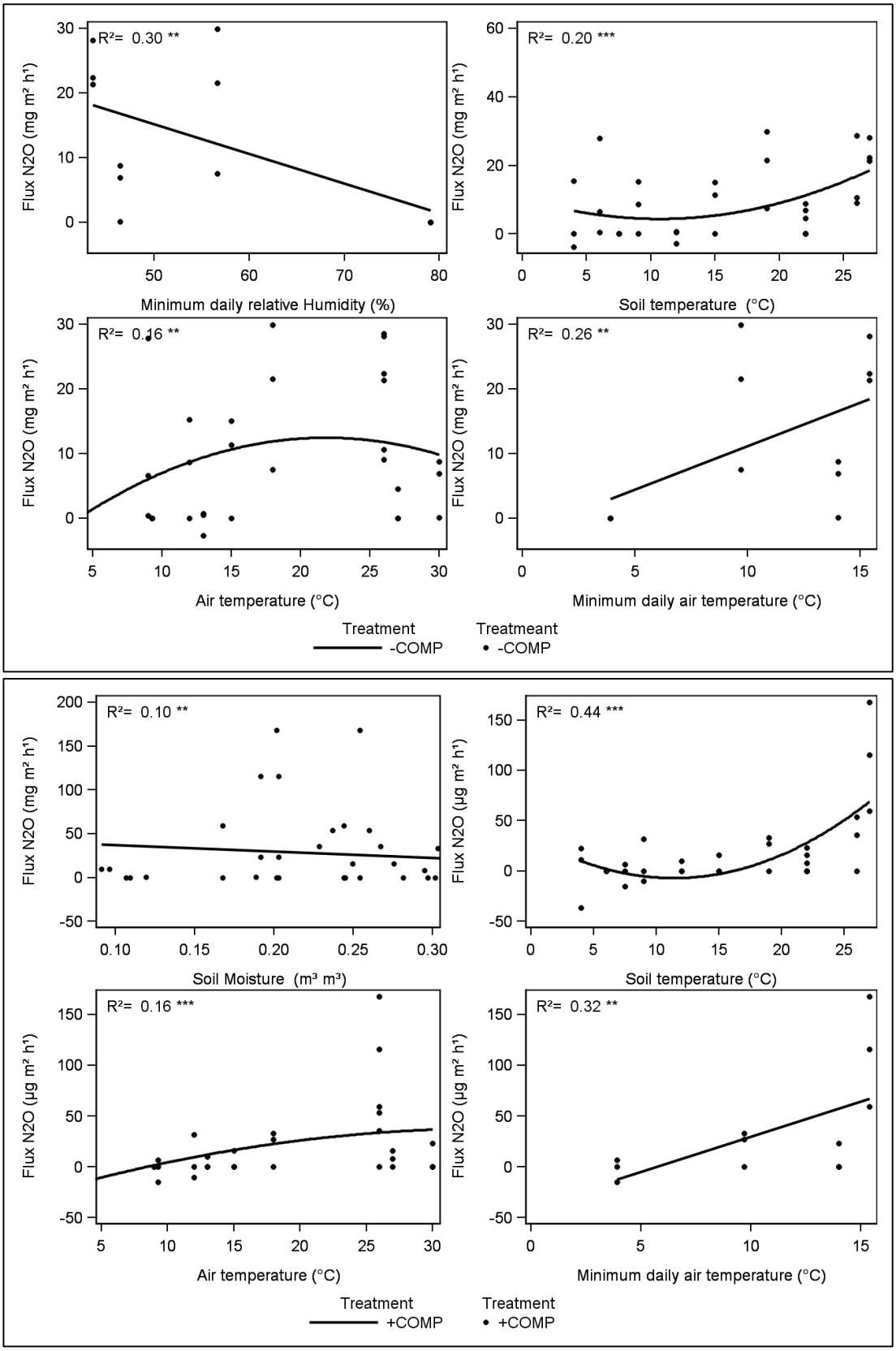

Figure 3.28 Significant relationships of environmental variables soil N_2O flux measured using coverboxes from compost amended plots (+COMP bottom panel) and controls (-COMP top panel) under *Miscanthus*.

of the variation in fluxes. Soil moisture was also significantly related to N_2O fluxes, though this relationship was relatively weak (R^2= 0.10), and, perhaps surprisingly, was negative (Figure 3.28).

3.3.7.6 CH_4 and environmental variables

CH_4 fluxes measured using SkyBeam were most closely related to relative humidity in the control treatment (R^2= 0.30) and the +COMP treatment (R^2= 0.19), with fluxes increasing with humidity in both (Figure 3.28). Both treatments also showed a significant negative relationship with solar radiation, and whilst it was a stronger relationship in the +COMP plots (R^2= 0.16) than the controls (R^2= 0.09), fluxes declined more quickly with radiation in the latter (Figure 3.29). This decline in fluxes was not a reduction in emission, since fluxes were predominantly negative, rather it indicates an increase in oxidation of CH_4. In addition to solar radiation and humidity, uptake of CH_4 increased with air temperature, though this relationship was weak for both the control plots (R^2= 0.05) and +COMP treatment (R^2= 0.04). This relationship suggests, for both treatments, that a shift from net emission to net uptake of CH_4 occurred at around 15^{o}C.

The monthly measurements of soil CH_4 flux demonstrated slightly different relationships with environmental variables. In fact, no variables were significantly related to the fluxes measured from the control plots. However, the relationship between CH_4 flux and air temperature was significant in the +COMP plots, and though it was better described by a non-linear relationship (R^2= 0.24) in the monthly data, it would indicated that at air temperatures above 15^{o}C CH_4 fluxes displayed a net uptake (Figure 3.30). The pattern was similar with soil temperature, though this relationship was less strong (R^2= 0.10). Two other variables significantly related to CH_4 fluxes were mean daily solar radiation (R^2= 0.24) and soil moisture (R^2= 0.17), and while the former was a positive relationship, with negative fluxes at low daily mean radiation and positive fluxes above a mean of 150 W m^{-2}, fluxes became more negative with increased soil moisture (Figure 3.30), though the soil was dry throughout the study, with moisture never exceeding 30%.

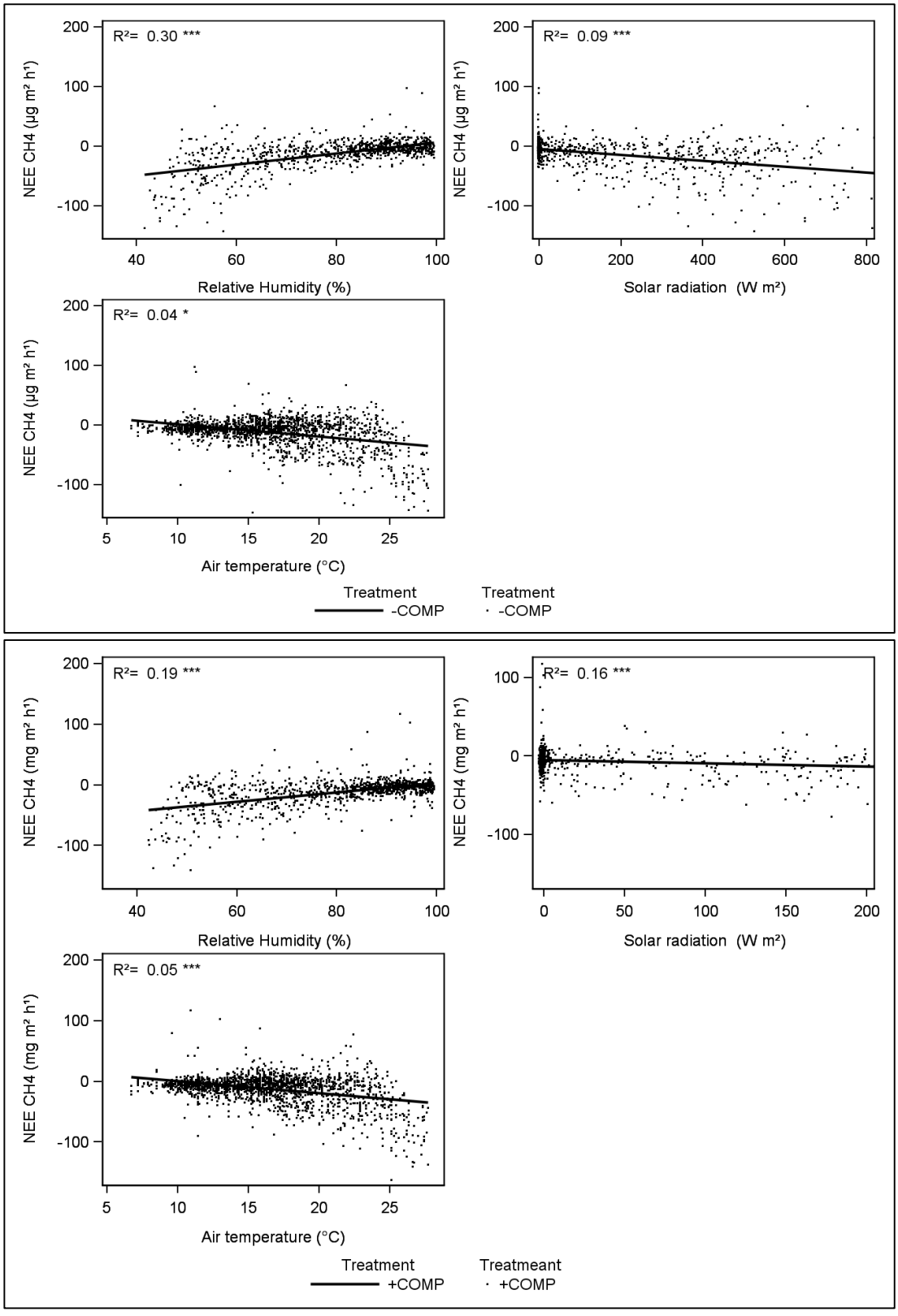

Figure 3.29 Relationship of NEE of CH_4 measured using SkyBeam to environmental variables from plots treated with compost (+COMP bottom panel) and controls (-COMP top panel). R^2 values and significance level are shown, (* p< 0.05, ** p< 0.01, *** p< 0.001). The model, linear or non-linear, with the best fit is displayed.

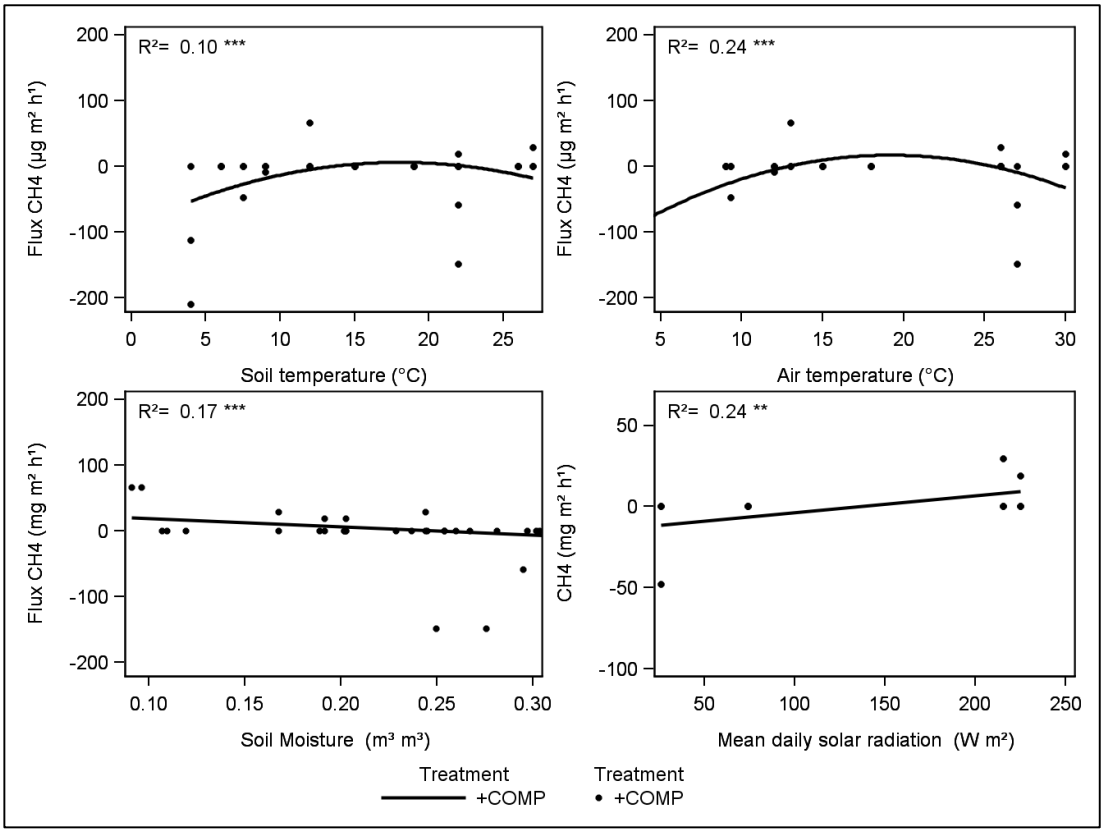

Figure 3.30 Significant relationships of environmental variables soil CH_4 flux measured using coverboxes from compost amended plots (+COMP) under *Miscanthus*. No significant relationships were found with the fluxes from the control (-COMP) plots. R^2 values and significance level are shown (* p< 0.05, ** p< 0.01, *** p< 0.001).

3.3.8 Multiple regression models

It was possible to account for at least 75 % of the variance in all the fluxes of all three gases from the +COMP treatment, though the –-COMP treatment was less well described. Solar radiation was the most important predictor of NEE of CO_2 from both treatments, (Equations 3.1 and 3.4), with daily rainfall significant for the –-COMP plots and soil moisture for the +COMP treatment. Solar radiation was also the most significant variable for N_2O flux from the –-COMP plots, though this model performed less well (R^2= 0.29, Equation 3.2). Air temperature had a bigger influence on N_2O flux from the +COMP plots than any other variable, and overall this model accounted for a much greater proportion of the variance in flux than in the control plots (R^2= 0.77, Equation 3.5). Air temperature was the most important variable in respect to CH_4 fluxes, and was the only variable significantly related to +COMP fluxes, accounting for 23% of the variance (Equation 3.3); it also had the most influence on CH_4 flux from the +COMP plots, and was incorporated in a model explaining 86% of the variation here (Equation 3.7). Soil respiration was very well described by a model including solar radiation and soil temperature (R^2= 0.93, Equation 3.4) in the –-COMP plots and was most strongly influenced by air temperature in the +COMP plots, with other significant variables being soil moisture and soil temperature (R^2= 0.91, Equation 3.8).

3.3.8.1 Control plots

NEE CO_2 (mg m^{-2} h^{-1}) = -8.4 * solar radiation (W m^{-2}) – 137 * daily rain (mm) + 1179

R^2= 0.85, p< 0.0001 **(Eq 3.1)**

NEE N_2O (µg m^{-2} h^{-1}) = -0.03 * solar radiation (W m^{-2}) + 2.3 * daily rain (mm) – 3.9

R^2= 0.29, p< 0.05 **(Eq 3.2)**

NEE CH_4 (µg m^{-2} h^{-1}) = -1.6 * air temperature (^oC) + 10.5

R^2= 0.23, p< 0.03 **(Eq 3.3)**

Soil respiration (mg m^{-2} h^{-1}) = -0.7 * solar radiation (W m^{-2}) + 11.2 * soil temperature (^oC) + 268

R^2= 0.93, p< 0.0001 **(Eq 3.4)**

3.3.8.2 Plots with compost

NEE CO_2 (mg m^{-2} h^{-1}) = -4.2 * solar radiation (W m^{-2}) + 198 * soil moisture (%) -833

R^2= 0.75, p< 0.0001 **(Eq 3.5)**

NEE N_2O (µg m^{-2} h^{-1}) = -11.0 * air temperature (^oC) + 7.5 * soil temperature (^oC) – 4.5 * daily rain (mm) + 30.4

R^2= 0.77, p< 0.0001 **(Eq 3.6)**

NEE CH_4 (µg m^{-2} h^{-1}) = -18.6 * air temperature (^oC) + 15.8 * soil temperature (^oC) – 7.4 daily rain (mm) -8.0

R^2= 0.86, p< 0.0001 **(Eq 3.7)**

Soil respiration (mg m^{-2} h^{-1}) = 48.3 * air temperature (^oC) + 130 * soil moisture (%) – 57.9 * soil temperature (^oC) – 73.6

R^2= 0.91, p< 0.0001 **(Eq 3.8)**

3.3.9 Diurnal patterns in trace gas fluxes

3.3.9.1 NEE measured using SkyBeam

The diurnal pattern for NEE of CO_2 was typified by positive fluxes through the night time and negative fluxes during the daytime. The transition from emission to uptake was relatively rapid, with an average flux of *ca.* 1000 mg m^{-2} h^{-1} at 06.00 but negative flux by 07.00 from –-COMP, indicating that photosynthesis quickly exceeded respiration (Figure 3.31). The transition was less quick in the +COMP plots, and tended to occur slightly later. The peak emissions CO_2 were on average approximately 1200 mg m^{-2} h^{-1} from –-COMP and 1000 mg m^{-2} h^{-1} from +COMP, and occurred between 01.00 and 02.00 (Figure 3.31). Night time NEE from the –-COMP plots tended to be slightly higher than the +COMP treatment, but during the day the difference was more pronounced, in the opposite direction, with maximum uptake in the region of -1500 mg m^{-2} h^{-1} in –-COMP *viz ca.* -800 mg m^{-2} h^{-1} from +COMP. The period of maximum uptake occurred between 10.00 and 16.00, but tended to be more

even in the +COMP treatment. The period during which NEE switched from negative to positive in the early evening was not so swift and typically occurred between 17.00 and 18.00 (Figure 3.31).

In a similar pattern to NEE of CO_2, N_2O also exhibited a diurnal trend of positive fluxes during the night time and negative fluxes during the day time (Figure 3.31, bottom panel). Maximum emission occurred between 03.00 and 04.00 and were in the region of 5 – 15 µg m^{-2} h^{-1}. From 05.00 fluxes consistently declined, in a manner less severe than displayed by CO_2, becoming negative around 09.00 and reaching maximum uptake at 16.00. Maximum uptake was *ca.* -20 µg m^{-2} h^{-1}, but the transition from uptake to emission during the evening was quicker than the opposite switch in the morning, and closely resembled the change from negative to positive displayed by that of CO_2 (Figure 3.31

CH_4 fluxes were on average negative throughout the entire day. However, these too displayed a diurnal pattern, characterised by fluxes close to zero during the period 21.00- 06.00, and oxidation through the day (Figure 3.31). After 06.00, in a fashion similar to that seen in CO_2 and N_2O, oxidation increased at a fairly constant rate until it peaked at *ca.* -40 µg m^{-2} h^{-1}, coinciding with the largest negative N_2O fluxes, but occurring 1-2 hours after the most negative CO_2 fluxes (Figure 3.31).

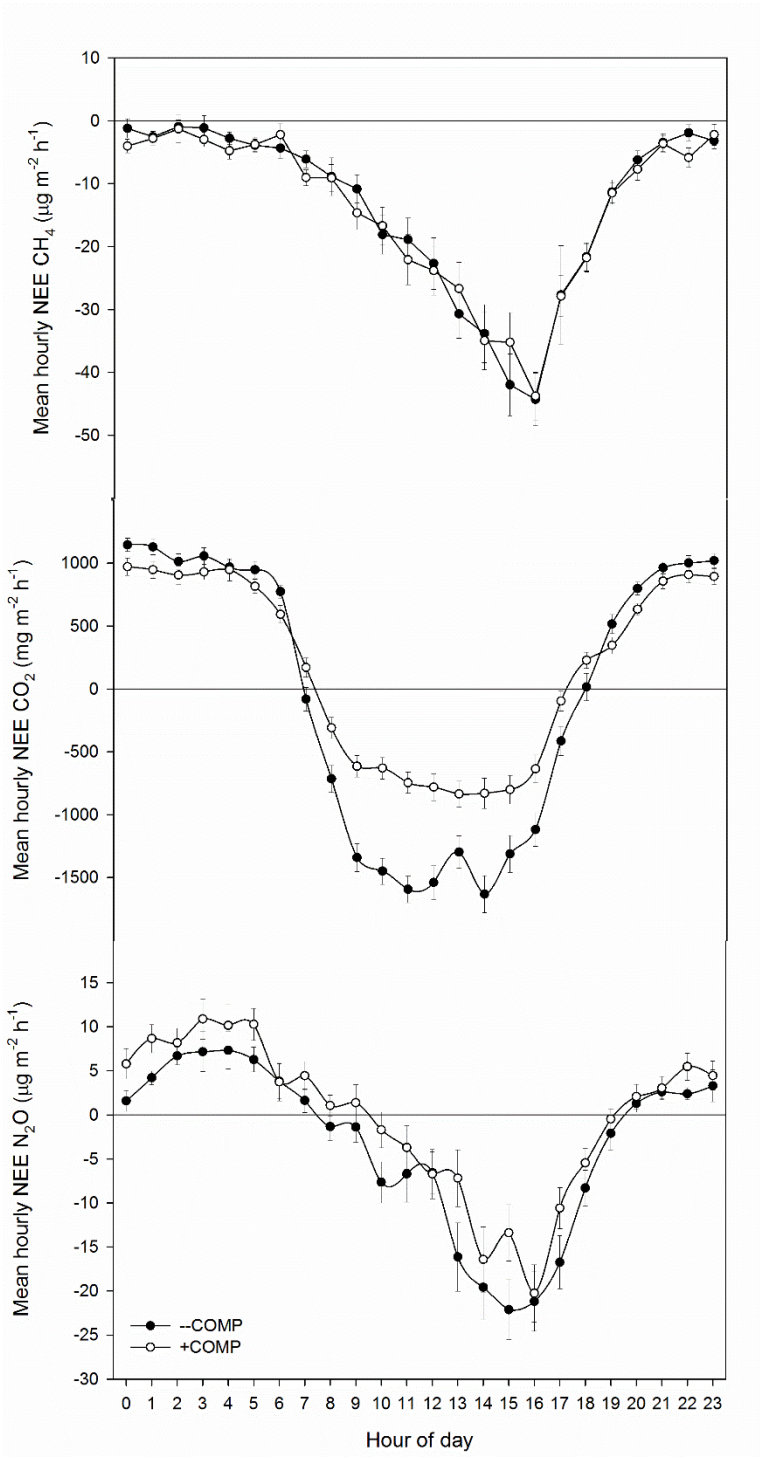

Figure 3.31 Diurnal pattern of NEE of CH_4 (top panel), CO_2 (middle panel) and N_2O (bottom panel) from *Miscanthus* amended with compost (+COMP) and a non-amended control (-COMP), as measured using SkyBeam between July and October 2013. Values displayed are means ± 1SE (n=3 * 51 days for CH_4 and N_2O and n= 3* 89 days for CO_2).

3.3.9.2 Soil respiration

The diurnal fluctuation in soil respiration was typified by lowest rates of respiration around 9.00 (Figure 3.32), which coincided with the lowest values of NEE of CO_2 (Figure 3.31, middle panel). However, respiration increased through the afternoon and continued to do so throughout the evening, reaching its daily peak at around 21.00 in the –-COMP controls: the pattern was similar for the +COMP plots, though the afternoon increase was steeper and peaked earlier at 15:00. Respiration tended to be higher in the +COMP treatment through the afternoon (Figure 3.32) as it increased more quickly after the daily minimum, which was in contrast to NEE of CO_2, which was lower in the –-COMP treatment during the day. During the night R_{soil} was similar for both treatments (Figure 3.31, middle panel). It was also apparent that the daily maxima and minima were approximately 20-30 mg m^{-2} h^{-1} higher in the +COMP treated plots, thought the absolute daily variation of *ca.* 40 mg m^{-2} h^{-1} was similar for both plots. This amplitude of diurnal variation was 15% and 14% of the daily maximum values for the –-COMP and +COMP plots respectively.

3.3.9.3 Drivers of diurnal patterns

The pattern of soil respiration did not simply follow the pattern of soil temperature, indicating this process was not simply temperature dependent. However, during the period from 09.00 to 17.00 it would seem that soil temperature could have been the key driver of soil respiration (Figure 3.33, top panel), and this period was used to estimate the magnitude of its influence, which was subtracted in order to calculate a temperature-independent respiration rate, referred to here as ‘baseline respiration’, (Figure 3.33, bottom panel).

NEE of N_2O and CH_4 tracked the pattern of baseline respiration throughout the night, (Figure 3.33). During the day time, particularly between 09.00 and 17.00 the trends in NEE diverged from respiration, whilst still following the same general pattern (Figure 3.33). The pattern in baseline respiration was also remarkably similar to that of NEE of CO_2, as measured using SkyBeam (Figure 3.34).

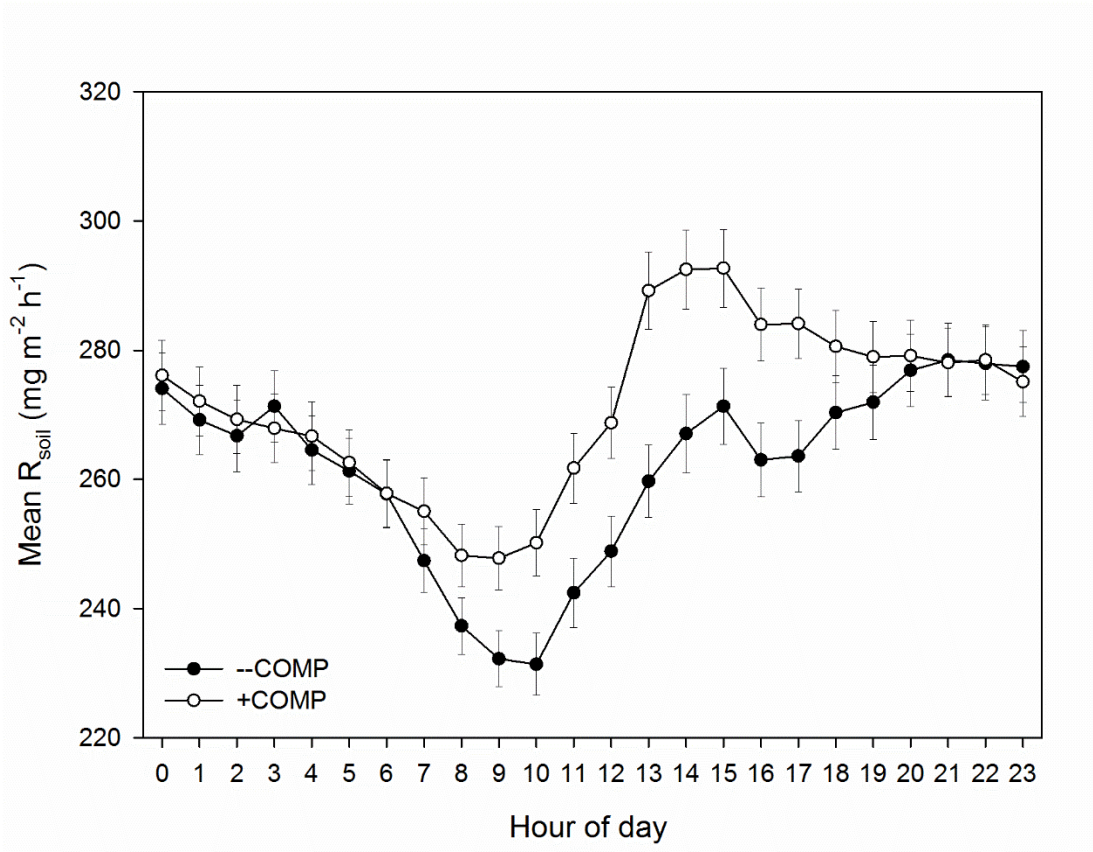

Figure 3.32 Diurnal pattern of R_{soil} from plots under *Miscanthus*, following a compost addition (+COMP) and untreated controls (-COMP). Values displayed are mean ± 1SE (n=3).

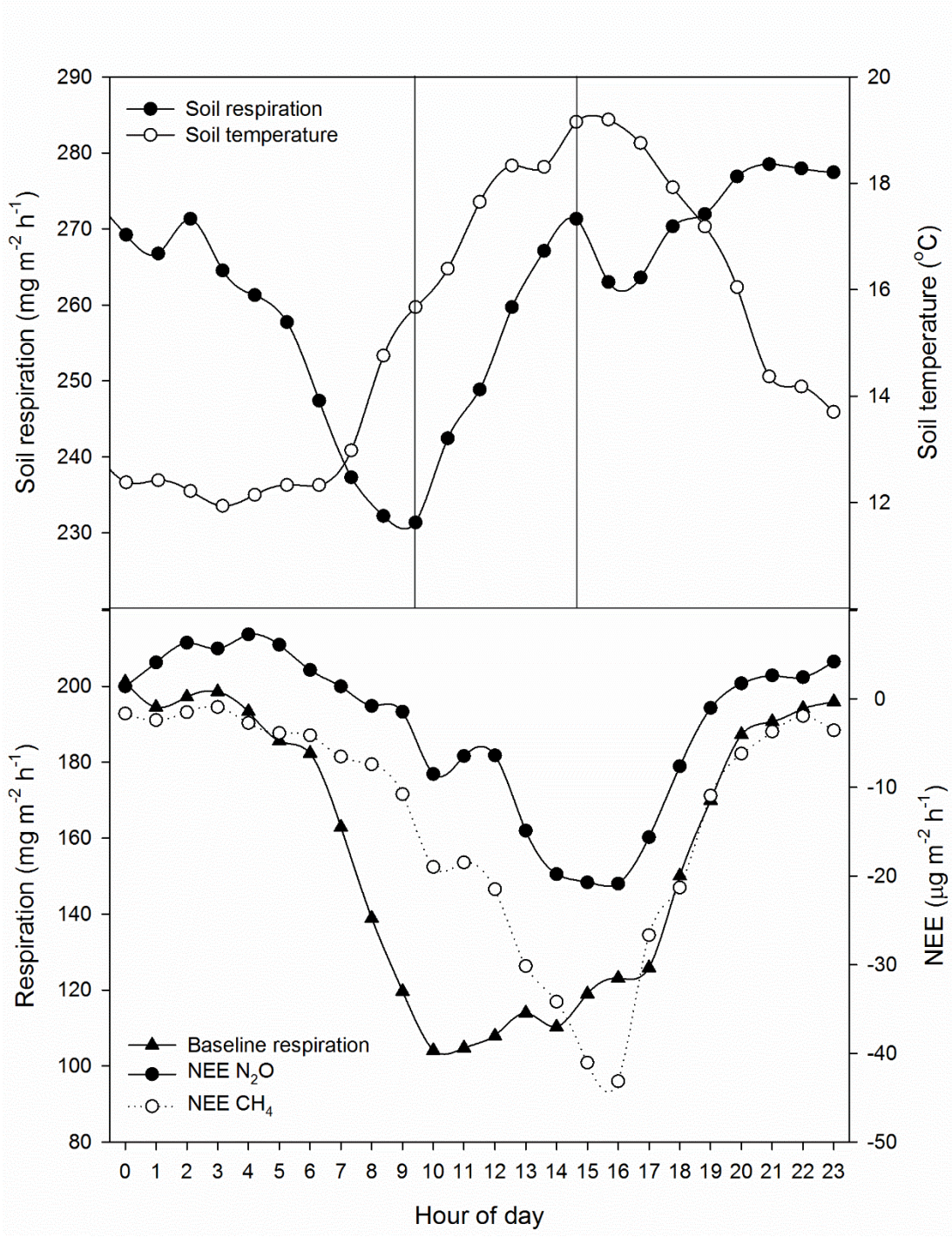

Figure 3.33 Top panel: diurnal pattern of soil respiration and soil temperature. The vertical lines indicate period of day when soil temperature appears to be the principal driver of respiration. Bottom panel: diurnal pattern of soil respiration with temperature dependent respiration subtracted (baseline respiration) and NEE of N_2O and CH_4 measured using SkyBeam. Values shown are means across the study period, only data from –-COMP treatment used.

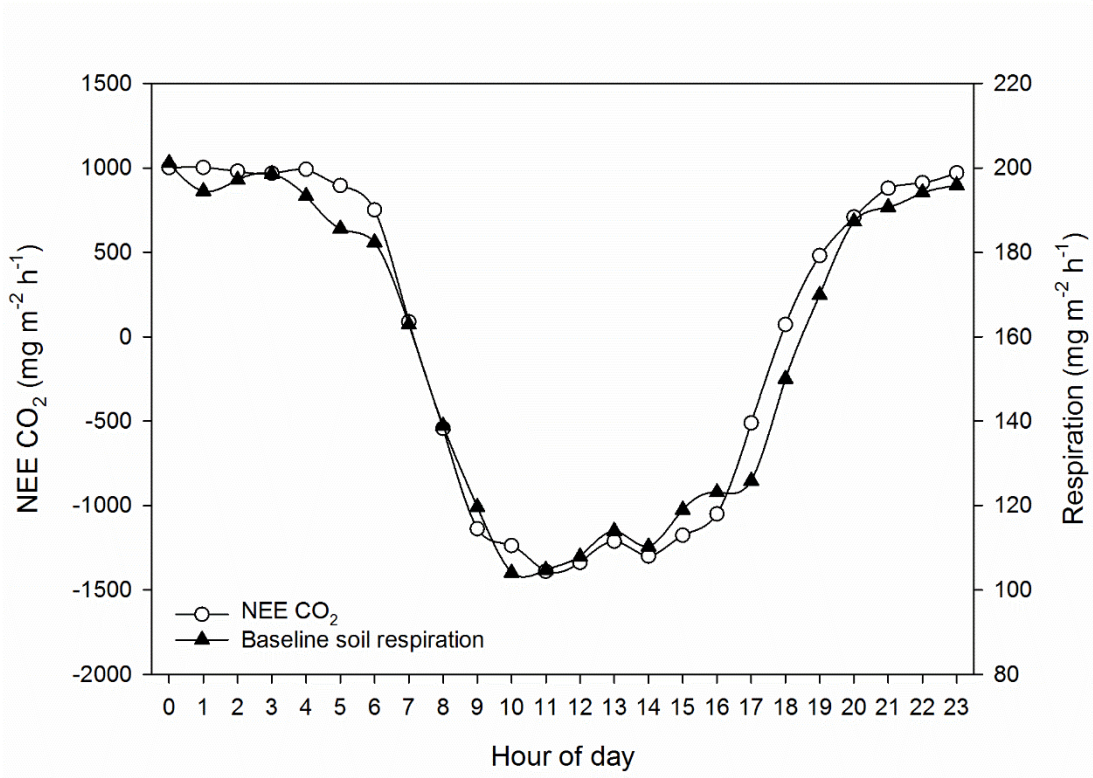

Figure 3.34 Diurnal patterns of NEE CO_2 from *Miscanthus* measured using SkyBeam and soil respiration using automated chambers. Negative values in NEE indicate net uptake of CO_2. Values shown are means across the study period from un-amended plots (-COMP).

3.4 Discussion

3.4.1 Evaluation of SkyBeam system

SkyBeam operated successfully and uninterrupted from the beginning of July until the first week of October 2013, and for a further few weeks throughout November and December 2013 until it was dismantled at the end of the year. In doing so the system completed a total of 20,000 chamber closures. Whilst ambitious designs for chambers to measure gas exchange by large vegetation have been proposed for many years (Eckardt, 1968), examples of implementation of such ideas are rare, and lack the automation required to produce continuous data (Mordacq *et al.*, 1991). The design of SkyBeam not only produced a dataset with 24 hour coverage over six months (Figure 3.18), but by using a single automatic chamber the *Miscanthus* crop at each measurement position was only enclosed for 10 minutes out of every hour, ensuring its isolation from the environment was kept to a minimum.

Due to the automated nature of both SkyBeam and the soil flux chambers employed in this study, flux data were generated for CO_2 for both night-time and day-time for a period of almost 6 months, at approximately hourly resolution. The same resolution data were generated for CH_4 and N_2O for two shorter, distinct, campaigns of 24 and 26 days respectively. Such CO_2 data were not delivered by EC since it is not really effective at collecting flux data at night due to the afore-mentioned problems of atmospheric stratification (Aubinet, 2008), with mathematical gap filling being a major limitation of the technique. The delivery of continuous data for NEE of CO_2 and soil respiration has shed light upon the underlying processes of NEE and raises questions about the way in which CO_2 fluxes are partitioned in many EC datasets. Similarly, the data delivered by SkyBeam differed from data generated using cover boxes, which were used exclusively only in the day-time and on a relatively infrequent monthly schedule, and this too has provided important information about interpretation of single daily measurements of soil GHG fluxes.

3.4.2 *Miscanthus* as a net carbon source

It is important to note that 2013 was an atypical year in terms of normal *Miscanthus* management. This was largely due to the non-standard harrowing of the *Miscanthus* field between the previous year's harvest and the emergence of new green shoots, in an effort to increase the yield by spreading the rhizomes more evenly. The previous year the crop had produced a below-expected yield, which had been attributed to the

heterogeneity of the original distribution of the rhizomes, sown at least 7 years previously. Tillage is known to increase soil respiration, since aerobic microbial activity is stimulated through increase exposure to atmospheric oxygen (e.g. Fiedler *et al.*, 2015). Due to the disturbance from tillage, it is suggested that 2013 was more typical of an establishment year and it is widely accepted that *Miscanthus* does not reach peak yields until around its sixth year (Arundale *et al.*, 2014, Christian *et al.*, 2008, Larsen *et al.*, 2014). The biomass harvested from the experimental plots in this study equated to *ca.* 2 t ha^{-1}, which is much less than optimum yields reported in this country, which can be in excess of 12 t ha^{-1} (Clifton-Brown *et al.*, 2004). During the establishment phase, yields gradually increase over the first 4-5 years and it was unsurprising, therefore, that this 2013 crop failed to exceed 1.5 m in height. This poor growth rate would help to explain why, according to SkyBeam data, the system was a net source for CO_2 over the study period. In addition to less aboveground biomass photosynthesising, turnover of belowground carbon has been shown to cause *Miscanthus* to be a net source of CO_2 during the first two years of establishment (Jorgensen *et al.*, 2014). It should also be pointed out that NEE of CO_2 was consistently at its lowest during the period immediately prior to equipment failure at the end of September 2013 (Figure 3.6), and so it is conceivable that had measurements continued the system would have been seen to be a sink for CO_2 over the course of the year.

3.4.3 Compost addition

3.4.3.1 Yield and soil properties

The biomass harvested from the +COMP plots, whilst not significantly lower than the –-COMP plots, suggested that the compost addition certainly did not increase yield in the experimental plots. One of the purported advantages of growing *Miscanthus* as a bioenergy crop is that it has very low nutrient requirements. In previous studies on fertiliser addition to *Miscanthus* there have been mixed results, with some studies showing increased yields with nitrogen application (Cosentino *et al.*, 2007, Ercoli *et al.*, 1999), but many that did not (Danalatos *et al.*, 2007, Muylle *et al.*, 2015, Teat *et al.*, 2015), and some that have seen effects vary across different sites (Haines *et al.*, 2015). It has been shown that *Miscanthus* grown with lower N input produces a higher quality feed stock for combustion, due to a reduction in the ash that it produces (Hodgson *et al.*, 2010). Green compost is not commonly applied to *Miscanthus*, though it may be used to aid phytoremediation of brownfield sites contaminated with

heavy metals (Lord, 2015), which may subsequently be used for bioenergy crop production. Since this was not such a site, it remains unclear exactly the aim of the farmer in making this application; it may be that *Miscanthus* acts as an inexpensive solution to disposal of waste materials. It did help the soil retain moisture, and in so doing may have slowed leaching of nutrients in soil water, which may have benefits in terms of yields in future years.

3.4.3.2 CO_2

Since the NEE of CO_2 is the product of the two general processes, respiration and photosynthesis, the potential existed for the compost to affect the balance by influencing either or both of these processes. The range of NEE from the +COMP treatment tended to be less than that from the –-COMP, with less uptake during the day, and lower emission through the night. The lower values during the day are reflected by the trend in lower standing biomass in those plots: less vegetation means less photosynthesis which also leads to less carbon being fixed in those plots and less autotrophic respiration. However, the soil respiration from the +COMP plots suggested that the compost was stimulating heterotrophic respiration during the first six weeks following application. There were only three replicates, and it is suggested that in future work a larger transect with more replication would help identify differences more easily. Green waste compost has been shown to increase soil respiration in some agricultural (Perez-Piqueres *et al.*, 2006, Vaughan *et al.*, 2011) and urban soils (Beesley, 2014).

3.4.3.3 N_2O

N_2O emissions from both treatments were generally low, in comparison to other agricultural systems where emissions may commonly be of the order of thousands of µg m^{-2} h^{-1} (Dobbie *et al.*, 1999). The peak soil fluxes measured using manual chambers were of a similar order of magnitude to those seen under *Miscanthus* when unfertilised (Drewer *et al.*, 2012, Jørgensen *et al.*, 1997). The peak fluxes measured using SkyBeam, however, were much higher and were more similar to the peaks often seen from fertilised arable crops (Smith *et al.*, 2012).

During the first period of high frequency N_2O measurements from SkyBeam, fluxes were higher from the +COMP treatment. This was most apparent during the first rainfall after measurements started during July 2013, when the highest fluxes from the soil chambers were also seen. As the first rain in over two weeks, this constituted a rewetting event, which have been shown to stimulate N_2O fluxes from agricultural

soils when fertilised with mineral nitrogen (Ruser *et al.*, 2006, Smith *et al.*, 2012), slurry (Rochette *et al.*, 2004) and especially when compacted (Beare *et al.*, 2009), but also from forest soils (Brumme *et al.*, 1999) and grasslands (Kim *et al.*, 2010). The likely cause of such bursts of N_2O emission is denitrification, as the precipitation causes a rapid rise in soil moisture and anaerobic microsites within the soil matrix. In well aerated soils, it has been suggested that prolonged dry periods allow a buildup of NO_3 through nitrification which is rapidly denitrified following rainfall (Kim *et al.*, 2010).

The current study suggests that the heightened effluxes of N_2O from the +COMP plots were not caused by increased input of nitrogen from the compost, since as green waste compost its carbon to nitrogen ratio is likely to have been very high, but due to the elevated soil moisture levels created by the compost amendment, which in turn made the soil more anaerobic and more suitable for N_2O production through denitrification.

3.4.3.4 CH_4

Over both measurement periods the SkyBeam data showed that the system was a net sink for CH_4, indicating that oxidation was the dominant CH_4 microbial process. It is perhaps surprising that there was no difference between the two compost treatments, since the compost increased the soil moisture. The elevated moisture might have been expected to stimulate CH_4 production due to increased anaerobic zones (McNamara *et al.*, 2008) and the occasion on which the highest efflux was recorded using manual chambers was during December 2013, when the soil was wettest.

3.4.4 Comparison of SkyBeam and manual chambers

Higher fluxes of N_2O and CH_4 were seen from the manual chambers than from the SkyBeam chambers within the same plots. The comparison was made between the closest temporal measurements, which was within two hours of each other. Despite this, there was an inevitable separation in time and space, neither of which cannot be discounted as a cause for the differences, especially given the diurnal variation in fluxes of both gases that were seen in this study. The second major difference was that SkyBeam included the vegetation within its chamber.

The presence of vegetation may play a role in GHG balance. Since it was first identified by Keppler *et al.* (2006), the formation of CH_4 by vegetation under UV-A stimulation has been further investigated and corroborated (Fraser *et al.*, 2015). CH_4 is further known to be transported via aerenchyma in vascular plants, particularly wetland species (Le Mer & Roger, 2001), where CH_4 formed in the anoxic rhizosphere is passively transported to the atmosphere. *Miscanthus sacchariflorus*, a species related to *Miscanthus x giganteus*, has been shown to be aerenchymous (Qin *et al.*, 2010) and it follows that the same may be true for *Miscanthus x giganteus*. In a CH_4 oxidising soil the concentration gradient could lead to CH_4 diffusing from the atmosphere through vegetation into the soil, meaning the presence of vegetation might increase the rate of CH_4 uptake from the air. Indeed, the presence of aerenchymous species has been shown to be able to reduce CH_4 emission from soils (Dinsmore *et al.*, 2009). Aerenchymous tissue has also been suggested to transport N_2O between soil and atmosphere along a concentration gradient (Jorgensen *et al.*, 2012, Pihlatie *et al.*, 2005, Rusch & Rennenberg, 1998), and so it may be a factor in the increased uptake of N_2O seen here in the SkyBeam chamber compared to the manual chambers.

3.4.5 Comparison of SkyBeam and EC system

NEE of CO_2 measured using SkyBeam differed to that measured using EC, in that the rate of uptake measured was lower in the former. Whilst fluxes were of a similar order of magnitude, it would appear that photosynthesis was not as strong from the SkyBeam experimental plots. It is entirely possible that, since the area covered by SkyBeam was smaller than the fetch of the EC system, there was a difference in the productivity of the crop between the two areas. The biomass harvested from the SkyBeam experimental plots was low, especially in comparison to the yields generally expected for *Miscanthus*. It is also possible that the crop in the SkyBeam area of the field developed more slowly than the field at large. It appeared as though the *Miscanthus* was photosynthesising most under SkyBeam during the period immediately prior to mechanical failure, in October 2013 (Figure 3.18), at a time when NEE from the EC system shows the field as a whole was not drawing down as much CO_2. The area of the field in which SkyBeam was assembled was close to a mature stand of various broadleaf trees (Figure 3.3), which, during the evening when the sun was in the west, cast a long shadow over the western side of the *Miscanthus* field. With no such obstacle shading the rest of the field, this will have affected the total radiation available to the *Miscanthus* in various parts of the field, and in fact the daily

mean values of radiation measured by the met station on SkyBeam were 81% of that measured by the system on the EC tower. This comparison is made with the caveat that no cross calibration was done between the two radiation sensors.

3.4.6 Diurnal patterns in trace gas fluxes

The diurnal pattern in NEE of CO_2 was entirely expected, with negative values seen in the day, due to photosynthesis, and positive values at night, when respiration was the dominant process. The pattern in soil respiration was not so straightforward, however. As seen in Chapter 2 of this thesis, the diurnal pattern of soil respiration under *Miscanthus* did not follow the expected pattern of a temperature dependent process, and this pattern was consistent between both compost treatments. It is widely accepted that soil respiration is controlled by either soil or air temperature and moisture (Buchmann, 2000), and this is the basis upon which NEE partitioning of EC data is generally conducted (Bhattacharyya *et al.*, 2013). It is clear that in this study that while temperature was an important controlling factor, there is a strong temperature independent influence on the diurnal pattern of soil respiration. It also raises questions regarding how EC data should be partitioned in future, and how reliable gap-filled night time data are.

Soil respiration is substrate limited, and increasing concentrations of labile carbon in the soil will cause an increase in respiration rate (Jones & Hodge, 1999, Kuzyakov, 2006), and it follows that soil respiration is controlled by photosynthesis (Kuzyakov & Cheng, 2001). The fact that in many ecosystems the peak in root exudation coincides with highest daily temperatures can mask the influence of carbon supply on respiration, though under forests, where the photosynthate may take up to four days to reach the rhizosphere, respiration and soil temperature can be decoupled (Ekblad & Hogberg, 2001). Under the *Miscanthus*, which in this year approached 2 m in height, it might be expected that the time taken for the photosynthate to reach the rhizosphere was shorter than that under mature forests, but longer than for shorter vegetation, thus explaining the peak in soil respiration which occurred in the early evening, and maintained high levels throughout the night, long after photosynthesis halted.

Once it is hypothesised that carbon supply might be the key driver of the diurnal pattern of soil respiration, the diurnal patterns in N_2O and CH_4 flux can be more easily interpreted. Where diurnal patterns in N_2O flux have been reported, the majority of

studies show increased emission through the day, reducing through the night, and temperature is reported as the driving influence (Das *et al.*, 2012, Hu *et al.*, 2013, Livesley *et al.*, 2008, Simek *et al.*, 2010, van der Weerden *et al.*, 2013). The diurnal pattern of N_2O uptake during light conditions, and release during darkness, has been shown at one arctic tundra site (Stewart *et al.*, 2012), where CH_4 and N_2O uptake occurred concurrently. That both net emission and net consumption of N_2O were seen over the course of the day under the *Miscanthus* indicates that there was more than one process governing NEE. Daytime net consumption exceeded emission, but this balance changed rapidly during the early evening, coinciding with the upturn in temperature independent soil respiration. Since respiration is carbon dependent, the increase in respiration rate might also be used as a proxy for carbon availability. Denitrification is a heterotrophic process which requires a C source (Firestone & Davidson, 1989), and so sudden availability of the day's photosynthate in the rhizosphere may stimulate a rapid increase in N_2O production through denitrification. Furthermore, with increasing soil respiration, it would be expected that O_2 concentration will decrease, providing better conditions for denitrification, due to the sensitivity of the enzyme nitric oxide reductase (NOR) to O_2 (Knowles, 1982).

N_2O uptake is most often reported in nitrogen limited soils with high soil moisture (Roobroeck *et al.*, 2010, Wrage *et al.*, 2004), and is generally attributed to the complete reduction of N_2O to N_2 as the final step in denitrification (Chapuis-Lardy *et al.*, 2007, Wu *et al.*, 2013). The net uptake reported here during the day occurred in a soil without a history of mineral N application, and the compost applied had a high C:N ratio, so it is to be expected that the soil under the *Miscanthus* had a low N concentration. However, the soil was generally dry, and rather than stimulating N_2O reduction, heavy rainfall was followed by the highest emissions seen. N_2O uptake by soil has been reported in dry soil with high O_2 concentration (Flechard *et al.*, 2005), and a similar sink has been shown to be due to microbial processes, since autoclaving the soil halted the process (Wu *et al.*, 2013). Net uptake under dry conditions may also be due to diffusion along a concentration gradient, where N_2O moves from the atmosphere down the soil profile to reduction sites at depth (Stewart *et al.*, 2012). One study suggested that another C4 species (*Zea mays*) may store or even metabolise N_2O (Grundmann *et al.*, 1993), a process which would also help to explain the lower N_2O flux seen in the SkyBeam chamber compared to the manual chambers. Alternatively, in the absence of NO_3^-, denitrifiers may use N_2O as an electron acceptor. This, however, would not explain the increase in emission of N_2O during

the night, unless there were also a diurnal pattern in NO_3 availability which would see the microbes preferentially use this, thus producing N_2O in the process.

It has been suggested recently that many (in some cases, more than 99%) reported negative N_2O fluxes should be discounted as within the detection limit of the system by which they were measured (Cowan *et al*., 2014). By considering all the measured variables used to calculate a flux, it is possible to propagate the associated error terms to estimate the limits of uncertainty in the flux calculation. In this study, if the manufacturer's accuracy of N_2O concentration (0.2 ppb at concentrations greater than 300 ppb (LGR, 2014)) is used conservatively and an accuracy of ± 1 ppb is assumed, and a further 1% error is estimated for other variables (temperature, pressure, area and volume), this yields a propagated error of ± 1.45 %, or a detection limit of *ca.* ± 30 µg m^{-2} h^{-1} (Figure 3.8). In this case, 24 of 82 negative fluxes would be rejected as zero, and a further 61 positive fluxes would rejected across both compost treatments. In the study by Cowan *et al.*, (2014) the sites used each received significant N input, either through mineral fertiliser application, manure or through faecal deposits of grazing livestock, thus it is argued that these systems were more conducive to N_2O emission than the *Miscanthus* crop in this study. The negative fluxes seen in Cowan *et al.* (2014) were a distinct minority of the measurements, none were greater than -10 µg N_2O-N m^{-2} h^{-1}, all of which would fall within the estimated detection limit of SkyBeam; more than 25% of the negative fluxes witnessed in the *Miscanthus* were greater than twice the detection limit, and negative fluxes overall represented approximately half the total number of fluxes. Whilst it is plausible that many small negative N_2O fluxes from agricultural fields may be due to analytical error, it would be unwise to reject all such fluxes out of hand, especially since there is a conceptual basis (Davidson *et al.*, 2000) and experimental evidence (Wu *et al.*, 2013) for biological uptake of N_2O in soils.

The diurnal pattern of CH_4 flux differed from that of N_2O, in that fluxes were never positive. This does not discount the possibility that both oxidation and production were occurring in the soil, but it does raise the possibility that the control of the diurnal pattern was the single process of oxidation, which increased through the day, until it halted in the early evening and didn't start again until the morning. In this study CH_4 emission was best described by a model including temperature as the major explanatory variable. Diurnal variation in CH_4 emissions have been reported on numerous occasions in wetland plants, with peaks in emission occurring during the afternoon (Wang & Han, 2005, Yu *et al.*, 2013b, Zhang & Ding, 2011), which are

attributed to transport through the plant. A similar pattern of increased uptake during the afternoon, reducing at night has been reported from above a forest system measured using EC (Wang *et al.*, 2013), though this was attributed to the breakdown of the atmospheric boundary layer at night interpreted as emission during the night. Since it is not a micrometeorological technique, SkyBeam was not subject to such uncertainties in night time flux measurements. PAR has been attributed as the control of increased CH_4 oxidation in a forest understory during the day, where a diurnal pattern similar to that seen in the *Miscanthus* of this study was reported (Sundqvist *et al.*, unpublished). Direct uptake of CH_4 has been seen in boreal plants (Sundqvist *et al.*, 2012), and should such a process be under stomatal control, it would explain why uptake halted coincidentally with photosynthesis.

3.5 Conclusions

Whilst it is difficult to draw any wide conclusions regarding the net GHG balance of *Miscanthus* cultivation from this study, it is valuable in that it provides information on the effects of specific farming practices on a mature *Miscanthus* crop. The data presented here show that tillage of *Miscanthus* strongly hinders crop development, at least in the short term. The addition of green waste compost did not give any improvement in yield, but it did cause elevated emission of N_2O, an important GHG. Whilst N_2O only played a small part in the GHG balance here, any practice that increases GHG emissions during the cultivation of the crop is detrimental to the potential carbon savings of biomass-derived energy. The measurements from SkyBeam indicated that the *Miscanthus* was a net source of GHGs, an important consideration for a crop whose sole function is to produce carbon-neutral energy.

Despite the discrepancy between NEE of CO_2 measured using SkyBeam and the EC tower in this field, there was a good general agreement between the two methods, and the advantage of a chamber approach was demonstrated by its ability to measure at the plot scale, at a spatial resolution fine enough to perform experimental contrasts, which is beyond the capability of micrometeorological techniques.

There were clear diurnal patterns in the fluxes of all three GHGs measured by SkyBeam, patterns not previously reported from this crop. By revealing these diurnal patterns, the need for continuous data of all three gases has been highlighted. If estimates of cumulative GHG are made from single daily measurements, then the potential for measuring at a time of day which will yield an inaccurate value is large.

This was established for soil respiration in Chapter 2 of this thesis, but has now been shown to be the case for both N_2O and CH_4 as well. The frequency with which flux measurements are made is extremely important. With particular focus on N_2O, large proportions of the annual budget might be emitted over the course of a couple of days. Had the manual measurement in July 2013 been made just two days later than it was, the cumulative flux estimate for N_2O from *Miscanthus* would have indicated it was a sink as opposed to a source. As it was, due to the timing of the manual chambers, and their inability to identify the diurnal pattern of fluxes, the manual chambers overestimated the flux of both CH_4 and N_2O in comparison to SkyBeam's continuous measurements.

There is also a discrepancy between flux estimates measured using simpler soil chambers and those which include vegetation and soil. This suggests that plants themselves play an important role in GHG flux, whether by direct metabolic processes or as a passive transport system through which GHGs may move bi-directionally between the soil and the atmosphere.

Further work must be undertaken in order to understand the key drivers of GHG fluxes, especially in respect to their diurnal variation. Only by understanding the diurnal pattern of each individual system will it be possible to ensure robust estimates of GHG budgets are being made, which will have great importance in our ability to mitigate anthropogenic climate change over the coming decades.

4 A comparison of greenhouse gas emissions from oilseed rape (*Brassica napus*) under different nitrogen treatments and methods of measurement

4.1 Introduction

One of the biggest global sources of N_2O is agriculture, where pasture land can be a large N_2O source due to animal urine and faecal deposits (see Williams *et al.*, 1999, Chadwick *et al.*, 2000, Bell *et al.*, 2015), and compaction due to trampling (Uchida *et al.*, 2008). Arable farming can also be a large emitter of N_2O, particularly as a result of the application of nitrogenous fertilisers (DEFRA, 2014a). In Chapter 3 of this thesis it was shown how amending a soil with green waste compost increased N_2O emissions and it was also clear that N_2O may be emitted in short-lived bursts of large fluxes. Given the correct combination conditions following fertiliser application, for example anaerobic soil conditions as a result of rainfall, a large proportion of the total annual N_2O flux may be emitted in just a few hours (Mummey *et al.*, 1997).

Mineral nitrogen may be applied to crops in various different forms, including ammonium nitrate (NH_4NO_3), and urea (CH_4N_2O). Depending on a soil's capacity for nitrification or denitrification, the type of fertiliser applied will affect the amount of nitrogen (N) lost as N_2O (Bateman & Baggs, 2005). Knowledge of a system's potential for N_2O production should enable a fertiliser strategy designed to minimise N_2O emissions, and therefore mitigate agricultural contribution to climate change. Restrictions already exist regarding the timing of fertiliser application with a view to preventing N losses through leaching and N_2O emissions (Environment Agency, 2015). In addition to N_2O emissions, N leaching from soils into groundwater can lead to problems such as eutrophication in watercourses (Kroeze & Seitzinger, 1998). Improved knowledge of N losses after fertiliser application will help to reveal where it is applied in excess, enabling the prevention of needless waste, but may also be key if an N_2O credit scheme, similar to that for CO_2 is introduced.

IPCC tier 1 emissions factors (EF) state that *ca.* 1% of applied N will be lost as N_2O over the course of the following year (De Klein *et al.*, 2006). If any credit scheme for N_2O is to be effective, then it is likely that EFs will be the way in which they are implemented (Millar *et al.*, 2010). It is therefore vital that their reliability is assessed empirically. If these EFs are shown to be robust through ground-truthed data, then it will reinforce any credit scheme. If, on the other hand, they are shown to be unreliable,

then a more accurate method for approximating emissions will be required to support such a scheme.

Trace gas fluxes may exhibit diurnal variation in both the amplitude and the direction of flux. This is to be expected for CO_2, where the gas is consumed by photosynthesis and produced by respiration. N_2O emissions may also display a diurnal pattern, and indeed in Chapter 3 of this thesis it was uniquely shown that NEE of N_2O under *Miscanthus* follows a cycle of net consumption during the day and emission at night. Diurnal patterns have been reported for N_2O in previous studies, but these have consistently shown peaks in emission during the afternoon and lower emission during the night, and generally attribute this to a temperature driven process (e.g. Christensen, 1983, Das *et al.*, 2012). Furthermore, it has been shown that CH_4 flux may also vary on a diurnal basis, as shown in Chapter 3.

In Chapter 3 it was shown that soil flux of N_2O and CH_4, when measured using soil-based opaque manual chambers, was higher than NEE of these two gases within the same experimental plots. Solar radiation was shown to play an important role in controlling not only NEE of CO_2, but N_2O as well. Whilst photosynthetically active radiation (PAR) has been suggested to play a role in diurnal patterns of N_2O flux, it has been used to explain increasing fluxes of N_2O during the day time, and the authors concluded that the relationship was actually due to the warming effect PAR had on microbial processes in the soil (Das *et al.*, 2012). Other studies have pointed out that the apparent Q_{10} of N_2O flux is too great to be driven by temperature alone, and that PAR may be in some way responsible for the additional increase in flux (Christensen, 1983).

SkyBeam (see Chapter 3) was an automated chamber system devised specifically to deliver a full GHG balance from the energy crop *Miscanthus* (*Miscanthus x giganteus*). Using this system the role that vegetation plays in N_2O and CH_4 flux was shown, as was the vital importance of high frequency measurements in capturing the inter- and intra-diurnal variability in trace gas fluxes. The system was a bespoke design for a specific challenge, and the scale of the equipment required to measure NEE from a crop which can grow in excess of 3 m make it impractical to deploy in fields of smaller vegetation. Here SkyLine is presented, a second independently developed automated system designed for use in more conventional crops than *Miscanthus*. The new system employs a single automated chamber, but is guided by a pair of parallel ropes to deliver the chamber to the correct positions. The use of

ropes ensures the potential length of the measurement transect is in excess 20 m, allowing in excess of 15 replicates. Aluminium trellis is used from which to suspend the guide ropes.

The long term study of monthly measurements in Chapter 2 showed that soil N_2O flux made a considerable contribution to the total GHG flux from barley (*Hordeum vulgare*). Here a second arable crop, oilseed rape (OSR, *Brassica napus*), is studied over the course of one month following fertiliser application. OSR is a member of the *brassica* genus, which includes broccoli, mustard and turnip. Whilst it has been used as an energy crop, it is more often cultivated for the high oil content of its seeds, which can be used in food production and cooking. It is often planted in rotation with wheat (*Triticum aestivum*) or barley, and will typically receive between 100 and 200 kg N ha^{-1} in fertiliser over the course of its cultivation. OSR was grown on 675 000 ha in the UK, constituting 11% of available agricultural land, with average yields of *ca.* 4 T ha^{-1} (DEFRA, 2014b) Understanding the response of OSR to N fertilisation, and developing the ability to reduce N_2O emissions from this crop would constitute a significant saving in the UK's agricultural GHG footprint.

This study investigated the effect of different N fertiliser treatments on the fluxes of all three biogenic GHGs from OSR. It also took the opportunity to investigate further the role vegetation and light play by measuring GHG flux from both soil and vegetation using both manual opaque chambers and an automated clear chamber from the same positions, and also using smaller opaque chambers to measure fluxes from the soil only.

4.2 Materials and methods

4.2.1 Study site

The study was conducted on a working farm in Lincolnshire, in the east midlands of the United Kingdom at which various research had been undertaken over the previous seven years, so its management had been well documented. In addition to arable crops, the farm is also used for the production of perennial crops *Miscanthus* (*Miscanthus x giganteus*) and willow (*Salix spp.*) for the purpose of energy production. The field in which the following experiments took place is used for annual arable crops in rotation, and the crop immediately preceding the oilseed rape (OSR) in this study had been spring barley.

Table 4.1 Overview of mineral nitrogen fertiliser applications to the OSR at the study site. The first application was prior to measurements commencing.

Date	*Fertiliser*	*Total product applied (kg ha^{-1})*	*Total NH_4-N (kg ha^{-1})*	*Total NO_3-N (kg ha^{-1})*
05/03/2014	Double Top[1] 18.8% NH_4-N 8.2% NO_3-N 30% SO_3	250	47	20.5
24/03/2014	Nitram[2] 17.2% NH_4-N 17.3% NO_3-N	200	34.4	34.6
01/04/2014	Nitram[2] 17.2% NH_4-N 17.3% NO_3-N	200	34.4	34.6

[1,2] Brand names of GrowHow products http://www.growhow.co.uk/ [2] 98.6% NH_4NO_3.

The OSR crop was drilled in the autumn of 2013, and all measurements during this study were made after crop emergence in March and April 2014. The OSR received its first treatment of mineral nitrogen (N) fertiliser a fortnight prior to the start of the measurement period, and then twice during the study (Table 4.1). Nitrogen treatments

were applied to the experimental plots to synchronise exactly with the fertiliser applications made by the farming contractor. Collars were left *in situ*, and fertiliser was weighed out and applied by hand to each chamber area on a *pro rata* basis to match the application rate to the field as a whole. An area of the OSR crop adjacent to the SkyLine study area was covered with plastic sheeting during the first fertiliser treatment prior to the deployment of equipment, and again during subsequent treatments. All equipment was deployed away from the tracks in the field created by tractors ('tramlines'; Figure 4.1), as access to the crop was continually required by the farming contractor throughout the study period.

4.2.2 Greenhouse gas flux measurements

GHG fluxes were measured at the site using manual static chambers (coverboxes) and SkyLine, with N_2O fluxes delivered from opaque coverboxes and a full suite of GHGs (CO_2, N_2O and CH_4) measured using SkyLine.

4.2.2.1 SkyLine design

SkyLine was an automated chamber-based system developed by the Mechanical and Electronic Workshops at the Department of Biology at the University of York. The basis of the design was a single chamber, suspended from a motorised trolley, in turn mounted on parallel horizontal Kevlar ropes (Figure 4.2). The ropes were held above the crop by trellis arches of 2 metres height, 18 metres apart, allowing the trolley to repeatedly traverse a pre-selected transect in the crop. Magnets embedded in the rope designated 'stops' at which the chamber automatically lowered to conduct a measurement. Landing bases for the chamber consisted of a flat, circular flange-ring with an inner diameter of 38 cm, which lay parallel to the soil surface. The flange had a perpendicular collar which was inserted below the soil surface in order to achieve a seal. The bases (henceforth 'rings') were analogous to the circular collars used for coverboxes and some automated chambers (e.g. Licor LI-8100 system, Licor, Lincoln NE). Upon completion of the programmed measurement period, the chamber was automatically lifted and the trolley moved to the next 'stop'. The sequence in which rings were sampled was programmable, allowing for randomisation or exclusion of specific rings if required. In addition to automated operation, the system could be controlled manually, allowing an operator to move the trolley between points, and drop and raise the chamber at will.

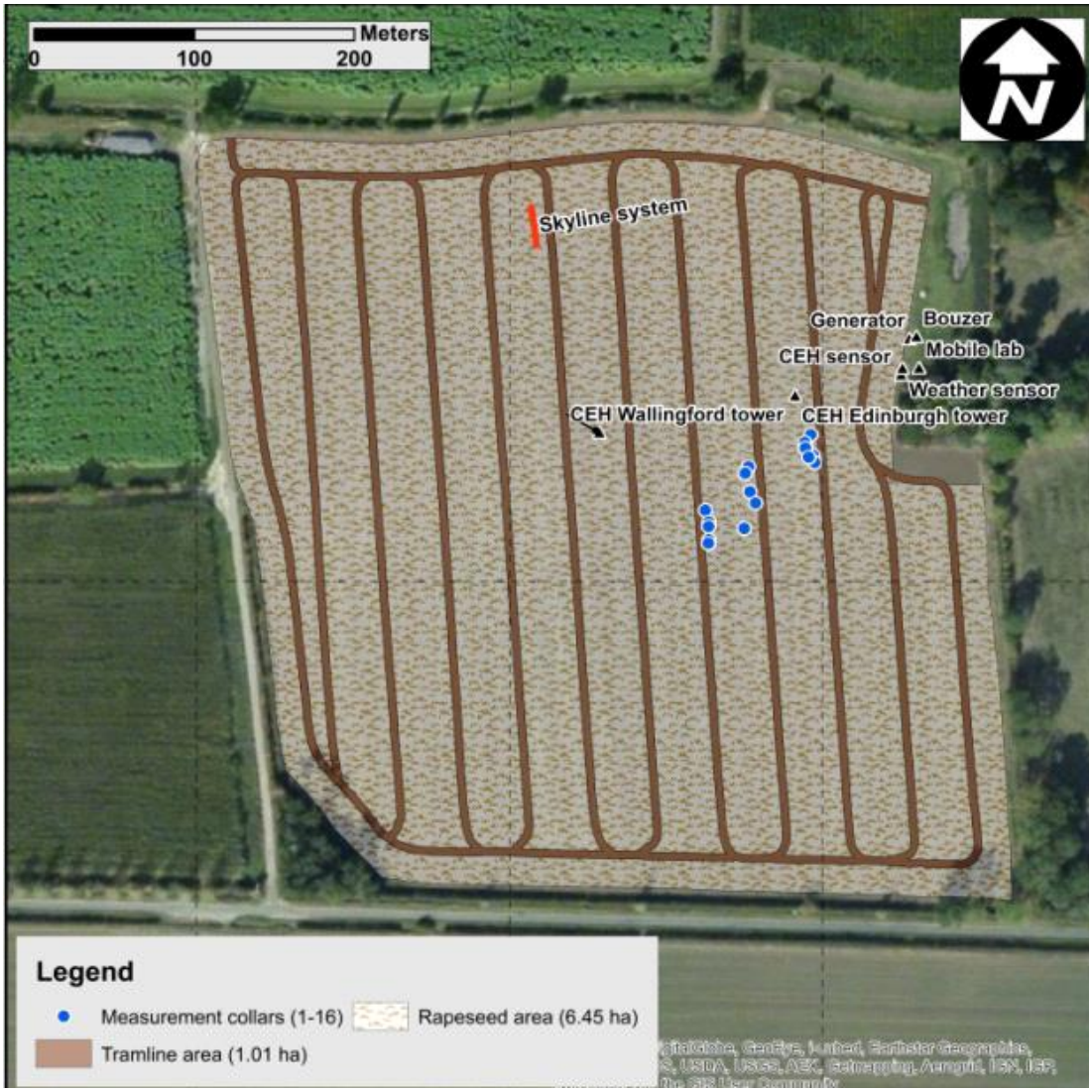

Figure 4.1 Aerial view of the OSR field. The SkyLine system is labelled towards the north of the field. Measurement collars 1-16 indicate where manual coverboxes were located. 'CEH Wallingford tower' is an eddy covariance (EC) system for CO_2, 'CEH Edinburgh' tower was an EC system for N_2O. To the east of the field were various pieces of equipment including a diesel generator for power supply and a met station. 'Tramlines' indicate the tracks used by tractors when treating the crop. The prevailing wind direction was from the southwest.

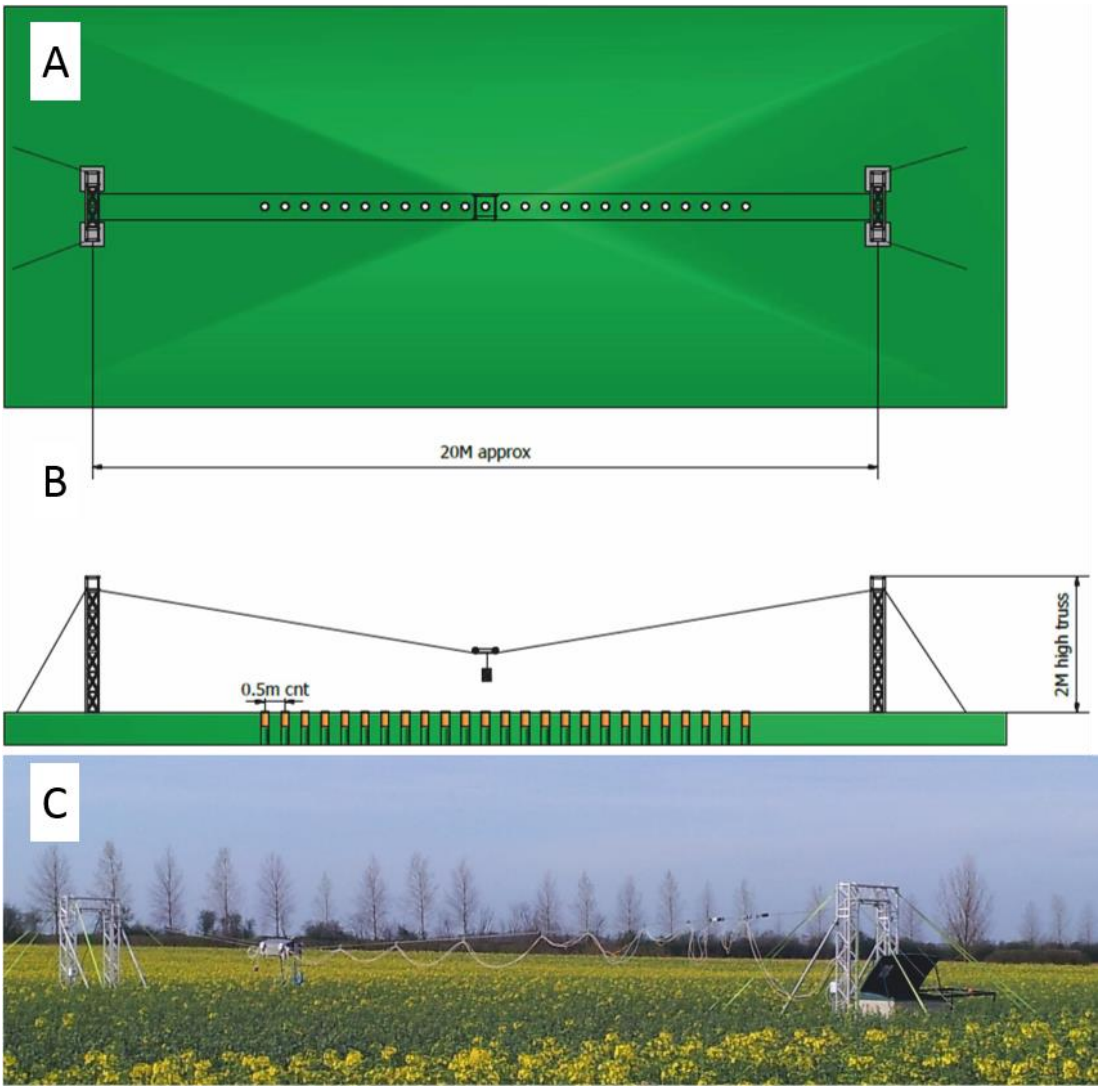

Figure 4.2 Aerial (A) and side-profile (B) schematics of the SkyLine system, showing the trellis arch supports at either end, supporting Kevlar ropes in between. The motorised trolley is depicted at the midpoint of the two supports. The system *in situ* (C) at the OSR field site. The LGR cavity ring down (CRD) analysers were housed in the garden box behind the right hand trellis support.

4.2.2.2 SkyLine chamber

The SkyLine chamber was a cylindrical chamber made of clear Perspex which allowed the transmission of light, thus enabling photosynthesis to continue, and therefore allowing the measurement of the net ecosystem exchange (NEE) of CO_2 to be measured from within the chamber. The chamber was designed as non-steady state dynamic chamber; that is, headspace gas was circulated from the chamber through analytical equipment and then returned. The rim at the base of the chamber was covered with a rubber seal which formed a gas-tight closure when dropped on the flange of the landing base (Figure 4.3). Inside the seal was a pressure sensor which was activated when the chamber landed on the collar and formed an air-tight seal.

A large chamber (internal diameter= 40.74 cm, height= 62 cm, volume= 80.8 L) was necessary to completely accommodate the OSR crop over which the measurements were made. Towards the end of the study, some binding of the crop was necessary, and pea netting was used for this purpose. The attenuation of light by the chamber was measured by simultaneously recording levels of photosynthetically active radiation (PAR) inside and outside of the chamber using two matched PAR sensors (QS-2 PAR quantum sensor, Delta-t Instruments, Cambridge UK) attached to a data logger (GP1, Delta-t Instruments, Cambridge UK), measuring at 1 Hz over a period of 21 days during the study period. After determining the effect of the chamber on light interception, CO_2 fluxes made using the SkyLine chamber were adjusted during hours of daylight (determined using the PAR data from an onsite met station) by using the equation from a light response curve, as described by Heinemeyer *et al.* (2013) (see Appendx C).

The aperture of the sampling tube was situated 10 cm from the top of the chamber (approximately 60 cm above the soil surface) and the return tube opened approximately 5 cm from the bottom lip of the chamber (Figure 4.3). This design was used in order to avoid sampling from directly above the soil surface, and to assist mixing of the headspace. There is some debate about the incorporation of fans to mix chamber headspaces (for a full discussion see (Davidson *et al.*, 2002) and the effect of such fans was also investigated in the current study.

In order to minimize pressure artefacts associated with closing a chamber over the soil, a vent was incorporated into the design of the chamber, after Xu *et al.* (2006).

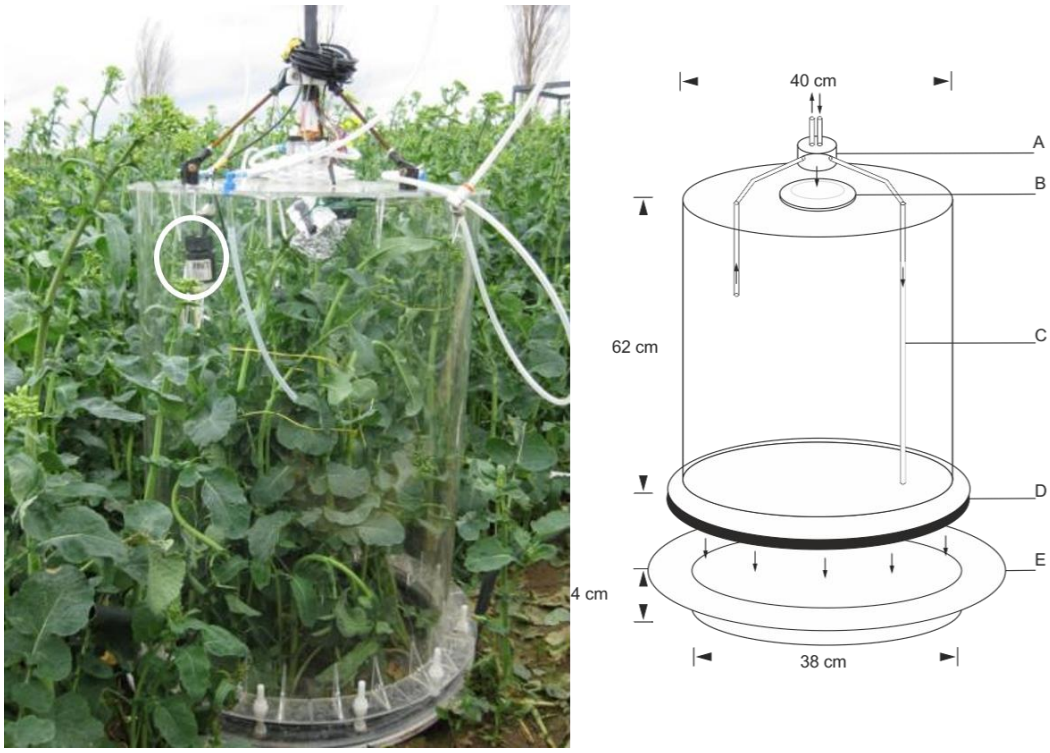

Figure 4.3 The SkyLine chamber *in situ* during a measurement over an OSR plant (left hand panel). Note the PAR sensor mounted within the chamber (circled). The schematic of the chamber (right hand panel) highlights the components and dimensions: **A**- manifold with attached gas lines. Arrows denote direction of flow; the sampling line draws from near the top (*circa* 10 cm) of the chamber and the return pipe opens near the base of the chamber. **B-** vent for pressure equalisation, after Xu *et al.* (2006). **C**- chamber constructed from clear Perspex, allowing the transmission of light and therefore permitting photosynthesis. **D**- gasket to ensure gas-tight seal between chamber and **E**- landing base.

4.2.2.3 Gas analysis

Housed in the motorised trolley was a Licor infrared gas analyser (IRGA, Li-8100, Licor, Lincoln NE) for measurement of CO_2 concentration. This apparatus was configured to control the SkyLine chamber as it would for a Licor long-term automated chamber, so that the length of chamber closure, the chamber volume and soil area covered were controlled and the Licor software used to calculate the CO_2 flux in units of µmol m^{-2} s^{-1}. Headspace gas was circulated from the chamber through an umbilical via polyethylene tubing (Bev-A-Line IV, Cole-Parmer, London UK) to the IRGA, before returning to the chamber.

In order to measure the fluxes of N_2O and CH_4, the exhaust from the IRGA was intercepted via a T-piece and passed through Bev-A-Line tubing to separate cavity ring-down (CRD) laser analysers (Los Gatos Research, CA USA) housed at one end of the SkyLine apparatus. The gas was circulated in series, and the stronger flow rate of the internal pump of the CH_4 analyser dictated that it was first in the sequence. A shunt for any over-pressure was used to compensate for different flow rates (see Appendix B). Both CRD analysers measured at 1 Hz, and fluxes were calculated as the change in concentration over time by linear regression, corrected for volume, temperature and soil area. In addition to CH_4 concentration, the first CRD also measured CO_2, which allowed for a second independent calculation of NEE.

4.2.2.4 Manual static chambers (coverboxes)

On 13 days between 19th March and 15th April 2014 the fluxes of N_2O were measured using manual static chambers (coverboxes), with measurements made between 09.00 and 18.00. The coverboxes were of the same diameter as the SkyLine chamber (40 cm), which allowed them to be fitted over the same rings. Chambers were deployed both under the SkyLine system, and at other areas within the rest of the OSR field (Figure 4.1). The chambers were circular in horizontal cross-section, and the main body consisted of two stacked opaque polypropylene sections, designed to gain clearance over the vegetation. These sections were clamped in place using bulldog clips, and a gasket formed a seal between the bottom section and the base ring, and between the lower and upper sections. The lid of the top section was flat aluminium sheeting; incorporated into the lid of the box was a vent for pressure equalisation and a three-way tap from which the headspace gas could be sampled.

Gas samples were taken through the tap using a 100 cm^3 syringe and stored in evacuated air-tight containers, and this was done at four time points (0, 20, 40 and

60 minutes). Samples were analysed for CO_2 and N_2O concentration by gas chromatography by the Centre for Ecology and Hydrology (CEH) Edinburgh, and fluxes were calculated by linear regression. Corrections were made for temperature, volume and area.

4.2.3 Experimental designs

4.2.3.1 Nitrogen treatment

The SkyLine system was assembled and, on 18th March 2014, the N_2O flux from all 18 rings was measured using manual operation of the system. The measured fluxes were used in order to arrange the rings into a blocked design for experimental manipulation, by ranking and grouping the most similar together. Five blocks of three rings were arranged and a single replicate of each treatment was assigned within each block at random. Prior to treatment the fluxes were compared using analysis of variance ($F_{[2,8]}$= 1.18, p= 0.3553), which showed no pre-treatment differences.

Three different forms of N addition were applied: NH_4NO_3 in the form of fertiliser (FER) (Table 4.1), NH_4 in the form of NH_4Cl (NH_4) and NO_3 in the form of $NaNO_3$ (NO_3). The three treatments were applied at the same time as the farmer treated the field. The fertiliser rings received the same dose as the rest of the field; the NH_4 and NO_3 treatments then received the same dose as the respective component parts of the fertiliser (i.e. NH_4: 34.4 kg N ha^{-1}; NO_3: 34.6 kg N ha^{-1}) . The chemicals for the treatments were weighed on a digital balance to 2 decimal places and applied to the experimental rings by hand. Care was taken to ensure the treatments were applied evenly throughout the rings, to mimic the action of the spreader used by the farming contractor. Treatments were applied on two occasions during the study period, directly mimicking the practices of the farmer. The first application took place on 24th March 2014, and the second one week later on the 1st April 2014.

The fluxes of three GHGs (CO_2, N_2O and CH_4) were followed using automated measurements from the SkyLine system, starting from the day of application until 11th April 2014. Chamber closures of 10 minutes were programmed for flux measurements, with a gap of 5 minutes between closures. Following this protocol, each cycle (the time to visit all 18 rings) was 270 minutes long, allowing for approximately six measurements at each sampling point per day.

4.2.3.2 Comparison of SkyLine and coverboxes

Opaque coverboxes were used to measure the N_2O flux from the OSR field on 13 days during the study period. In order to achieve this, 16 chambers were deployed throughout the field (Figure 4.1). Additional measurements were made with coverboxes from the 8 rings under the SkyLine system that received the FER treatment (equivalent of 200 kg ha^{-1} of Nitram fertiliser, on two occasions). The total cumulative flux of N_2O measured using the coverbox method was calculated and compared to the total N_2O flux measured using the SkyLine system for the same period (25th March to 10th April, since no coverbox measurements were taken on 24th March).

In order to test the hypothesis that individual N_2O flux measurements would not differ between the SkyLine chamber and the static chambers, on four days during the study period (19th, 25th, 27th March, 10th April 2014) manual measurements were taken using the SkyLine chamber, which was shaded with reflective cloth to mimic the opacity of the static chamber. This was an opportunistic additional hypothesis, and in order not to interfere with the primary comparison of automated measurements and coverboxes, these measurements were taken after the coverbox sampling. At the end of the 60 minute measurement period, the coverbox was lifted to purge the headspace, but left raised above the vegetation to keep it darkened. Each coverbox was then removed in turn and replaced with the shaded SkyLine chamber, which was closed for 10 minutes and the headspace circulated sequentially through the CRD analysers for N_2O CO_2 and CH_4 (Appendix B) as in the automated measurements.

4.2.3.3 Comparison of light and dark N_2O fluxes

In order to test whether the flux of N_2O differed under light and dark measurement conditions, comparisons were made between April 8th -9th 2014 through a combination of manual operation of the SkyLine system, and the use of smaller, opaque flux chambers to exclude the vegetation. For this experiment, only the 8 FER rings under the SkyLine system were used. Small base rings (10 cm diameter) were inserted into the soil at the base of the vegetation inside the SkyLine rings. In order to measure GHG flux from the soil, opaque cylindrical chambers (dimensions: diameter x height y) were placed on the base rings and sealed with an air-tight rubber band (Figure 4.4). Headspace gas was circulated through the LGR analysers for five minutes and fluxes calculated using linear regression. An initial round of measurements was made commencing around 10:00 on the 8th April, with all of the rings exposed to light. Measurements were taken from the small soil chamber and the large SkyLine

chamber sequentially. Since it was hypothesised that the fluxes measured with the SkyLine chamber were principally driven by processes in the soil, the measurements from the small chambers were used to assign the rings into four pairs. This was done by ranking the fluxes and grouping similar rings: the vegetation in one ring of each pair was shaded, and the other left unshaded. Three subsequent rounds of measurements were made through the evening of April 8th and a further round started at 08:00 on the following morning (April 9th). The ring of each pair to be shaded was assigned at random, as was the order in which the rings of each pair would be sampled. Shading of the plant was achieved with reflective cloth to avoid warming, and gaps were left at the base of the vegetation in order to allow the headspace to circulate freely during flux measurements (Figure 4.4). For each SkyLine measurement the chamber was then closed for ten minutes, with a gap of five minutes to purge the chamber.

4.2.4 Ancillary measurements

Soils were sampled from within the chamber bases on a weekly basis throughout the study. Soil inorganic N was measured through extraction in 1 M KCl and analysis of the filtered extract using a Bran-Luebbe AA3 autoanalyser, and soil moisture was determined by oven drying at 105 ^{o}C until constant mass. High frequency (1 minute, averaged over 15 minutes) measurements of soil moisture and temperature at 5 cm depth were made using temperature and moisture probes (UA-001-64 & S-SMD-M005, Hoboware, Onset Corporation, MA USA), and quantum sensors measured PAR (ambient and inside the SkyLine chamber; SKP 215, Skye Instruments, Powys, Wales, UK). Other meteorological variables were provided by CEH Edinburgh courtesy of a met station sited with their EC system at the site, and rainfall data were obtained from the Met Office for the nearby station detailed in Chapter 2. Aboveground biomass of OSR was destructively harvested by hand at the end of the study, prior to grain filling, by CEH Lancaster and oven dried to constant weight.

4.2.5 Statistical analyses

All statistical analyses were conducted using SAS (SAS 9.3, SAS Institute, NC USA), and graphs were produced with Sigmaplot (Sigmaplot 12.5, Systat Software). Where necessary, fluxes were transformed in order to normalize them. Mean N_2O flux rates were log transformed and the reciprocal of the mean CO_2 fluxes were used for repeated measures analysis. Repeated analyses were performed on the flux rates

and the daily total fluxes of CO_2, CH_4 and N_2O using a mixed effects model with PROC MIXED (ring and block as random effects).

Analysis of variance was carried out on cumulative flux of CO_2 CH_4 and N_2O from the nitrogen treatments over the whole period to test for treatment. The fluxes of CO_2 measured using Licor and LGR analysers were tested for correlation and the statistic reported is Pearson's correlation. In the chamber comparison experiment the methods were tested for differences using a paired t test for each time point. A paired t-test was also used for the light and dark contrast experiment. Cumulative fluxes were calculated by trapezoidal integration.

Figure 4.4 Example of a FER ring with shaded vegetation. The shroud did not go all the way to the soil surface in order to allow gas to circulate. Inside the large SkyLine ring is a small opaque chamber, allowing measurement of GHG flux from just the soil.

4.3 Results

4.3.1 Nitrogen treatment

Initial fluxes of N_2O (24th – 30th March) were positive, but low, and not exceeding 250 µg m^{-2} h^{-1} (Figure 4.5). Four days after the first N addition, fluxes began to increase, particularly for the fertiliser treatment. A technical fault prevented data from being collected automatically on March 28th, but manual measurements were obtained in the afternoon of March 29th. This round of measurements suggests that there may have been a peak in emissions in the intervening period (Figure 4.5), since fluxes from both all treatments were close to 500 µg m^{-2} h^{-1} at this point. Fluxes then continued at this higher rate, and, indeed, were still high up to the second N addition on April 1st. By the time the second addition was applied the flux in the FER treatment was approaching 1000 µg m^{-2} h^{-1}, and a trend towards higher fluxes from this treatment started to become apparent over the following few days (Figure 4.5).

When analysed for the entire study period, there was a significant difference in N_2O flux between treatments, $F_{[2,423]}$=12.10, p<0.0001, and there was a significant interaction between treatment and time during the study, $F_{[144,423]}$= 1.44, p< 0.003. The FER rings showed distinct peaks in flux during the afternoons of March 31st to April 6th. These peaks increased steadily from *ca.* 500 µg m^{-2} h^{-1} on the 31st to a maximum of 3131 µg m^{-2} h^{-1} on the 6th April. From the afternoon of April 6th the NH_4 rings demonstrated slightly higher fluxes than the other two treatments for three consecutive cycles, and the highest mean N_2O flux (4266 µg m^{-2} h^{-1}) was recorded from the NH_4 rings on April 6th. In the first part of the study period (24th to 28th March) the NO_3 rings tended to show slightly higher fluxes, but after the second N application these were the slowest to respond, with fluxes not exceeding 1000 µg m^{-2} h^{-1} until April 5th.

There was a strong correlation between the flux of CO_2 independently measured using the IRGA and CRD analysis systems (Figure 4.6), r= 0.97, p< 0.0001. There were no significant differences in the NEE of CO_2 (calculated with Licor software) between the three N treatments (Figure 4.7). Positive fluxes were apparent during hours of darkness, when respiration was the dominant process, and negative fluxes were seen during the daytime when the OSR was photosynthesising. The amplitude of the oscillation between positive and negative fluxes increased through the study

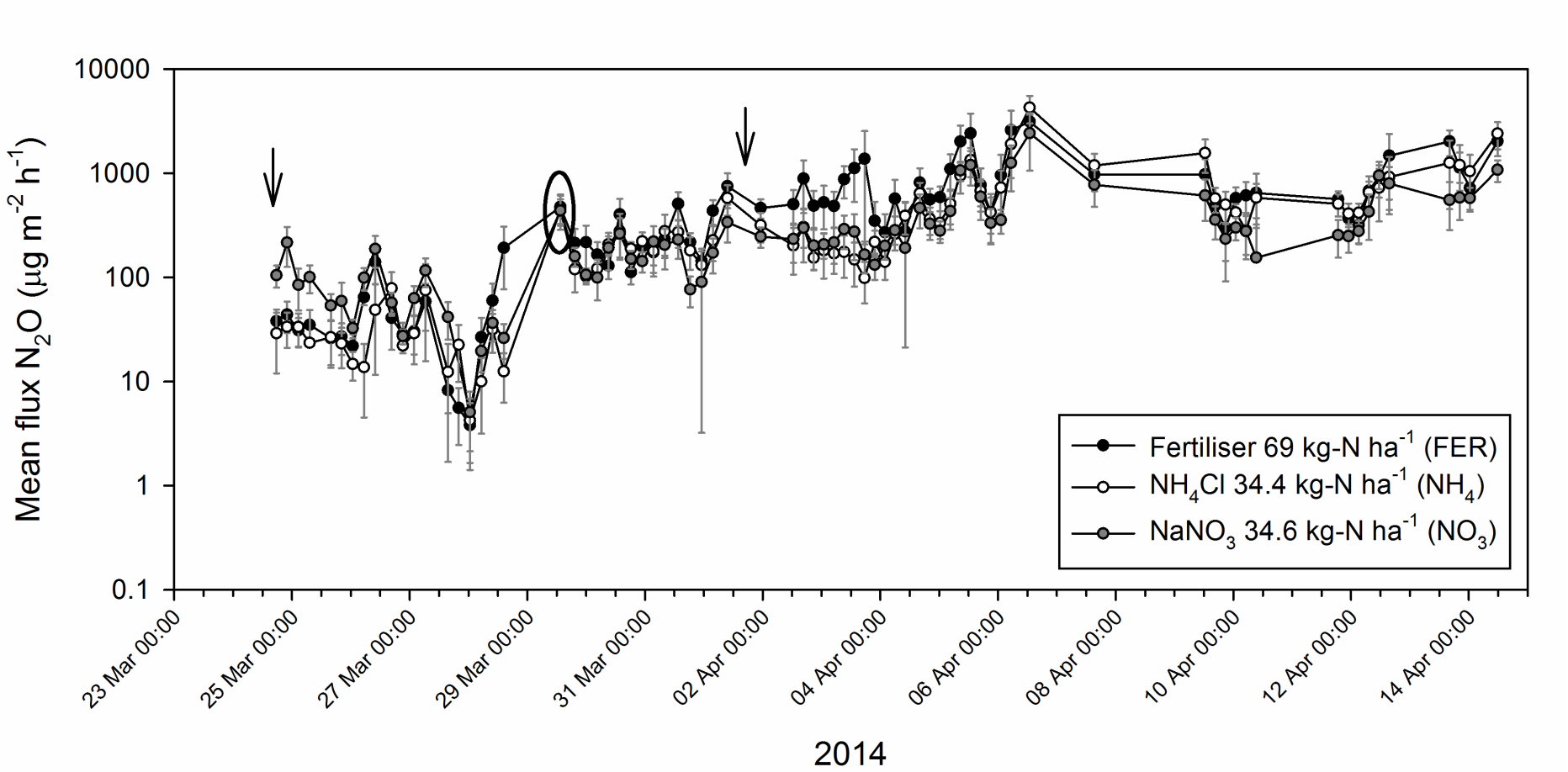

Figure 4.5 N_2O flux from OSR under three nitrogen treatments, from automated measurements using the SkyLine system, with data from one parallel cycle of manual measurements (inside the black elipse). Data shown are means ± 1SE, n= 5, note the log_{10} scale. Arrows denote the timing of treatment application

.

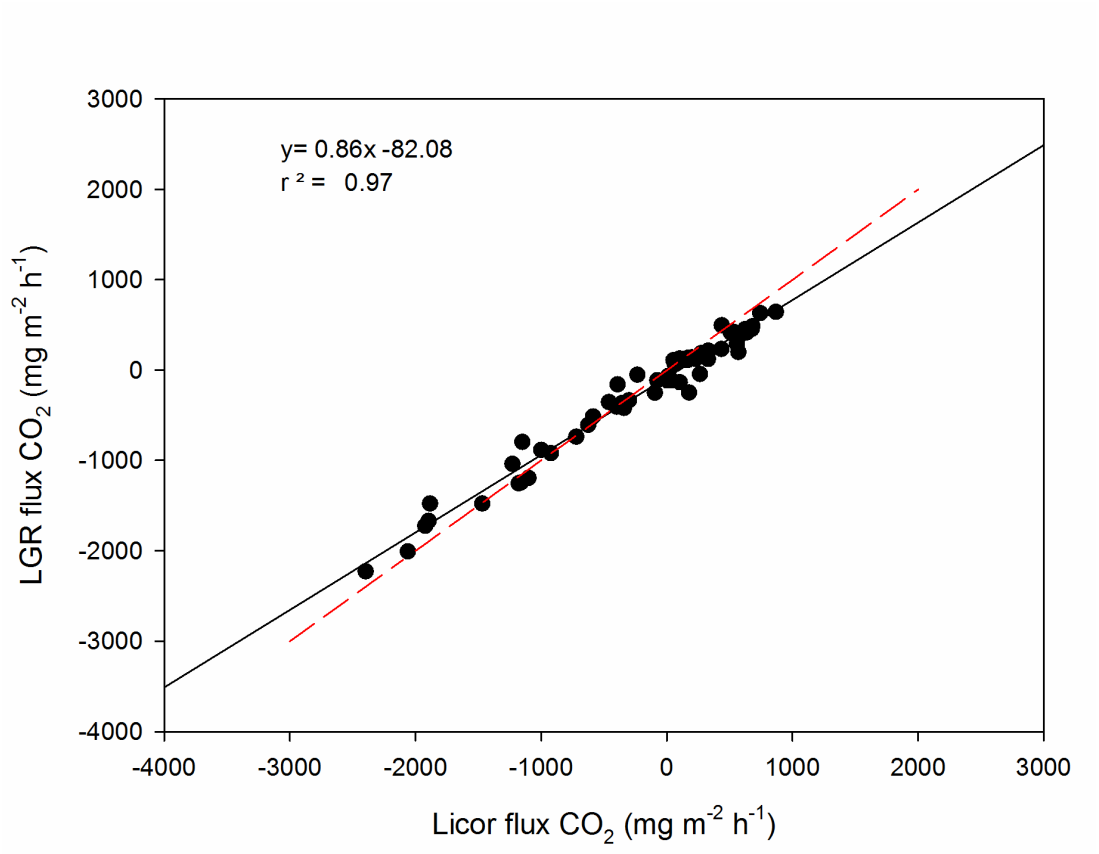

Figure 4.6 Comparison of CO_2 flux calculated using IRGA software (Licor, Lincoln NE) and cavity ring down laser LGR (Los Gatos Research, CA). The solid line is the regression line (equation shown top left), and the dashed line represents the 1:1 line.

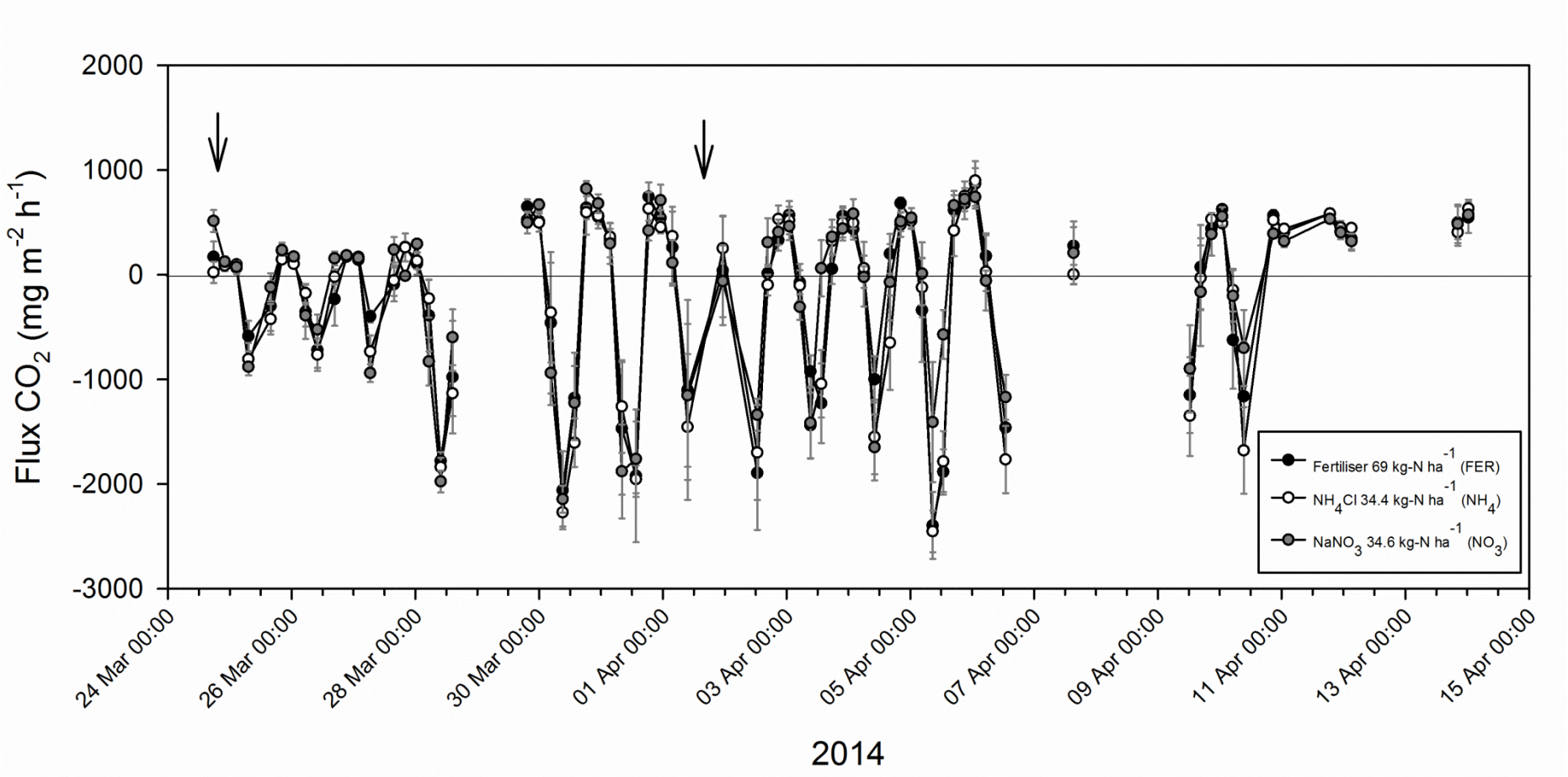

Figure 4.7 Mean NEE of CO_2 ±1SE from OSR following three nitrogen treatments measured with the SkyLine system. Arrows denote the timings of treatment application. Negative flux indicates net uptake of CO_2 and positive flux release.

period as the crop grew and flowered. Peaks in positive flux can be seen overnight e.g. March 30-31st (700 mg m^{-2} h^{-1}) and April 5-6th (898 mg m^{-2} h^{-1}). These peaks followed the two days that showed the greatest uptake in CO_2 (maxima of -1953 mg m^{-2} h^{-1} and -1765 mg m^{-2} h^{-1} respectively).

There were also no significant differences in the CH_4 flux between the three treatments $F_{[2,359]}$= 0.08, p= 0.9271 (Figure 4.8). Fluxes were often negative, indicating the soil was taking up CH_4, though they were close to zero: the minimum flux (greatest uptake) was -54 µg m^{-2} h^{-1} from the FER treatment and the maximum (greatest emission) 39 µg m^{-2} h^{-1} from the NO_3 treatment. There did not appear to have been any response to the application of the nitrogen treatments on either occasion.

The daily total N_2O flux was significantly different between nitrogen treatments (Figure 4.9) $F_{[2, 149]}$= 4.48, p< 0.013, although there were only three individual days during which there was a significant effect. On the 24th March, following the first application of nitrogen, the NO_3 rings emitted more N_2O than either the NH_4 or FER plots. For the majority of the study period the FER rings were the highest emitters of N_2O, though this wasn't statistically significant until April 2nd; by April 11th the NO_3 rings were emitting less than the other two treatments (Figure 4.9). It is also evident that the total amount of N_2O produced from all three treatments doubled in the space of 48 hours, between April 7th-9th. There was also a further peak in N_2O emission over April 12th. However, despite the FER treatment consistently producing more N_2O, by the end of the study there were no differences between the total N_2O produced by the different forms of nitrogen; FER 357 ± 67 mg N_2O m^{-2}, NH_4 306 ± 82 mg N_2O m^{-2}, NO_3 196 ± 66 mg N_2O m^{-2}, $F_{[2,12]}$= 1.31 p=0.31. The total N_2O-N lost from the system by the three treatments was: FER 2.27 ± 0.42 kg N_2O-N ha^{-1} (1.77 ± 0.33% of total N applied); NH_4 1.95 ± 0.52 kg N_2O-N ha^{-1} (2.83 ± 0.75%); NO_3 1.25 ± 0.42 kg N_2O-N ha1 (1.80 ± 0.60%).

There were no differences in the total daily NEE of CO_2 between treatments $F_{[2,156]}$=0.38, p=0.69. The OSR was a net sink for CO_2, with the total accumulation being: FER 136.73 ± 21.26 g CO_2 m^{-2}, NH_4 167.03 ± 12.55 g CO_2 m^{-2}, NO_3 112.75 ± 22.36 g CO_2 m^{-2}. The effect of treatment on total NEE of CO_2 was not significant $F_{[2.12]}$= 2.00, p=0.17, with NH_4 tending towards being the greatest sink and NO_3 the weakest sink. Despite fixing carbon over the whole study period, there were individual

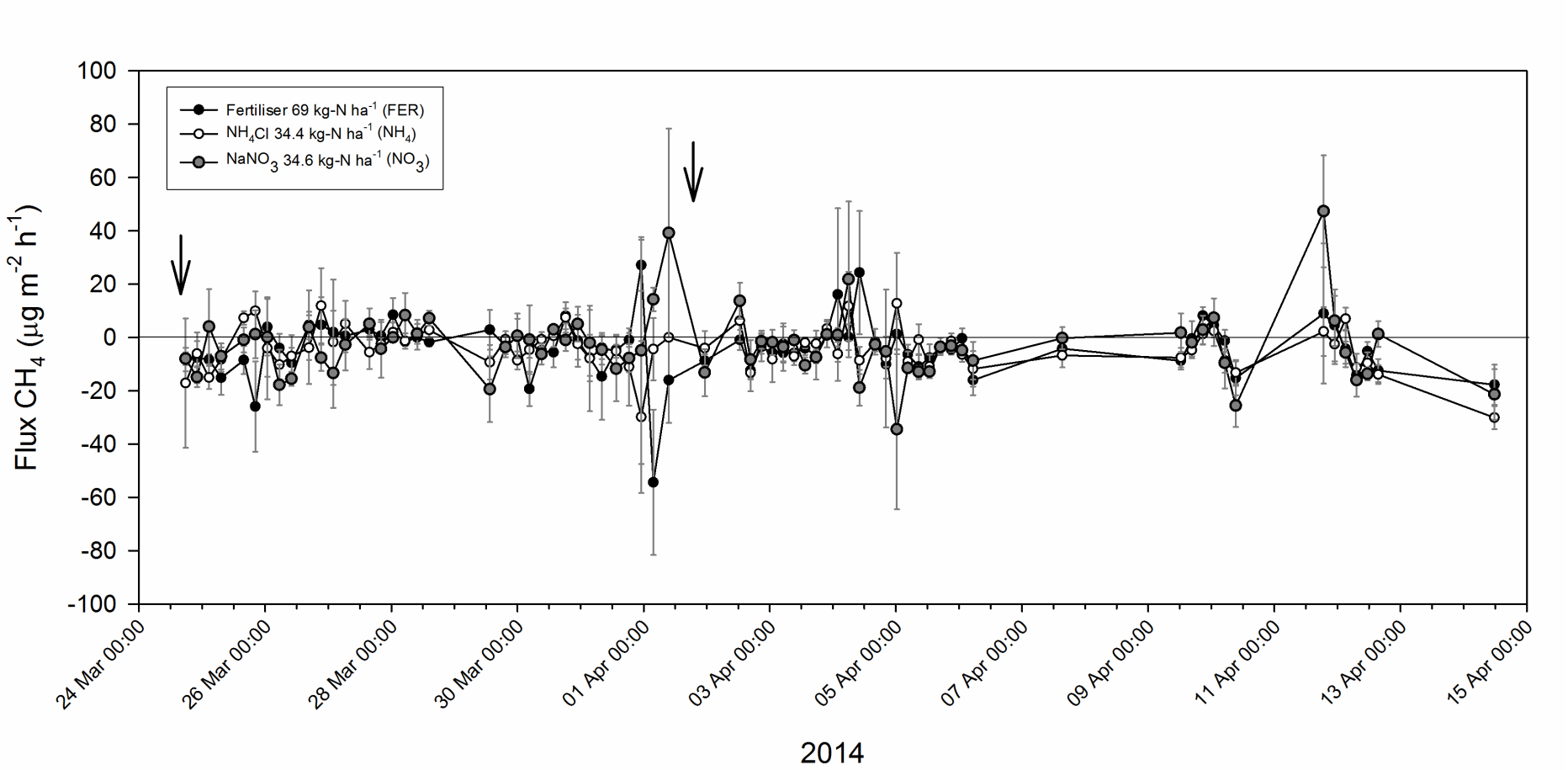

Figure 4.8 Mean CH_4 flux (±1SE, n=5) from OSR following three nitrogen treatments measured using the SkyLine system. Negative fluxes indicate uptake and positive fluxes release. Arrows indicate timing of treatment applications.

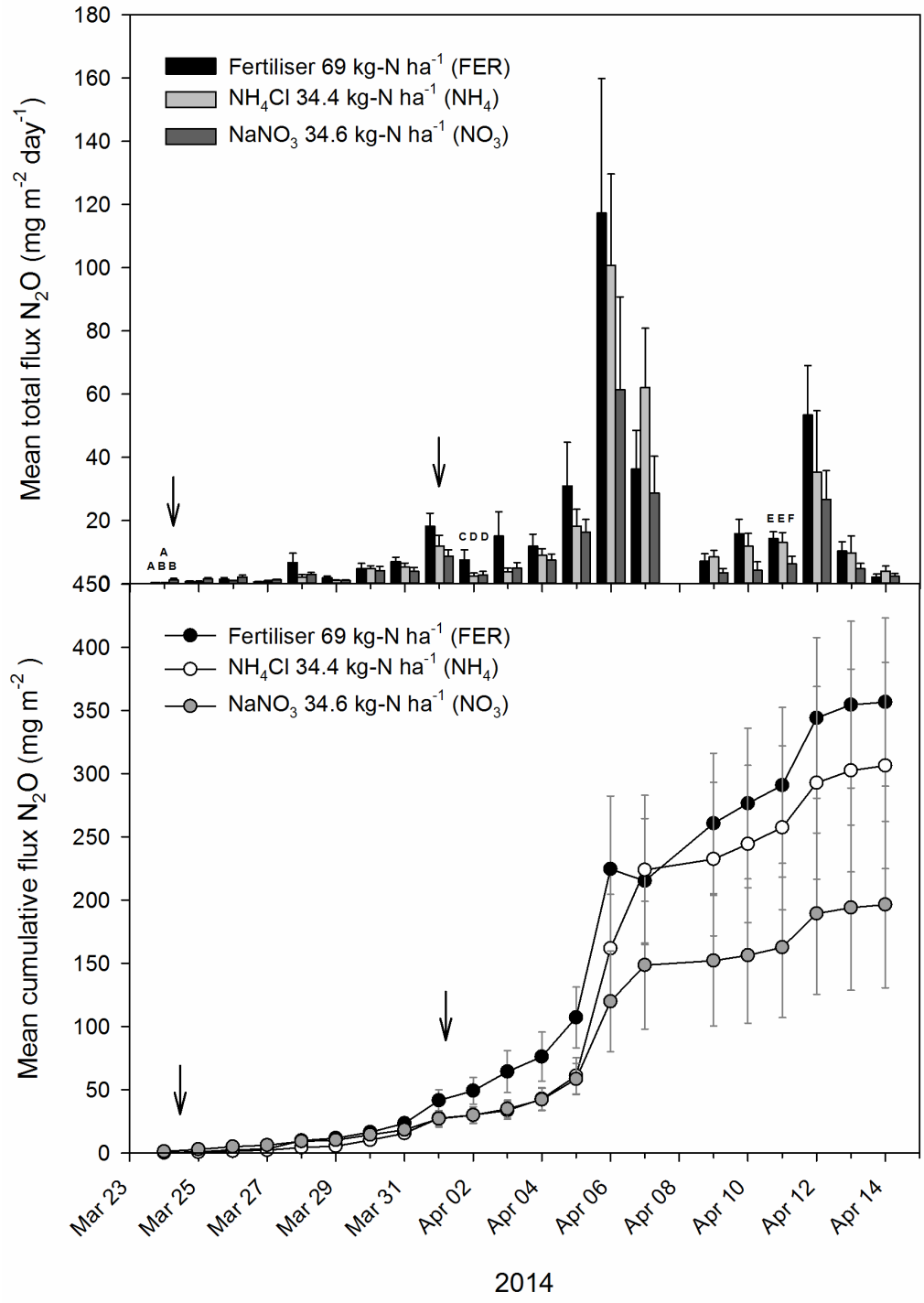

Figure 4.9 The daily mean total (top panel) and cumulative (bottom panel) fluxes of N_2O from OSR following three nitrogen treatments, measured using the SkyLine system. Error bars ±1SE, n=5. Arrows indicate timing of nitrogen application. Letters are used to denote daily significant differences (alpha= 0.05) between treatments.

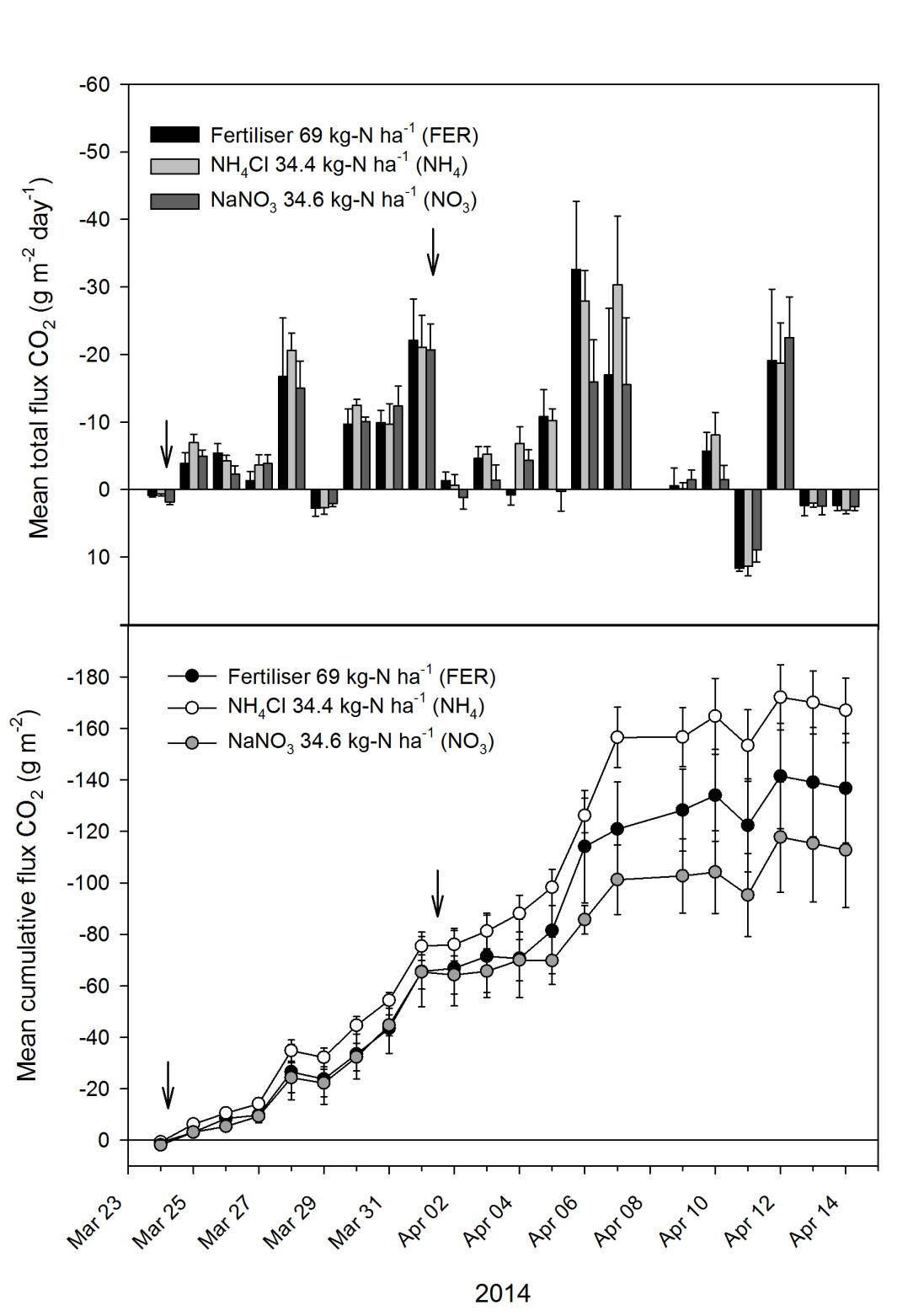

Figure 4.10: The daily mean total (top panel) and cumulative (bottom panel) NEE of CO_2 from OSR following three nitrogen treatments, measured using the SkyLine system. Error bars ±1SE, n=5. Arrows indicate timing of nitrogen applications. The vertical axis has an inverted scale: negative fluxes indicate uptake and positive fluxes emission.

days during which the system was a net source for CO_2 (Figure 4.10): the day of the first application (March 24th) and March 29th, where all three nitrogen treatments displayed a net loss of CO_2, but also April 2nd, 4th and 5th when individual treatments were losing carbon whilst the other two fixed it.

Whilst CH_4 fluxes were generally small, they were also largely negative; until April 11th the OSR system was a net sink under all three treatments (Figure 4.11). There were sporadic occurrences of a single treatment being a source over a 24 hour period, but there was no clear pattern: however, one such day of emissions on April 12th flipped the NO_3 treatment from a sink to a source. There was a significant treatment effect $F_{[2,152]}= 8.10$, $p< 0.001$, and the total flux over the study period was higher from the NO_3 rings than from the FER and NH_4 $F_{[2.12]}= 5.90$, $p< 0.02$. However, due to the fluxes being so small in comparison to those of N_2O and CO_2, CH_4 plays a very small part in the total GHG balance.

The overall GHG balance for the OSR system during this study period was negative, with CO_2-eq derived from the IPCC fifth assessment report (Myhre *et al.*, 2013), it is therefore a GHG sink (Figure 4.12). The contribution of CH_4 to the overall balance is negligible: the treatment in which CH_4 had the greatest effect was FER (-0.08 ± 0.02 g CO_2-eq m^{-2}) which represents approximately 0.26 % of the total GHG balance, but N_2O had much more influence. Emissions of 106.31 ± 19.83 g CO_2-eq m^{-2} (FER), 91.33 ± 24.31 g CO_2-eq m^{-2} (NH_4) and 58.54 ± 19.60 g CO_2-eq m^{-2} (NO_3) greatly reduced the effect of the GHG sink that is driven by the CO_2 uptake: the N_2O fluxes of the FER, NH_4 and NO_3 treatments represent reductions of 77.75 ± 14.50 %, 54.67 ± 14.55 % and 51.92 ± 17.39 % respectively. The overall GHG balance did not differ between nitrogen treatments $F_{[6,8]}= 0.89$, $p>0.54$.

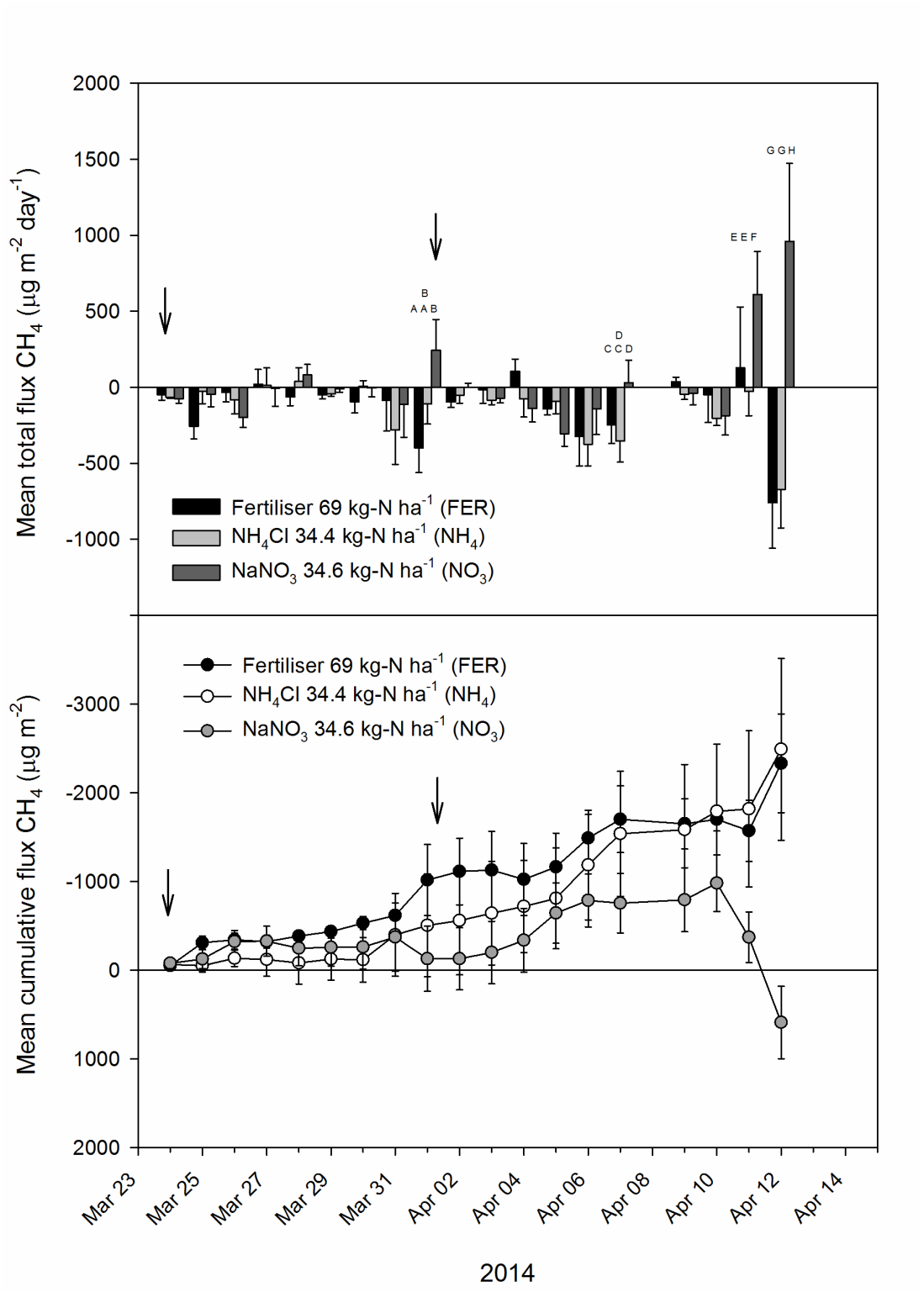

Figure 4.11 The daily mean total (top panel) and cumulative (bottom panel) NEE of CO_2 from OSR following three nitrogen treatments, measured using the SkyLine system. Error bars ±1SE, n=5. Arrows indicate timing of nitrogen applications. The bottom panel has an inverted vertical axis: negative fluxes indicate uptake and positive fluxes emission. Letters are used to denote daily significant differences (alpha= 0.05) between treatments.

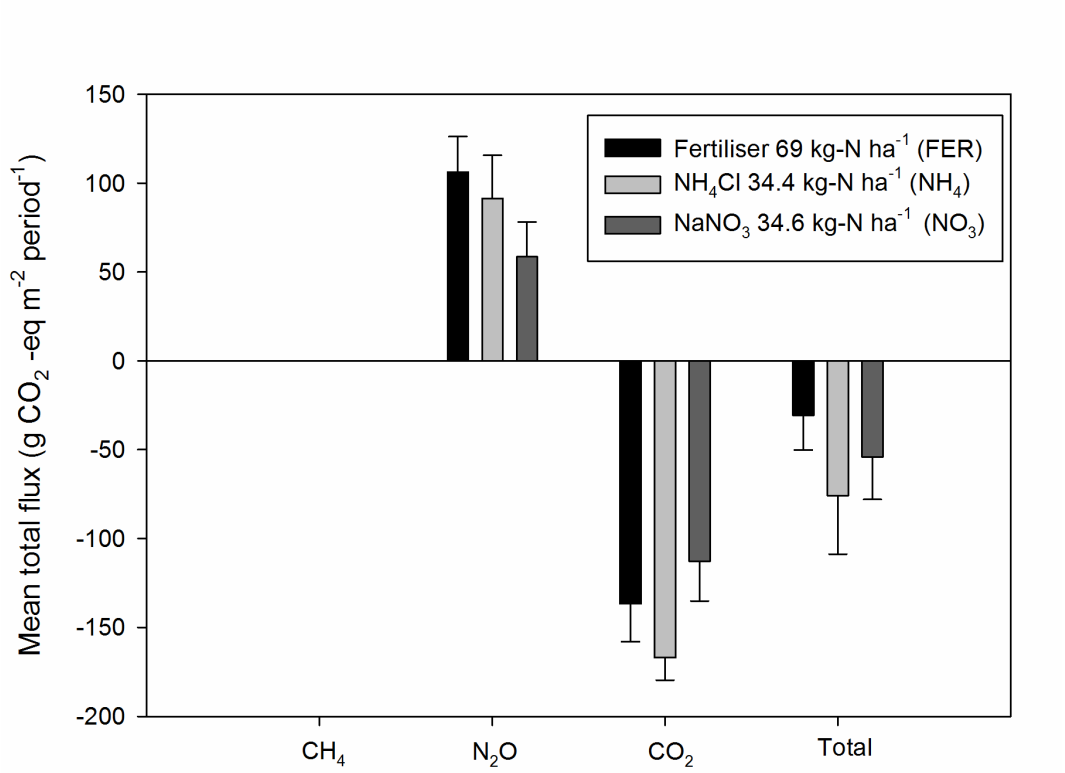

Figure 4.12 The relative contribution of each gas to the total GHG balance from the OSR under three nitrogen treatments, measured using the SkyLine system. Total flux is expressed in terms of CO_2 equivalents over 100 years using the latest emissions factors (IPCC 2013). The contribution of CH_4 is so small it cannot be seen at this scale. Negative flux indicates uptake (net sink) and positive fluxes emission (net source)

4.3.2 Chamber comparison

N_2O fluxes measured with coverboxes from the FER rings under SkyLine exhibited a similar general pattern to those of the automated measurements: they increased over the study period (25th March – 10th April, Figure 4.13) following the application of the Nitram fertiliser. The N_2O flux increased from 184.6 ± 45.4 µg m^{-2} h^{-1} on March 25th (one day after the first fertiliser application) to 3551.2 ± 512.9 µg m^{-2} h^{-1} on the 10th April. This is slightly higher than the peak flux from the automated SkyLine measurements (3131.4 ± 508.3 µg m^{-2} h^{-1}) which was recorded on 6th April. Of the eight days that coverbox measurements were taken from the FER rings under SkyLine, two occasions (19th March and 14th April) fell outside the period during which SkyLine was running automatically. These two days have been dropped from this analysis.

Using the remaining six occasions to calculate the total flux of N_2O for the period gives an estimate that is nearly five times higher than using the higher frequency SkyLine data (Figure 4.14): 1170.1 ± 184.0 mg N_2O m^{-2} versus 242.3 ± 39.8 mg N_2O m^{-2} which was highly significant, $t_{[7]}$= -6.07, p< 0.0006. It should be pointed out that all the manual static chamber measurements were taken during daylight hours.

Fluxes of N_2O measured using the opaque static chambers were higher than those measured with manual operation of a darkened SkyLine chamber. This was significant on two of the four days that this comparison was undertaken: 25th March $t_{[7]}$=-4.36, p< 0.004 and 10th April $t_{[6]}$=6.31, p<0.001 (Figure 4.15). On the other two occasions, the apparently large differences between the two chamber types were driven by single rings: on 19th March, fluxes were relatively evenly matched between the two techniques, save for ring 17, where the flux of 314.0 µg m^{-2} h^{-1} from the coverbox was nearly 50 times higher than the flux in the SkyLine chamber (7.0 µg m^{-2} h^{-1}). On 27th March the ring with the highest flux measured with coverboxes was ring 1 (3261.2 µg m^{-2} h^{-1}) which was nearly four times large than ring 14 (819.4 µg m^{-2} h^{-1}), which was the next largest. Ring 1 also produced the highest coverbox flux on 10th April (4275 µg m^{-2} h^{-1}), though the fluxes were more evenly distributed on this occasion, when the next highest flux was 3642.4 µg m^{-2} h^{-1} from ring 2. Generally there was a similar pattern demonstrated by both techniques: high and low coverbox fluxes were also high or low with the SkyLine chamber. With the exception of 19th March the highest coverbox flux was also the highest SkyLine flux, and the lowest fluxes were the same on each day except for 27th March.

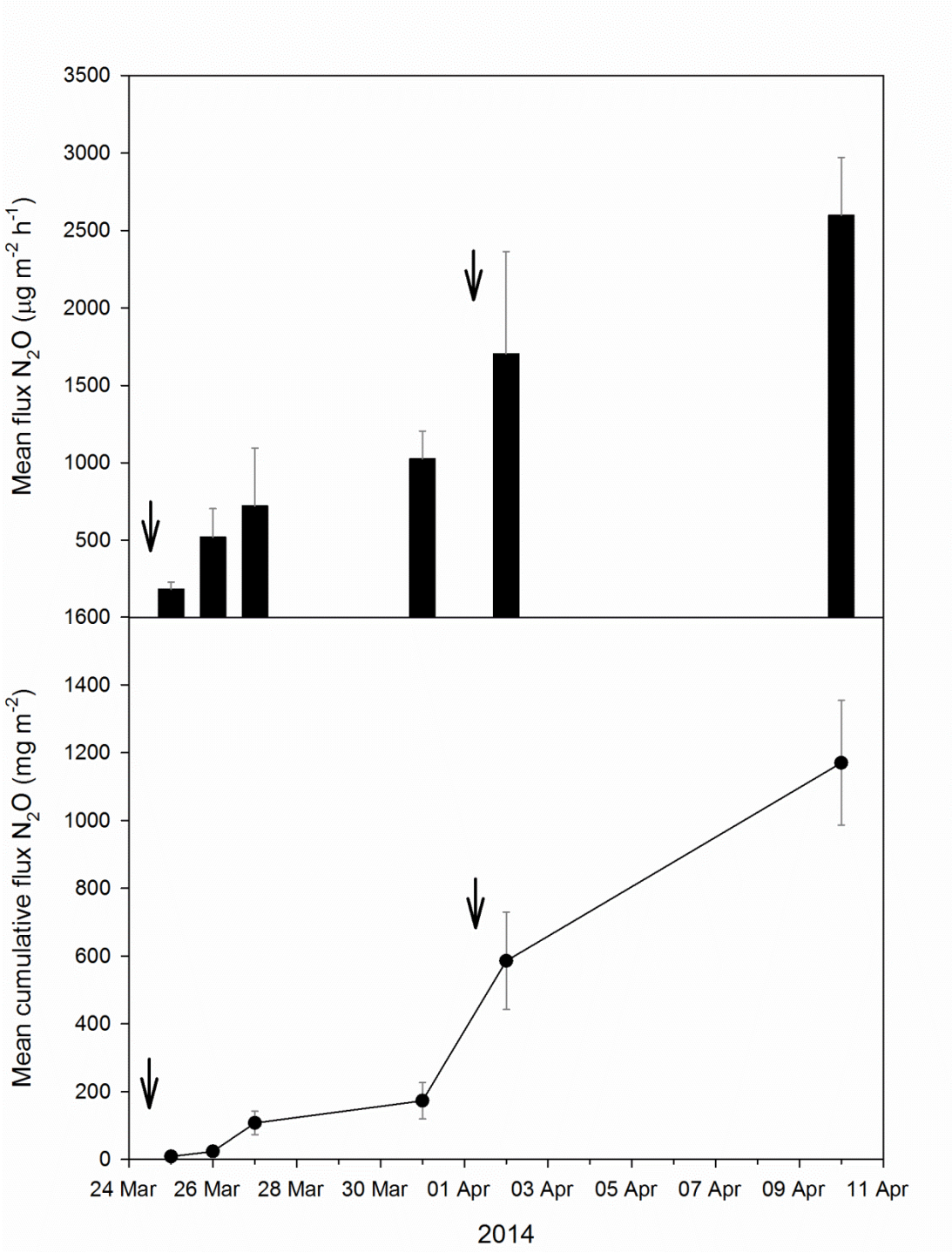

Figure 4.13 N_2O flux from the FER rings (2 applications of Nitram NH_4NO_3 fertiliser at 200 kg ha^{-1}) measured using coverboxes (top panel) and the cumulative flux of N_2O calculated from these measurements (bottom panel). All values are means ± 1 SE, n=8. The arrows indicate the timings of fertiliser application.

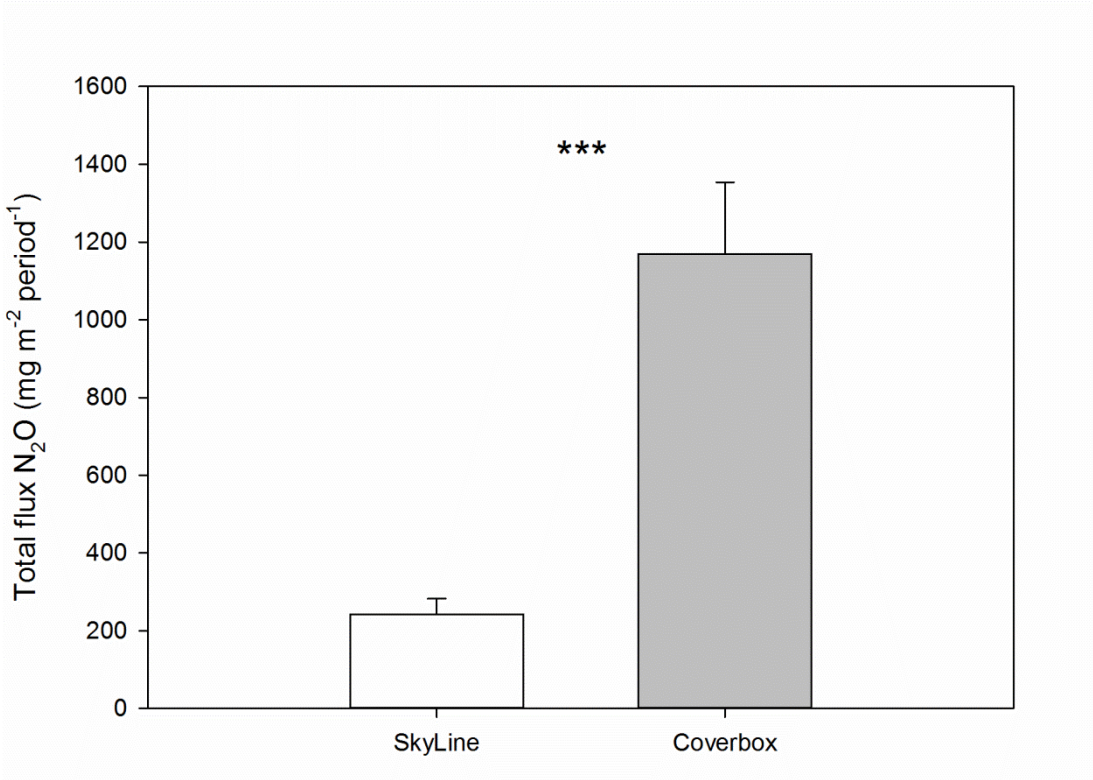

Figure 4.14 The total flux of N_2O from the FER treatment (2 doses of NH_4NO_3 Nitram fertiliser at 200kg ha^{-1}) calculated from trapezoidal integration of measurements from the SkyLine system and manual coverboxes for the period 25 March 2014 – 10th April 2014. Values shown are means ± 1SE, n=8. *** denotes significant difference ($p < 0.001$), paired t-test.

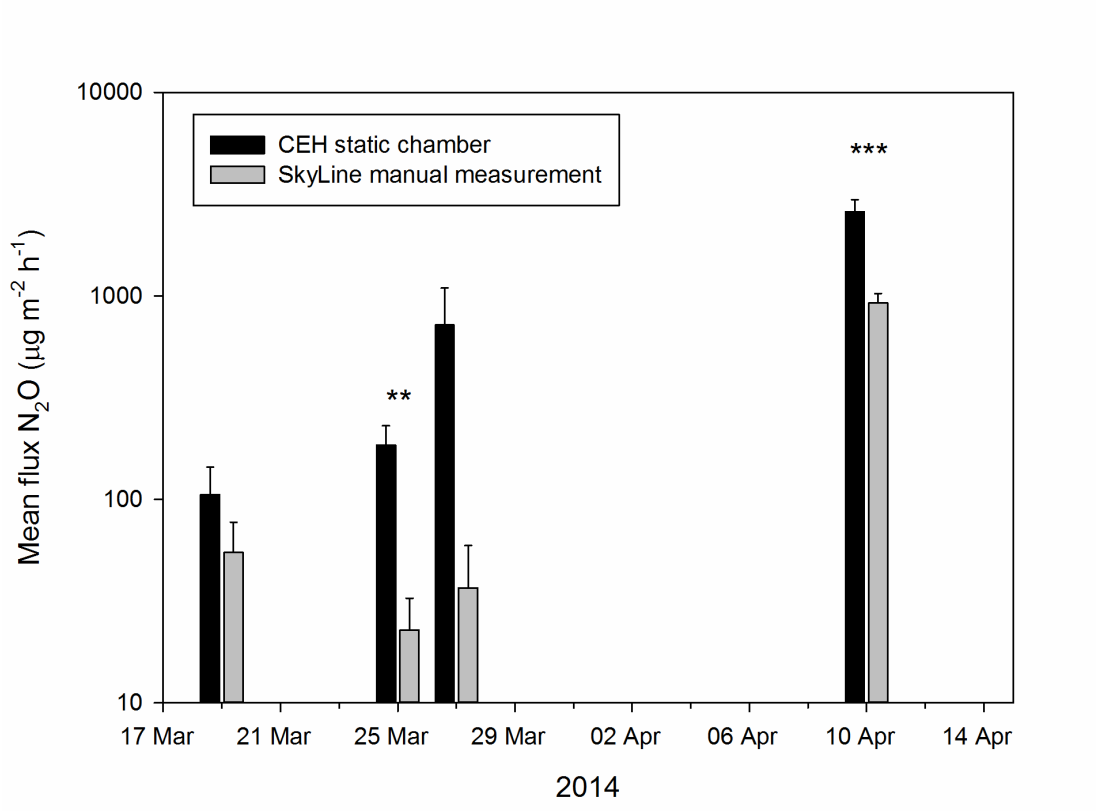

Figure 4.15 Comparison of N_2O flux from OSR measured using opaque static chambers (coverboxes) and a manually operated shaded SkyLine chamber. Measurements taken from vegetation treated with the equivalent of 200 kg ha^{-1} Nitram fertiliser (NH_4NO_3) on two occasions. Significant differences are shown: ** $p<0.01$ *** $p<0.001$. Values are means ± 1SE n=8.

4.3.3 Dark and light comparison

After the first round of measurements with the small soil flux chambers, six rings displayed similar fluxes of N_2O, which made three evenly matched pairs. Two other rings (17 and 18), were badly mismatched, so were removed from the analyses presented here. As a consequence, the number of replicates per treatment was reduced to three for the soil flux chambers. The same pairings did not hold for the measurements from the large chamber, since the fluxes did not display the same pattern, so all eight rings have been included in the analyses of these fluxes.

There was no significant effect of shading on N_2O flux from either the soil chambers or the SkyLine measurements (Figure 4.16). However, fluxes were higher from the soil chambers than from the SkyLine chambers $F_{[1,60]}= 38.54$, $p<0.0001$. The fluxes measured from the SkyLine chamber during this comparison were of a similar magnitude to those already measured through automated operation, and the highest fluxes measured with coverboxes. Remarkably, the soil chamber fluxes were up to six times larger.

The change in flux through time approached significance ($F_{[4,60]}= 2.41$, $p= 0.059$), but there was no interaction between time and chamber size ($F_{[4.60]}= 1.41$, $p> 0.24$). This change in time was represented by increases through the afternoon, before a decline in fluxes as night fell. By the following morning fluxes were beginning to increase once more. A similar diurnal pattern in N_2O fluxes was also apparent from the higher frequency automated measurements: this pattern is apparent in both the soil and SkyLine chamber measurements.

Since initial N_2O fluxes from the soil chambers were more evenly matched than the SkyLine measurements, these were used to investigate the change in flux following the shading treatment. There were no significant differences in the change between shaded and unshaded rings (Figure 4.17); in the first round following shading (45 minutes after), both treatments increased in flux, and they were very similar $t_{[2]}=0.35$, $p> 0.75$. By the next round of measurements (*ca.* 240 minutes), the flux from the shaded rings had decreased, whilst the flux from the unshaded rings continued to rise, and a trend appeared which suggests that the treatments started to differ, $t_{[2]}=2.67$, $p< 0.13$. Prior to the next round of measurements the sun set and both treatments were deprived of light, and fluxes from all rings decreased. At this point the shaded rings were producing lower fluxes than prior to treatment,

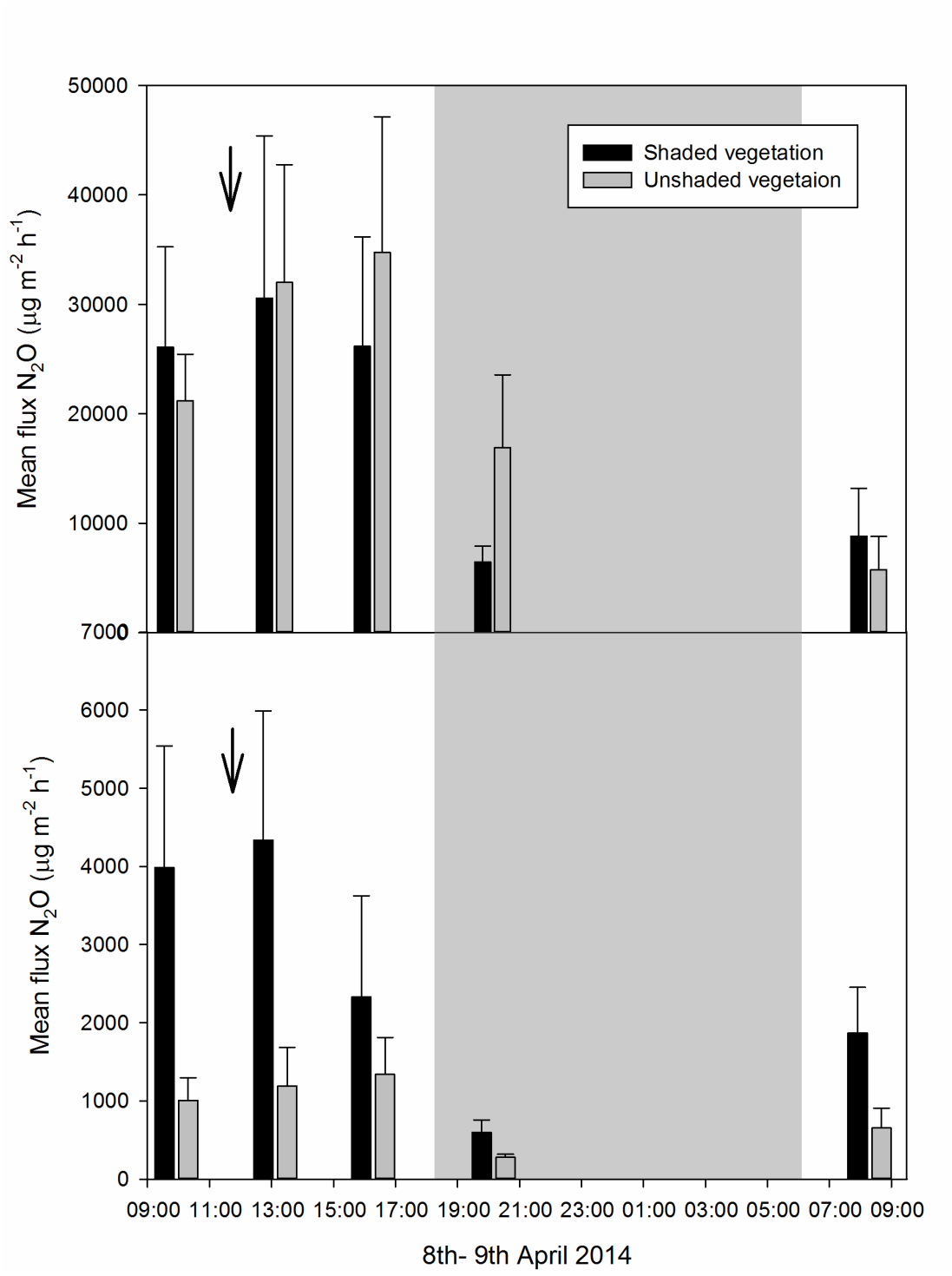

Figure 4.16 Comparison of mean ± 1 SE N_2O fluxes with shaded and unshaded OSR vegetation. The top panel shows fluxes from small soil chambers, the bottom panel from the rings using the SkyLine chamber. The grey shaded area shows hours of darkness, and the arrow denotes the time at which the shrouding was implemented; the first round of measurements (prior to shrouding) was used for statistical grouping. Soil flux measurements

were paired; one unbalanced pair was removed from the analysis (n=3 (see text)); SkyLine measurements were not paired, so all rings were included (n=4).

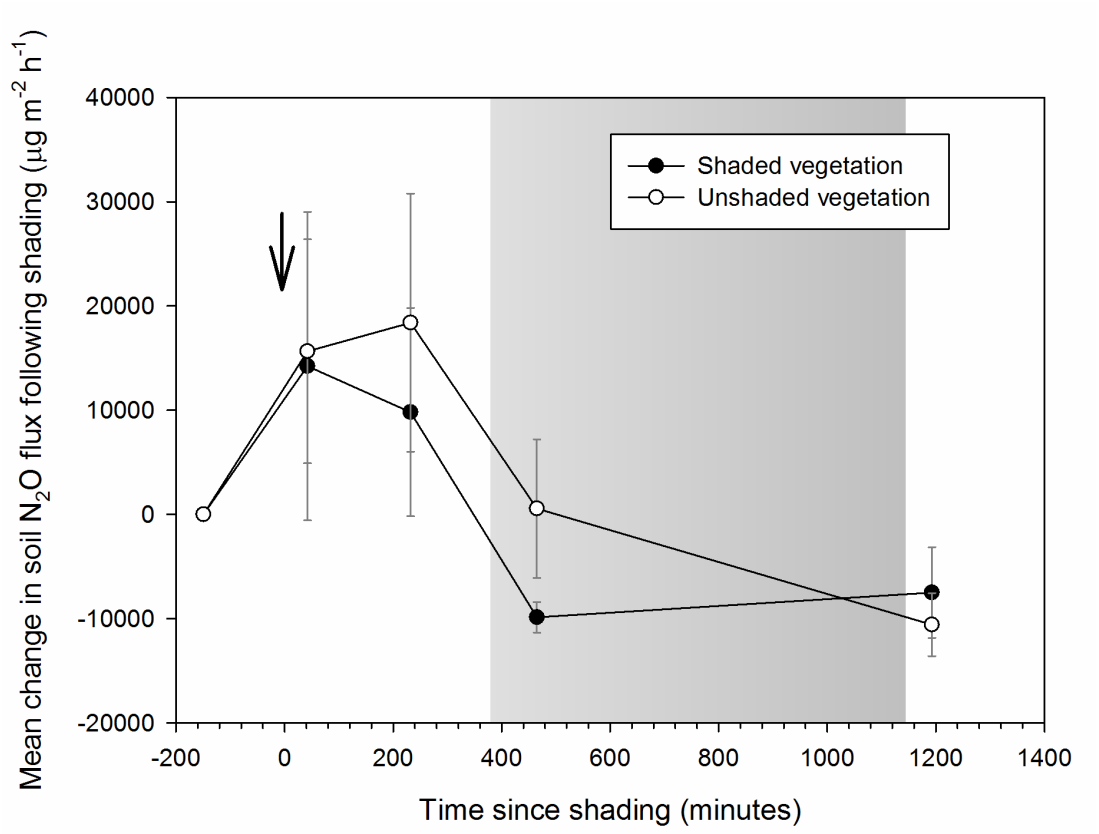

Figure 4.17 Change in N_2O flux following shading vegetation. Shaded area indicates night time.

whereas the unshaded rings were still emitting as much N_2O as pre-treatment. Fluxes were lower than initial values when the next series of measurements were made at 08.55 the following morning, nearly 24 hours following the first round.

4.3.4 Environmental variables

Radiation (solar and photosynthetically active radiation (PAR)), and temperature (air temperature, at canopy height and soil temperature) all displayed similar diurnal patterns, with peaks in the afternoon and lowest values during the night (Figure 4.18). Of the four positions at which temperature was measured (air, canopy height, soil surface and soil at 5 cm depth), the daily variation was greatest in the canopy and smallest in the soil.

The concentration of NO_3 and NH_4 in the soil increased following both applications of nitrogen; all rings were measured prior to nitrogen treatment, with mean NH_4-N concentrations of 37.9 ± 7.8 mg kg^{-1} (FER), 35.0 ± 4.0 mg kg^{-1} (NH_4) and 30.3 ± 14.9 mg kg^{-1} and mean NO_3-N counts of 5.5 ± 1.2 mg kg^{-1} (FER), 5.7 ± 0.8 mg kg^{-1} (NH_4) 4.7 ± 0.4 mg kg^{-1} (NO_3) (Figure 4.19). Only the FER rings were sampled for the rest of the study period, which involved four more measurements of soil N. Four days following nitrogen application, NO_3-N concentration had risen to 24.9 ± 5.1 mg kg^{-1}, and dropped to 20.7 ± 3.3 mg kg^{-1} on April 1st, just prior to the second N addition. A week later NO_3-N had increased again to 27.4 ± 3.1 mg kg^{-1}, before a final concentration of 24.1 ± 3.3 mg kg^{-1} was recorded on April 15th. Soil NH_4-N, after an initial increase following the first N application (up to 60.18 ± 7.40 mg kg^{-1} on 28th March), then remained relatively stable with means of 69.0 ± 12.0 mg kg^{-1}, 66.0 ± 6.8 mg kg^{-1} and 55.2 ± 9.1 mg kg^{-1} on 1st, 9th and 15th April respectively, despite a second N application.

Volumetric soil moisture was characterised by three distinct peaks (28th March, 1st and 7th April), followed by gradual declines. The gravimetric soil water content followed a similar pattern, but had less variability.

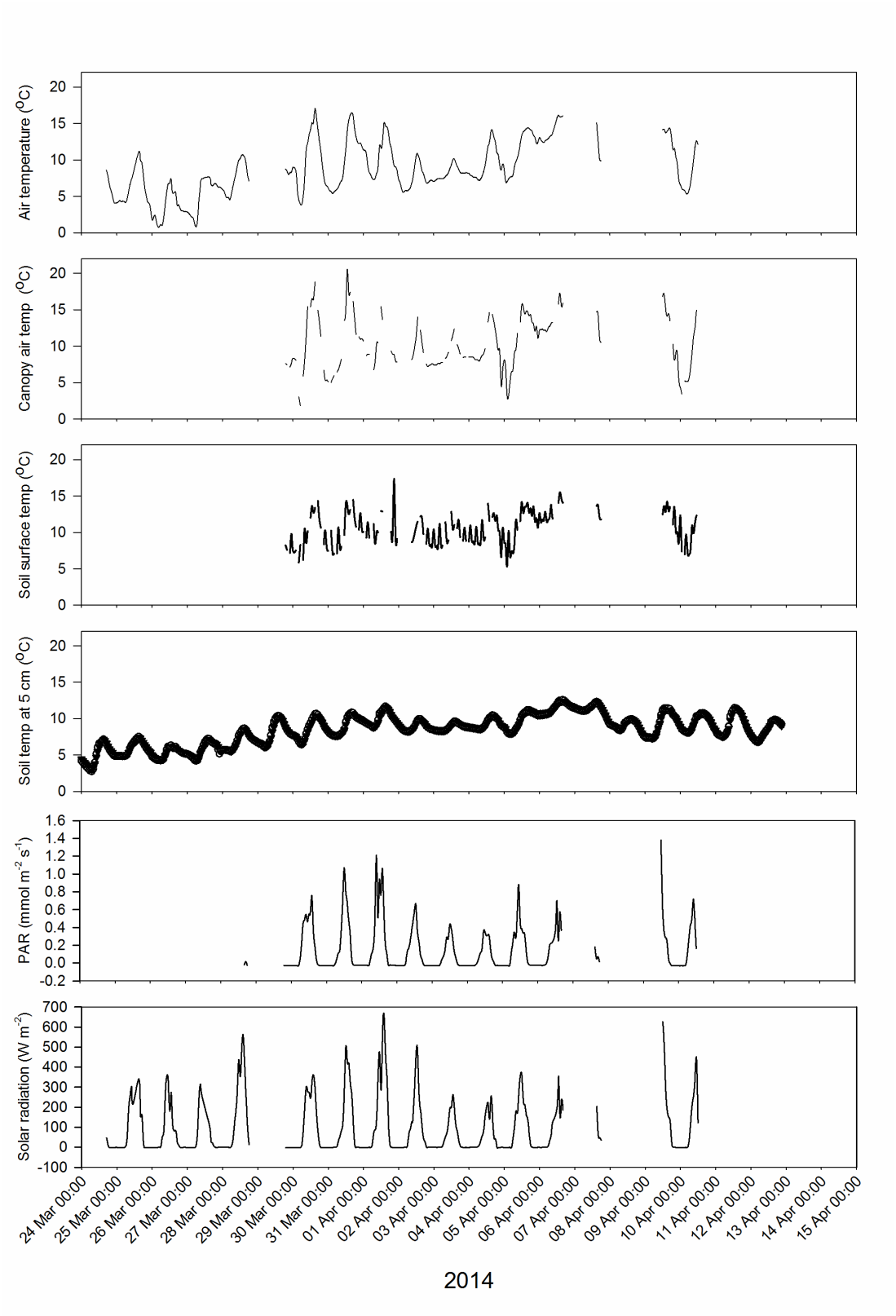

Figure 4.18 Hourly mean measurements of temperature (temp) at various heights relative to the ground, photosynthetically active radiation (PAR) and solar radiation at the study site.

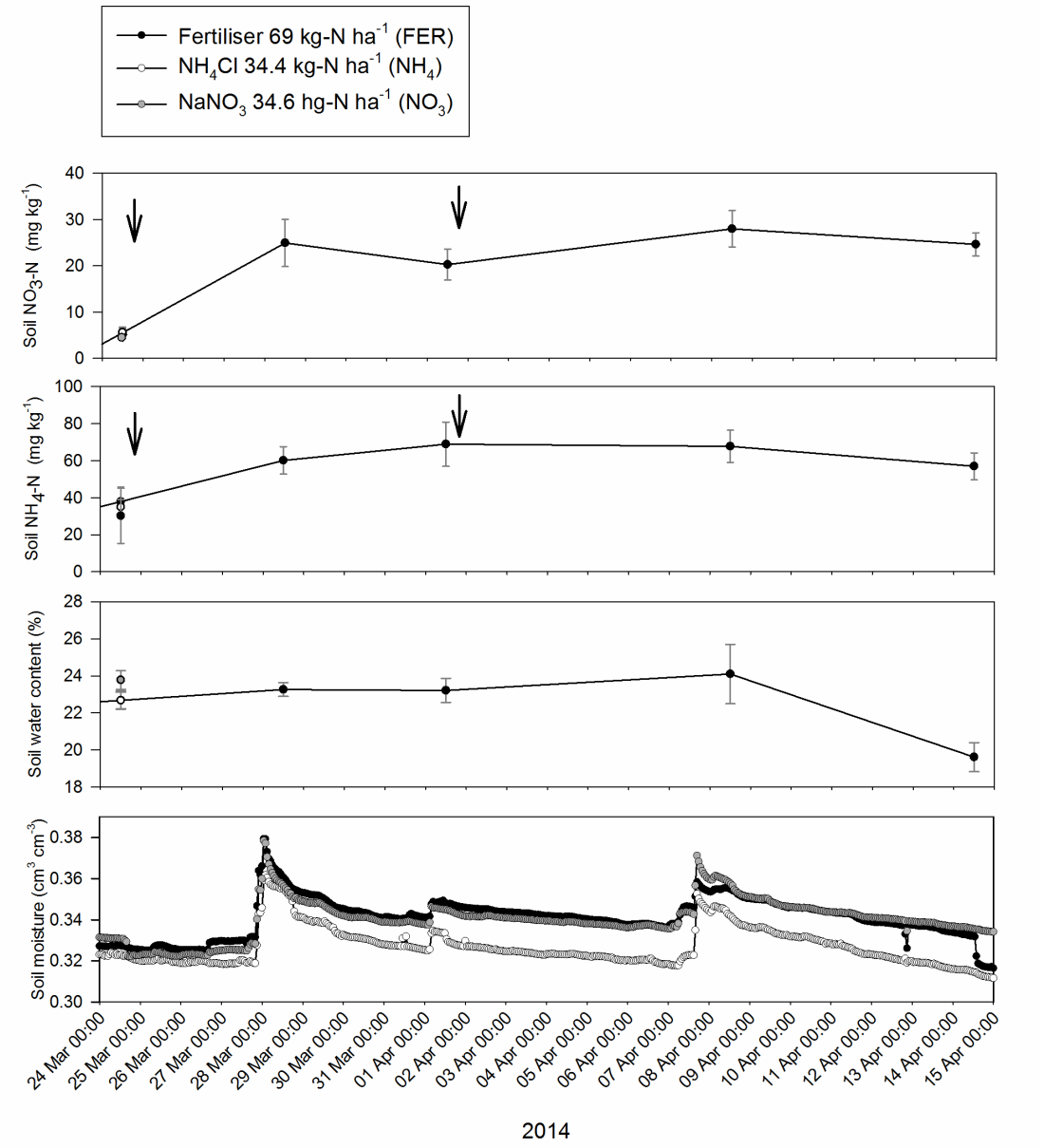

Figure 4.19 Hourly mean soil moisture (bottom panel) at 5 cm depth and daily mean ± 1 SE (n=5) soil properties for three different N treatments in the OSR. The daily means are data from the control (FER) treatment only. Arrows denote timings of nitrogen applications.

There was a strong positive correlation between air temperature and soil temperature (Figure 4.20). Temperature measurements at canopy height and soil surface, whilst also positively correlated with the other temperature measurements, had a slightly distorted relationship, possibly due to sunstrike of the equipment, or a fault in the equipment itself. For this reason data from the canopy height and soil surface are discounted from further analysis. The correlation matrix also shows that PAR and solar radiation are strongly positively correlated. Both PAR and solar radiation had a moderately positive correlation with air and soil temperature. The relationship with soil temperature was weaker most likely due to the insulating effect of the upper soil surfaces.

4.3.5 Simple regression models

There were weak negative relationships between CO_2 flux and temperature (Figure 4.21), with air temperature explaining between eight and thirteen percent of the variance in the flux (FER R^2= 0.08, NH_4 R^2 = 0.13, NO_3 R^2= 0.11). Soil temperature was barely significant for NH_4 treatment only (R^2 = 0.02), but this was a very weak negative relationship. The variables which explained the greatest variation in CO_2 flux were solar radiation and PAR. The relationship between light and CO_2 was strongly negative and non-linear, indicating that the most negative net CO_2 flux (highest levels of photosynthesis) occurred at when levels of sunlight were highest. The variation between the effect of light on each treatment was smaller for solar radiation (FER R^2= 0.61, NH_4 R^2= 0.59, NO_3 R^2= 0.61). A greater variation between nitrogen treatments in response to PAR was seen (FER R^2= 0.83, NH_4 R^2= 0.87, NO_3 R^2= 0.74). There were no variables with a significant relationship with CH_4 flux (Figure 4.22).

Many environmental variables showed a significant relationship with N_2O flux (Figure 4.23). Volumetric soil moisture explained a small amount of the variance for all treatments (FER R^2= 0.04, NH_4 R^2= 0.02, NO_3 R^2= 0.03), though the slope of these relationships was very close to zero. There was a positive relationship between sunlight and N_2O flux for all treatments: solar radiation explained between four and seven percent of the variance (FER R^2= 0.05, NH_4 R^2= 0.07, NO_3 R^2= 0.04). PAR was similar in its effectiveness as a predictor of N_2O flux for two treatments, but interestingly much better for the NO_3 treated replicates (FER R^2= 0.05, NH_4 R^2= 0.05, NO_3 R^2= 0.19); the slope of the lines was similar for all three treatments, however. The best single predictor of N_2O flux for the FER and NH_4 treatments was soil

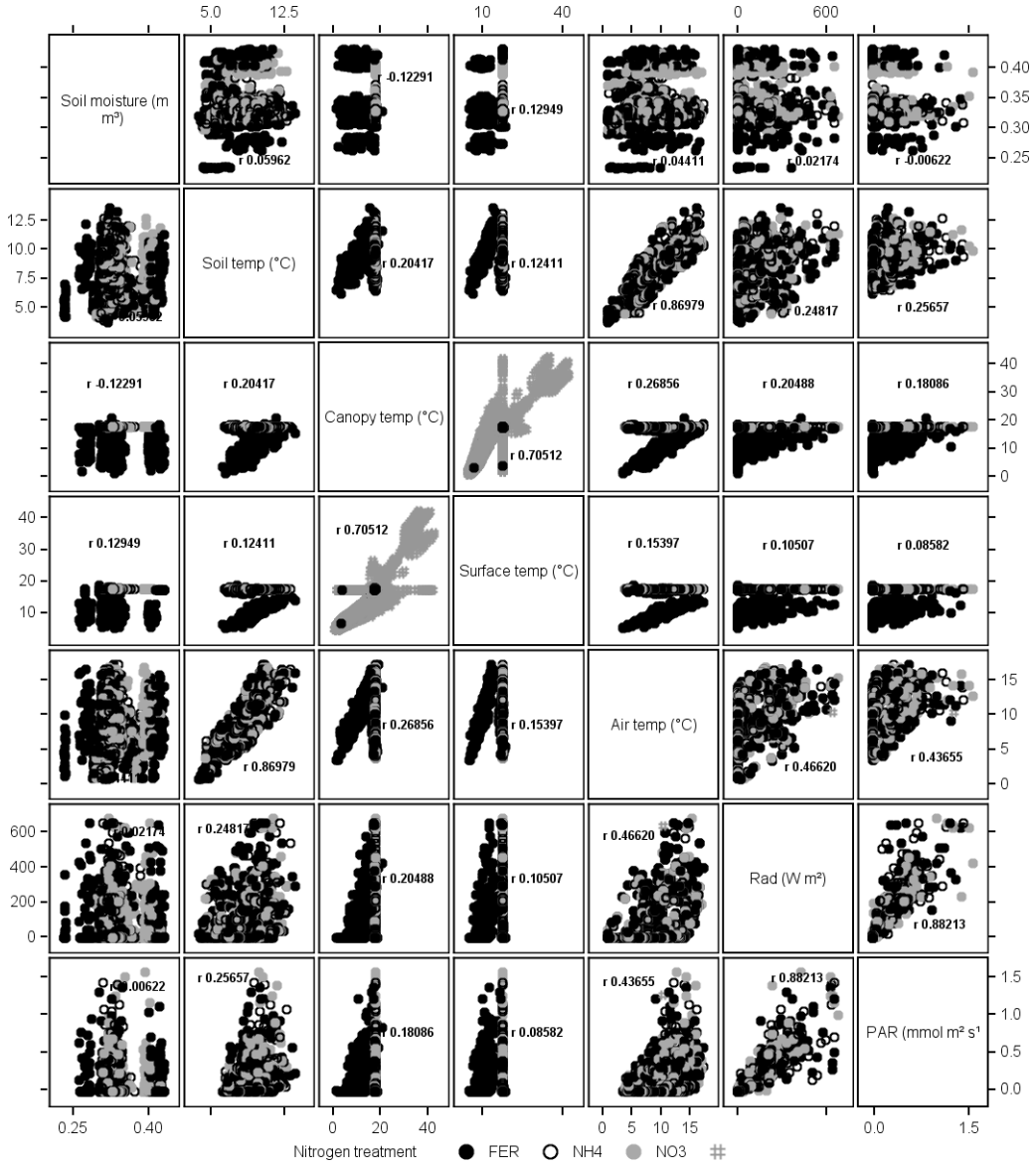

Figure 4.20 Correlation matrix of the measured environmental variables at the OSR field site over the experimental period. Pearson's correlation coefficient is shown inset in each panel. The scatter plots include data from all three Nitrogen treatments.

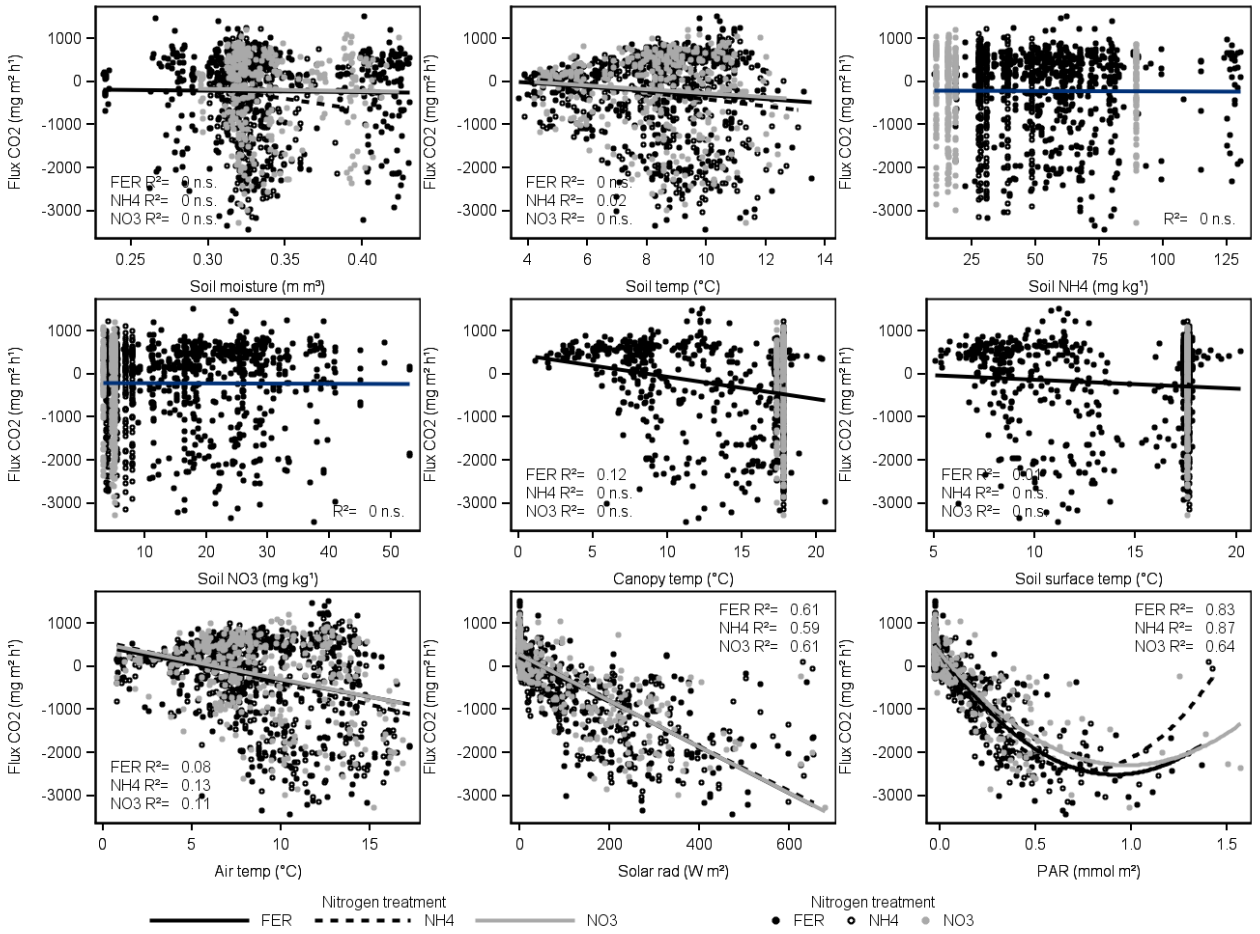

Figure 4.21 Linear regression models for NEE of CO_2 from OSR under three nitrogen treatments. R^2 statistics are included where significant.

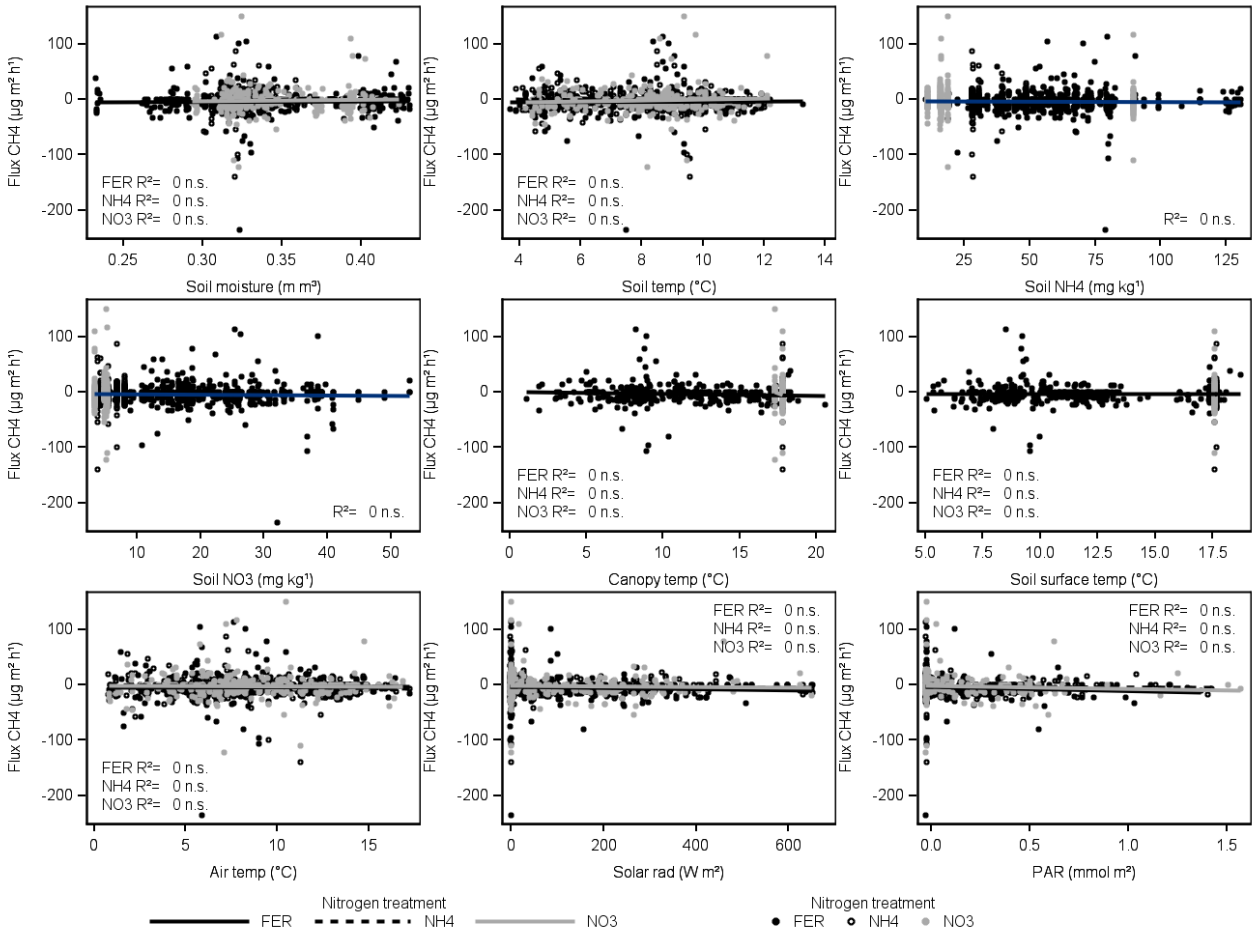

Figure 4.22 Linear regression between environmental factors and CH_4 flux from three different nitrogen treatments under OSR. Significant R^2 values are displayed

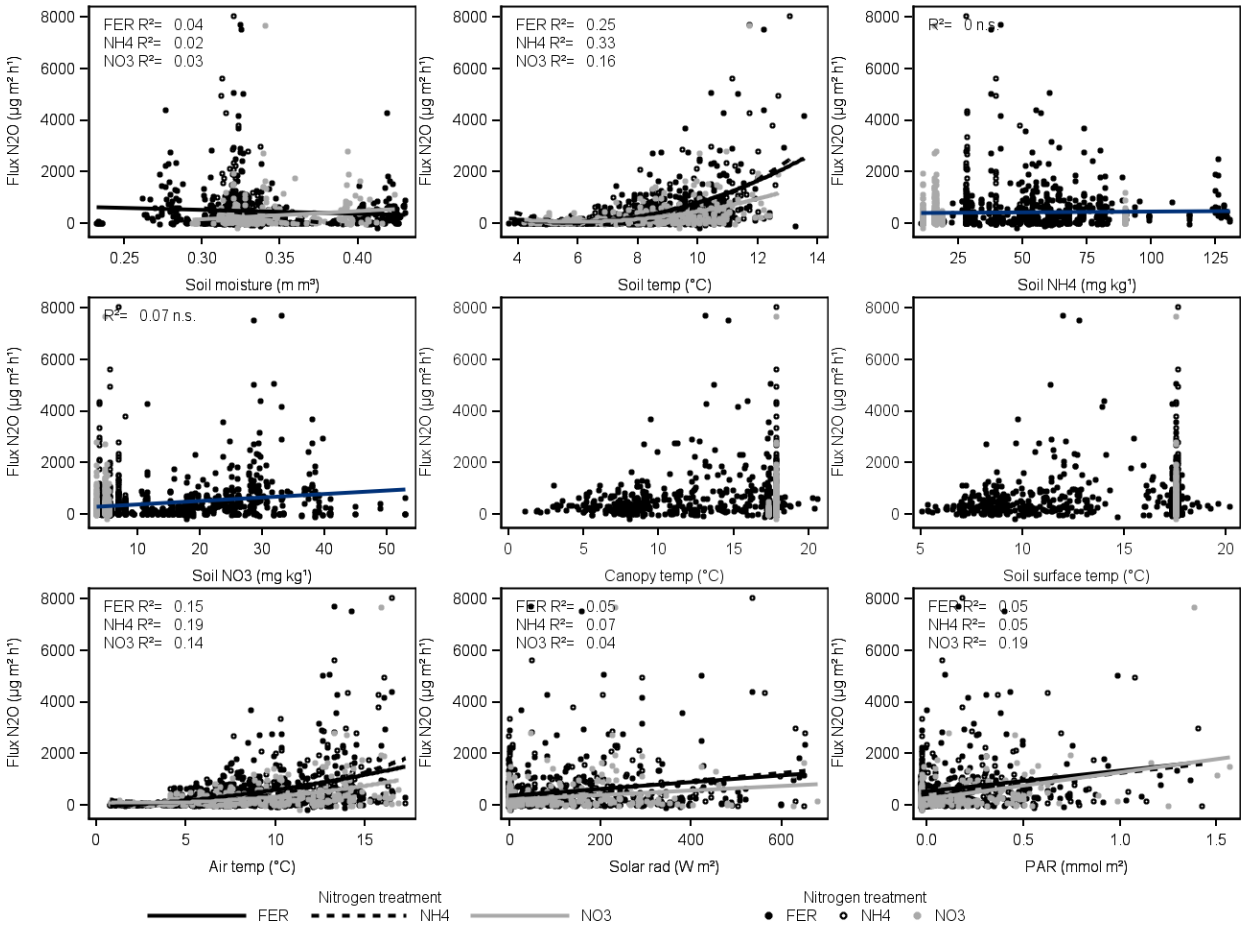

Figure 4.23 Linear regression models between environmental variables and N_2O flux from OSR under three different nitrogen treatments

temperature (FER R^2= 0.25, NH_4 R^2= 0.33, NO_3 R^2= 0.16), in a non-linear relationship; air temperature was not as good a predictor for FER and NH_4 treatments, but almost as good for NO_3 (FER R^2= 0.15., NH_4 R^2= 0.19, NO_3 R^2= 0.14).

4.3.6 Multiple regression

With the exception of soil NO_3-N, NH_4-N and gravimetric soil water content (GWC), the measured environmental variables were used as independent predictors of N_2O flux in stepwise regression models to explain variation in diurnal N_2O flux and the variation between days over the study period. Canopy temperature and soil surface temperature were not included in the models, due to the inclusion of air temperature and soil temperature.

4.3.6.1 Daily total N2O flux

The variation in daily total N_2O flux is more clearly related to the measured environmental variables than the single regressions explaining instantaneous N_2O fluxes (Table 4.2). The most important variable for total daily fluxes was the daily minimum air temperature, which explained 43%, 54% and 48% of the variation in FER, NH_4 and NO_3 treatments respectively, and 44% of all the treatments combined. The other variables that featured in all of the models were the maximum solar radiation- which was responsible for 11- 18% of the variation for individual treatments and 18% overall- and maximum volumetric soil moisture: 16% (FER), 15% (NH_4), 18% (NO_3) and 13% overall. The final models explained between 80-85% of the variance for individual treatments and 74% for all treatments combined, yielding final equations for daily total flux (F_d (mg m^{-2} day^{-1})) of:

FER F_d **= 8.1*min air temp + 0.08*max solar radiation – 4550*max soil moisture +1866**

NH_4 F_d **= 8.7*min air temp + 0.06*max solar radiation – 3390*max soil moisture +1373**

NO_3 F_d **= 4.6*min air temp + 0.04*max solar radiation – 2538*max soil moisture +1038**

All F_d **= 7.1*min air temp + 0.06*max solar radiation – 3489*max soil moisture +1425**

Table 4.2 Stepwise regression models to explain the mean daily total N_2O flux from OSR under three different nitrogen treatments, and all treatments together. “Max” indicates the maximum daily value of a variable, “min” the daily minimum; β= standardised estimate of a variable.

Step		*Treatment*			
		FER	*NH_4*	*NO_3*	*ALL*
1	Variable	Min air temp	Min air temp	Min air temp	Min air temp
	β	0.51	0.42	0.46	0.44
	r^2	0.43	0.54	0.48	0.44
	p	<0.009	<0.002	<0.005	<0.0001
2	Variable	Max soil moisture	Max solar radiation	Max solar radiation	Max soil moisture
	β	-0.53	-0.42	-0.54	-0.47
	r^2	0.16	0.11	0.18	0.05
	p	<0.06	<0.09	<0.03	0.001
3	Variable	Max solar radiation	Max soil moisture	Max soil moisture	Max solar radiation
	β	0.63	0.72	0.65	0.64
	r^2	0.23	0.15	0.19	0.18
	p	<0.004	<0.02	<0.004	<0.0001
Final	Intercept	1866	1373	1038	1425
	r^2	0.81	0.80	0.85	0.74
	p	<0.0001	0.0003	0.0002	<0.0001

4.3.6.2 Diurnal trend in N2O fluxes

There was a clear diurnal pattern in N_2O fluxes, with higher rates of emission during daylight hours, a pattern still evident despite the gradual increase in emissions following applications of mineral nitrogen. The effect of this is shown by the difference in flux estimates for total N_2O flux for the period when using either only measurements taken during the day or during the night (Figure 4.24). Daytime measurements across all three N treatments yield a higher value (336.1 ± 55.5 mg m^{-2}) than night time measurements (156.4 ± 24.0 mg m^{-2}), $F_{[1,24]}$= 9.5, p< 0.006. Clearly, since using fluxes measured through the day provides a total flux that is more than twice that from night time fluxes this questions the accuracy of estimates based solely upon day time measurements.

To better illustrate the diurnal pattern, N_2O fluxes were normalised to the highest daily value, yielding values between 0 and 1 (Figure 4.25). This removed the effect of increasing N_2O fluxes following nitrogen addition. The normalised N_2O fluxes peaked during the afternoon and the lowest values were around midnight (Figure 4.25).

The normalised fluxes and the independent variables were averaged over each cycle; models were constructed for individual nitrogen treatments, and again for all fluxes. Variables that were less frequently than daily were not included in the diurnal models. As these models were attempting to explain diurnal variation, only days where coverage of flux measurements spanned the whole 24 hour period were used (thus excluding 8 of the 21 days of the study period). The most important variable for explaining N_2O flux in the NH_4 treatment was PAR; for the FER, NO_3 and all treatments combined it was solar radiation. No other variables were significant in the models, the equations of which are shown below, where F_{norm}=normalised flux N_2O:

FER F_{norm}**= 0.001* solar radiation + 0.57** R^2**= 0.23, p<0.0001**

NH_4 F_{norm}**= 0.61* PAR +0.56** R^2**= 0.30, p<0.0001**

NO_3 F_{norm}**= 0.001* solar radiation + 0.59** R^2**= 0.21, p<0.002**

All F_{norm}**= 0.001* solar radiation + 0.57** R^2**= 0.23, p<0.0001**

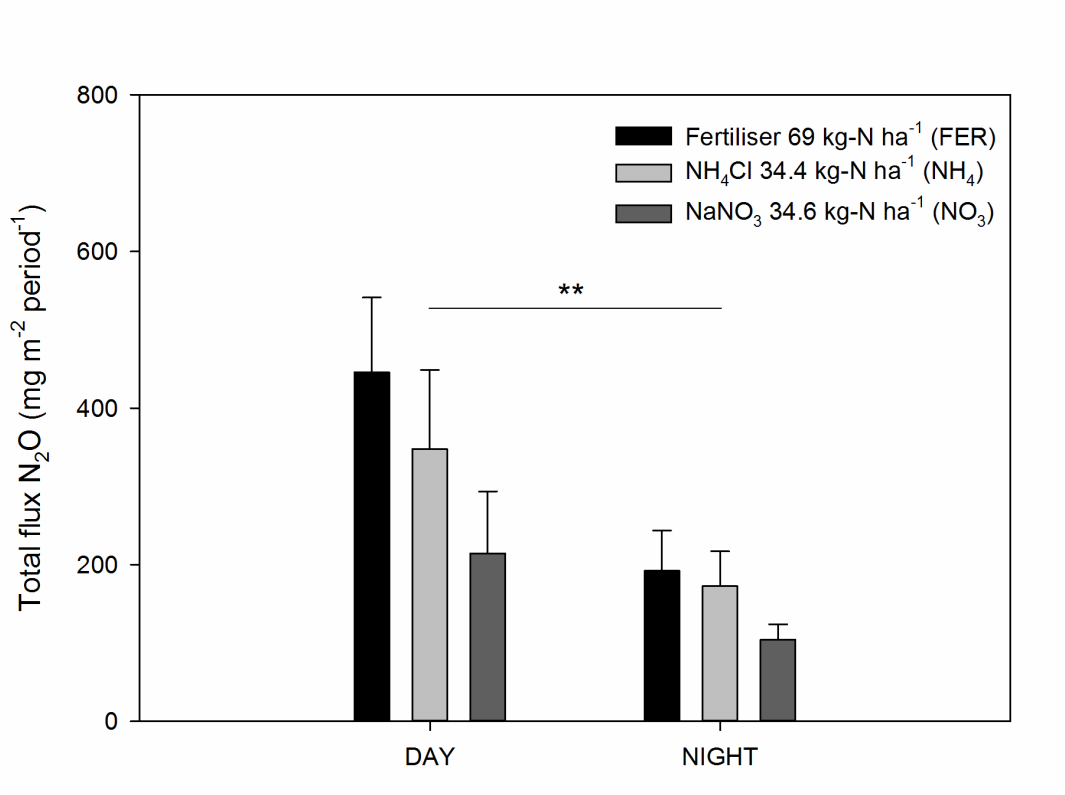

Figure 4.24 The mean (± 1SE, n=5) total estimated flux of N_2O from OSR under three different nitrogen treatments from automated SkyLine measurements, separated into data collected during the day and data collected at night (periods of 0 W m^{-2} solar radiation). ** denotes significant difference $p < 0.01$.

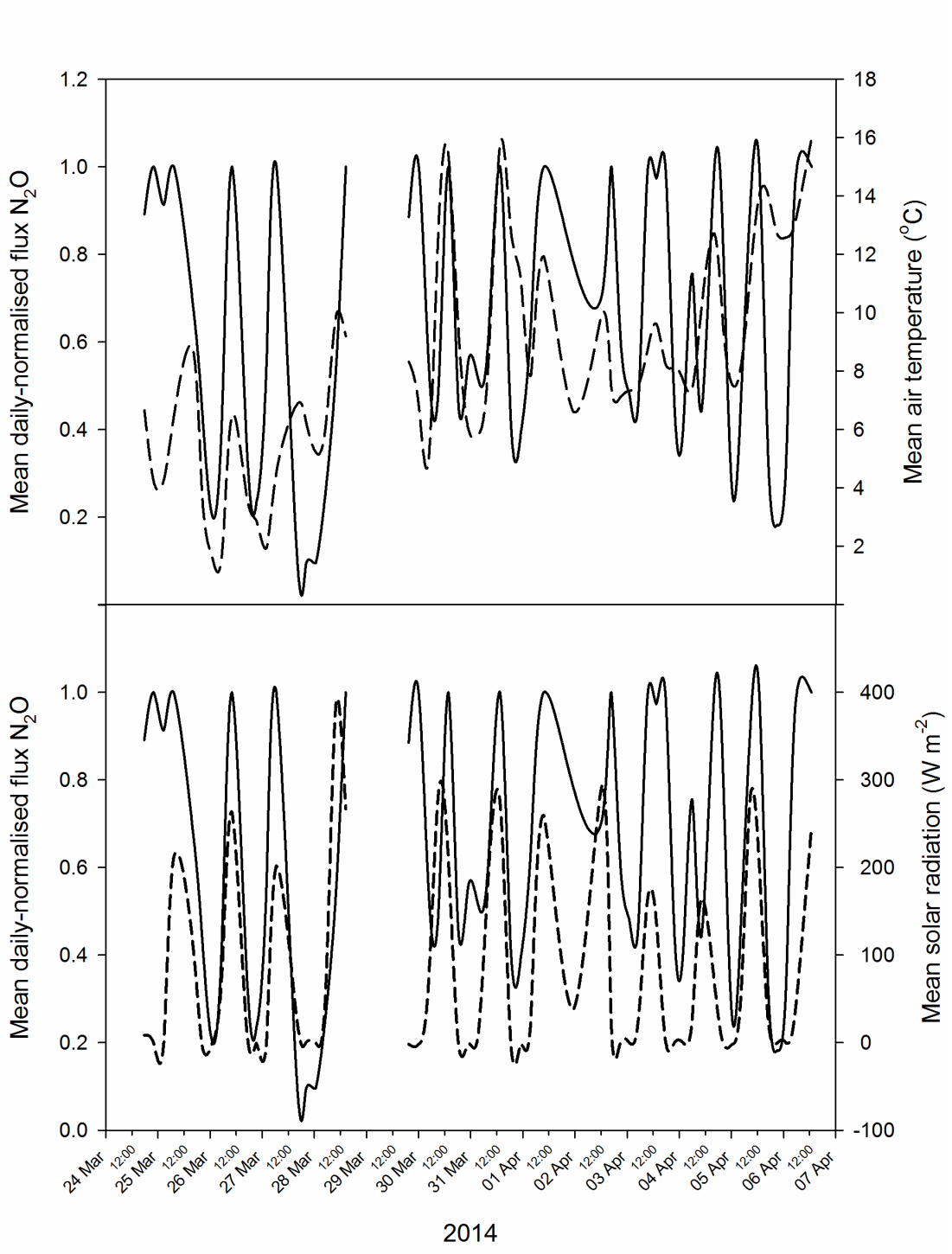

Figure 4.25 Mean N_2O fluxes by cycle normalised to the highest daily mean (FER treatment only, solid line) from SkyLine rings flowing two applications of Nitram fertiliser (NH_4NO_3). Solar radiation (bottom panel, dashed line) and air temperature (top panel, dashed line) averaged over the same period as the flux measurements are also shown.

4.3.7 Plant biomass and soil pH

There were no significant differences between the total biomass of OSR between the nitrogen treatments. However, the soil from the NH_4 treated rings was more acidic (pH 5.7) than the NO_3 rings (pH 6.3) ($F_{[2,15]}$= 7.13, p< 0.007). The soil pH of the FER treatment did not differ (pH 6.0) from either of the other treatments.

In both the NH_4 and NO_3 treatments there was a significant correlation between soil pH and the total N_2O flux for the study period. This nature of this relationship differed between the two treatments, however: in NH_4 there was a negative relationship between total N_2O and pH (r= -0.89, p= 0.04), but the relationship was positive in the NO_3 treatment (r= 0.91, p= 0.03). The FER treatment did not display any relationship with pH.

4.4 Discussion

4.4.1 SkyLine automated flux system

The SkyLine system enabled the measurement of three trace gases, CO_2, CH_4 and N_2O from over OSR at high frequency for a period of 21 days. The system successfully completed 1322 closures, providing nearly 4000 individual flux measurements, yielding a near-continuous dataset (measuring each replicate approximately every four hours). Using a clear chamber, enclosing both the soil and the vegetation, ensured the flux data were of NEE of the three gases of interest. NEE data of such high frequency from over tall vegetation is almost unprecedented without using eddy covariance (EC) equipment. The advantage that SkyLine has over EC is that its spatial resolution allowed the testing of hypotheses through manipulative experiments; the inability to deliver such spatial resolution is one of the shortcomings of the EC technique.

An automated chamber system for measurement of N_2O is described by Breuer *et al.* (2000), which utilised an in-line gas chromatograph (GC) with electron capture detector (ECD), in conjunction with an IRGA for measurement of CO_2. This system has subsequently been adapted and used in several studies under subtropical rainforest (Rowlings *et al.*, 2012) and semi-arid agricultural soils (Barton *et al.*, 2008, Morris *et al.*, 2013). SkyLine has several advantages over these systems, foremost being the number of replicates it can provide. The number of chambers accommodated in the aforementioned studies were three (Rowlings *et al.*, 2012), five, six (Barton *et al.*, 2008) and twelve (Morris *et al.*, 2013), as opposed to eighteen by SkyLine. Another system similar to the Breuer system is described by Nishimura (2005), which provided six replicates.

The number of replicates SkyLine can provide is limited principally by the distance between the vertical supports across which the ropes are suspended. It is thought that this distance might be increased to as much as 50 m, and over more homogeneous landscapes (e.g. grassland) where a smaller chamber footprint is required for representative measurements, the number of replicates might be increased to 50. Studies over pasture are being conducted with the equipment with 30 replicates (Stockdale & Ineson, unpublished). A limiting factor becomes the time required to complete a full measurement cycle. A drawback to the Breuer system is that each measurement required a chamber closure of between 45 and 60 minutes,

and whilst the chamber lid was opened in between measurements, the protocol meant that each chamber was closed for 30- 50% of the study period. The SkyLine system, with a 10 minute closure for each replicate in every four hour cycle reduced the time the vegetation was enclosed to less than 5% of the study period. SkyLine, with its use of in line laser analysers, also negated the requirement for storage of samples for laboratory analysis, as carried out with manual chamber measurements, or with accumulating automated systems such as SIGMA (Ambus *et al.*, 2010, Juszczak & Augustin, 2013).

4.4.2 Nitrogen treatment effect

Methane fluxes were small throughout the study, and largely negative, indicating uptake of CH_4 through oxidation by soil microbes. However, whilst the FER and NH_4 treatments were net sinks for CH_4, the NO_3 treated rings were a net source. On all days where there were significant differences in the total daily flux of CH_4, the NO_3 rings were consistently the cause of these differences, with net emission as opposed to consumption. Both NH_4^+ and NO_3^- have been shown to inhibit CH_4 oxidation (Dunfield & Knowles, 1995), and while NH_4^+ does so as a competitive inhibitor, NO_3^- not only inhibits competitively but also through the subsequent production of NO_2^- from denitrification and by reducing the pH of the soil.

CO_2 fluxes followed a clear diurnal pattern, with net uptake during the day and net emission at night. Fluxes were well described through the relationship with PAR, which also explains the occurrence of the largest emissions overnight following days with the greatest uptake, as carbon fixed through photosynthesis was respired by soil microbes and the vegetation. Rapid respiration of carbon fixed through photosynthesis has been shown in cereal crops (Gregory & Atwell, 1991), and the time lag between peak photosynthesis and respiration is known to be of the order of hours for grasses and herbs (Kuzyakov & Gavrichkova, 2010). There were no differences between either the total CO_2 flux or the plant biomass between treatments which indicates that the system was not nitrogen limited.

The differences in individual N_2O fluxes between the three treatments exhibited over the study period suggests both nitrification and denitrification were important to N_2O production at this site. Firestone & Davidson (1989) cite NH_4^+ concentrations as the principal proximal control on nitrification. The same authors recognise oxygen concentration, carbon supply and NO_3^- as limiting factors for denitrification, and state

that oxygen levels are the most important in fertilised soils, since the reductase enzymes are inhibited by O_2 (Knowles, 1982); it is thought that the threshold above which no nitrification occurs is *ca.* 70-75% water-filled pore space (WFPS) (Bateman & Baggs, 2005, Well *et al.*, 2006), and that nitrification peaks at 60% WFPS (Bateman & Baggs, 2005). That the NO_3 rings produced most N_2O over the 24 hours following the first treatment application suggests that denitrification was the dominant process at that time. This is supported by the relative concentrations of soil NO_3-N (less than 8 mg kg^{-1}) and NH_4-N (*ca.* 30 mg kg^{-1}) prior to nitrogen application, which suggest that NO_3^- was the limiting factor to N_2O production at the time of application. Previous studies at this site have measured the bulk density of the soil to be *ca.* 1.2-1.6 g cm^{-3} (Case *et al.*, 2012, Case *et al.*, 2014, Drewer *et al.*, 2012), and if a particle density of 2.65 g cm^{-3} is assumed, then the highest soil moisture content measured at the site (0.38 cm^3 cm^{-3}) approximates to 70-100% WFPS, and the lowest (0.32 cm^3 cm^{-3}) to 60-80%. It follows, then, that for much of the study period conditions were probably favourable for both processes to occur concurrently.

N_2O production from both nitrification and denitrification provides an explanation for the fact that there was no significant difference between nitrogen treatments for the total N_2O flux over the study period. Whereas N_2O from the NO_3 treatment must be a product of denitrification, N_2O from both FER and NH_4 treatments could have been produced by both processes. The NO_3^- portion of the fertiliser might be reduced via denitrification, but the NH_4^+ will produce N_2O during nitrification, and then the resulting NO_3^- will also feed into denitrification; similarly, any N_2O immediately coming from the NH_4 treatment will have been the product of nitrification, but later may have continued to be produced by either the oxidation of NH_4^+ or the reduction of the NO_3- produced. Despite receiving twice as much mineral N, the FER rings did not produce more N_2O overall, which indicates that following the two N applications the system was not nitrogen limited.

4.4.3 Controls of N_2O flux

Individual N_2O fluxes showed significant relationships with several variables, but the variable which explained most of the variation in the FER and NH_4 treatments was soil temperature; the most important variable for explaining fluxes from NO_3 treatments was PAR. The effect of PAR was probably a proxy for labile carbon input to the soil from the OSR root exudates as the vegetation photosynthesized. As one of the three principal limiting factors in denitrification described in Firestone &

Davidson (1989), available soil carbon drives denitrification directly, and also indirectly by creating anaerobic zones as a result of the heterotrophic respiration it stimulates in the soil (Farquharson & Baldock, 2008). As microbial processes, both nitrification and denitrification are directly affected by temperature, hence the relationship between soil temperature and N_2O flux in the FER and NH_4 treatments. It also explains temperature's importance in the NO_3 treatment, where it was the most closely associated environmental variable after PAR.

Perhaps most surprising is that the relationship between individual N_2O flux and soil moisture was found to be so weak in this study. Explaining just 2-4% of individual N_2O fluxes in this study, soil moisture is often found to be one of the key drivers of N_2O production (Dobbie & Smith, 2003b, Skiba & Smith, 2000, Skiba *et al.*, 1998), though this is not always the case (Kaiser *et al.*, 1996). The lack of a close relationship to individual fluxes might be due to the soil moisture content never dropped to a point where it became limiting. It also may be the result of the simultaneous occurrence of two processes (nitrification and denitrification) with different optima with regard to soil moisture (Farquharson & Baldock, 2008). Whilst both these are reasonable explanations, other factors appeared to be exerting a greater influence over N_2O fluxes at this site.

The daily total flux of N_2O was largely explained (80-85% of the variation in individual treatments, 74% overall) by the measured daily values of minimum air temperature, maximum solar radiation level and maximum volumetric soil moisture content. Previous studies have identified soil mineral-N content as a key factor in N_2O production from agricultural soils (Abdalla *et al.*, 2010, Dobbie & Smith, 2003b, Jahangir *et al.*, 2012), though it may only be a significant factor when soil moisture is not limiting (Jones *et al.*, 2007). It should be noted that the frequency of soil N data in this study was not high enough to be of use to regression modelling. The inclusion of solar radiation in this study's model is rare, if not unique: whilst carbon is occasionally included as soil organic carbon (SOC) or dissolved organic carbon (DOC) in models explaining fluxes from agricultural soils (e.g. Harrison & Matson, 2003, Kaiser *et al.*, 1996, Petersen *et al.*, 2008)), parkland (Lemke *et al.*, 1998) and fens (Ambus & Christensen, 1993), PAR or solar radiation are never included as independent variables in such models. Since denitrification is a heterotrophic process, it follows that it is reliant on the amount of carbon entering the system, which ultimately is driven by photosynthesis which is directly proportional to levels of PAR and solar radiation, as shown here in this study.

4.4.4 Diurnal pattern of N_2O flux

There was a clear daily pattern in N_2O flux throughout the study period at this site. Highest rates of N_2O emission were seen in the afternoon, and the lowest fluxes through the night. When these fluxes were normalized to the highest daily value, the diurnal trend was a sinusoidal pattern much like that displayed by CO_2 flux, though inverted, as CO_2 uptake peaked during daylight hours. This was in direct contrast to the diurnal pattern seen from the *Miscanthus* crop at the same site during the previous year (Chapter 2 of this thesis).

A diurnal pattern in N_2O flux has been reported several times before from agricultural field studies, over bare soil (Blackmer *et al.*, 1982, Ryden *et al.*, 1978) and pasture (Christensen, 1983, Das *et al.*, 2012, Livesley *et al.*, 2008, Simek *et al.*, 2010), which all showed peaks in N_2O emissions in the afternoon. Similar daily peaks were shown from bare soil in Scotland and grassland in Brazil (Alves *et al.*, 2012), whereas a greenhouse study with monoliths of two different soil types showed confounding diurnal patterns, with daytime peaks of N_2O flux from a sandy loam and night-time peaks from a peaty-gley (Smith *et al.*, 1998b). Many of these authors attributed the principal cause of diurnal trends to soil temperature (Alves *et al.*, 2012, Blackmer *et al.*, 1982, Livesley *et al.*, 2008) which has also been shown to drive diurnal patterns in the laboratory (Hatch *et al.*, 2005). Smith *et al.* (1998b) also describe soil temperature as the controlling factor of daily N_2O flux, and that the night-time peaks are due to N_2O being produced deeper in the soil profile, hence a lag between air temperature and soil temperature at the N_2O production microsites. Christensen (1983), whilst acknowledging the role of soil temperature, proposed that PAR may influence N_2O flux; Das *et al.* (2012) specifically investigated the role of PAR in N_2O flux, but concluded that the influence was limited to the warming effect it had on the upper layers of soil. The results of this study showed, on the other hand, that it was solar radiation (and in one instance PAR) that drove the diurnal pattern in N_2O flux in this system, and not air or soil temperature.

4.4.5 Dark and light N_2O flux

If solar radiation was the cause of diurnal peaks in N_2O emissions, it would be expected to see a reduction in N_2O flux following shading of the vegetation. The logic behind this is that the shaded vegetation stops photosynthesising, thus the carbon supply to the soil is slowed, causing the rate of denitrification to slow. When the first

round of measurements were taken following experimental shading (40 minutes after shading), fluxes for both shaded and unshaded treatments had increased, suggesting that the supply of carbon in the soil had not yet been affected. The second round of measurements took place over 200 minutes after, and there was perhaps the start of a trend of dropping fluxes in the shaded treatment, whilst the unshaded fluxes continued to rise. The experiment suffered from a low number of replicates (n=3), and no statistical difference was found. By the time the third round of measurements were taken, the sun had set and all plants were in darkness (the suggestion of lower fluxes from the shaded replicates was still apparent).

Of two studies which have attempted to investigate the effect of light on measured N_2O flux by using clear and opaque chambers, one (Stewart *et al.*, 2012) found that soils acting as a sink for N_2O in light switched to a source in opaque chambers. This, however, was a study from an N limited tundra landscape, though it is precisely the same effect described in Chapter 3 of this thesis. A second study in a salt marsh in the northeastern United States saw N_2O emission increase in opaque chambers compared to clear chambers (Moseman-Valtierra *et al.*, 2011), which was attributed to denitrification inhibition by increased oxygen levels in the sediments as a consequence of photosynthesis, which is a situation specific to coastal environments and not relevant to an agricultural system. In order to investigate the hypothesis that shading vegetation will decrease N_2O flux in a denitrifying agricultural soil, further experimentation is required, with higher frequency measurements following shading.

4.4.6 Chamber comparisons

There was a large discrepancy between the fluxes measured with manual static chambers and the SkyLine system. In paired comparisons fluxes tended to be higher from the manual chambers than from the darkened SkyLine chamber (Figure 4.15). Due to the logistics of the operation, the coverbox measurements were always made first, with the SkyLine measurement taking place a minimum of 75 minutes after the opaque chambers were placed. The flux measurements from SkyLine was therefore made after the vegetation had been darkened for over an hour, sometimes as long as two hours. The results of the shading experiment above suggest that this darkening may slow N_2O flux due to cutting off the carbon supply to the soil for denitrification. If this is the case then the manual measurement process itself may be responsible for altering the N_2O flux subsequently measured by SkyLine.

The second way that the paired manual chamber and SkyLine measurements differ is that the coverboxes were placed from late morning into the afternoon, which has been shown in this study and others (e.g. Alves *et al.*, 2012, Christensen, 1983)) to be the peak time for emissions. So the bias in taking manual measurements in the current study was two-fold: they were invariably made at the time of peak N_2O flux where SkyLine measured the flux as the peak declined, and they reduced the rate of N_2O flux for subsequent SkyLine measurements.

The total N_2O flux for the study period measured using manual measurements was nearly five times higher than the total derived from automated SkyLine measurements. This reflects two contrasting aspects of the measurement regimes of the two systems: the first is influenced by the frequency of measurements, and the second is the effect of a clear chamber compared to an opaque chamber. Concerns have long been raised regarding the practice of using a single daily measurement from which to extrapolate daily, monthly, or even annual fluxes (Ryden *et al.*, 1978). The extent to which manual measurements might overestimate fluxes is largely dependent upon the amplitude of the diurnal variation and the time of day at which the measurement is made. In extreme cases, daily maxima might be 15 times higher than the minima (Simek *et al.*, 2010) which opens up the possibility of greatly overestimating the true flux; various comparisons of fluxes calculated with single daily measurements and more frequent data show overestimates in the region of 60% (Maljanen *et al.*, 2001), 31-49% (Yao *et al.*, 2009b) and 21% (Brumme & Beese, 1992). The results here show a bigger discrepancy than those elsewhere, but using day-time measurements from SkyLine alone gave a two-fold difference in the estimate of total N_2O flux for the period than if night time measurements were used. If only the maximum daily values from SkyLine are used, then the manual chamber measurements still estimated the total N_2O flux to be more than twice as high for the same period. Further explanation for this may be found in the comparison of the fluxes derived from the small, opaque soil chambers and the large clear SkyLine chamber.

The N_2O fluxes measured using small soil chambers were much higher than in the clear SkyLine chamber, indeed, up to 30 times higher (Figure 4.16). The principal differences between the chambers were: the area covered (SkyLine 0.12 m^2, soil chamber 0.009 m^2), the chamber volume (SkyLine 83 L, soil chamber 2.6 L), the opacity of the soil chamber and the fact that the SkyLine chamber included the vegetation and the soil chamber did not. Due to the exclusion of vegetation, the soil chambers very quickly saw a large buildup (up to 3000 ppm) of CO_2, which did not

occur in the SkyLine chamber where photosynthesis reduced the CO_2 concentration in the headspace. According to Fick's law, buildup of CO_2 within the soil chamber reduced efflux from soil pores which will have resulted in anaerobic zones in the soil surface layers and further stimulated denitrification, thus increasing N_2O production (Figure 4.26). Depending on the CO_2 accumulation within the headspace of the large static manual chambers, which were in place for one hour (c.f. 10 minutes for the SkyLine chamber), a similar process may have occurred.

Augmenting the effects of this process is the fact that the large static chambers were not mixed, except by minor disturbance of the air through pumping the syringe at the discrete sampling times; in between sampling, the headspace will have settled, leaving CO_2 concentrations to be highest immediately above the soil surface (Schneider *et al.*, 2009), increasing anaerobic microsites in the soil pores and stimulating N_2O production through denitrification. Since it is suggested here that cutting off light to vegetation did not reduce the carbon supply for denitrification until after one hour, it is feasible that an initial increase in N_2O production is one 'artefact' of the opaque static chamber method used here.

A further possible explanation for the apparent increased fluxes in the small soil chambers is the inclusion of N_2O hotspots in its footprint. N_2O production is notoriously spatially heterogeneous; it has been shown in the high variance between individual rings in this study and in many previous investigations (Clayton *et al.*, 1994, Velthof *et al.*, 1996, Turner *et al.*, 2008, Chadwick *et al.*, 2014,), even over very small (< 1 m) distances (Ambus & Christensen, 1994). At the end of the current study the entire upper 10 cm of soil was taken intact from the base of one of the small soil chambers and incubated in the laboratory; it was found through systematic paring down of the soil core that almost all the N_2O flux from that chamber had been derived from a volume of soil approximately 1 cm^3 (Ineson & Toet, personal communication). Such hot spots are likely to be found close to the roots of the vegetation where exudates provided a labile carbon source for denitrification. Since the roots of OSR are small, they do not reach the circumference of the landing bases of the SkyLine chamber (40 cm diameter)

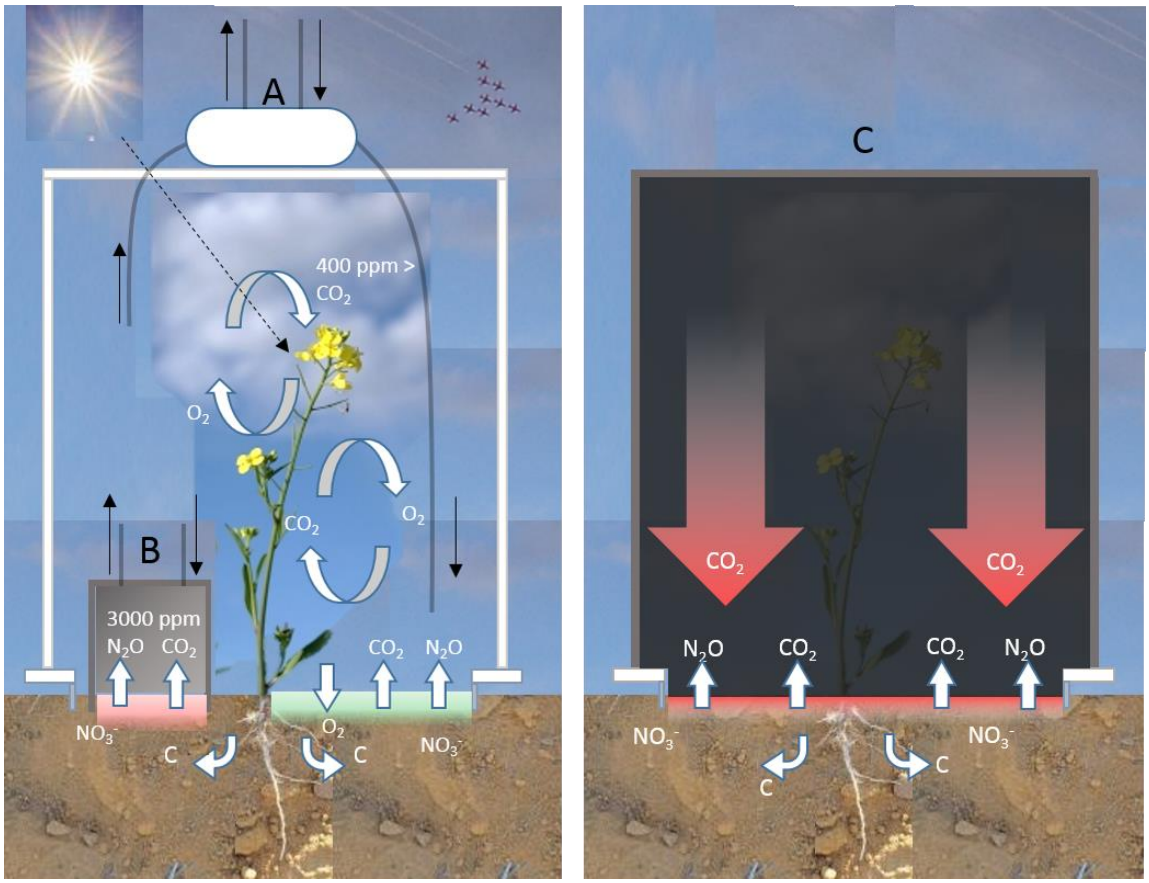

Figure 4.26 Schematic of the proposed chamber dynamics of the clear SkyLine chamber (A), the opaque soil flux chamber (B) and the large opaque manual chamber (C). Open arrows denote chemical flows, the dashed line indicates the travel of light and closed arrow flow of gas for sampling. Left panel: high concentrations of CO_2 in the soil chamber reduce the diffusion gradient and therefore the efflux from the soil, increasing anaerobic pockets and stimulating increased N_2O production through denitrification. Photosynthesis by the OSR in the SkyLine chamber reduces CO_2 concentrations and so the soil remains more aerated than in the soil chamber, and the flow rate of 0.4 l min^{-1} ensures the headspace is well mixed. Root exudates provide a carbon source for both respiration and denitrification in the soil. Right panel: there is no flow of headspace gas in the large manual chamber in between sampling; during this period the CO_2 from respiration settles at the bottom of the chamber as it is heavier than air, which slows diffusion of O_2 into the soil and creates more anaerobic pockets where N_2O production from denitrification increases.

within which the small chamber bases sat (11 cm diameter see; Figure 4.4 for an example of where the small chamber bases were placed), close to the base of the vegetation and the roots. The proportion of the small landing bases' area which will have encompassed roots (or have been in close proximity to them) will have been greater than that of the larger landing bases, thus increasing the likelihood of the occurrence of hotspots per unit area in the small chambers.

4.4.7 Total N_2O flux and GHG balance

The N_2O emissions measured using SkyLine during this study were high in comparison to other studies of agricultural systems. The results from the FER treatment presented here amount to a total emission of ca 2.3 kg N ha^{-1} over the 21 days of measurements, with a peak daily emission of ca 770 g N_2O-N ha^{-1} day^{-1} and a maximum mean individual flux of more than 2000 µg N_2O-N m^{-2} h^{-1} in the FER treatment and nearly 3000 µg N_2O-N m^{-2} h^{-1} in the NH_4 treatment. According to a comprehensive review of N_2O fluxes from agricultural soils (Stehfest & Bouwman, 2006) the total flux reported here was above the mean (and median values) for fertiliser rate and study length. It is, however, below the mean values for crop type (though OSR is included in the category "other" in Stehfest & Bouwman (2006), which includes anything that isn't a legume, grass or cereal), although it is greater than the median total flux.

The fluxes found here are consistently higher than others for temperate systems. A Danish study reported a peak emission of N_2O of *ca.* 94 µg m^{-2} h^{-1} following application of 124 kg N ha^{-1} as pig slurry (Chatskikh *et al.*, 2008); the same paper reports no peak in emissions from a prior fertiliser treatment of 71 kg N ha^{-1} as NH_4NO_3. The total N_2O produced during the cultivation of the OSR crop equated to an average of 6.8 g N ha^{-1} day^{-1}, which is considerably less than 100 g N ha^{-1} day^{-1}, which is what the FER treatment in this chapter averaged. In an intercropping experiment in Canada, a maximum mean N_2O flux of ca 60 g N ha^{-1} day^{-1} was reported, though this was based on a single monthly measurement in each of four months, taken during the day-time (Beaudette *et al.*, 2010).

Also in Canada, Asgedom *et al.* (2014) used weekly manual chamber measurements and reported peak emissions of *ca.* 175 g N ha^{-1} day^{-1} approximately one month after application of *ca.* 140 kg N ha^{-1} urea fertiliser, and a total emission of 2.48 kg N ha^{-1}

for the entire growth cycle of the OSR. Peaks of ca 500 µg N_2O-N m^{-2} hr^{-1} from OSR were seen in an unreplicated experiment in Germany (Hellebrand *et al.*, 2003), following 150 kg N ha^{-1} unspecified fertilizer type which yielded an annual total emission of 3.89 kg N ha^{-1}. Also in Germany, peak fluxes of approaching 400 µg N_2O-N m^{-2} h^{-1} were reached after fertiliser applications to OSR (which totaled 150 kg N ha^{-1}) in each of three consecutive years (Kavdir *et al.*, 2008) with bursts of N_2O emission persistently seen throughout the year (200-400 µg N_2O-N m^{-2} h^{-1}) months after fertiliser application. To put these values in context, N_2O flux measured from OSR in a drier climate (maximum measured WFPS < 30%) following fertiliser application (75 kg-N urea) was an order of magnitude smaller: maximum hourly N_2O flux during the year was < 40 µg N_2O-N m^{-2} h^{-1}, and the annual flux was < 140 g-N ha^{-1} (Barton *et al.*, 2010).

The emissions factor (EF) for fertiliser is defined as the proportion of applied N emitted to the atmosphere as N_2O, and the range given for mineral fertilisers is by the IPCC is 0.3-3% (De Klein *et al.*, 2006). This range does not account for crop type, and OSR is associated with a lower EF than grassland or leafy crops (Dobbie & Smith, 2003b). Commonly, the EF from experimental fertiliser additions is calculated as:

(N_2O from N application – N_2O from control) / total N applied * 100

In the current study, there was no untreated control since it was not part of the hypotheses under test. It is only possible, therefore, to express the total N_2O flux in terms of the total N application, which ranged from 1.8-2.8% across the three nitrogen treatments. This is likely to be an overestimate of the actual EF for the measurement period, though it is calculated over just 21 days and so does not account for N_2O emissions which will have occurred after the cessation of measurements. Assuming further N_2O emissions occurred throughout the year, the EF for this system will have been at the upper limit of the IPCC estimate. Reported values from OSR range from 0.02% (Barton *et al.*, 2008), 0.06% (Barton *et al.*, 2010) where fluxes were low, 0.7% (Skiba *et al.*, 1998) under high N input (235 kg N ha^{-1} $year^{-1}$), to values greater than 2.5% (Merino *et al.*, 2012) and even over 3.2% (Kaiser & Ruser, 2000).

The large N_2O flux at this site has implications for the GHG balance for the production of the crop. Using the data for three GHGs from the SkyLine system the site had a

negative GWP; however, the balance was close to neutral, with the N_2O emissions largely counteracting the sink effect of photosynthesis. Further bursts of N_2O emissions could easily tip the balance, and certainly, if the data from the manual chambers were used to provide an estimate of total GHG flux, the system would be estimated to have had a positive net effect on radiative forcing. This serves to highlight the importance of fully accounting for all GHGs when assessing the impacts in terms of GWP. Since OSR is the principal feedstock for biodiesel in Germany (de Vries *et al.*, 2014) it is vital that accurate measurement of N_2O flux is included in any lifecycle analysis (LCA), and it emphasises the need to move away from first generation energy crops.

4.5 Conclusions

The value of automated chamber systems has been reinforced in the findings presented here. The spatial resolution provided by the SkyLine system enabled an experimental contrast to be performed into the effect of different nitrogen fertilisers on GHG fluxes from OSR. The findings showed that both nitrification and denitrification played an important role in N_2O production at this site. The OSR was a net sink for GHGs, but the contribution of N_2O to the GHG balance negated *ca.* 50% of the total GHG gains from photosynthesis. The absence of a difference both in the total N_2O flux and the above ground biomass between the fertiliser treatment and the nitrate and ammonium treatments, which received half as much nitrogen as the fertiliser, indicated that the system was not N limited and that the fertiliser had been applied in excess. CH_4 fluxes were not a significant element of the GHG budget at this site.

The high frequency of flux measurements from SkyLine revealed a strong diurnal pattern in N_2O fluxes, characterised by peaks of emission through the afternoon and lower emissions at night, and this pattern was explained best with its relationship to solar radiation as opposed to temperature. It is suggested, due to this relationship with sunlight, that carbon supply from the plant played an important role in the diurnal pattern of N_2O fluxes.

N_2O flux measurements made using opaque manual chambers were significantly lower than those made using SkyLine. It is hypothesised that, in altering the light available to the vegetation, the manual chambers had a direct influence on the denitrification process in the soil. In addition, cumulative flux estimates of N_2O using

manual measurements overestimated the total flux by 5 times compared to the estimate using SkyLine measurements, principally due to the inherent bias caused by measuring during the afternoon when fluxes were highest, and this finding reinforces the necessity of high frequency measurements to enable accurate estimates of GHG fluxes to be made. Further work needs to be undertaken to investigate the role that solar radiation has on the diurnal pattern of N_2O fluxes.

5 General discussion

5.1 Evaluation of the novel systems presented

The aim of this study was to develop novel automated technologies to deliver full GHG budgets from a range of crop systems. The use of automated techniques allowed the delivery of near-continuous data for soil respiration, NEE and fluxes of N_2O and CH_4. The nature of these data has yielded vital new information on the diurnal cycles of trace gas fluxes, the differences in diurnal cycles between different crops, and the drivers of GHG fluxes.

SkyBeam and SkyLine were both deployed with great success, in two medium-term GHG experiments. The challenges in measuring from two very different crops, namely *Miscanthus* and OSR, were varied. It was particularly pleasing to produce a virtually uninterrupted four month dataset using SkyBeam from its initial deployment. Dropping a chamber consistently and accurately over a crop the size of *Miscanthus* was in and of itself a feat worthy of note. The scale of the chamber makes SkyBeam almost unique in its objective, and where Mordacq *et al.* (1991) used a chamber to measure gas exchange over small trees, it was not an automated system, and the enclosed vegetation was isolated from ambient environmental conditions for long periods of time.

Among the shortcomings of SkyBeam was the cumbersome nature of the supporting structures, and the time required for installation. Whilst this was time well-invested, considering the amount of data generated over the course of half a year, it does not reflect such a practical solution for shorter study periods. The success of SkyBeam led to the development of SkyLine, a much more adaptable system. Its reliance on shorter, lightweight support structures and ropes instead of a rigid beam made SkyLine easier to transport, quicker to install and able to measure from a longer transect. In work subsequent to this study, SkyLine has been deployed at five further sites, for up to a year, and has now measured from over grassland and clear fell forest, in addition to the measurements from OSR. Its flexibility as a platform for GHG measurements has been demonstrated by the use of standing tree trunks in the forest study from which to suspend its ropes, in place of aluminium trellis. It has also been used to measure GHG fluxes from over water as well as land.

The use of a single chamber is not only cost-effective, but it means that the measurement positions are only isolated from the environment for a maximum of ten minutes at a time; in between flux measurements the crop and soil are exposed to ambient environmental conditions. A common design for previous automated chamber systems has incorporated a permanent base in the soil, with a lid closing for measurements (Morris *et al.*, 2013, Pape *et al.*, 2009, Rowlings *et al.*, 2012). The sides of a collar (in the case of Pape (2009) these are 43 cm high) will inevitably have an effect on the internal microclimate. The analysers employed by both SkyLine and SkyBeam enabled fluxes to be calculated over a short period of time, which minimised the potential for changes in the headspace microclimate to effect the fluxes such as temperature (Butterbach-Bahl *et al.*, 2011) or pressure artefacts (Pumpanen *et al.*, 2004). In contrast, automated systems which utilise a inline GC (Nishimura *et al.*, 2005) require chamber closure times of at least 30 minutes, which can have adverse effects on the accuracy of flux measurements (Heinemeyer & McNamara, 2011).

5.2 The influence of N_2O on GHG balance

In this study the flux of N_2O from two different crops, barley and OSR, has been shown to be a major contributor to the net GHG balance. In the OSR N_2O emissions negated up to 50% of the carbon gains from photosynthesis. The total N_2O flux was comparable from barley over its cultivation, and depending on the NEE (not measured in this study), it had the potential to turn a net GHG sink into a net source. The estimated emission factor (EF) from the OSR ranged from 1.8 to 2.8% across the nitrogen treatments, and the total N_2O flux (413 mg m^{-2}) produced from under the barley equated to an EF of *ca.* 1.45%, though it should be noted that in lacking an untreated control, and not measuring for a full year, these numbers are not EFs in the strictest sense. These EFs are both higher than the default 1% Tier 1 IPCC guideline figure, but fall within the uncertainty range (De Klein *et al.*, 2006). These results add weight to the EFs reported in Reay *et al.* (2012) which include indirect emissions, which ranged from 1.8 to 3.8%.

The nitrogen addition study in Chapter 3 did not attempt to measure leaching of applied N, but the fact that N_2O emissions were not higher in the fertiliser (FER) treatment than either the nitrate or ammonium treatments, despite receiving twice as much mineral N, might suggest that much of the applied N did indeed run off. The absence of an increase in the total biomass from the FER treatments at the end of

the study might support this, but without measuring N content of the biomass it is not possible to be certain of this; it may be that after treatment application the system was neither N limited, nor was the excess N incorporated into the vegetation. Very recently it has been suggested that indirect emissions of N_2O from water courses caused by fertiliser runoff might be underestimated by as much as 40% (Turner *et al.*, 2015), which highlights the serious issue that use of excess N in agriculture. This raises important questions regarding the attitude towards fertiliser use in agriculture. Clearly the current study reflects the unsuitability of first generation crops for biofuel production due to fertiliser-derived emissions. This is a serious matter which needs to be addressed, since for example Europe's largest economy, Germany, uses OSR as its principal biodiesel feedstock (de Vries *et al.*, 2014), and 12% of global cereals are predicted to be diverted to bioethanol production by 2022 (OECD-FAO, 2013). It has been shown that, in terms of GHG balance, it is only lignocellulosic feedstocks such as *Miscanthus*, other perennial grasses and waste products that will offer a benefit from biofuel production (Searchinger *et al.*, 2008), and the findings of the current study would not contradict that conclusion. Application of green waste compost was also shown to increase N_2O fluxes in *Miscanthus* compared to untreated controls. Whilst the fluxes were very low in respect to those seen from the other two crops in this study, in the cultivation of energy crops, every effort should be made to maximise the GHG benefit. Any bioenergy production which receives nitrogen application is inevitably going to be questionable in terms of its GHG gains (Reay *et al.*, 2012).

There is a wider question regarding fertiliser application to arable land. Economically, fertiliser use is a trade-off between yield improvement and cost of fertiliser, and so long as the yield increase is financially more advantageous to farmers that the outlay, fertiliser will continue to be applied in excess (Davidson *et al.*, 2014). It has been suggested that by issuing financial incentives to landusers for reducing N_2O emissions, N fertiliser derived emissions could be reduced by 50% (Millar *et al.*, 2010). Other approaches include improving nitrogen use efficiency (NUE) in crops (Davidson *et al.*, 2014) or use of slow release fertilisers (Chien *et al.*, 2009).

5.3 Diurnal patterns in trace gas fluxes

It was striking to find such a marked difference in the diurnal pattern of soil respiration between different crops grown on adjacent fields (Chapter 2), especially given that

soil respiration is often described as a function of soil or air temperature (Bhattacharyya *et al.*, 2013, Buchmann, 2000). It is clear from the data presented in Chapters 2 and 3 that there was a strong temperature-independent influence on respiration, particularly under the *Miscanthus*, and that this is often ignored when night time EC data are processed (Bhattacharyya *et al.*, 2013).

The cause for the discrepancy between the barley and *Miscanthus* in this study cannot be fully explained here, though it is hypothesised that assimilated carbon moving through the vegetation to the soil is the driver. It is known that photosynthate moves through larger vegetation at slower rates than through short plant species (Bradford *et al.*, 2012, Kuzyakov & Gavrichkova, 2010, Liu *et al.*, 2006, Savage *et al.*, 2013), and so it is possible that carbon arriving at the soil peaked later in the day under *Miscanthus* than barley, thus stimulated a later peak in soil respiration.

Diurnal patterns in N_2O flux have been reported on several occasions (Christensen, 1983, Das *et al.*, 2012, Hu *et al.*, 2013, Livesley *et al.*, 2008), but without exception these report diel variations of highest flux in the afternoon or early evening and lowest through the night. These studies all deal exclusively with N_2O emission, and in that respect the data presented in Chapter 4 from OSR are consistent with their findings. In contrast to the majority of these authors' interpretation, the current study found a closer relationship between solar radiation and N_2O flux than with temperature.

The exact opposite pattern in N_2O flux was witnessed in the *Miscanthus*, where it was shown that net uptake of N_2O occurred during the day, but net emission at night. The only instance of such a pattern of uptake during light conditions and release in the dark has been seen in an arctic tundra, and was demonstrated using opaque and clear chambers (Stewart *et al.*, 2012). Such a pattern is difficult to interpret, since the biological processes governing N_2O production and reduction are rather convoluted (Butterbach-Bahl *et al.*, 2013), but it is assumed that N_2O consumption occurs when reduction to N_2 exceeds production (Chapuis-Lardy *et al.*, 2007). The reason for this to vary over the course of a day needs further investigation, but the presence of vegetation may be key, since it might store or metabolise N_2O (Grundmann *et al.*, 1993) or act as a passive gas transport channel from higher ambient concentrations to reduction sites further down the soil profile (Clough *et al.*, 1999). If vegetative transport is mediated by stomata, then it would halt when photosynthesis ceased and

the stomata closed. Since the N_2O emission increase seen coincided with soil respiration, it is possible that it was driven by production from heterotrophic denitrification.

CH_4 flux in *Miscanthus* also exhibited a diurnal pattern. As was consistent across all three crops, oxidation was the dominant CH_4 process at this site, which was a net sink in all of the current studies. In the *Miscanthus*, unlike the OSR and the barley, there was a strong pattern of peak uptake during the day, and fluxes closer to zero at night. It was demonstrated that temperature was the major explanatory variable, which is consistent with a microbial process. It cannot be discounted that the vegetation itself was taking up CH_4 as has been seen in boreal plants (Sundqvist *et al.*, 2012), and this also would explain the abrupt halt of uptake when the plant stopped photosynthesising.

5.4 Automated vs manual measurements and the effect of sampling frequency

There have been several comparisons made of fluxes measured using automated systems and manual chambers, and they tend to take one of two approaches. The first involves direct comparison of techniques measuring the same flux at the same frequency (Ambus & Robertson, 1998, Heinemeyer & McNamara, 2011, Pumpanen *et al.*, 2004). The second approach is comparing the total flux estimated between different measurement frequencies (Laville *et al.*, 1997, van der Weerden *et al.*, 2013, Yu *et al.*, 2013a). The current study has enabled comparisons between techniques on both of these levels, across a variety of crop types.

5.4.1 Comparison of static and dynamic chambers

In Chapter 3 measurements of CH_4 and N_2O flux using manual static chambers were made from within the same experimental plots as the SkyBeam chamber. It was shown that CH_4 and N_2O fluxes from the manual chambers were significantly higher than those made by SkyBeam. This was not designed as an experimental comparison, and is described with the caveat that SkyBeam was a clear chamber which enclosed the vegetation, and the manual chambers covered the soil only. However, when manual chambers were deployed over the OSR in Chapter 4, these were measuring from the exact same positions as SkyLine, and so included

vegetation in the flux. In this instance the fluxes were again much higher for N_2O. The caveat in this instance is that again the manual chambers were opaque and SkyLine clear. Static chambers have been shown to underestimate CO_2 fluxes (Heinemeyer & McNamara, 2011, Pumpanen *et al.*, 2004), so whether the discrepancy in this study is due to temporal separation, opacity of the chambers or the presence of vegetation cannot be ruled out.

5.4.2 Comparison of monthly and sub daily measurements

Estimates of cumulative soil respiration were made from barley and *Miscanthus* in Chapter 3, using monthly data from a Licor survey chamber and *ca.* hourly measurements using Licor automated chambers. Measurements were made from the same collars for both techniques. In the *Miscanthus* the monthly measurements consistently overestimated the cumulative flux, compared to the hourly data. The trend was not significant in the barley. Low frequency measurements have been shown to give lower estimates than high frequency measurements of cumulative flux on for N_2O (van der Weerden *et al.*, 2013), and CH_4 (Yu *et al.*, 2013a). In this study the over estimation of cumulative flux is attributed to the insensitivity of a single measurement on one day per month to the inter- and intradiel variation. In particular under the *Miscanthus*, by not including the early morning in monthly measurements, the lowest fluxes were missed and so the measurements were biased.

A similar bias was introduced in the comparison between manual measurements and automated measurements of N_2O in Chapter 4, where the manual chambers were deployed only during the day, during the period of peak daily fluxes, and SkyLine measurements included the night time fluxes, which were the lowest.

5.4.3 Comparisons of light and dark

The diurnal pattern of N_2O flux suggested that had an effect on N_2O fluxes in Chapter 4. This was reinforced by the importance of solar radiation in the multiple regression models for N_2O flux, but also in the shading experiment that was performed. Although the comparison was flawed, the trend for lower fluxes under shaded vegetation indicated that with further replication statistical significance might be demonstrated.

Counter intuitively, the measurements of N_2O flux from the opaque manual chambers were significantly higher than those from the clear chamber in Chapter 4. An explanation is proposed for this (see Section 4.4.6), which is reinforced by the theory of Moseman-Valtierra (2011) when a similar increase in fluxes was seen in darkened chambers.

The effect of heightened N_2O fluxes from darkened soil chambers compared to clear NEE chambers was consistent between measurements made in the *Miscanthus* and OSR. In Chapters 3 and 4 the presence of vegetation in clear chambers was associated with reduced N_2O flux. This lends weight to the idea that photosynthesising vegetation maintains higher O_2 levels within the chamber and so inhibits denitrification (Moseman-Valtierra *et al.*, 2011). Darkened chambers, whether they enclosed vegetation (Manual chambers, Chapter 4) or not (small soil chambers, Chapter 4; manual chambers, Chapter 3), create anaerobic environments due to the buildup of CO_2 and stimulate N_2O production through denitrification. A drop in O_2 concentration would also explain the elevated CH_4 fluxes from the manual chambers in Chapter 3 in comparison to the SkyBeam chamber. If such a process is occurring, it would represent a hitherto undescribed chamber artefact.

Diffusion gradients are known to build up inside chambers which can have an effect on the apparent flux (Healy *et al.*, 1996, Heinemeyer & McNamara, 2011). If, due to the opacity of the chamber, the chamber itself were altering the flux process, and not just inaccurately measuring it, questions regarding the use of opaque chambers arise which need to be addressed. Chambers are specifically recommended to be opaque, especially those which are required to be closed for tens of minutes, in order to reduce the warming effect that a clear chamber can have (Butterbach-Bahl *et al.*, 2011, Rochette & Eriksen-Hamel, 2008). It may be that by avoiding one chamber artefact (warming), another equally serious one is introduced (stimulation of N_2O).

5.5 Environmental controls of trace gas flux

Several consistent patterns emerged from the relationships between trace gas fluxes and the measured environmental variables (Table 5.1). Solar radiation and air temperature both displayed negative relationships with NEE in the OSR and *Miscanthus*. Due to the auto correlative nature of incoming radiation and air temperature, the two variables' associations with trace gas fluxes were consistently

Table 5.1 Summary table of significant relationships between environmental variables and trace gas fluxes, across all chapters. +sign = positive relationships, (i.e. greater emission with increasing values of the independent variable) and – sign = negative relationships (i.e. reduced emission/ greater uptake with increasing values of the independent variables). Frequency is defined as H= hourly measurements, M= monthly measurements.

	NEE		Soil Respiration				CH_4						N_2O					
Crop	*Miscanthus*	OSR	*Miscanthus*		Barley		*Miscanthus*		Barley		OSR		*Miscanthus*		Barley		OSR	
Frequency	H	H	H	M	H	M	H	M	H	M	H	M	H	M	H	M	H	M
Variable																		
Air temperature	-	-	+		+		-	-					+	+			+	
Soil temperature			+	+	+									+		+	+	
Soil moisture				-		-							+	-		-	-	
Solar radiation	-	-	+	+	+		-							+		+	+	
Relative humidity	+	+		-			+							-				

the same. In the case of NEE, it is the solar radiation which is the driver of the relationship, since it is sunlight which stimulates photosynthesis, and this was reflected in individual regressions in Chapters 3 and 4, where radiation was the variable with the closest relationship with NEE. Soil respiration, N_2O flux and CH_4 flux are all the products of microbial processes, and as such it is to be expected that temperature would have an important influence on them. Soil temperature is often described as strongly influencing soil respiration (Buchmann, 2000, Kane *et al.*, 2003, Kutsch & Kappen, 1997). The relationships seen in this study were not so straightforward. Whereas soil respiration under barley followed a typical temperature dependent diurnal pattern (see Chapter 2), respiration under *Miscanthus* did not, with a lagged element to the pattern of diurnal variation (see Chapters 2 and 3). Whilst there was certainly a strong temperature associated influence on respiration under the *Miscanthus*, there was an independent process also driving respiration. It is suggested here that the temperature independent element was due to carbon supply. In their warming experiment, Fitter *et al.* (1999) showed that it was photosynthetically active radiation which drove increased soil respiration due to greater allocation of belowground carbon, as opposed to the increase in temperature, to which plants acclimatised. Various approaches have been used to demonstrate the relationship between photosynthate and soil respiration, such as girdling (Hogberg *et al.*, 2002, Hogberg *et al.*, 2001) and isotopic labelling of CO_2 (Kuzyakov & Cheng, 2001), which have shown the influence that recent photosynthate has on soil respiration. That solar radiation was also shown to be significantly associated with N_2O flux from all three crops might initially be dismissed as due to its close relationship with temperature. However, in the OSR it was shown to be the variable with the closest relationship with the diurnal variation in N_2O flux, which has led to the hypothesis that it was carbon supply which drove this pattern in fluxes here. Solar radiation was also seen to be important in multiple regression models explaining N_2O flux from *Miscanthus*.

Soil temperature was also positively related to soil N_2O flux, in both barley and *Miscanthus*. A range of Q_{10} OF 2.2 to 7.1 has been reported for soil N_2O flux (Alves *et al.*, 2012), and the values in this thesis do not contradict those findings. It is perhaps surprising that no effect of soil temperature was seen in CH_4 fluxes, though this was perhaps down to the very low fluxes seen across all crops.

Air temperature exhibited the similar relationships to fluxes as soil temperature, which is to be expected since the two variables are inextricably linked. This was one of the few variables with which CH_4 flux was significantly associated in any of the three crops. CH_4 flux under *Miscanthus* declined with increasing air temperature. In this case this decline represented an increase in CH_4 oxidation, which has been shown in previous studies (Butterbach-Bahl & Papen, 2002).

Negative effects of soil moisture on soil respiration in barley and *Miscanthus* can be attributed to reduced O_2 levels in the soil with increasing moisture levels. The negative relationship with N_2O flux seen in all three crops was somewhat surprising. Whilst in anoxic conditions caused by very high soil moisture levels N_2O reduction is known to exceed N_2O production (Chapuis-Lardy *et al.*, 2007), the soils during this study were rarely waterlogged, and so it is more difficult to explain this relationship with that mechanism. Ordinarily, N_2O flux would be expected to increase with soil moisture as anaerobic conditions stimulate denitrification (Dobbie & Smith, 2003b, Skiba *et al.*, 1998). Indeed, the hourly measurements of N_2O from *Miscanthus* did demonstrate a more conventional positive relationship with soil moisture, and this is most likely to the extra sensitivity in data interpretation that comes with higher frequency measurements.

5.6 Future work

The work described in the current study has produced several important questions that should be addressed in order to further the understanding of the processes controlling trace gas fluxes. The most pressing issue is to establish the driver of the differing diurnal cycles of N_2O flux. How common is such diurnal variation in N_2O? High frequency measurements are required from a range of plant soil systems to characterise any existing patterns. It is clear that if two different crops grown on adjacent fields (same soil type) exhibited opposite patterns in diel N_2O patterns, it is entirely possible that current understanding of N_2O fluxes is inadequate. Does recently assimilated photosynthate drive the diel pattern seen in the OSR? If so, it may be possible to show this through manipulating the levels of radiation arriving at the plants. The biggest challenge when manipulating light levels is decoupling light and temperature. Low energy LED grow lamps are available which give off little heat, and these may offer the opportunity to manipulate night time light levels without raising temperature, to establish whether diurnal N_2O cycles could be disrupted.

Of equal interest is the uptake of N_2O from well aerated, N limited soils. Through laboratory incubations an understanding is growing that N_2O uptake in aerated soils is much more common than previously reported (Stockdale, personal communication). Since N_2O has such a large GWP, understanding all the mechanisms governing its production and consumption is vital to our ability to mitigate emissions. Ascertaining whether aerobic uptake of N_2O by soils is simply reduction of N_2O to N_2, or a previously undescribed assimilatory pathway for N would be of great interest.

Since our knowledge of the drivers of N_2O production, especially at fine temporal resolution is rather poor, it is becoming clearer that in addition to high frequency measurements of soil temperature and moisture, measurements of the chemical properties of the soil need to be made more often. High frequency data on mineral N and dissolved organic nitrogen and carbon (DON and DOC) within the chamber might be very useful in terms of explaining observed fluxes, and predictive modelling of emissions.

It was apparent in the study from OSR, as has been shown in various other studies, that N_2O fluxes can be driven by very small 'hotspots'. The work in Chapter 4 enabled the detection of such a hotspot, which was extracted in a soil core and microbial analysis of the soil is planned. It may be that hotpots are responsible for the majority of the total landscape N_2O flux, and as such it is a matter of urgency that we discover exactly what is creating these hotspots.

Further investigation into the differences in soil respiration under various crops species will also be of great value, especially in terms of accurately partitioning NEE from EC data. Communication with computer modellers invariably includes the request for more measurements of flux to be made to validate models. In order to enable simulations of GHG emissions under various scenarios to be as accurate as possible, it is essential that robust flux measurements are made from a variety of land uses.

5.7 **Summary**

From the work presented here it is apparent how crucial N_2O is in term of GHG balance, and that it is essential that is quantified accurately and reliably. If N_2O flux is

to be estimated through the use of emissions factors, then they must be verified so that they are more precise than the default Tier 1 EFs, around which there has been shown to be much variance. Direct measurements of GHGs taken at high frequency are capable of providing important information regarding the temporal and spatial variation of. Measurements made with SkyBeam and SkyLine in *Miscanthus* and OSR demonstrated how large, fleeting bursts of N_2O emissions characterise N_2O flux, and that these short-lived events may contribute major proportions of an annual GHG budget. It is pleasing to hear that revised substrate-specific EFs are being prepared for the UK based upon a comprehensive regime of direct measurements (Chadwick, *personal communication*).

The work in the OSR reinforced the understanding that continued use of first generation crops for bioenergy production will not provide substantial gains in terms of GHGs. The application of nitrogenous fertiliser ensures that N_2O emissions counteract much of the carbon gain from crop growth, and the remaining 'carbon credit' will be subsumed by further inherent emissions from transportation, fertiliser manufacturing and processing of the feedstock. *Miscanthus* provides a much more promising opportunity in terms of bioenergy. Its low N_2O emissions ensured that the major contributor to the GHG balance was CO_2. In this current study the field of *Miscanthus* was seen as a net source according to measurements made by SkyBeam. This, however, was an atypical year, with tillage creating conditions more akin to an establishment year for the crop and stimulating a large turnover of soil C, and the yield of the crop itself very poor. Subsequent years with less disturbance should see an improvement in yield, which will drive more uptake of CO_2 and create a strong GHG sink.

Addition of compost to the *Miscanthus* did not improve the yield, and in fact it increased N_2O emissions, and there was the suggestion it may also have increased CO_2 losses from the soil. Since no measurements of soil quality were made in this study it is not possible to state whether there were any unseen benefits gained from this compost application, and it is possible that it may stimulate improvements to the crop in years beyond this study. The conclusions drawn here, however, are that the compost was detrimental to the GHG balance and so such practices should be avoided where possible. It is also recommended that the soil be disturbed as little as

possible, meaning farmers should refrain from tilling the soil in which perennial crops are cultivated.

The strong and differing diurnal patterns in fluxes of all three GHGs, across different crops raises serious implications for how trace gas sampling regimes should be structured in the future. Rates of soil respiration in particular varied in the timings of peak fluxes between crops on adjacent fields. If flux estimates are to be based on single daily measurements then the timing of these is crucial, since by measuring in the early morning the discrepancies between crops might be entirely different or non-existent in the afternoon. The total opposite behaviour of N_2O fluxes in *Miscanthus* and OSR demonstrated the importance of taking measurements throughout a 24 hour cycle. In *Miscanthus* uptake during the day was replaced by emission at night, and so raises the very real possibility that measuring at the 'wrong' time of day might lead a researcher to draw wholly inaccurate conclusions as to whether a system is a net source or sink. Equally, due to the depression of N_2O emissions in the OSR during the night, a cumulative flux based entirely upon day time measurements will overestimate the magnitude of the crop as a source.

The use of clear, automated chamber systems for the measurement of trace gas fluxes has enabled the quantification of a full GHG balance for two crops. Both SkyLine and SkyBeam provided a flexible measurement platform with which manipulative experiments were performed. This is due to the spatial resolution of the chamber, which is not achievable with EC systems. The potential to use such systems, in conjunction with micrometeorological techniques to gain a more thorough understanding of trace gas fluxes is large, and it will also be possible to gain important insight into the challenges of scaling up from small footprints to larger scales.

Appendix A

Testing of the SkyBeam system at the University of York.

Fluxes of CO_2 were measured from grass sward plots under a prototype of SkyBeam, using the SkyBeam chamber and clear Licor Li-8100 103 chambers and an IRGA. Chambers of each type were paired within each plot and the order in which they were used (SkyBeam (gantry), Licor) was randomised. The null hypothesis that there would be no significant difference between the CO_2 flux measurements made using SkyBeam and Licor chambers was tested, using Wilcoxon signed rank test which showed there was no significant difference between the methods (S= -9, n=6, p> 0.05).

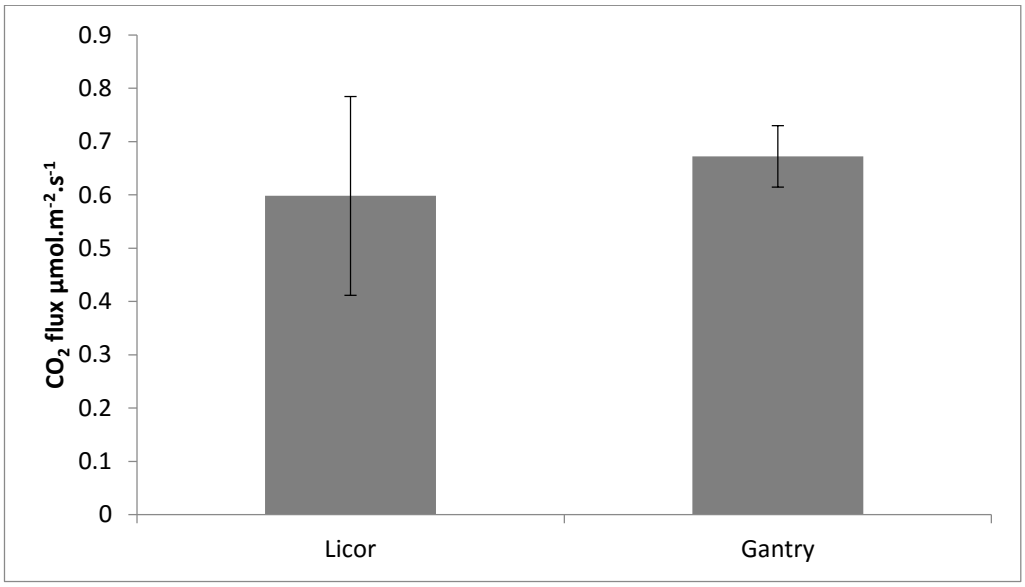

Appendix B

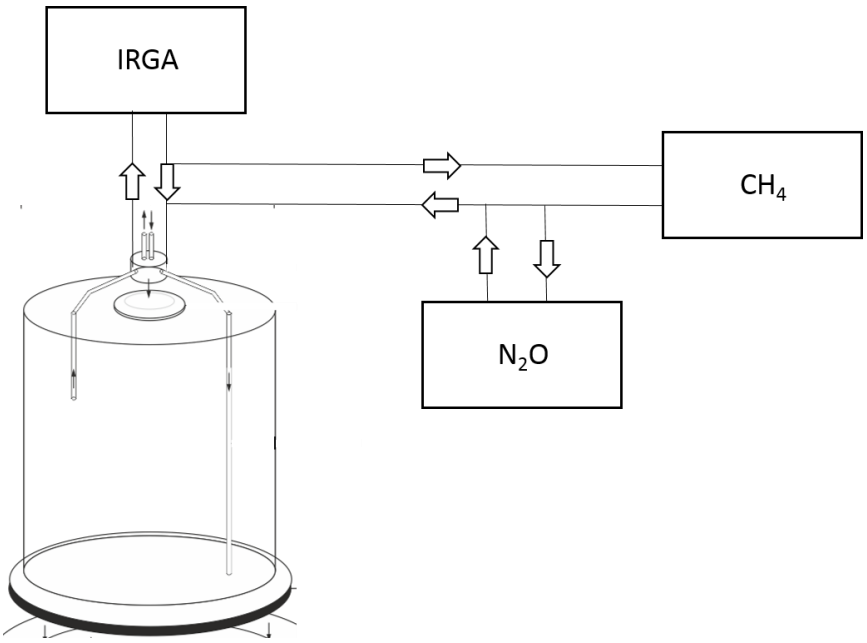

Schematic of the analyser set up. Headspace gas travelled from the chamber and to the IRGA and back in a loop, with the exhaust from the IRGA being subsampled by the CH_4 LGR analyser. In turn the exhaust from the CH_4 analyser was subsampled by the N_2O analyser. Arrows denote the direction of flow.

Appendix C

NEE fluxes were adjusted, after Heinemeyer *et al.* (2013), according to the light response curve of NEE and the attenuation of light by the chamber.

The light attenuation by the Skybeam chamber demonstrated by the results of linear regression of internal and external PAR

Internal PAR= 0.60 * External PAR +0.04 R^2= 0.85, p< 0.0001

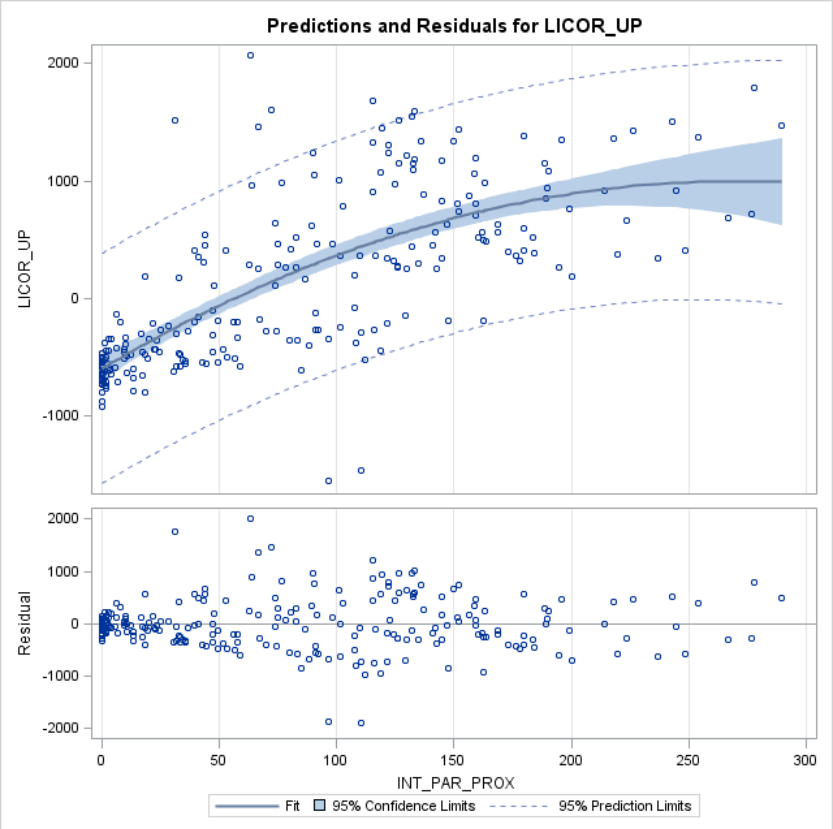

Light response curve:

NEE= 11.8 * Solar radiation – 0.02 * solar radiation^2 R^2= 0.54, p< 0.0001

The light attenuation by the SkyLine chamber demonstrated by the results of linear regression of internal and external PAR:

Internal PAR= 0.71 * External PAR -0.02 R^2= 0.88, p< 0.0001

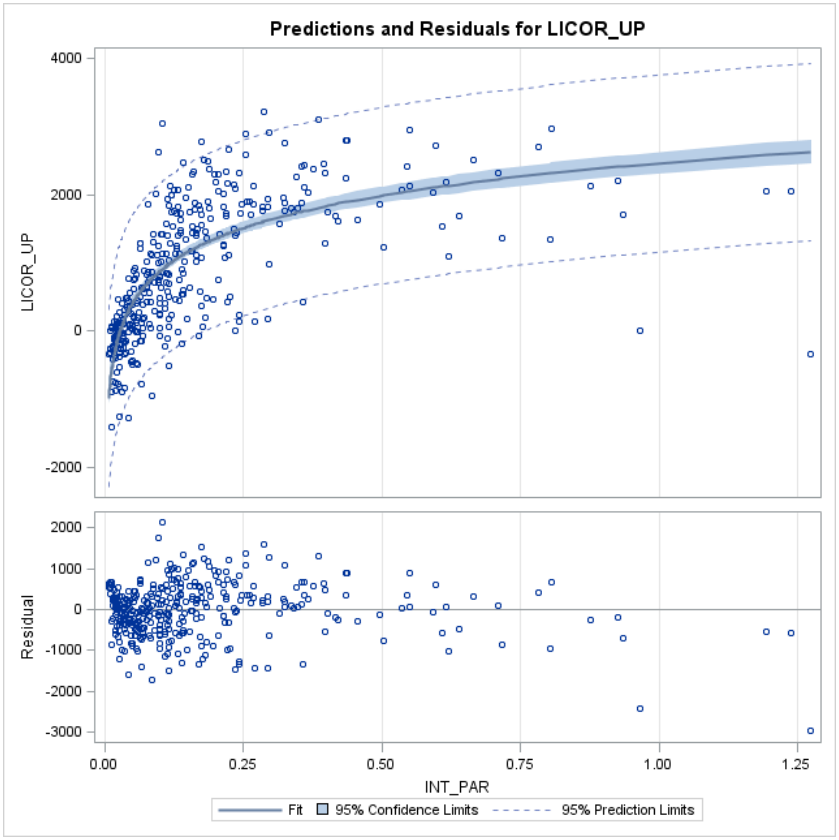

Light response curve of NEE inside the SkyLine chamber

NEE= 685 * Log_{10} (Internal PAR) + 2460 R^2= 0.55, p< 0.0001

List of references

Abdalla M, Jones M, Ambus P, Williams M (2010) Emissions of nitrous oxide from Irish arable soils: effects of tillage and reduced N input. Nutrient Cycling in Agroecosystems*,* **86**, 53-65.

Adler PR, Del Grosso SJ, Parton WJ (2007) Life-cycle assessment of net greenhouse-gas flux for bioenergy cropping systems. Ecological Applications*,* **17**, 675-691.

Agency E (2015) The nitrate pollution prevention regulations 2015. pp Page, Controller of Her Majesty's Stationery Office.

Albanito F, Saunders M, Jones MB (2009) Automated diffusion chambers to monitor diurnal and seasonal dynamics of the soil CO_2 concentration profile. European Journal of Soil Science*,* **60**, 507-514.

Albertsson AC, Andersson SO, Karlsson S (1987) The mechanism of biodegradation of polyethylene. Polymer Degradation and Stability*,* **18**, 73-87.

Alvaro-Fuentes J, Cantero-Martinez C, Lopez MV, Arrue JL (2007) Soil carbon dioxide fluxes following tillage in semiarid Mediterranean agroecosystems. Soil & Tillage Research*,* **96**, 331-341.

Alves BJR, Smith KA, Flores RA *et al.* (2012) Selection of the most suitable sampling time for static chambers for the estimation of daily mean N_2O flux from soils. Soil Biology & Biochemistry*,* **46**, 129-135.

Ambus P, Christensen S (1993) Denitrification variability and control in a riparian fen irrigated with agricultural drainage water. Soil Biology & Biochemistry*,* **25**, 915-923.

Ambus P, Christensen S (1994) Measurement of N_2O emission from a fertilsed grassland- an analysis of spatial variability. Journal of Geophysical Research-Atmospheres*,* **99**, 16549-16555.

Ambus P, Robertson GP (1998) Automated near-continuous measurement of carbon dioxide and nitrous oxide fluxes from soil. Soil Science Society of America Journal*,* **62**, 394-400.

Ambus P, Skiba U, Drewer J, Jones SK, Carter MS, Albert KR, Sutton MA (2010) Development of an accumulation-based system for cost-effective chamber measurements of inert trace gas fluxes. European Journal of Soil Science*,* **61**, 785-792.

Arif MAS, Houwen F, Verstraete W (1996) Agricultural factors affecting methane oxidation in arable soil. Biology and Fertility of Soils*,* **21**, 95-102.

Arundale RA, Dohleman FG, Heaton EA, McGrath JM, Voigt TB, Long SP (2014) Yields of *Miscanthus x giganteus* and *Panicum virgatum* decline with stand age in the Midwestern USA. Global Change Biology Bioenergy, **6**, 1-13.

Asgedom H, Tenuta M, Flaten DN, Gao XP, Kebreab E (2014) Nitrous oxide emissions from a clay soil receiving granular urea formulations and dairy manure. Agronomy Journal, **106**, 732-744.

Aubinet M (2008) Eddy covariance CO_2 flux measurements in nocturnal conditions: An analysis of the problem. Ecological Applications, **18**, 1368-1378.

Bahn M, Schmitt M, Siegwolf R, Richter A, Bruggemann N (2009) Does photosynthesis affect grassland soil-respired CO_2 and its carbon isotope composition on a diurnal timescale? New Phytologist, **182**, 451-460.

Baldocchi DD (2003) Assessing the eddy covariance technique for evaluating carbon dioxide exchange rates of ecosystems: past, present and future. Global Change Biology, **9**, 479-492.

Baldocchi DD, Wilson KB (2001) Modeling CO_2 and water vapour exchange of a temperate broadleaved forest across hourly to decadal time scales. Ecological Modelling, **142**, 155-184.

Barrena I, Menendez S, Dunabeitia M *et al.* (2013) Greenhouse gas fluxes (CO_2, N_2O and CH_4) from forest soils in the Basque Country: Comparison of different tree species and growth stages. Forest Ecology and Management, **310**, 600-611.

Barton L, Kiese R, Gatter D, Butterbach-Bahl K, Buck R, Hinz C, Murphy DV (2008) Nitrous oxide emissions from a cropped soil in a semi-arid climate. Global Change Biology, **14**, 177-192.

Barton L, Murphy DV, Kiese R, Butterbach-Bahl K (2010) Soil nitrous oxide and methane fluxes are low from a bioenergy crop (canola) grown in a semi-arid climate. Global Change Biology Bioenergy, **2**, 1-15.

Bateman EJ, Baggs EM (2005) Contributions of nitrification and denitrification to N_2O emissions from soils at different water-filled pore space. Biology and Fertility of Soils, **41**, 379-388.

Beare MH, Gregorich EG, St-Georges P (2009) Compaction effects on CO_2 and N_2O production during drying and rewetting of soil. Soil Biology & Biochemistry, **41**, 611-621.

Beaudette C, Bradley RL, Whalen JK, McVetty PBE, Vessey K, Smith DL (2010) Tree-based intercropping does not compromise canola (*Brassica napus* L.) seed oil yield and reduces soil nitrous oxide emissions. Agriculture Ecosystems & Environment, **139**, 33-39.

Beesley L (2014) Respiration (CO_2 flux) from urban and pen-urban soils amended with green waste compost. Geoderma, **223**, 68-72.

Behnke GD, David MB, Voigt TB (2012) Greenhouse Gas Emissions, Nitrate Leaching, and Biomass Yields from Production of *Miscanthus x giganteus* in Illinois, USA. Bioenergy Research, **5**, 801-813.

Bell MJ, Rees RM, Cloy JM, Topp CFE, Bagnall A, Chadwick DR (2015) Nitrous oxide emissions from cattle excreta applied to a Scottish grassland: Effects of soil and climatic conditions and a nitrification inhibitor. Science of the Total Environment, **508**, 343-353.

Bender M, Conrad R (1995) Effect of CH_4 concentrations and soil conditions on the induction of CH_4 oxidation activity. Soil Biology & Biochemistry, **27**, 1517-1527.

Bertholdsson NO, Brantestam AK (2009) A century of Nordic barley breeding-Effects on early vigour root and shoot growth, straw length, harvest index and grain weight. European Journal of Agronomy, **30**, 266-274.

Bhattacharyya P, Neogi S, Roy KS, Rao KS (2013) Gross primary production, ecosystem respiration and net ecosystem exchange in Asian rice paddy: an eddy covariance-based approach. Current Science, **104**, 67-75.

Biraud S, Ciais P, Ramonet M *et al.* (2002) Quantification of carbon dioxide, methane, nitrous oxide and chloroform emissions over Ireland from atmospheric observations at Mace Head. Tellus Series B-Chemical and Physical Meteorology, **54**, 41-60.

Blackmer AM, Robbins SG, Bremner JM (1982) Diurnal variability in rate of emission of nitrous oxide from soils. Soil Science Society of America Journal, **46**, 937-942.

Bond-Lamberty B, Wang CK, Gower ST (2004) A global relationship between the heterotrophic and autotrophic components of soil respiration? Global Change Biology, **10**, 1756-1766.

Boon A, Robinson JS, Chadwick DR, Cardenas LM (2014) Effect of cattle urine addition on the surface emissions and subsurface concentrations of greenhouse gases in a UK peat grassland. Agriculture Ecosystems & Environment, **186**, 23-32.

Boot-Handford ME, Abanades JC, Anthony EJ *et al.* (2014) Carbon capture and storage update. Energy & Environmental Science, **7**, 130-189.

Bouma TJ, Nielsen KL, Eissenstat DM, Lynch JP (1997) Estimating respiration of roots in soil: Interactions with soil CO_2, soil temperature and soil water content. Plant and Soil, **195**, 221-232.

Bradford MA, Ineson P, Wookey PA, Lappin-Scott HM (2001) Role of CH_4 oxidation, production and transport in forest soil CH_4 flux. Soil Biology & Biochemistry, **33**, 1625-1631.

Bradford MA, Strickland MS, DeVore JL, Maerz JC (2012) Root carbon flow from an invasive plant to belowground foodwebs. Plant and Soil, **359**, 233-244.

Breuer L, Papen H, Butterbach-Bahl K (2000) N_2O emission from tropical forest soils of Australia. Journal of Geophysical Research-Atmospheres, **105**, 26353-26367.

Brumme R, Beese F (1992) Effects of liming and nitrogen fertilisation on emissions of CO_2 and N_2O from a temperate forest. Journal of Geophysical Research-Atmospheres, **97**, 12851-12858.

Brumme R, Borken W, Finke S (1999) Hierarchical control on nitrous oxide emission in forest ecosystems. Global Biogeochemical Cycles, **13**, 1137-1148.

Brummell ME, Siciliano SD (2011) Measurement of carbon dioxide, methane, nitrous oxide and water potential in soil ecosystems. Methods in Enzymology, Vol 46: Research on Nitrification and Related Processes, Pt B, **496**, 115-137.

Buchmann N (2000) Biotic and abiotic factors controlling soil respiration rates in *Picea abies* stands. Soil Biology & Biochemistry, **32**, 1625-1635.

Burrows EH, Bubier JL, Mosedale A, Cobb GW, Crill PM (2005) Net ecosystem exchange of carbon dioxide in a temperate poor fen: a comparison of automated and manual chamber techniques. Biogeochemistry, **76**, 21-45.

Businger JA, Oncley SP (1990) Flux measurement with conditional sampling. Journal of Atmospheric and Oceanic Technology, **7**, 349-352.

Butterbach-Bahl K, Baggs EM, Dannenmann M, Kiese R, Zechmeister-Boltenstern S (2013) Nitrous oxide emissions from soils: how well do we understand the processes and their controls? Philosophical transactions of the Royal Society of London. Series B, Biological sciences, **368**, 20130122.

Butterbach-Bahl K, Kiese R, Liu CY (2011) Measurements of biosphere-atmosphere exchange of CH_4 in terrestrial ecosystems. In: *Methods in Enzymology: Methods in Methane Metabolism, Vol 495, Pt B.* (eds Rosenzweig AC, Ragsdale SW) pp Page. San Diego, Elsevier Academic Press Inc.

Butterbach-Bahl K, Papen H (2002) Four years continuous record of CH_4-exchange between the atmosphere and untreated and limed soil of a N-saturated spruce and beech forest ecosystem in Germany. Plant and Soil, **240**, 77-90.

ButterbachBahl K, Papen H, Rennenberg H (1997) Impact of gas transport through rice cultivars on methane emission from rice paddy fields. Plant Cell and Environment, **20**, 1175-1183.

Cadoux S, Ferchaud F, Demay C *et al.* (2014) Implications of productivity and nutrient requirements on greenhouse gas balance of annual and perennial bioenergy crops. Global Change Biology Bioenergy, **6**, 425-438.

Case SDC, McNamara NP, Reay DS, Whitaker J (2012) The effect of biochar addition on N_2O and CO_2 emissions from a sandy loam soil - The role of soil aeration. Soil Biology & Biochemistry, **51**, 125-134.

Case SDC, McNamara NP, Reay DS, Whitaker J (2014) Can biochar reduce soil greenhouse gas emissions from a *Miscanthus* bioenergy crop? Global Change Biology Bioenergy, **6**, 76-89.

Castaldi S (2000) Responses of nitrous oxide, dinitrogen and carbon dioxide production and oxygen consumption to temperature in forest and agricultural light-textured soils determined by model experiment. Biology and Fertility of Soils, **32**, 67-72.

Caughey SJ, Wyngaard JC, Kaimal JC (1979) Turbulence in the evloving stable boundary layer. Journal of the Atmospheric Sciences, **36**, 1041-1052.

Chadwick DR, Cardenas L, Misselbrook TH *et al.* (2014) Optimizing chamber methods for measuring nitrous oxide emissions from plot-based agricultural experiments. European Journal of Soil Science, **65**, 295-307.

Chadwick DR, Pain BF, Brookman SKE (2000) Nitrous oxide and methane emissions following application of animal manures to grassland. Journal of Environmental Quality, **29**, 277-287.

Chandra RP, Arantes V, Saddler J (2015) Steam pretreatment of agricultural residues facilitates hemicellulose recovery while enhancing enzyme accessibility to cellulose. Bioresource Technology, **185**, 302-307.

Chapuis-Lardy L, Wrage N, Metay A, Chotte J-L, Bernoux M (2007) Soils, a sink for N_2O? A review. Global Change Biology, **13**, 1-17.

Chatskikh D, Olesen JE (2007) Soil tillage enhanced CO_2 and N_2O emissions from loamy sand soil under spring barley. Soil & Tillage Research, **97**, 5-18.

Chatskikh D, Olesen JE, Hansen EM, Elsgaard L, Petersen BM (2008) Effects of reduced tillage on net greenhouse gas fluxes from loamy sand soil under winter crops in Denmark. Agriculture Ecosystems & Environment, **128**, 117-126.

Cherubini F, Bird ND, Cowie A, Jungmeier G, Schlamadinger B, Woess-Gallasch S (2009) Energy- and greenhouse gas-based LCA of biofuel and bioenergy systems: Key issues, ranges and recommendations. Resources Conservation and Recycling, **53**, 434-447.

Chien SH, Prochnow LI, Cantarella H (2009) Recent developments of fertiliser producction and use to improve nutrient efficiency amd minimise environmental impacts. In: *Advances in Agronomy, Vol 102.* (ed Sparks DL). San Diego, Elsevier Academic Press Inc.

Chirinda N, Olesen JE, Porter JR, Schjonning P (2010) Soil properties, crop production and greenhouse gas emissions from organic and inorganic fertilizer-based arable cropping systems. Agriculture Ecosystems & Environment, **139**, 584-594.

Christensen S (1983) Nitrous oxide emission from a soil under permanent grass-seasonal and diurnal fluctuationss as influenced by manuring and fertilisation. Soil Biology & Biochemistry, **15**, 531-536.

Christian DG, Riche AB, Yates NE (2008) Growth, yield and mineral content of *Miscanthus x giganteus* grown as a biofuel for 14 successive harvests. Industrial Crops and Products, **28**, 320-327.

Christiansen JR, Korhonen JFJ, Juszczak R, Giebels M, Pihlatie M (2011) Assessing the effects of chamber placement, manual sampling and headspace mixing on CH_4 fluxes in a laboratory experiment. Plant and Soil, **343**, 171-185.

Ciais P, C. Sabine, G. Bala, L. Bopp, V. Brovkin, J. Canadell, A. Chhabra, R. DeFries, J. Galloway, M. Heimann, C. Jones, C. Le Quéré, R.B. Myneni, S. Piao and P. Thornton, (2013) Carbon and Other Biogeochemical Cycles. In: Climate Change 2013: The Physical Science Basis. Contribution of Working Group I to the Fifth Assessment Report of the Intergovernmental Panel on Climate Change. Cambridge University Press, Cambridge, United Kingdom and New York, NY, USA.

Ciais P, Wattenbach M, Vuichard N *et al.* (2010) The European carbon balance. Part 2: croplands. Global Change Biology, **16**, 1409-1428.

Clapp LW, Semmens MJ, Novak PJ, Hozalski RM (2004) Model for *in situ* perchloroethene dechlorination via membrane-delivered hydrogen. Journal of Environmental Engineering-Asce, **130**, 1367-1381.

Clayton H, Arah JRM, Smith KA (1994) Measurement of nitrous oxide emissions from fertilised grassland using closed chambers. Journal of Geophysical Research-Atmospheres, **99**, 16599-16607.

Clifton-Brown JC, Breuer J, Jones MB (2007) Carbon mitigation by the energy crop, *Miscanthus*. Global Change Biology, **13**, 2296-2307.

Clifton-Brown JC, Stampfl PF, Jones MB (2004) *Miscanthus* biomass production for energy in Europe and its potential contribution to decreasing fossil fuel carbon emissions. Global Change Biology, **10**, 509-518.

Clough TJ, Jarvis SC, Dixon ER, Stevens RJ, Laughlin RJ, Hatch DJ (1999) Carbon induced subsoil denitrification of ^{15}N-labelled nitrate in 1 m deep soil columns. Soil Biology & Biochemistry, **31**, 31-41.

Conen F, Neftel A (2007) Do increasingly depleted delta N-15 values of atmospheric N_2O indicate a decline in soil N_2O reduction? Biogeochemistry, **82**, 321-326.

Conen F, Smith KA (1998) A re-examination of closed flux chamber methods for the measurement of trace gas emissions from soils to the atmosphere. European Journal of Soil Science, **49**, 701-707.

Conrad R (1996) Soil microorganisms as controllers of atmospheric trace gases (H_2, CO, CH_4, OCS, N_2O, and NO). Microbiological Reviews, **60**, 609-.

Conrad R (2009) The global methane cycle: recent advances in understanding the microbial processes involved. Environmental Microbiology Reports, **1**, 285-292.

Cosentino SL, Patane C, Sanzone E, Copani V, Foti S (2007) Effects of soil water content and nitrogen supply on the productivity of *Miscanthus x giganteus* in a Mediterranean environment. Industrial Crops and Products, **25**, 75-88.

Cowan NJ, Famulari D, Levy PE, Anderson M, Reay DS, Skiba UM (2014) Investigating uptake of N_2O in agricultural soils using a high-precision dynamic chamber method. Atmospheric Measurement Techniques, **7**, 4455-4462.

Crutzen PJ, Mosier AR, Smith KA, Winiwarter W (2008) N_2O release from agro-biofuel production negates global warming reduction by replacing fossil fuels. Atmospheric Chemistry and Physics, **8**, 389-395.

Danalatos NG, Archontoulis SV, Mitsios I (2007) Potential growth and biomass productivity of *Miscanthus x giganteus* as affected by plant density and N-fertilization in central Greece. Biomass & Bioenergy, **31**, 145-152.

Das BT, Hamonts K, Moltchanova E, Clough TJ, Condron LM, Wakelin SA, O'Callaghan M (2012) Influence of photosynthetically active radiation on diurnal N_2O emissions under ruminant urine patches. New Zealand Journal of Agricultural Research, **55**, 319-331.

Davidson EA, Galloway JN, Millar N, Leach AM (2014) N-related greenhouse gases in North America: innovations for a sustainable future. Current Opinion in Environmental Sustainability, **9-10**, 1-8.

Davidson EA, Keller M, Erickson HE, Verchot LV, Veldkamp E (2000) Testing a conceptual model of soil emissions of nitrous and nitric oxides. Bioscience, **50**, 667-680.

Davidson EA, Matson PA, Vitousek PM, Riley R, Dunkin K, Garciamendez G, Maass JM (1993) Processes regulating soil emissions of NO and N_2O in a seasonally dry tropical forest. Ecology, **74**, 130-139.

Davidson EA, Savage K, Verchot LV, Navarro R (2002) Minimizing artifacts and biases in chamber-based measurements of soil respiration. Agricultural and Forest Meteorology, **113**, 21-37.

Davis MP, David MB, Mitchell CA (2013) Nitrogen Mineralization in Soils Used for Biofuel Crops. Communications in Soil Science and Plant Analysis*,* **44**, 987-995.

Davis SC, Parton WJ, Dohleman FG, Smith CM, Del Grosso S, Kent AD, DeLucia EH (2010) Comparative Biogeochemical Cycles of Bioenergy Crops Reveal Nitrogen-Fixation and Low Greenhouse Gas Emissions in a *Miscanthus x giganteus* Agro-Ecosystem. Ecosystems*,* **13**, 144-156.

De Klein C, Novoa RS, Ogle S *et al.* (2006) N_2O emissions from managed soils, and CO_2 emissions from lime and urea application. IPCC Guidelines for National Greenhouse Gas Inventories, Prepared by the National Greenhouse Gas Inventories Programme*,* **4**.

De Klein C, Harvey M (2012) Nitrous Oxide Chamber Methodology Guidelines.

de Vries SC, van de Ven GWJ, van Ittersum MK (2014) First or second generation biofuel crops in Brandenburg, Germany? A model-based comparison of their production-ecological sustainability. European Journal of Agronomy*,* **52**, 166-179.

DECC (2011) UK Renewable Energy Roadmap. Department of Energy & Climate Change 3 Whitehall Place London SW1A 2AW.

DECC (2015) Annual statement of emissions for 2013. Controller of Her Majesty's Stationery Office.

DEFRA (2014a) Agricultural emissions reporting.

DEFRA (2014b) Farming statistics, final crop areas, yields, livestock populations and agricultural workforce at June 2014. pp Page, Office for National Statistics.

Denmead OT (1995) Novel meteorological methods for measuring trace gas fluxes. Philosophical Transactions of the Royal Society of London Series a-Mathematical Physical and Engineering Sciences*,* **351**, 383-396.

Denmead OT (2008) Approaches to measuring fluxes of methane and nitrous oxide between landscapes and the atmosphere. Plant and Soil*,* **309**, 5-24.

Denmead OT, Harper LA, Freney JR, Griffith DWT, Leuning R, Sharpe RR (1998) A mass balance method for non-intrusive measurements of surface-air trace gas exchange. Atmospheric Environment*,* **32**, 3679-3688.

Desjardins RL, Brach EJ, Alvo P, Schuepp PH (1982) Aircraft monitoring of surface carbon dioxide exchange. Science*,* **216**, 733-735.

Ding WX, Cai ZC, Tsuruta H (2005) Plant species effects on methane emissions from freshwater marshes. Atmospheric Environment*,* **39**, 3199-3207.

Dinsmore KJ, Skiba UM, Billett MF, Rees RM (2009) Effect of water table on greenhouse gas emissions from peatland mesocosms. Plant and Soil, **318**, 229-242.

Dobbie KE, McTaggart IP, Smith KA (1999) Nitrous oxide emissions from intensive agricultural systems: Variations between crops and seasons, key driving variables, and mean emission factors. Journal of Geophysical Research-Atmospheres, **104**, 26891-26899.

Dobbie KE, Smith KA (2003a) Impact of different forms of N fertiliser on N_2O emissions from intensive grassland. Nutrient Cycling in Agroecosystems, **67**, 37-46.

Dobbie KE, Smith KA (2003b) Nitrous oxide emission factors for agricultural soils in Great Britain: the impact of soil water-filled pore space and other controlling variables. Global Change Biology, **9**, 204-218.

Don A, Osborne B, Hastings A *et al.* (2012) Land-use change to bioenergy production in Europe: implications for the greenhouse gas balance and soil carbon. Global Change Biology Bioenergy, **4**, 372-391.

Dowdell RJ, Smith KA, Crees R, Restall SWF (1972) Field studies of ethylene in the soil atmosphere: equipment and preliminary results. Soil Biology and Biochemistry, **4**, 325-331.

Drewer J, Finch JW, Lloyd CR, Baggs EM, Skiba U (2012) How do soil emissions of N_2O, CH_4 and CO_2 from perennial bioenergy crops differ from arable annual crops? Global Change Biology Bioenergy, **4**, 408-419.

Dunfield P, Knowles R (1995) Kinetics of methane oxidation by nitrate, nitrite and ammonium in a humisol. Applied and Environmental Microbiology, **61**, 3129-3135.

Dupin HJ, McCarty PL (1999) Mesoscale and microscale observations of biological growth in a silicon pore imaging element. Environmental Science & Technology, **33**, 1230-1236.

Duyzer JH, Verhagen HLM, Weststrate JH, Bosveld FC (1992) Measurement of the dry deposition flux of NH_3 on to coniferous forest. Environmental Pollution, **75**, 3-13.

Eckardt FE (1968) Techniques de mesure de la photosynthèse sur le terrain basées sur l'emploi d'enceintées climatisées. In: *Fonctionnement des écosystèmes terrestres au niveau de la production primaire.* (ed Eckardt FE). Vaillant-Carmanne, S.A. (Belgium), UNESCO.

Ekblad A, Hogberg P (2001) Natural abundance of C-13 in CO_2 respired from forest soils reveals speed of link between tree photosynthesis and root respiration. Oecologia, **127**, 305-308.

Elsgaard L, Gorres CM, Hoffmann CC, Blicher-Mathiesen G, Schelde K, Petersen SO (2012) Net ecosystem exchange of CO_2 and carbon balance for eight temperate

organic soils under agricultural management. Agriculture Ecosystems & Environment, **162**, 52-67.

Ercoli L, Mariotti M, Masoni A, Bonari E (1999) Effect of irrigation and nitrogen fertilisation on biomass yield and efficiency of energy use in crop production of *Miscanthus*. Field Crops Research, **63**, 3-11.

Fang C, Moncrieff JB (1998) Simple and fast technique to measure CO_2 profiles in soil. Soil Biology & Biochemistry, **30**, 2107-2112.

Farquharson R, Baldock J (2008) Concepts in modelling N_2O emissions from land use. Plant and Soil, **309**, 147-167.

Fest BJ, Livesley SJ, Drosler M, van Gorsel E, Arndt SK (2009) Soil-atmosphere greenhouse gas exchange in a cool, temperate *Eucalyptus delegatensis* forest in south-eastern Australia. Agricultural and Forest Meteorology, **149**, 393-406.

Fiedler SR, Buczko U, Jurasinski G, Glatzel S (2015) Soil respiration after tillage under different fertiliser treatments - implications for modelling and balancing. Soil & Tillage Research, **150**, 30-42.

Fierer N, Chadwick OA, Trumbore SE (2005) Production of CO_2 in soil profiles of a California annual grassland. Ecosystems, **8**, 412-429.

Finocchiaro R, Tangen B, Gleason R (2014) Greenhouse gas fluxes of grazed and hayed wetland catchments in the US Prairie Pothole Ecoregion. Wetlands Ecology and Management, **22**, 305-324.

Firestone MK, Davidson EA (1989) Microbial basis of NO and N_2O production in soil. In: *Exchange of trace gases between terrestrial ecosystems and the atmosphere* (eds EO Andreae and DS Schimel) pp 7-21. John Wiley & Sons.

Fitter AH, Self GK, Brown TK, Bogie DS, Graves JD, Benham D, Ineson P (1999) Root production and turnover in an upland grassland subjected to artificial soil warming respond to radiation flux and nutrients, not temperature. Oecologia, **120**, 575-581.

Flechard CR, Neftel A, Jocher M, Ammann C, Fuhrer J (2005) Bi-directional soil/atmosphere N_2O exchange over two mown grassland systems with contrasting management practices. Global Change Biology, **11**, 2114-2127.

Flessa H, Wild U, Klemisch M, Pfadenhauer J (1998) Nitrous oxide and methane fluxes from organic soils under agriculture. European Journal of Soil Science, **49**, 327-335.

Forster P, Ramaswamy V, Artaxo P *et al.* (2007) Changes in atmospheric constituents and in radiative forcing. Chapter 2. In: *Climate Change 2007. The Physical Science Basis*.

Fowler D, Hargreaves KJ, Macdonald JA, Gardiner B (1995) Methane and CO_2 exchange over peatland and the effects of afforestation. Forestry, **68**, 327-334.

Frankenberg C, Meirink JF, van Weele M, Platt U, Wagner T (2005) Assessing methane emissions from global space-borne observations. Science, **308**, 1010-1014.

Fraser WT, Blei E, Fry SC, Newman MF, Reay DS, Smith KA, McLeod AR (2015) Emission of methane, carbon monoxide, carbon dioxide and short-chain hydrocarbons from vegetation foliage under ultraviolet irradiation. Plant Cell and Environment, **38**, 980-989.

Gauci V, Gowing DJG, Hornibrook ERC, Davis JM, Dise NB (2010) Woody stem methane emission in mature wetland alder trees. Atmospheric Environment, **44**, 2157-2160.

Gauder M, Butterbach-Bahl K, Graeff-Honninger S, Claupein W, Wiegel R (2012) Soil-derived trace gas fluxes from different energy crops - results from a field experiment in Southwest Germany. Global Change Biology Bioenergy, **4**, 289-301.

Godfray HCJ, Beddington JR, Crute IR *et al.* (2010) Food Security: The Challenge of Feeding 9 Billion People. Science, **327**, 812-818.

Goodroad LL, Keeney DR (1985) Site of nitrous oxide production in field soils. Biology and Fertility of Soils, **1**, 3-7.

Gopalakrishnan G, Negri MC, Snyder SW (2011) A Novel Framework to Classify Marginal Land for Sustainable Biomass Feedstock Production. Journal of Environmental Quality, **40**, 1593-1600.

Grabmer W, Graus M, Lindinger C, Wisthaler A, Rappengluck B, Steinbrecher R, Hansel A (2004) Disjunct eddy covariance measurements of monoterpene fluxes from a Norway spruce forest using PTR-MS. International Journal of Mass Spectrometry, **239**, 111-115.

Grace J, Lloyd J, McIntyre J *et al.* (1995) Fluxes of carbon dioxide and water vapour over an undisturbed tropical forest in south west Amazonia. Global Change Biology, **1**, 1-12.

Grace P, Van Der Weerden TJ, Kelly K, Rees RM, Skiba UM (2012) Automated greenhouse gas measurements in the field. In: *Nitrous oxide chamber methodology guidelines.* (eds De Klein CAM, Harvey MJ) pp Page. Wellington, New Zealand, Ministry for Primary Industries.

Gregorich EG, Rochette P, VandenBygaart AJ, Angers DA (2005) Greenhouse gas contributions of agricultural soils and potential mitigation practices in Eastern Canada. Soil & Tillage Research, **83**, 53-72.

Gregory PJ, Atwell BJ (1991) The fate of carbon in pulse-labelled crops of barley and wheat. Plant and Soil, **136**, 205-213.

Grondahl L, Friborg T, Christensen TR *et al.* (2008) Spatial and inter-annual variability of trace gas fluxes in a heterogeneous high-arctic landscape. Advances in Ecological Research, Vol 40, **40**, 473-498.

Grundmann GL, Lensi R, Chalamet A (1993) Delayed NH_3 and N_2O uptake by maize leaves. New Phytologist, **124**, 259-263.

Guckland A, Corre MD, Flessa H (2010) Variability of soil N cycling and N_2O emission in a mixed deciduous forest with different abundance of beech. Plant and Soil, **336**, 25-38.

Haines SA, Gehl RJ, Havlin JL, Ranney TG (2015) Nitrogen and Phosphorus Fertilizer Effects on Establishment of Giant *Miscanthus*. Bioenergy Research, **8**, 17-27.

Han G-x, Zhou G-s, Xu Z-z (2008) Temporal variation of soil respiration and its affecting factors in a maize field during maize growth season. Shengtaixue Zazhi, **27**, 1698-1705.

Hargreaves KJ, Skiba U, Fowler D, Arah J, Wienhold FG, Klemedtsson L, Galle B (1994) Measurement of nitrous oxide emission from fertilised grassland using micrometeorological techniques. Journal of Geophysical Research-Atmospheres, **99**, 16569-16574.

Harris Z, Spake R, Taylor G (2015) Land use change to bioenergy: A meta-analysis of soil carbon and GHG emissions. Biomass and Bioenergy *in press.*

Harrison J, Matson P (2003) Patterns and controls of nitrous oxide emissions from waters draining a subtropical agricultural valley. Global Biogeochemical Cycles, **17**, 13.

Hatch D, Trindade H, Cardenas L, Carneiro J, Hawkins J, Scholefield D, Chadwick D (2005) Laboratory study of the effects of two nitrification inhibitors on greenhouse gas emissions from a slurry-treated arable soil: impact of diurnal temperature cycle. Biology and Fertility of Soils, **41**, 225-232.

Healy RW, Striegl RG, Russell TF, Hutchinson GL, Livingston GP (1996) Numerical evaluation of static-chamber measurements of soil-atmosphere gas exchange: Identification of physical processes. Soil Science Society of America Journal, **60**, 740-747.

Heath J, Ayres E, Possell M *et al.* (2005) Rising atmospheric CO_2 reduces sequestration of root-derived soil carbon. Science, **309**, 1711-1713.

Heinemeyer A, Di Bene C, Lloyd AR *et al.* (2011) Soil respiration: implications of the plant-soil continuum and respiration chamber collar-insertion depth on measurement and modelling of soil CO_2 efflux rates in three ecosystems. European Journal of Soil Science*,* **62**, 82-94.

Heinemeyer A, Gornall J, Baxter R, Huntley B, Ineson P (2013) Evaluating the carbon balance estimate from an automated ground-level flux chamber system in artificial grass mesocosms. Ecology and Evolution*,* **3**, 4998-5010.

Heinemeyer A, McNamara NP (2011) Comparing the closed static versus the closed dynamic chamber flux methodology: Implications for soil respiration studies. Plant and Soil*,* **346**, 145-151.

Hellebrand HJ, Kern J, Scholz V (2003) Long-term studies on greenhouse gas fluxes during cultivation of energy crops on sandy soils. Atmospheric Environment*,* **37**, 1635-1644.

Hodgson EM, Fahmi R, Yates N *et al.* (2010) *Miscanthus* as a feedstock for fast-pyrolysis: Does agronomic treatment affect quality? Bioresource Technology*,* **101**, 6185-6191.

Hogberg P, Nordgren A, Agren GI (2002) Carbon allocation between tree root growth and root respiration in boreal pine forest. Oecologia*,* **132**, 579-581.

Hogberg P, Nordgren A, Buchmann N *et al.* (2001) Large-scale forest girdling shows that current photosynthesis drives soil respiration. Nature*,* **411**, 789-792.

Hong E, Kim D, Kim J *et al.* (2015) Optimization of alkaline pretreatment on corn stover for enhanced production of 1.3-propanediol and 2,3-butanediol by *Klebsiella pneumoniae* AJ4. Biomass & Bioenergy*,* **77**, 177-185.

Hortnagl L, Wohlfahrt G (2014) Methane and nitrous oxide exchange over a managed hay meadow. Biogeosciences*,* **11**, 7219-7236.

Hu Z-h, Zhou Y-p, Cut H-l, Chen S-t, Xiao Q-T, Liu Y (2013) Effects of Diurnal Warming on Soil N_2O Emission in Soybean Field. Huanjing Kexue*,* **34**, 2961-2967.

Hutsch BW (2001) Methane oxidation in non-flooded soils as affected by crop production - invited paper. European Journal of Agronomy*,* **14**, 237-260.

Ineson P, Cotrufo MF, Bol R, Harkness DD, Blum H (1996) Quantification of soil carbon inputs under elevated CO_2:C-3 plants in a C-4 soil. Plant and Soil*,* **187**, 345-350.

IPCC (2011) Summary for policy makers. In: *IPCC Special Report on Renewable Energy Sources and Climate Change Mitigation.* (eds O. Edenhofer RPM, Y. Sokona, K. Seyboth, P. Matschoss, S. Kadner, T., Zwickel PE, G. Hansen, S. Schlömer, C.

von Stechow) pp Page. Cambridge, United Kingdom and New York, NY, USA., Cambridge University Press.

IPCC (2014) Climate Change 2014: Synthesis Report. Contribution of Working Groups I, II and III to the Fifth Assessment Report of the Intergovernmental Panel on Climate Change [Core Writing Team, R.K. Pachauri and L.A. Meyer (eds.)]. IPCC, Geneva, Switzerland.

Jacobs A, Rauber R, Ludwig B (2009) Impact of reduced tillage on carbon and nitrogen storage of two Haplic Luvisols after 40 years. Soil & Tillage Research, **102**, 158-164.

Jahangir MMR, Khalil MI, Johnston P *et al.* (2012) Denitrification potential in subsoils: A mechanism to reduce nitrate leaching to groundwater. Agriculture Ecosystems & Environment, **147**, 13-23.

Jeuffroy MH, Baranger E, Carrouee B *et al.* (2013) Nitrous oxide emissions from crop rotations including wheat, oilseed rape and dry peas. Biogeosciences, **10**, 1787-1797.

Jiang JY, Hu ZH, Sun WJ, Huang Y (2010) Nitrous oxide emissions from Chinese cropland fertilized with a range of slow-release nitrogen compounds. Agriculture Ecosystems & Environment, **135**, 216-225.

Johnson JMF, Archer D, Barbour N (2010) Greenhouse Gas Emission from Contrasting Management Scenarios in the Northern Corn Belt. Soil Science Society of America Journal, **74**, 396-406.

Jones DL, Hodge A (1999) Biodegradation kinetics and sorption reactions of three differently charged amino acids in soil and their effects on plant organic nitrogen availability. Soil Biology & Biochemistry, **31**, 1331-1342.

Jones SK, Rees RM, Skiba UM, Ball BC (2007) Influence of organic and mineral N fertiliser on N_2O fluxes from a temperate grassland. Agriculture Ecosystems & Environment, **121**, 74-83.

Jorgensen CJ, Struwe S, Elberling B (2012) Temporal trends in N_2O flux dynamics in a Danish wetland - effects of plant-mediated gas transport of N_2O and O_2 following changes in water level and soil mineral-N availability. Global Change Biology, **18**, 210-222.

Jørgensen SV, Cherubini F, Michelsen O (2014) Biogenic CO_2 fluxes, changes in surface albedo and biodiversity impacts from establishment of a *Miscanthus* plantation. Journal of Environmental Management, **146**, 346-354.

Jørgensen RN, Jørgensen BJ, Nielsen NE, Maag M, Lind AM (1997) N_2O emission from energy crop fields of *Miscanthus* "Giganteus" and winter rye. Atmospheric Environment, **31**, 2899-2904.

Juszczak R, Augustin J (2013) Exchange of the Greenhouse Gases Methane and Nitrous Oxide Between the Atmosphere and a Temperate Peatland in Central Europe. Wetlands, **33**, 895-907.

Kaiser EA, Eiland F, Germon JC *et al.* (1996) What predicts nitrous oxide emissions and denitrification N-loss from European soils? Zeitschrift Fur Pflanzenernahrung Und Bodenkunde, **159**, 541-547.

Kaiser EA, Kohrs K, Kucke M, Schnug E, Heinemeyer O, Munch JC (1998) Nitrous oxide release from arable soil: Importance of N-fertilization, crops and temporal variation. Soil Biology & Biochemistry, **30**, 1553-1563.

Kaiser EA, Ruser R (2000) Nitrous oxide emissions from arable soils in Germany - An evaluation of six long-term field experiments. Journal of Plant Nutrition and Soil Science, **163**, 249-259.

Kaltschmitt M, Reinhardt GA, Stelzer T (1997) Life cycle analysis of biofuels under different environmental aspects. Biomass & Bioenergy, **12**, 121-134.

Kammann C, Grunhage L, Jager HJ (2001a) A new sampling technique to monitor concentrations of CH_4, N_2O and CO_2 in air at well-defined depths in soils with varied water potential. European Journal of Soil Science, **52**, 297-303.

Kammann C, Grunhage L, Jager HJ, Wachinger G (2001b) Methane fluxes from differentially managed grassland study plots: the important role of CH_4 oxidation in grassland with a high potential for CH_4 production. Environmental Pollution, **115**, 261-273.

Kane ES, Pregitzer KS, Burton AJ (2003) Soil respiration along environmental gradients in Olympic National Park. Ecosystems, **6**, 326-335.

Karl T, Apel E, Hodzic A, Riemer DD, Blake DR, Wiedinmyer C (2009) Emissions of volatile organic compounds inferred from airborne flux measurements over a megacity. Atmospheric Chemistry and Physics, **9**, 271-285.

Kavdir Y, Hellebrand HJ, Kern J (2008) Seasonal variations of nitrous oxide emission in relation to nitrogen fertilization and energy crop types in sandy soil. Soil & Tillage Research, **98**, 175-186.

Keppler F, Hamilton JTG, Brass M, Rockmann T (2006) Methane emissions from terrestrial plants under aerobic conditions. Nature, **439**, 187-191.

Kessavalou A, Mosier AR, Doran JW, Drijber RA, Lyon DJ, Heinemeyer O (1998) Fluxes of carbon dioxide, nitrous oxide, and methane in grass sod and winter wheat-fallow tillage management. Journal of Environmental Quality, **27**, 1094-1104.

Keymer DP, Kent AD (2014) Contribution of nitrogen fixation to first year *Miscanthus x giganteus*. Global Change Biology Bioenergy, **6**, 577-586.

Kim DG, Mishurov M, Kiely G (2010) Effect of increased N use and dry periods on N_2O emission from a fertilized grassland. Nutrient Cycling in Agroecosystems, **88**, 397-410.

King JC, Lachlan-Cope TA, Ladkin RS, Weiss A (2008) Airborne measurements in the stable boundary layer over the Larsen Ice Shelf, Antarctica. Boundary-Layer Meteorology, **127**, 413-428.

Kludze HK, Delaune RD, Patrick WH (1993) Aerenchyma formation and methane and oxygen exchange in rice. Soil Science Society of America Journal, **57**, 386-391.

Knittel K, Boetius A (2009) Anaerobic Oxidation of Methane: Progress with an Unknown Process. In: *Annual Review of Microbiology.* pp Page. Palo Alto, Annual Reviews.

Knowles R (1982) Denitrification. Microbiological Reviews, **46**, 43-70.

Koga N, Tsuruta H, Sawamoto T, Nishimura S, Yagi K (2004) N_2O emission and CH_4 uptake in arable fields managed under conventional and reduced tillage cropping systems in northern Japan. Global Biogeochemical Cycles, **18**, 11.

Kozlova EA, Manning AC, Kisilyakhov Y, Seifert T, Heimann M (2008) Seasonal, synoptic, and diurnal-scale variability of biogeochemical trace gases and O_2 from a 300-m tall tower in central Siberia. Global Biogeochemical Cycles, **22**.

Kroeze C, Seitzinger SP (1998) Nitrogen inputs to rivers, estuaries and continental shelves and related nitrous oxide emissions in 1990 and 2050: a global model. Nutrient Cycling in Agroecosystems, **52**, 195-212.

Kutsch WL, Kappen L (1997) Aspects of carbon and nitrogen cycling in soils of the Bornhoved lake district .2. Modelling the influence of temperature increase on soil respiration and organic carbon content in arable soils under different managements. Biogeochemistry, **39**, 207-224.

Kuzyakov Y (2006) Sources of CO_2 efflux from soil and review of partitioning methods. Soil Biology & Biochemistry, **38**, 425-448.

Kuzyakov Y, Cheng W (2001) Photosynthesis controls of rhizosphere respiration and organic matter decomposition. Soil Biology & Biochemistry, **33**, 1915-1925.

Kuzyakov Y, Gavrichkova O (2010) REVIEW: Time lag between photosynthesis and carbon dioxide efflux from soil: a review of mechanisms and controls. Global Change Biology, **16**, 3386-3406.

Laine A, Sottocornola M, Kiely G, Byrne KA, Wilson D, Tuittila E-S (2006) Estimating net ecosystem exchange in a patterned ecosystem: Example from blanket bog. Agricultural and Forest Meteorology, **138**, 231-243.

Larsen SU, Jorgensen U, Kjeldsen JB, Laerke PE (2014) Long-Term *Miscanthus* Yields Influenced by Location, Genotype, Row Distance, Fertilization and Harvest Season. Bioenergy Research*,* **7**, 620-635.

Laughlin RJ, Stevens RJ (2003) Changes in composition of nitrogen-15-labeled gases during storage in septum-capped vials. Soil Science Society of America Journal*,* **67**, 540-543.

Laville P, Henault C, Renault P *et al.* (1997) Field comparison of nitrous oxide emission measurements using micrometeorological and chamber methods. Agronomie*,* **17**, 375-388.

Laville P, Jambert C, Cellier P, Delmas R (1999) Nitrous oxide fluxes from a fertilised maize crop using micrometeorological and chamber methods. Agricultural and Forest Meteorology*,* **96**, 19-38.

Le Mer J, Roger P (2001) Production, oxidation, emission and consumption of methane by soils: A review. European Journal of Soil Biology*,* **37**, 25-50.

Leegood RC (2008) Roles of the bundle sheath cells in leaves of C_3 plants. Journal of Experimental Botany*,* **59**, 1663-1673.

Lemke RL, Izaurralde RC, Nyborg M (1998) Seasonal distribution of nitrous oxide emissions from soils in the Parkland region. Soil Science Society of America Journal*,* **62**, 1320-1326.

Leuning R, Moncrieff J (1990) Eddy covariance CO_2 flux measurements using open-path and closed-path CO_2 analysers- corrections for aanalysing water vapour sensitivity and damping of fluctuations in air sampling tubes. Boundary-Layer Meteorology*,* **53**, 63-76.

Lewandowski I, Clifton-Brown JC, Scurlock JMO, Huisman W (2000) *Miscanthus*: European experience with a novel energy crop. Biomass & Bioenergy*,* **19**, 209-227.

Li CS, Frolking S, Butterbach-Bahl K (2005) Carbon sequestration in arable soils is likely to increase nitrous oxide emissions, offsetting reductions in climate radiative forcing. Climatic Change*,* **72**, 321-338.

Li Z, Kelliher FM (2005) Determining nitrous oxide emissions from subsurface measurements in grazed pasture: A field trial of alternative technology. Australian Journal of Soil Research*,* **43**, 677-687.

Lin X, Wang S, Ma X *et al.* (2009) Fluxes of CO_2, CH_4, and N_2O in an alpine meadow affected by yak excreta on the Qinghai-Tibetan plateau during summer grazing periods. Soil Biology & Biochemistry*,* **41**, 718-725.

Liu Q, Edwards NT, Post WM, Gu L, Ledford J, Lenhart S (2006) Temperature-independent diel variation in soil respiration observed from a temperate deciduous forest. Global Change Biology, **12**, 2136-2145.

Livesley SJ, Kiese R, Graham J, Weston CJ, Butterbach-Bahl K, Arndt SK (2008) Trace gas flux and the influence of short-term soil water and temperature dynamics in Australian sheep grazed pastures of differing productivity. Plant and Soil, **309**, 89-103.

Loescher HW, Law BE, Mahrt L, Hollinger DY, Campbell J, Wofsy SC (2006) Uncertainties in, and interpretation of, carbon flux estimates using the eddy covariance technique. Journal of Geophysical Research-Atmospheres, **111**, 19.

Lord RA (2015) Reed canarygrass (*Phalaris arundinacea*) outperforms *Miscanthus* or willow on marginal soils, brownfield and non-agricultural sites for local, sustainable energy crop production. Biomass & Bioenergy, **78**, 110-125.

Lotscher M, Gayler S (2005) Contribution of current photosynthates to root respiration of non-nodulated *Medicago sativa*: Effects of light and nitrogen supply. Plant Biology, **7**, 601-610.

Ma WK, Schautz A, Fishback L-AE, Bedard-Haughn A, Farrell RE, Siciliano SD (2007) Assessing the potential of ammonia oxidizing bacteria to produce nitrous oxide in soils of a high arctic lowland ecosystem on Devon Island, Canada. Soil Biology & Biochemistry, **39**, 2001-2013.

Mahrt L (2010) Computing turbulent fluxes near the surface: Needed improvements. Agricultural and Forest Meteorology, **150**, 501-509.

Makita N, Kosugi Y, Kamakura M (2014) Linkages between diurnal patterns of root respiration and leaf photosynthesis in *Quercus crispula* and *Fagus crenata* seedlings. Journal of Agricultural Meteorology, **70**, 151-162.

Maljanen M, Hytonen J, Martikainen PJ (2001) Fluxes of N_2O, CH_4 and CO_2 on afforested boreal agricultural soils. Plant and Soil, **231**, 113-121.

Matson PA, Harriss RC (2009) *Biogenic trace gases: measuring emissions from soil and water*, John Wiley & Sons.

Matsuura S, Mori A, Hojito M, Kanno T, Sasaki H (2011) Evaluation of a portable chamber system for soil CO_2 efflux measurement and the potential errors caused by internal compensation and water vapor dilution. Journal of Agricultural Meteorology, **67**, 127-137.

Maughan M, Bollero G, Lee DK *et al.* (2012) *Miscanthus x giganteus* productivity: the effects of management in different environments. Global Change Biology Bioenergy, **4**, 253-265.

Mays KL, Shepson PB, Stirm BH, Karion A, Sweeney C, Gurney KR (2009) Aircraft-Based Measurements of the Carbon Footprint of Indianapolis. Environmental Science & Technology, **43**, 7816-7823.

McMillen RT (1988) An eddy correlation technique with extended applicability to non-simple terrain. Boundary-Layer Meteorology, **43**, 231-245.

McNamara NP, Plant T, Oakley S, Ward S, Wood C, Ostle N (2008) Gully hotspot contribution to landscape methane (CH_4) and carbon dioxide (CO_2) fluxes in a northern peatland. Science of the Total Environment, **404**, 354-360.

Meijide A, Cardenas LM, Sanchez-Martin L, Vallejo A (2010) Carbon dioxide and methane fluxes from a barley field amended with organic fertilizers under Mediterranean climatic conditions. Plant and Soil, **328**, 353-367.

Merino P, Artetxe A, Castellon A, Menendez S, Aizpurua A, Estavillo JM (2012) Warming potential of N_2O emissions from rapeseed crop in Northern Spain. Soil & Tillage Research, **123**, 29-34.

Millar N, Robertson GP, Grace PR, Gehl RJ, Hoben JP (2010) Nitrogen fertilizer management for nitrous oxide (N_2O) mitigation in intensive corn (maize) production: an emissions reduction protocol for US Midwest agriculture. Mitigation and Adaptation Strategies for Global Change, **15**, 185-204.

Mills R, Glanville H, McGovern S, Emmett B, Jones DL (2011) Soil respiration across three contrasting ecosystem types: comparison of two portable IRGA systems. Journal of Plant Nutrition and Soil Science, **174**, 532-535.

Miranda AC, Miranda HS, Lloyd J *et al.* (1997) Fluxes of carbon, water and energy over Brazilian cerrado: An analysis using eddy covariance and stable isotopes. Plant Cell and Environment, **20**, 315-328.

Moore T, Roulet N, Knowles R (1990) Spatial and temporal variations of methane flux from subarctic northern boreal fens. Global Biogeochemical Cycles, **4**, 29-46.

Mordacq L, Ghashghaie J, Saugier B (1991) A simple field method for measuring gas exchange of small trees. Functional Ecology, **5**, 572-576.

Mori A, Hojito M, Kondo H, Matsunami H, Scholefield D (2005) Effects of plant species on CH_4 and N_2O fluxes from a volcanic grassland soil in Nasu, Japan. Soil Science and Plant Nutrition, **51**, 19-27.

Morris SG, Kimber SWL, Grace P, Van Zwieten L (2013) Improving the statistical preparation for measuring soil N_2O flux by closed chamber. Science of the Total Environment, **465**, 166-172.

Moseman-Valtierra S, Gonzalez R, Kroeger KD *et al.* (2011) Short-term nitrogen additions can shift a coastal wetland from a sink to a source of N_2O. Atmospheric Environment*,* **45**, 4390-4397.

Mummey DL, Smith JL, Bolton H (1997) Small-scale spatial and temporal variability of N_2O flux from a shrub-steppe ecosystem. Soil Biology & Biochemistry*,* **29**, 1699-1706.

Muylle H, Van Hulle S, De Vliegher A, Baert J, Van Bockstaele E, Roldan-Ruiz I (2015) Yield and energy balance of annual and perennial lignocellulosic crops for bio-refinery use: A 4-year field experiment in Belgium. European Journal of Agronomy*,* **63**, 62-70.

Myhre G, D. Shindell, F.-M. Bréon, W. Collins, J. Fuglestvedt, J. Huang, D. Koch, J.-F. Lamarque, D. Lee, B. Mendoza, T. Nakajima, A. Robock, G. Stephens, T. Takemura and H. Zhang (2013) Anthropogenic and Natural Radiative Forcing. In: Climate Change 2013: The Physical Science Basis. Contribution of Working Group I to the Fifth Assessment Report of the Intergovernmental Panel on Climate Change. Cambridge University Press, Cambridge, United Kingdom and New York, NY, USA.

Nastari P (2012) Sugar and ethanol production - where Brazil stands in 2020? International Sugar Journal*,* **114**, 74-78.

Nishimura S, Sudo S, Akiyama H, Yonemura S, Yagi K, Tsuruta H (2005) Development of a system for simultaneous and continuous measurement of carbon dioxide, methane and nitrous oxide fluxes from croplands based on the automated closed chamber method. Soil Science and Plant Nutrition*,* **51**, 557-564.

Norman JM, Kucharik CJ, Gower ST *et al.* (1997) A comparison of six methods for measuring soil-surface carbon dioxide fluxes. Journal of Geophysical Research-Atmospheres*,* **102**, 28771-28777.

OECD-FAO (2013) Agricultural outlook 2013-2022.

Oikawa PY, Grantz DA, Chatterjee A, Eberwein JE, Allsman LA, Jenerette GD (2014) Unifying soil respiration pulses, inhibition, and temperature hysteresis through dynamics of labile soil carbon and O_2. Journal of Geophysical Research-Biogeosciences*,* **119**, 521-536.

Oliver RJ, Finch JW, Taylor G (2009) Second generation bioenergy crops and climate change: a review of the effects of elevated atmospheric CO_2 and drought on water use and the implications for yield. Global Change Biology Bioenergy*,* **1**, 97-114.

Oncley SP, Delany AC, Horst TW, Tans PP (1993) Verification of flux measurement using relaxed eddy accumulation. Atmospheric Environment Part a-General Topics*,* **27**, 2417-2426.

Orchard VA, Cook FJ (1983) Relationship between soil respiratin and soil-moisture. Soil Biology & Biochemistry, **15**, 447-453.

Palmer MM, Forrester JA, Rothstein DE, Mladenoff DJ (2014) Conversion of open lands to short-rotation woody biomass crops: site variability affects nitrogen cycling and N_2O fluxes in the US Northern Lake States. Global Change Biology Bioenergy, **6**, 450-464.

Pape L, Ammann C, Nyfeler-Brunner A, Spirig C, Hens K, Meixner FX (2009) An automated dynamic chamber system for surface exchange measurement of non-reactive and reactive trace gases of grassland ecosystems. Biogeosciences, **6**, 405-429.

Park K-H, Wagner-Riddle C, Gordon RJ (2010) Comparing methane fluxes from stored liquid manure using micrometeorological mass balance and floating chamber methods. Agricultural and Forest Meteorology, **150**, 175-181.

Parton WJ, Mosier AR, Ojima DS, Valentine DW, Schimel DS, Weier K, Kulmala AE (1996) Generalized model for N-2 and N_2O production from nitrification and denitrification. Global Biogeochemical Cycles, **10**, 401-412.

Paustian K, Six J, Elliott ET, Hunt HW (2000) Management options for reducing CO_2 emissions from agricultural soils. Biogeochemistry, **48**, 147-163.

Perdomo C, Irisarri P, Ernst O (2009) Nitrous oxide emissions from an Uruguayan argiudoll under different tillage and rotation treatments. Nutrient Cycling in Agroecosystems, **84**, 119-128.

Perez-Piqueres A, Edel-Hermann W, Alabouvette C, Steinberg C (2006) Response of soil microbial communities to compost amendments. Soil Biology & Biochemistry, **38**, 460-470.

Petersen SO (1999) Nitrous oxide emissions from manure and inorganic fertilizers applied to spring barley. Journal of Environmental Quality, **28**, 1610-1618.

Petersen SO, Hoffmann CC, Schafer CM *et al.* (2012) Annual emissions of CH_4 and N_2O, and ecosystem respiration, from eight organic soils in Western Denmark managed by agriculture. Biogeosciences, **9**, 403-422.

Petersen SO, Schjonning P, Thomsen IK, Christensen BT (2008) Nitrous oxide evolution from structurally intact soil as influenced by tillage and soil water content. Soil Biology & Biochemistry, **40**, 967-977.

Pihlatie M, Ambus P, Rinne J, Pilegaard K, Vesala T (2005) Plant-mediated nitrous oxide emissions from beech (*Fagus sylvatica*) leaves. New Phytologist, **168**, 93-98.

Pitt J, LE Breton M, Allen G *et al.* (2015) The development and evaluation of airborne in situ N_2O and CH_4 sampling using a Quantum Cascade Laser Absorption Spectrometer (QCLAS). development, **8**, 8859-8902.

Poll C, Marhan S, Back F, Niklaus PA, Kandeler E (2013) Field-scale manipulation of soil temperature and precipitation change soil CO_2 flux in a temperate agricultural ecosystem. Agriculture Ecosystems & Environment, **165**, 88-97.

Pryor SC, Larsen SE, Sorensen LL, Barthelmie RJ (2008) Particle fluxes above forests: Observations, methodological considerations and method comparisons. Environmental Pollution, **152**, 667-678.

Pumpanen J, Kolari P, Ilvesniemi H *et al.* (2004) Comparison of different chamber techniques for measuring soil CO_2 efflux. Agricultural and Forest Meteorology, **123**, 159-176.

Qin X-Y, Xie Y-H, Chen X-S (2010) Comparative Study on the Aerenchyma of Four Dominant Wetland Plants in Dongting Lake. Wuhan Zhiwuxue Yanjiu, **28**, 400-405.

Rabot E, Cousin I, Henault C (2015) A modeling approach of the relationship between nitrous oxide fluxes from soils and the water-filled pore space. Biogeochemistry, **122**, 395-408.

Ragauskas AJ, Williams CK, Davison BH *et al.* (2006) The path forward for biofuels and biomaterials. Science, **311**, 484-489.

Raich JW, Schlesinger WH (1992) The global carbon dioxide flux in soil respiration and its relaitionship to vegetation and climate. Tellus Series B-Chemical and Physical Meteorology, **44**, 81-99.

Raich JW, Tufekcioglu A (2000) Vegetation and soil respiration: Correlations and controls. Biogeochemistry, **48**, 71-90.

Reay DS, Davidson EA, Smith KA, Smith P, Melillo JM, Dentener F, Crutzen PJ (2012) Global agriculture and nitrous oxide emissions. Nature Climate Change, **2**, 410-416.

Reay DS, Grace J (2007) Carbon Dioxide: Importance, Sources and Sinks. In: *Greenhouse Gas Sinks.* (eds Reay DS, Hewitt CN, Smith KA, Grace J), Cabi Publishing-C a B Int, Cabi Publishing, Wallingford 0X10 8DE, Oxon, UK.

Reay DS, Nedwell DB (2004) Methane oxidation in temperate soils: effects of inorganic N. Soil Biology & Biochemistry, **36**, 2059-2065.

Rees RM, Baddeley JA, Bhogal A *et al.* (2013) Nitrous oxide mitigation in UK agriculture. Soil Science and Plant Nutrition, **59**, 3-15.

Regina K, Pihlatie M, Esala M, Alakukku L (2007) Methane fluxes on boreal arable soils. Agriculture Ecosystems & Environment, **119**, 346-352.

Reichstein M, Tenhunen J, Roupsard O *et al.* (2003) Inverse modeling of seasonal drought effects on canopy CO_2/H_2O exchange in three Mediterranean ecosystems. Journal of Geophysical Research-Atmospheres, **108**.

Reicosky DC, Dugas WA, Torbert HA (1997) Tillage-induced soil carbon dioxide loss from different cropping systems. Soil & Tillage Research, **41**, 105-118.

Reiners WA (1968) Carbon dioxide evolution from floor of three Minnesota forests. Ecology, **49**, 471-&.

Roberts WP, Chan KY (1990) Tillage induced increases in carbon dioxide loss from the soil. Soil & Tillage Research, **17**, 143-151.

Rochette P (2011) Towards a standard non-steady-state chamber methodology for measuring soil N_2O emissions. Animal Feed Science and Technology, **166-67**, 141-146.

Rochette P, Angers DA, Chantigny MH, Bertrand N, Cote D (2004) Carbon dioxide and nitrous oxide emissions following fall and spring applications of pig slurry to an agricultural soil. Soil Science Society of America Journal, **68**, 1410-1420.

Rochette P, Eriksen-Hamel NS (2008) Chamber measurements of soil nitrous oxide flux: Are absolute values reliable? Soil Science Society of America Journal, **72**, 331-342.

Roobroeck D, Butterbach-Bahl K, Brueggemann N, Boeckx P (2010) Dinitrogen and nitrous oxide exchanges from an undrained monolith fen: short-term responses following nitrate addition. European Journal of Soil Science, **61**, 662-670.

Rowe MD, Fairall CW, Perlinger JA (2011) Chemical sensor resolution requirements for near-surface measurements of turbulent fluxes. Atmospheric Chemistry and Physics, **11**, 5263-5275.

Rowe RL, Street NR, Taylor G (2009) Identifying potential environmental impacts of large-scale deployment of dedicated bioenergy crops in the UK. Renewable & Sustainable Energy Reviews, **13**, 260-279.

Rowlings DW, Grace PR, Kiese R, Weier KL (2012) Environmental factors controlling temporal and spatial variability in the soil-atmosphere exchange of CO_2, CH_4 and N_2O from an Australian subtropical rainforest. Global Change Biology, **18**, 726-738.

Rusch H, Rennenberg H (1998) Black alder (*Alnus glutinosa* (L.) Gaertn.) trees mediate methane and nitrous oxide emission from the soil to the atmosphere. Plant and Soil, **201**, 1-7.

Ruser R, Flessa H, Russow R, Schmidt G, Buegger F, Munch JC (2006) Emission of N_2O, N-2 and CO_2 from soil fertilized with nitrate: Effect of compaction, soil moisture and rewetting. Soil Biology & Biochemistry, **38**, 263-274.

Ryden JC, Lund LJ, Focht DD (1978) Direct in-field measurement of nitrous oxide from soils. Soil Science Society of America Journal, **42**, 731-737.

Saarnio S, Silvola J (1999) Effects of increased CO_2 and N on CH_4 efflux from a boreal mire: a growth chamber experiment. Oecologia, **119**, 349-356.

Salome C, Nunan N, Pouteau V, Lerch TZ, Chenu C (2010) Carbon dynamics in topsoil and in subsoil may be controlled by different regulatory mechanisms. Global Change Biology, **16**, 416-426.

Sanz-Cobena A, Garcia-Marco S, Quemada M, Gabriel JL, Almendros P, Vallejo A (2014) Do cover crops enhance N_2O, CO_2 or CH_4 emissions from soil in Mediterranean arable systems? Science of the Total Environment, **466**, 164-174.

Savage K, Davidson EA, Tang J (2013) Diel patterns of autotrophic and heterotrophic respiration among phenological stages. Global Change Biology, **19**, 1151-1159.

Schmid HP (1994) Source areas for scalars and scalar fluxes. Boundary-Layer Meteorology, **67**, 293-318.

Schneider J, Kutzbach L, Schulz S, Wilmking M (2009) Overestimation of CO_2 respiration fluxes by the closed chamber method in low-turbulence nighttime conditions. Journal of Geophysical Research-Biogeosciences, **114**, 10.

Schonbach P, Wolf B, Dickhofer U *et al.* (2012) Grazing effects on the greenhouse gas balance of a temperate steppe ecosystem. Nutrient Cycling in Agroecosystems, **93**, 357-371.

Schutz H, Conrad R, Goodwin S, Seiler W (1988) Emission of hydrogen from deep and shallow fresh water environments. Biogeochemistry, **5**, 295-311.

Searchinger T, Heimlich R, Houghton RA *et al.* (2008) Use of US croplands for biofuels increases greenhouse gases through emissions from land-use change. Science, **319**, 1238-1240.

Shvaleva A, Silva FCE, Costa JM *et al.* (2014) Comparison of methane, nitrous oxide fluxes and CO_2 respiration rates from a Mediterranean cork oak ecosystem and improved pasture. Plant and Soil, **374**, 883-898.

Simek M, Brucek P, Hynst J (2010) Diurnal fluxes of CO_2 and N_2O from cattle-impacted soil and implications for emission estimates. Plant Soil and Environment, **56**, 451-457.

Singh BK, Bardgett RD, Smith P, Reay DS (2010) Microorganisms and climate change: terrestrial feedbacks and mitigation options. Nature Reviews Microbiology, **8**, 779-790.

Sitch S, Friedlingstein P, Gruber N *et al.* (2015) Recent trends and drivers of regional sources and sinks of carbon dioxide. Biogeosciences, **12**, 653-679.

Skiba U, Jones SK, Dragosits U *et al.* (2012) UK emissions of the greenhouse gas nitrous oxide. Philosophical Transactions of the Royal Society B-Biological Sciences, **367**, 1175-1185.

Skiba U, Smith KA (2000) The control of nitrous oxide emissions from agricultural and natural soils. Chemosphere - Global Change Science, **2**, 379-386.

Skiba UM, Sheppard LJ, MacDonald J, Fowler D (1998) Some key environmental variables controlling nitrous oxide emissions from agricultural and semi-natural soils in Scotland. Atmospheric Environment, **32**, 3311-3320.

Smith KA, Ball T, Conen F, Dobbie KE, Massheder J, Rey A (2003) Exchange of greenhouse gases between soil and atmosphere: interactions of soil physical factors and biological processes. European Journal of Soil Science, **54**, 779-791.

Smith KA, Clayton H, Arah JRM *et al.* (1994) Micrometeorological and chamber methods for measurement of nitrous oxide fluxes between soils and the atmosphere-overview and conclusions. Journal of Geophysical Research-Atmospheres, **99**, 16541-16548.

Smith KA, Dobbie KE, Thorman R, Watson CJ, Chadwick DR, Yamulki S, Ball BC (2012) The effect of N fertiliser forms on nitrous oxide emissions from UK arable land and grassland. Nutrient Cycling in Agroecosystems, **93**, 127-149.

Smith KA, McTaggart IP, Dobbie KE, Conen F (1998a) Emissions of N_2O from Scottish agricultural soils, as a function of fertilizer N. Nutrient Cycling in Agroecosystems, **52**, 123-130.

Smith KA, Thomson PE, Clayton H, McTaggart IP, Conen F (1998b) Effects of temperature, water content and nitrogen fertilisation on emissions of nitrous oxide by soils. Atmospheric Environment, **32**, 3301-3309.

Smith P, Bustamante M, Ahammad H *et al.* (2014) Agriculture, forestry and other land use (AFOLU). Climate change, 1-179.

Smith R, Slater FM (2010) The effects of organic and inorganic fertilizer applications to *Miscanthus x giganteus*, *Arundo donax* and *Phalaris arundinacea*, when grown as energy crops in Wales, UK. Global Change Biology Bioenergy, **2**, 169-179.

Soussana JF, Allard V, Pilegaard K *et al.* (2007) Full accounting of the greenhouse gas (CO_2, N_2O, CH_4) budget of nine European grassland sites. Agriculture Ecosystems & Environment, **121**, 121-134.

Sreenivasulu N, Schnurbusch T (2012) A genetic playground for enhancing grain number in cereals. Trends in Plant Science, **17**, 91-101.

St Clair S, Hillier J, Smith P (2008) Estimating the pre-harvest greenhouse gas costs of energy crop production. Biomass & Bioenergy, **32**, 442-452.

Stehfest E, Bouwman L (2006) N_2O and NO emission from agricultural fields and soils under natural vegetation: summarizing available measurement data and modeling of global annual emissions. Nutrient Cycling in Agroecosystems, **74**, 207-228.

Stewart KJ, Brummell ME, Farrell RE, Siciliano SD (2012) N_2O flux from plant-soil systems in polar deserts switch between sources and sinks under different light conditions. Soil Biology & Biochemistry, **48**, 69-77.

Stocker T, Qin D, Plattner G-K *et al.* (2014) *Climate change 2013: The physical science basis*, Cambridge University Press Cambridge, UK, and New York.

Strullu LSL, Cadoux S, Preudhomme M, Jeuffroy MH, Beaudoin N (2011) Biomass production and nitrogen accumulation and remobilisation by *Miscanthus x giganteus* as influenced by nitrogen stocks in belowground organs. Field Crops Research, **121**, 381-391.

Styles D, Gibbons J, Williams AP *et al.* (2015) Consequential life cycle assessment of biogas, biofuel and biomass energy options within an arable crop rotation. Global Change Biology Bioenergy, **7**, 1305-1320.

Sundqvist E, Crill P, Molder M, Vestin P, Lindroth A (2012) Atmospheric methane removal by boreal plants. Geophysical Research Letters, **39**, 6.

Teat AL, Neufeld HS, Gehl RJ, Gonzales E (2015) Growth and Yield of *Miscanthus x giganteus* Grown in Fertilized and Biochar-Amended Soils in the Western North Carolina Mountains. Castanea, **80**, 45-58.

Thauer RK (1998) Biochemistry of methanogenesis: a tribute to Marjory Stephenson. Microbiology-UK, **144**, 2377-2406.

Thies B, Bendix J (2011) Satellite based remote sensing of weather and climate: recent achievements and future perspectives. Meteorological Applications, **18**, 262-295.

Tjiputra JF, Olsen A, Bopp L *et al.* (2014) Long-term surface pCO_2 trends from observations and models. Tellus Series B-Chemical and Physical Meteorology, **66**, 24.

Toma Y, Fernandez FG, Sato S *et al.* (2011) Carbon budget and methane and nitrous oxide emissions over the growing season in a *Miscanthus sinensis* grassland in Tomakomai, Hokkaido, Japan. Global Change Biology Bioenergy*,* **3**, 116-134.

Turner DA, Chen D, Galbally IE *et al.* (2008) Spatial variability of nitrous oxide emissions from an Australian irrigated dairy pasture. Plant and Soil*,* **309**, 77-88.

Turner PA, Griffis TJ, Lee X, Baker JM, Venterea RT, Wood JD (2015) Indirect nitrous oxide emissions from streams within the US Corn Belt scale with stream order. Proceedings of the National Academy of Sciences.

Turnipseed AA, Pressley SN, Karl T *et al.* (2009) The use of disjunct eddy sampling methods for the determination of ecosystem level fluxes of trace gases. Atmospheric Chemistry and Physics*,* **9**, 981-994.

Twine TE, Kustas WP, Norman JM *et al.* (2000) Correcting eddy-covariance flux underestimates over a grassland. Agricultural and Forest Meteorology*,* **103**, 279-300.

Tyner WE (2012) Biofuels and agriculture: a past perspective and uncertain future. International Journal of Sustainable Development and World Ecology*,* **19**, 389-394.

Uchida Y, Clough TJ, Kelliher FM, Sherlock RR (2008) Effects of aggregate size, soil compaction, and bovine urine on N_2O emissions from a pasture soil. Soil Biology & Biochemistry*,* **40**, 924-931.

van der Weerden TJ, Clough TJ, Styles TM (2013) Using near-continuous measurements of N_2O emission from urine-affected soil to guide manual gas sampling regimes. New Zealand Journal of Agricultural Research*,* **56**, 60-76.

van der Weijde T, Kamei CLA, Torres AF, Vermerris W, Dolstra O, Visser RGF, Trindade LM (2013) The potential of C4 grasses for cellulosic biofuel production. Frontiers in Plant Science*,* **4**, 18.

Vaughan SM, Dalal RC, Harper SM, Menzies NW (2011) Effect of fresh green waste and green waste compost on mineral nitrogen, nitrous oxide and carbon dioxide from a Vertisol. Waste Management*,* **31**, 1720-1728.

Vellinga OS, Gioli B, Elbers JA, Holtslag AAM, Kabat P, Hutjes RWA (2010) Regional carbon dioxide and energy fluxes from airborne observations using flight-path segmentation based on landscape characteristics. Biogeosciences*,* **7**, 1307-1321.

Velthof GL, Jarvis SC, Stein A, Allen AG, Oenema O (1996) Spatial variability of nitrous oxide fluxes in mown and grazed grasslands on a poorly drained clay soil. Soil Biology & Biochemistry*,* **28**, 1215-1225.

Venterea RT, Spokas KA, Baker JM (2009) Accuracy and Precision Analysis of Chamber-Based Nitrous Oxide Gas Flux Estimates. Soil Science Society of America Journal*,* **73**, 1087-1093.

Vitousek PM, Aber JD, Howarth RW *et al.* (1997) Human alteration of the global nitrogen cycle: Sources and consequences. Ecological Applications, **7**, 737-750.

von Arnold K, Nilsson M, Hanell B, Weslien P, Klemedtsson L (2005) Fluxes of CO_2, CH_4 and N_2O from drained organic soils in deciduous forests. Soil Biology & Biochemistry, **37**, 1059-1071.

Wang K, Liu C, Zheng X *et al.* (2013) Comparison between eddy covariance and automatic chamber techniques for measuring net ecosystem exchange of carbon dioxide in cotton and wheat fields. Biogeosciences, **10**, 6865-6877.

Wang ZP, Han XG (2005) Diurnal variation in methane emissions in relation to plants and environmental variables in the Inner Mongolia marshes. Atmospheric Environment, **39**, 6295-6305.

Warneke S, Macdonald BCT, Macdonald LM, Sanderman J, Farrell M (2015) Abiotic dissolution and biological uptake of nitrous oxide in Mediterranean woodland and pasture soil. Soil Biology & Biochemistry, **82**, 62-64.

Wei D, Xu R, Tenzin T, Wang YS, Wang YH (2015) Considerable methane uptake by alpine grasslands despite the cold climate: *in situ* measurements on the central Tibetan Plateau, 2008-2013. Global Change Biology, **21**, 777-788.

Well R, Kurganova I, de Gerenyu VL, Flessa H (2006) Isotopomer signatures of soil-emitted N_2O under different moisture conditions - A microcosm study with arable loess soil. Soil Biology & Biochemistry, **38**, 2923-2933.

Wienhold FG, Frahm H, Harris GW (1994) Measurements of N_2O fluxes from fertilised grassland using a fast response analyser. Journal of Geophysical Research-Atmospheres, **99**, 16557-16567.

Williams DL, Ineson P, Coward PA (1999) Temporal variations in nitrous oxide fluxes from urine-affected grassland. Soil Biology & Biochemistry, **31**, 779-788.

Woli KP, David MB, Darmody RG, Mitchell CA, Smith CM (2010) Assessing the nitrous oxide mole fraction of soils from perennial biofuel and corn-soybean fields. Agriculture Ecosystems & Environment, **138**, 299-305.

Wrage N, Lauf J, del Prado A *et al.* (2004) Distinguishing sources of N_2O in European grasslands by stable isotope analysis. Rapid Communications in Mass Spectrometry, **18**, 1201-1207.

Wrage N, Velthof GL, van Beusichem ML, Oenema O (2001) Role of nitrifier denitrification in the production of nitrous oxide. Soil Biology & Biochemistry, **33**, 1723-1732.

Wu DM, Dong WX, Oenema O, Wang YY, Trebs I, Hu CS (2013) N_2O consumption by low-nitrogen soil and its regulation by water and oxygen. Soil Biology & Biochemistry*,* **60**, 165-172.

Xu LK, Furtaw MD, Madsen RA, Garcia RL, Anderson DJ, McDermitt DK (2006) On maintaining pressure equilibrium between a soil CO_2 flux chamber and the ambient air. Journal of Geophysical Research-Atmospheres*,* **111**.

Yan YP, Sha LQ, Cao M *et al.* (2008) Fluxes of CH_4 and N_2O from soil under a tropical seasonal rain forest in Xishuangbanna, Southwest China. Journal of Environmental Sciences-China*,* **20**, 207-215.

Yang M, Zhang J, Kuittinen S, Vepsalainen J, Soininen P, Keinanen M, Pappinen A (2015) Enhanced sugar production from pretreated barley straw by additive xylanase and surfactants in enzymatic hydrolysis for acetone-butanol-ethanol fermentation. Bioresource Technology*,* **189**, 131-137.

Yao ZS, Zheng XH, Xie BH *et al.* (2009a) Comparison of manual and automated chambers for field measurements of N_2O, CH_4, CO_2 fluxes from cultivated land. Atmospheric Environment*,* **43**, 1888-1896.

Yao ZS, Zheng XH, Xie BH *et al.* (2009b) Comparison of manual and automated chambers for field measurements of N_2O, CH_4, CO_2 fluxes from cultivated land. Atmospheric Environment*,* **43**, 1888-1896.

Yu L, Wang H, Wang G *et al.* (2013a) A comparison of methane emission measurements using eddy covariance and manual and automated chamber-based techniques in Tibetan Plateau alpine wetland. Environmental Pollution*,* **181**, 81-90.

Yu LF, Wang H, Wang GS *et al.* (2013b) A comparison of methane emission measurements using eddy covariance and manual and automated chamber-based techniques in Tibetan Plateau alpine wetland. Environmental Pollution*,* **181**, 81-90.

Zenone T, Chen JQ, Deal MW *et al.* (2011) CO_2 fluxes of transitional bioenergy crops: effect of land conversion during the first year of cultivation. Global Change Biology Bioenergy*,* **3**, 401-412.

Zhang W, Mo JM, Yu GR, Fang YT, Li DJ, Lu XK, Wang H (2008) Emissions of nitrous oxide from three tropical forests in Southern China in response to simulated nitrogen deposition. Plant and Soil*,* **306**, 221-236.

Zhang XB, Wu LH, Sun N, Ding XS, Li JW, Wang BR, Li DC (2014) Soil CO_2 and N_2O Emissions in Maize Growing Season Under Different Fertiliser Regimes in an Upland Red Soil Region of South China. Journal of Integrative Agriculture*,* **13**, 604-614.

Zhang YH, Ding WX (2011) Diel methane emissions in stands of *Spartina alterniflora* and *Suaeda salsa* from a coastal salt marsh. Aquatic Botany*,* **95**, 262-267.

Zhang ZH, Duan JC, Wang SP *et al.* (2013) Effects of seeding ratios and nitrogen fertilizer on ecosystem respiration of common vetch and oat on the Tibetan plateau. Plant and Soil*,* **362**, 287-299.

Zhou MH, Zhu B, Bruggemann N, Bergmann J, Wang YQ, Butterbach-Bahl K (2014) N2O and CH_4 Emissions, and NO_3^- Leaching on a crop-yield basis from a subtropical rain-fed wheat-maize rotation in response to different types of nitrogen fertilizer. Ecosystems*,* **17**, 286-301.